AD_____

Award Number: DAMD17-98-1-8517

TITLE: Bone-97 Alcohol and Skeletal Adaptation to Mechanical Usage

PRINCIPAL INVESTIGATOR: Russell Turner, Ph.D.

CONTRACTING ORGANIZATION: Mayo Clinic and Foundation
Rochester, Minnesota 55905

REPORT DATE: October 2002

TYPE OF REPORT: Final

PREPARED FOR: U.S. Army Medical Research and Materiel Command
Fort Detrick, Maryland 21702-5012

DISTRIBUTION STATEMENT: Approved for Public Release;
Distribution Unlimited

AD_____

Award Number: DAMD17-00-1-0096

TITLE: Molecular Mechanisms of Prostate Cancer Cell Death

PRINCIPAL INVESTIGATOR: Vincent L. Cryns, M.D.

CONTRACTING ORGANIZATION: Northwestern University
Chicago, Illinois 60611

REPORT DATE: April 2003

TYPE OF REPORT: Final

PREPARED FOR: U.S. Army Medical Research and Materiel Command
Fort Detrick, Maryland 21702-5012

REPORT DOCUMENTATION PAGE

Form Approved
OMB No. 074-0188

1. AGENCY USE ONLY (Leave blank)	2. REPORT DATE	3. REPORT TYPE AND DATES COVERED
	April 2003	Final (15 Mar 00 - 14 Mar 03)

4. TITLE AND SUBTITLE
Molecular Mechanisms of Prostate Cancer Cell Death

5. FUNDING NUMBERS
DAMD17-00-1-0096

6. AUTHOR(S)
Vincent L. Cryns, M.D.

7. PERFORMING ORGANIZATION NAME(S) AND ADDRESS(ES)
Northwestern University
Chicago, Illinois 60611

E-Mail:v-cryns@northwestern.edu

8. PERFORMING ORGANIZATION REPORT NUMBER

9. SPONSORING / MONITORING AGENCY NAME(S) AND ADDRESS(ES)
U.S. Army Medical Research and Materiel Command
Fort Detrick, Maryland 21702-5012

10. SPONSORING / MONITORING AGENCY REPORT NUMBER

11. SUPPLEMENTARY NOTES
Original contains color plates: All DTIC reproductions will be in black and white.

12a. DISTRIBUTION / AVAILABILITY STATEMENT
Distribution authorized to U.S. Government agencies only (proprietary information, Apr 03). Other requests for this document shall be referred to U.S. Army Medical Research and Materiel Command, 504 Scott Street, Fort Detrick, Maryland 21702-5012.

12b. DISTRIBUTION CODE

13. Abstract ***(Maximum 200 Words)*** *(abstract should contain no proprietary or confidential information)*

Using a novel expression cloning strategy and secondary functional screen of a human prostate cancer cDNA library, we have identified one new, functionally relevant caspase substrate: the mismatch repair protein MLH1 implicated in a variety of cancers including those of the prostate. We have demonstrated that human MLH1 is specifically cleaved by caspase-3 (but not by other caspases) at Asp^{418} *in vitro*. Furthermore, we have shown that MLH1 is rapidly proteolyzed by caspase-3 in prostate cancer cells induced to undergo apoptosis by treatment with TNF-related apoptotosis-inducing ligand (TRAIL) or the topoisomerase II inhibitor etoposide, which induces DNA double-strand breaks. Importantly, proteolysis of MLH1 by caspase-3 triggers its partial redistribution from the nucleus to the cytoplasm. In addition, a capase-3 cleavage-resistant D418E MLH1 mutant inhibits etoposide-induced apoptosis but has little effect on TRAIL-induced apoptosis. These results indicate that MLH1 is specifically targeted for proteolysis by caspase-3, and this proteolytic event promotes the execution of apoptotic signals initiated by DNA double-strand breaks. In this way, our results suggest a novel function of MLH1 in the response to DNA double-strand breaks that is deregulated by caspase proteolysis. These experiments, then, may lead to novel treatments for prostate cancer that specifically target MLH1.

14. SUBJECT TERMS	15. NUMBER OF PAGES
apoptosis, caspase, programmed cell death, signal transduction	51
	16. PRICE CODE

17. SECURITY CLASSIFICATION OF REPORT	18. SECURITY CLASSIFICATION OF THIS PAGE	19. SECURITY CLASSIFICATION OF ABSTRACT	20. LIMITATION OF ABSTRACT
Unclassified	Unclassified	Unclassified	Unlimited

Table of Contents

Cover.....

SF 298.....2

Table of Contents.....3

Introduction.....4

Body.....5-7

Key Research Accomplishments.....8

Reportable Outcomes.....8

Conclusions.....9

References.....10

Bibliography and Personnel.....11

Appendices.....12-50

Introduction

Apoptosis or programmed cell death is a genetically regulated cellular suicide response that is activated in prostate cancer cells by androgen ablation and irradiation. Indeed, the tumoricidal activity of these treatment modalities stems from their ability to induce apoptosis in prostate cancer cells (1). Caspases are a conserved family of cysteine proteases that are universal effectors of programmed cell death (2, 3). However, the molecular mechanisms by which caspases induce prostate cancer cell death are largely unknown. We *hypothesize* that caspases kill prostate cancer cells by cleaving and altering the activity of key intracellular proteins. To test this hypothesis, we propose to screen a prostate cDNA library for caspase substrates using a novel expression cloning strategy that we have recently developed (4-7). The specific objectives, then, are: (1) To isolate cDNAs encoding caspase substrates from a prostate cDNA library; and (2) To identify/characterize those caspase substrates identified in objective 1 whose proteolysis directly promotes prostate cancer cell death. In these experiments, then, we will apply a novel expression cloning strategy that we have recently developed (and validated) to systematically identify caspase substrate(s) whose proteolysis directly contributes to prostate cancer apoptosis. The major innovative aspect of our approach is that it allows us to directly and rapidly identify these critical caspase target(s): no other systematic strategies to isolate functionally relevant caspase substrates have been described.

Using this strategy, we have identified one clearly functionally relevant caspase substrate whose proteolysis promotes prostate cancer cell death in response to some stimuli: the mismatch repair protein MLH1 implicated in a variety of cancers including those of the prostate. Hence, we will focus on deciphering the mechanisms by which caspase cleavage of MLH1 promotes prostate cancer cell death. **We hypothesize (i) that MLH1 inhibits apoptosis induced by some types of DNA damage; and (ii) that caspase proteolysis of MLH1 specifically disrupts its DNA repair and anti-apoptotic functions.** These studies, then, will provide novel insights into the mechanisms of prostate cancer apoptosis, and they may thereby lead to new therapies for prostate cancer that specifically target MLH1.

Body

Task 1. **Preparation of Small Pools from a Prostate cDNA library, Months 1-4:**
Completed in year one of the grant.

Task 2. **Screen Small Pools for Caspase Substrates, Months 4-12:**
Completed in year one of the grant. 22 novel caspase substrate cDNAs were identified from a human prostate cancer cDNA library (listed in Table 1). 3 previously identified caspase substrates (indicated by asterisks) were also isolated in this screen, confirming its validity.

Table. 1. Caspase Substrates Identified in Human Prostate Carcinoma cDNA Library Screen

Caspase Substrates	Function
I. Regulatory Protein	
MLH1 (mut L homologue 1)	DNA mismatch repair
Integrin β4	Cell adhesion/cell survival
HER2 (ERB2)	Tyrosine kinase receptor
Protein phosphatase 1B2	Phosphatase
VCP (Valosin-containing protein)	Proteasome pathway
Complement component 4A	Complement host defense
Complement component 4B (2x)	Complement host defense
CDP (CCAAT displacement protein)	Transcriptional repression
SRP54 (Signal Recognition Particle 54 kDa)	Secretory protein targeting
Lysyl-tRNA synthetase	tRNA synthesis
II. Structural Proteins	
Actin, α-2 (2x)	Actin microfilament system
Actin, γ-2 (2x)	Actin microfilament system
Filamin A*	Actin binding protein
Actinin, α-1	Actin binding protein
Vimentin*	Intermediate filament protein
Cytokeratin 18*	Intermediate filament protein
Myosin heavy polypeptide 11 (2x)	Contractile protein
III. Novel Proteins/Proteins of Unknown Function	
Breast cancer associated gene 1 protein (AF126181)	Unknown
Cisplatin resistance associated gene (NM_006697)	Unknown
N-myc downstream regulated gene 2 (XM_007500)	Unknown
Hypothetical protein FLJ10233 (NM_018034)	Unknown

Task 3. **Secondary Functional Screen of Caspase Substrates Isolated in Task 2, Months 6-16:**

Completed in year two of the grant. Of the 22 novel caspase substrate cDNAs identified in the screen, one was found to alter the sensitivity of transfected PC-3 prostate carcinoma cells to some apoptotic stimuli: a partial cDNA encoding MLH1, a DNA mismatch repair (MMR) gene implicated in the pathogenesis of many cancers including prostate carcinoma (8-10). Although these results do not exclude the possibility that additional caspase substrate cDNAs isolated in Task 2 might contribute to prostate cancer apoptosis, we decided to focus on the one clearly functionally relevant caspase substrate identified in this screen, *viz.*, MLH1. Furthermore, the recent observation that MMR defects and MLH1 mutations occur in prostate cancer (9, 11-13) underscores the potential clinical relevance of our studies.

Task 4. **Detailed Analyses of the Functionally Relevant Caspase Substrate Identified in Task 3 (MLH1), Months 12-36:**

Completed in years two and three. These results are detailed in a manuscript currently in preparation entitled "Proteolysis of the Mismatch Repair Protein MLH1 by Caspase-3 Promotes Apoptosis induced by DNA Double-Strand Breaks" (manuscript included in appendix). We intend to submit this manuscript for publication within 2 weeks. In this manuscript, we demonstrate that human MLH1 was isolated as a caspase-3 substrate by small pool expression cloning using a human prostate adenocarcinoma cDNA library (Fig. 1 in the manuscript). We then show that human MLH1 is specifically cleaved by caspase-3 (and not by other caspases tested) *in vitro* (Fig. 2A in the manuscript). By mutating the Asp residue (Asp^{418}) at a potential caspase-3 cleavage site to a Glu residue, we demonstrate that the resulting mutant MLH1 protein (D418E) is resistant to proteolysis by caspase-3, thereby indicating that Asp^{418} is indeed the caspase-3 cleavage site (Fig. 2B in the manuscript). Next, we demonstrate that MLH1 is rapidly cleaved in PC-3 prostate carcinoma cells induced to undergo apoptosis by treatment with TRAIL (a promising therapeutic cytokine that preferentially induces apoptosis in cancer cells (14, 15)) or in TSU-Pr1 carcinoma cells treated with etoposide (a chemotherapeutic agent that induces DNA double-strand breaks (16)) (Fig. 3A in the manuscript). The broad spectrum caspase inhibitor zVAD-fmk antagonizes TRAIL- or etoposide-induced MLH1 proteolysis, indicating that caspases are responsible for the apoptotic cleavage of MLH1 (Fig. 3B in the manuscript). Furthermore, we observed that MLH1 is not cleaved in caspase-3-deficient MCF-7 cells induced to undergo apoptosis (Fig. 3C in the manuscript). Hence, MLH-1 is a specific proteolytic substrate of caspase-3.

In this same manuscript, we demonstrate that proteolysis of MLH1 by caspase-3 has several important functional consequences. First, caspase cleavage of MLH1 triggers its partial redistribution from the nucleus to the cytoplasm. As shown in Fig. 4 in the appended manuscript, the amino-terminal caspase cleavage product of MLH1 (N-MLH1) is found in both the cytoplasm and nucleus of transfected PC-3 cells. In contrast, both full-length MLH1 and the carboxyl-terminal cleavage product (C-MLH1) are present predominantly in the nucleus, as would be expected for a protein involved in DNA repair.

To determine whether caspase proteolysis of MLH1 is sufficient to induce apoptosis, we transfected PC-3 prostate carcinoma cells with GFP-tagged cDNAs encoding full-length MLH1, the amino-terminal (N-MLH1) or the carboxyl-terminal (C-MLH1) caspase cleavage products. None of these cDNAs were sufficient to induce apoptosis in PC-3 cells (Fig. 5 in the manuscript). In contrast, these cells were sensitive to apoptosis induction by the carboxyl-terminal caspase cleavage product of RAD21 (C-RAD21), a proteolytic product we have previously shown to be sufficient to trigger apoptotic cell death (7) (Fig. 5). To examine whether the proteolytic cleavage of MLH1 by caspase-3 is necessary for the execution of apoptosis, we transiently transfected PC-3 cells with GFP-vector or cDNAs encoding GFP-tagged WT or

D418E mutant MLH1. After 24 hours, cells were treated with TRAIL or etoposide (a chemotherapeutic drug which selectively induces DNA double-strand breaks(16)). As shown in Fig. 6 in the appended manuscript, the cleavage-resistant D418E mutant MLH1 protected PC-3 cells from etoposide-induced apoptosis, but had little effect on TRAIL-induced apoptosis. **Taken together, these findings indicate that caspase proteolysis of MLH1 promotes apoptosis induced by DNA double-strand breaks.** Indeed, they suggest that caspase-3 inactivates MLH1's anti-apoptotic/repair function in response to DNA double-strand breaks.

Key Research Accomplishments

- Using a novel small pool expression cloning strategy to screen a human prostate cancer cDNA library, we identified 22 new caspase substrates.
- Using our secondary functional screen to identify caspase substrate cDNAs that alter the sensitivity of prostate cancer cells to apoptosis, we identified one novel caspase substrate that is clearly functionally relevant: the DNA mismatch repair gene product MLH1.
- We have demonstrated that MLH1 is specifically cleaved by caspase-3 at Asp^{418} *in vitro.*
- We have demonstrated that MLH1 is cleaved by caspases in prostate cancer cells undergoing apoptosis in response to diverse stimuli.
- We have also demonstrated that caspase-3 is required for the apoptotic proteolysis of MLH1.
- We have constructed GFP-tagged cDNAs encoding wild-type MLH1, D418E (caspase cleavage-resistant) MLH1, and each of its caspase cleavage products.
- We have demonstrated that caspase proteolysis of MLH1 has important functional consequences, *viz.*, the partial redistribution of MLH1 from the nucleus to the cytoplasm.
- We have demonstrated that neither full-length MLH1 nor its cleavage products induces apoptosis in PC-3 prostate carcinoma cells, indicating that MLH1 proteolysis is not sufficient to induce apoptosis.
- We have demonstrated that a caspase cleavage-resistant D418E mutant MLH1 protects PC-3 prostate carcinoma cells from apoptosis induced by etoposide (a chemotherapeutic agent which induces DNA double-strand breaks), thereby indicating that MLH1 proteolysis promotes apoptosis in response to DNA double-strand breaks.

Reportable Outcomes

Manuscript in preparation: Chen F, Arseven O, and VL Cryns. Proteolysis of the Mismatch Repair Protein MLH1 by Caspase-3 Promotes Apoptosis induced by DNA Double-Strand Breaks. Manuscript in appendix. We anticipate submitting this manuscript for publication by May 1, 2003.

Grant funded: Department of Defense Breast Cancer Research Program 2001 "Caspase Cleavage of HER2: A Novel Apoptotic Pathway in Breast Cancer". HER2 was identified as a novel caspase substrate in our screen performed in year one, and this new grant focuses on the role of caspase cleavage of HER2 in breast cancer apoptosis (no overlap with the present award).

Presentation: "Caspase Proteolytic Signaling: A Dead End" Chicago Prostate Club, Northwestern University Medical School, Chicago, IL, December 2000.

Presentation: "Caspase Proteolytic Signaling: A Dead End" Apoptosis Interest Group Chicago, Northwestern University Medical School, Chicago, IL, April 2001.

Conclusions

Using our novel expression cloning strategy and secondary functional screen, we have identified one clearly functionally relevant caspase substrate that *inhibits* prostate cancer cell death in response to chemotherapeutic drugs that induce DNA double-strand breaks: the mismatch repair protein MLH1 implicated in a variety of cancers including those of the prostate. We have demonstrated that human MLH1 is specifically cleaved by caspase-3 at Asp^{418} *in vitro*. Furthermore, MLH1 is rapidly proteolyzed by caspase-3 in prostate cancer cells induced to undergo apoptosis by treatment with TNF-related apoptotosis-inducing ligand (TRAIL) or the topoisomerase II inhibitor etoposide, which induces DNA double-strand breaks. Importantly, proteolysis of MLH1 by caspase-3 triggers its partial redistribution from the nucleus to the cytoplasm. In addition, a capase-3 cleavage-resistant D418E MLH1 mutant inhibits etoposide-induced apoptosis but has little effect on TRAIL-induced apoptosis. These results indicate that MLH1 is specifically targeted for proteolysis by caspase-3, and this proteolytic event promotes the execution of apoptotic signals initiated by DNA double-strand breaks.

These experiments, then, have provided us with novel insights into the molecular mechanisms of prostate cancer apoptosis. Because apoptosis plays a critical role in the progression and treatment of prostate cancer, our studies may lead to novel, highly selective therapies for prostate cancer. For instance, our studies suggest that inhibition of MLH1 may sensitize prostate cancer cells to apoptosis induced by chemotherapeutic drugs which induce DNA double-strand breaks.

Refererences

1. Denmeade, S.R., Lin, X.S., and Isaacs, J.T. 1996. Role of programmed (apoptotic) cell death during the progression and therapy for prostate cancer. *Prostate* 28:251-265.
2. Cryns, V.L., and Yuan, J. 1998. Proteases to die for. *Genes & Dev* 12:1551-1570.
3. Thornberry, N.A., and Lazebnik, Y. 1998. Caspases: enemies within. *Science* 281:1312-1316.
4. Lustig, K.D., Stukenberg, T., McGarry, T., King, R.W., Cryns, V.L., Mead, P., Zon, L., Yuan, J., and Kirschner, M.W. 1997. Small pool expression screening: a novel strategy for the identification of genes involved in cell cycle control, apoptosis and early development. *Methods Enzymol* 283:83-99.
5. Cryns, V., Byun, Y., Rana, A., Mellor, H., Lustig, K., Ghanem, L., Parker, P., Kirschner, M., and Yuan, J. 1997. Specific proteolysis of the kinase protein kinase C-related kinase 2 by caspase-3 during apoptosis: Identification by a novel small pool expression cloning strategy. *J Biol Chem* 272:29449-29453.
6. Byun, Y., Chen, F., Chang, R., Trivedi, M., Green, K., and Cryns, V.L. 2001. Caspase cleavage of vimentin disrupts intermediate filaments and promotes apoptosis. *Cell Death Differ* 8:443-450.
7. Chen F., Kamradt M., Mulcahy M., Byun Y., Xu H., McKay M.J., and Cryns V.L. 2002. Caspase proteolysis of the cohesin component RAD21 promotes apoptosis. *J Biol Chem* 2002; 277:16775-16781.
8. Bronner, C.E., Baker, S.M., Morrison, P.T., Warren, G., Smith, L.G., Lescoe, M.K., Kane, M., Earabino, C., Lipford, J., Lindblom, A., et al. 1994. Mutation in the DNA mismatch repair gene homologue hMLH1 is associated with hereditary non-polyposis colon cancer. *Nature* 368:258-261.
9. Chen, Y., Wang, J., Fraig, M.M., Metcalf, J., Turner, W.R., Bissada, N.K., Watson, D.K., and Schweinfest, C.W. 2001. Defects in DNA mismatch repair in human prostate cancer. *Cancer Res* 61:4112-4121.
10. Papadopoulos, N., Nicolaides, N.C., Wei, Y.F., Ruben, S.M., Carter, K.C., Rosen, C.A., Haseltine, W.A., Fleischmann, R.D., Fraser, C.M., Adams, M.D., et al. 1994. Mutation of a mutL homolog in hereditary colon cancer. *Science* 263:1625-1629.
11. Boyer, J.C., Umar, A., Risinger, J.I., Lipford, J.R., Kane, M., Yin, S., Barrett, J.C., Kolodner, R.D., and Kunkel, T.A. 1995. Microsatellite instability, mismatch repair deficiency, and genetic defects in human cancer cell lines. *Cancer Res* 55:6063-6070.
12. Gao, X., Wu, N., Grignon, D., Zacharek, A., Liu, H., Salkowski, A., Li, G., Sakr, W., Sarkar, F., Porter, A.T., et al. 1994. High frequency of mutator phenotype in human prostatic adenocarcinoma. *Oncogene* 9:2999-3003.
13. Uchida, T., Wada, C., Wang, C., Ishida, H., Egawa, S., Yokoyama, E., Ohtani, H., and Koshiba, K. 1995. Microsatellite instability in prostate cancer. *Oncogene* 10:1019-1022.
14. Sheridan, J.P., Marsters, S.A., Pitti, R.M., Gurney, A., Skubatch, M., Baldwin, D., Ramakrishnan, L., Gray, C.L., Baker, K., Wood, W.I., Goddard, A.D., Godowski, P., and Ashkenazi, A. 1997. Control of TRAIL-induced apoptosis by a family of signaling and decoy receptors. *Science* 277:818-821.
15. Ashkenazi, A., Pai, R.C., Fong, S., Leung, S., Lawrence, D.A., Marsters, S.A., Blackie, C., Chang, L., McMurtrey, A.E., Hebert, A., DeForge, L., Koumenis, I.L., Lewis, D., Harris, L., Bussiere, J., Koeppen, H., Shahrokh, Z., and Schwall, R.H. 1999. Safety and antitumor activity of recombinant soluble Apo2 ligand. *J Clin Invest* 104:155-162.
16. Froelich-Ammon, S., and Osheroff, N. 1995. Topoisomerase poisons: harnessing the dark side of enzyme mechanism. *J Biol Chem* 270:21429-21432.

Bibliography

1. Chen F, Arseven O, and **Cryns VL**. Proteolysis of the Mismatch Repair Protein MLH1 by Caspase-3 Promotes Apoptosis induced by DNA Double-Strand Breaks. Manuscript in preparation.

2. Chen F, Kamradt M, Chang R, Mulcahy M, Byun Y, Xu H, McKay MJ, and **Cryns VL**. Caspase proteolysis of the cohesin component RAD21 promotes apoptosis. *J Biol Chem* 2002 277:16775-16781.

Both manuscripts included in the appendix.

Personnel Supported by this Award

1. Vincent L. Cryns, MD, Principal Investigator

2. Feng Chen, MD, Research Associate

Appendices

1. Biosketch

2. Manuscripts:

Chen F, Arseven O, and VL Cryns. Proteolysis of the Mismatch Repair Protein MLH1 by Caspase-3 Promotes Apoptosis induced by DNA Double-Strand Breaks. Manuscript in preparation.

Chen F, Kamradt M, Chang R, Mulcahy M, Byun Y, Xu H, McKay MJ, and **Cryns VL**. Caspase proteolysis of the cohesin component RAD21 promotes apoptosis. *J Biol Chem* 2002 277:16775-16781.

BIOGRAPHICAL SKETCH

Provide the following information for the key personnel in the order listed for Form Page 2.
Follow the sample format for each person. **DO NOT EXCEED FOUR PAGES.**

NAME	POSITION TITLE
Vincent L. Cryns, M.D.	Assistant Professor

EDUCATION/TRAINING *(Begin with baccalaureate or other initial professional education, such as nursing, and include postdoctoral training.)*

INSTITUTION AND LOCATION	DEGREE *(if applicable)*	YEAR(s)	FIELD OF STUDY
Harvard College, Cambridge, MA	A.B.	1983	Biochemistry
Harvard Medical School, Boston, MA	M.D.	1987	Medicine

A. Postions and Honors

Professional Experience:

1987-1988 Intern in Internal Medicine, Massachusetts General Hospital, Boston, MA
1988-1990 Resident in Internal Medicine, Dartmouth-Hitchcock Medical Center, Hanover, NH
1990-1993 Clinical and Research Fellow in Medicine, Endocrine Unit, Massachusetts General Hospital and Harvard Medical School, Boston, MA
1992-1997 Instructor, Harvard Medical School
1994-1997 Clinical Assistant in Medicine, Massachusetts General Hospital
1997- Assistant Professor in Medicine, Feinberg School of Medicine, Northwestern University
1997- Member, Robert H. Lurie Comprehensive Cancer Center, Northwestern University
1997- Member, Feinberg Cardiovascular Research Center, Feinberg School of Medicine, Northwestern University
1998- Attending Physician, Northwestern Memorial Hospital
1999- Admissions Committee, Medical Scientist Training Program, Feinberg School of Medicine, Northwestern University
2002- Chair, Admissions Committee, Integrated Biology Program, Feinberg School of Medicine, Northwestern University

Research Training:

1991-1995 Molecular Pathogenesis of Endocrine Neoplasia, mentor: Dr. Andrew Arnold, Harvard Medical School
1995-1997 Molecular Mechanisms of Apoptosis, mentor: Dr. Junying Yuan, Harvard Medical School

Honors and Awards:

1980-1983 Harvard National Scholar
1983 A. B. *Summa cum laude* in biochemistry, Harvard College
1983 *Phi Beta Kappa*, Harvard College
1983-1987 Harvard College Graduate National Scholar
1990- Diplomate, American Board of Internal Medicine
1991 Nettie Karpin Award, Endocrine Society
1992-1993 Individual National Research Service Award, NIH
1993 Young Investigator Award, American Soc. for Bone & Mineral Research
1994 Senior Fellows Award, Endocrine Society
1994- Diplomate, Endocrinology, Diabetes and Metabolism (ABIM)
1993-1998 NIH Mentored Clinical Scientist Development Award
2000-2003 Young Investigator Award, Department of Defense, Prostate Cancer Research Program
2002- Member, Pathobiology 1 and Concept-6 Grant Review Panels, Department of Defense, Breast Cancer Research Program

B. Selected Peer-Reviewed Publications

St. Germain DL, Dittrich W, Morganelli CM, **Cryns VL**. Molecular cloning by hybrid arrest of translation in *Xenopus laevis* oocytes: identification of a cDNA encoding the type I iodothyronine 5'-deiodinase from rat liver. *J Biol Chem* 1990; 265:20087-20090.

Cryns VL, Alexander JM, Klibanski A, Arnold A. The retinoblastoma gene in human pituitary tumors. *J Clin. Endocrinol Metab*1993; 77: 644-646.

Cryns VL, Thor A, Xu H-J, Hu S-X, Wierman ME, Vickery AL, Benedict WF, Arnold A. Loss of the retinoblastoma tumor-suppressor gene in parathyroid carcinoma. *N Engl J Med* 1994; 330:757-761.

Cryns VL, Rubio M-P, Thor AD, Louis DN, Arnold A. p53 abnormalities in human parathyroid carcinoma. *J Clin Endocrinol Metab* 1994; 78:1320-1324.

Cryns VL, Yi SM, Tahara H, Gaz RD, Arnold A. Frequent loss of chromosome arm 1p DNA in parathyroid adenomas. *Genes Chromosom Cancer* 1995; 13:9-17.

Baron JA, Comi RJ, **Cryns VL**, Brinck-Johnsen T, Mercer GN. The effect of cigarette smoking on adrenal cortical hormones. *J Pharmacol Exp Ther* 1995; 272:151-155.

Tahara H, Smith AP, Gaz RD, **Cryns VL**, Arnold A. Genomic localization of novel candidate tumor suppressor gene loci in human parathyroid adenomas. *Cancer Res* 1996; 56: 599-605.

Cryns VL, Bergeron L, Zhu H, Li H, Yuan J. Specific cleavage of α-fodrin during Fas- and tumor necrosis factor-induced apoptosis is mediated by an interleukin-1β-converting enzyme/Ced-3 protease distinct from the poly(ADP-ribose) polymerase protease. *J Biol Chem* 1996; 271:31277-31282.

Lustig KD, Stukenberg T, McGarry T, King RW, **Cryns VL**, Mead P, Zon L, Yuan J, Kirschner MW. Small pool expression screening: identification of genes involved in cell cycle control, apoptosis, and early development. *Methods Enzymol* 1997; 283:83-99.

Li H, Bergeron L, **Cryns VL**, Pasternack MS, Zhu H, Shi L, Greenberg A, Yuan J. Activation of caspase-2 in apoptosis. *J Biol Chem* 1997; 272:21010-21017.

Cryns VL, Byun Y, Rana A, Mellor H, Lustig K, Ghanem L, Parker P, Avruch J, Kirschner MW, Yuan J. Specific proteolysis of the kinase protein kinase C-related kinase 2 by caspase-3 during apoptosis: Identification by a novel small pool expression cloning strategy. *J Biol Chem* 1997; 272:29449-29453.

Cryns VL, Yuan J. Proteases to die for. *Genes & Dev.* 1998; 12:1551-1570.

Holly TA, Drincic A, Byun Y, Nakamura S, Harris K, Klocke FJ, **Cryns VL**. Caspase inhibition reduces myoctye cell death induced by myocardial ischemia and reperfusion *in vivo*. *J Mol Cell Cardiol* 1999; 31:1709-1715.

Bialik S, **Cryns VL**, Drincic A, Miyata S, Wollowick AL, Srinivasan A, Kitsis RN. The mitochondrial apoptotic pathway is activated by serum and glucose deprivation in cardiac myocytes. *Circ Res* 1999; 85:403-414.

Abraha A, Ghoshal N, Gamblin TC, **Cryns V**, Berry RW, Kuret J, Binder LI. C-terminal modification and truncation in the polymerization of tau in vitro and in Alzheimer's disease. *J Cell Sci* 2000; 113:3737-3745.

Lee C, Janulis L, Ilio K, Shah A, Park I, Kim S, **Cryns V**, Pins M, Bergan R. In vitro models of prostate apoptosis: Clusterin as an antiapoptotic mediator. *Prostate* 2000; 45(S9):21-24.

Talanian RV, Brady KD, **Cryns VL**. Caspases as targets for anti-inflammatory and anti-apoptotic drug discovery. *J Med Chem* 2000; 43:3351-3371.

Byun Y, Chen F, Chang R, Trivedi M, Green KJ, **Cryns VL**. Caspase cleavage of vimentin disrupts intermediate filaments and promotes apoptosis. *Cell Death Differ* 2001; 8:443-450.

Kamradt MJ, Chen F, **Cryns VL**. The small heat shock protein αB-crystallin negatively regulates cytochrome c- and caspase-8-dependent activation of caspase-3 by inhibiting its autoproteolytic maturation. *J Biol Chem* 2001; 276:16059-16063.

Chen F, Kamradt M, Mulcahy M, Byun Y, Xu H, McKay MJ, **Cryns VL**. Caspase proteolysis of the cohesin component RAD21 promotes apoptosis. *J Biol Chem* 2002; 277:16775-16781.

Kamradt MC, Chen F, Sam S, **Cryns VL**. The small heat shock protein αB-crystallin negatively regulates apoptosis during myogenic differentiation by inhibiting caspase-3 activation. *J Biol Chem* 2002; 277:38731-38736.

Chen F, Chang R, Trivedi M, Capetanaki Y, **Cryns VL**. Caspase proteolysis of desmin produces a dominant-negative inhibitor of intermediate filaments and promotes apoptosis. *J Biol Chem* 2003; 278:6848-6853.

Proteolysis of the Mismatch Repair Protein MLH1 by Caspase-3 Promotes Apoptosis induced by DNA Double-Strand Breaks

Feng Chen, Onur Arseven, and Vincent L. Cryns

Robert H. Lurie Comprehensive Cancer Center and the Department of Medicine, Feinberg School of Medicine, Northwestern University, Chicago, IL 60611, USA.

Corresponding author:

Vincent Cryns

Tarry 15-755

Feinberg School of Medicine

Northwestern University

303 E. Chicago Ave.

Chicago, IL 60611

Tel: (312) 503-0644

Fax: (312) 908-9032

e-mail: v-cryns@northwestern.edu

Running Title: Caspase Cleavage of MLH1 Promotes Etoposide-induced Apoptosis

Abstract

Caspases are critical pro-apoptotic proteases that execute cell death signals by selectively cleaving proteins as Asp residues to alter their function. Caspases trigger apoptotic chromatin degradation by directly activating caspase-activated DNase (CAD) and by inactivating a number of enzymes that sense or repair DNA damage. We have identified the mismatch repair protein MLH1 as a novel caspase-3 substrate by screening small pools of a human prostate adenocarcinoma cDNA library for cDNAs encoding caspase substrates. Human MLH1 is specifically cleaved by caspase-3 at Asp^{418} *in vitro*. Furthermore, MLH1 is rapidly proteolyzed by caspase-3 in cancer cells induced to undergo apoptosis by treatment with TNF-related apoptotosis-inducing ligand (TRAIL) or the topoisomerase II inhibitor etoposide, which induces DNA double-strand breaks. Importantly, proteolysis of MLH1 by caspase-3 triggers its partial redistribution from the nucleus to the cytoplasm. In addition, a capase-3 cleavage-resistant D418E MLH1 mutant inhibits etoposide-induced apoptosis but has little effect on TRAIL-induced apoptosis. These results indicate that MLH1 is specifically targeted for proteolysis by caspase-3, and this proteolytic event promotes the execution of apoptotic signals initiated by DNA double-strand breaks.

Introduction

The caspase family of cysteine proteases are essential effectors of the apoptotic cell death program that catalyze many of the biochemical and morphological events of apoptosis by their concerted proteolytic actions on a subset of intracellular proteins (1, 2). Caspases are organized in a proteolytic cascade in which initiator procaspases are activated by oligomerization via recruitment to distinct caspase-activating complexes; these apoptotic signals are then amplified by the mitochondria. In the extrinsic pathway, ligands of the tumor necrosis factor (TNF)-α family (*e.g.*, TNF-α, TNF-related apoptosis-inducing ligand (TRAIL), and Fas) bind to their death domain-containing receptors, an event which leads to the recruitment of the death domain-containing protein FADD, and subsequently, to the recruitment and activation of procaspases-8 and -10 to receptor complexes (1-5). In the intrinsic pathway, caspase-2, rather than caspase-9, has recently emerged as the likely initiator caspase activated by genotoxic stress such as DNA damage and chemotherapeutic drugs (6-8). In response to these stimuli, procaspase-2 is recruited to a large cytosolic complex, the components of which have yet to be identified (but are apparently different from the apoptosome discussed below), resulting in its oligomerization and activation (8). Importantly, the apoptotic signals initiated by death ligands or genotoxic stress are amplified by the mitochondria: caspase-8 (extrinsic pathway) and caspase-2 (intrinsic pathway) trigger the mitochondrial release of cytochrome c and other pro-apototic mediators such as Smac/DIABLO (6, 7, 9-12). Procaspase-9 is then activated by oligomerization in the apoptosome, a large cytosolic complex composed of cytochrome c, Apaf-1 and ATP (13, 14). Caspases-8 -9, and -10 then proteolyze and activate downstream caspases, including caspases-3, -6 and -7, which execute the apoptotic cell death signal by cleaving a number of intracellular protein targets (5, 15, 16).

The oligonucleosomal degradation of chromosomal DNA is one of the defining irreversible features of apoptotic cells that facilitates packaging the fragmented genome into apoptotic bodies (1, 17). Caspases promote DNA fragmentation by a variety of mechanisms.

First, at least under certain circumstances, caspases induce the mitochondrial release of AIF and endonuclease G, which interact with each other to induce chromosomal DNA fragmentation (18-20). Second, caspases proteolyze and inactivate ICAD (also known as DFF-45), an inhibitor of the caspase-activated DNase (CAD) (21-23). ICAD normally binds to and suppresses the DNase activity of CAD. Caspase cleavage of ICAD releases it from CAD, thereby activating CAD, which degrades DNA between nucleosomes. Third, caspases cleave several enzymes which sense or repair damaged DNA, including poly (ADP-ribose) polymerase (PARP), RAD21, RAD51, ATM, the catalytic subunit of the DNA-dependent protein kinase, the Bloom Syndrome protein (BLM), and BRCA1 (24-31). In the case of RAD21, caspase cleavage generates a pro-apoptotic carboxyl terminal product that is sufficient to induce apoptosis (25, 26). In this way, caspases promote DNA fragmentation by activating apoptotic DNases and by systematically subverting the DNA repair machinery.

Here we report that MLH1, a component of the conserved DNA mismatch repair (MMR) complex, is a novel and specific caspase-3 substrate. Indeed, our results are the first to indicate a linkage between caspases and MMR proteins. The MMR system recognizes and repairs mispaired or unpaired nucleotides that result from errors in DNA replication (32, 33). The mammalian homologues of the *E. Coli* MutS protein form heterodimers (MSH2-MSH6 and MSH2-MSH3) that bind to nucleotide mismatches and recruit heterodimers of the MutL homologues (MLH1-PMS2, MLH1-PMS1, or MLH1-MLH3) to base mismatches (32, 34). These MLH1-containing heterodimers, in turn, function as adaptor proteins which link the MutS proteins to the DNA repair/replication machinery, resulting in the strand-specific excision and repair of the mismatch-containing, newly synthesized DNA strand. Inactivating mutations of *MLH1* and *MSH2* occur commonly in hereditary nonpolyposis colon cancer and less commonly in other carcinomas, and they result in a "mutator" phenotype characterized by instability of repetitive microsatellite DNA sequences (33, 35-38). MMR proteins have also been implicated in homologous recombination repair of DNA double-strand breaks (DSBs), cell cycle checkpoint

activation, and in the execution of the apoptotic response to DNA damage induced by alkylating agents or other drugs which modify nucleotides (39-46).

In the present manuscript, we show that MLH1 is rapidly and specifically cleaved by caspase-3 at Asp^{418} in cells induced to undergo apoptosis by treatment with TRAIL (intrinsic apoptototic pathway) or etoposide (extrinsic apoptotic pathway); the latter chemotherapeutic drug inhibits topoisomerase II and selectively induces DNA DSBs (47). Furthermore, we demonstrate that proteolysis of MLH1 triggers its partial relocalization from the nucleus to the cytoplasm and contributes to the execution of apoptosis induced by DNA DSBs. In this way, our results suggest a novel function of MLH1 in the response to DNA DSBs that is deregulated by caspase proteolysis.

Materials and Methods

Plasmid Constructs. cDNAs encoding GFP-tagged full-length MLH1, the amino-terminal caspase cleavage product (N-MLH1, amino acids 1-418) or the carboxyl-terminal caspase cleavage product (C-MLH1, amino acids 419-756) were made by PCR amplification of wild-type human MLH1 (kindly provided by Dr. R. D. Kolodner) using the following oligonucleotide primers: 5'-GGCCCTCGAGGCCAAAATGTCGTTCGTG-3' and 5-GGCCCCGCGGACACCT-CTCAAAGACTTT-3' (full-length MLH1), 5'-GGCCCTCGAGGCCAAAATGTCGTTCGTG-3' and 5'-GGCCCCGCGGATCTGTCTTATCCTCTGT-3' (N-MLH1), or 5'-GGCCCTCGAGAT-GATTTCTAGTGGCAGGGCT-3' and 5-GGCCCCGCGGACACCTCTCAAAGACTTT-3' (C-MLH1). Each amplified PCR product was digested with *Xho*I and *Sac*2 and subcloned into pEGFP-N1 (Clontech). All cDNAs were verified by DNA sequencing.

Small Pool Expression Cloning. Small pool expression cloning to identify cDNAs encoding caspase substrates was performed as described previously (25, 48-50) with the following exceptions. Small pools (48 cDNAs/pool) of a human prostate adenocarcinoma cDNA library (Invitrogen, catalogue no. 11597010) were used to make ^{35}S-labeled protein pools with the TNT SP6 Coupled Transcription/Translation system (Promega) as described previously (48, 49). ^{35}S-labeled protein pools were incubated with buffer control or 25 ng of caspase-1, -2, -3 or -8 for 1 h at 37°C; the cleavage reactions were then separated by SDS-PAGE and visualized by autoradiography as described (48, 49). Single cDNAs encoding putative caspase substrates were isolated by systematically subdividing small cDNA pools and retesting the corresponding ^{35}S-labeled protein pools as above (48, 49).

Caspase Cleavage of MLH1 *In Vitro*. ^{35}S-labeled full-length human MLH1 was incubated with buffer, 2.5 ng or 25 ng of caspases-1, -2, -3, -6, -7 or -8 for 1 hr at 37°C, and the reactions analyzed as described previously (49, 51). A potential caspase-3 cleavage site in MLH1 (Asp^{418}) was specifically altered to a Glu residue with the QuickChange Site-Directed Mutagenesis kit

(Stratagene) using the following primers: 5'-GAGGATAAGACAGAGATTTCTAGTGGCA-GG-3' and 5'-CCTGCCACTAGAAATCTCTGTCTTATCCTC-3'. The entire coding sequence of the mutant D418E MLH1 was sequenced to verify the unique, intended mutation. ^{35}S-labeled D418E MLH1 was examined for sensitivity to caspase-3 cleavage as above.

Cell Culture, Apoptosis Induction, and Immunoblotting. Human PC-3 prostate carcinoma cells, TSU-Pr1 bladder carcinoma cells, and MCF-7 breast carcinoma cells were all grown in DMEM (Mediatech) with 10% heat-inactivated fetal calf serum (Invitrogen) added. Three apoptotic inducers were used in these studies: soluble TRAIL (purified as below) and TNF-α (R&D Systems), which activate the death receptor apoptotic pathway (1, 2), and etoposide (Sigma), a topoisomerase II inhibitor that induces DNA DSBs (47). Recombinant soluble TRAIL (amino acids 95-281) was produced in *E. coli* from pET15b plasmid (Novagen) containing a truncated TRAIL cDNA (52), and the His-tagged protein was purified under native conditions with the Qia*express* System (Qiagen) as described previously (53). PC-3 cells were treated with 2 μg/ml TRAIL for 0-16 h, while TSU-Pr1 cells were treated with 50 μM etoposide for 0-36 h. Immunoblotting of whole cell lysates was performed as described previously (51) using the following antibodies: an MLH1 mAb (BD Biosciences), a PKCδ polyclonal antibody (Santa Cruz Biotechnology), a procaspase-3 mAb (BD Biosciences), or a RAD21 polyclonal antibody (25). To determine whether caspases were responsible for the apoptotic proteolysis of MLH1, PC-3 or TSU-Pr1 cells were pre-incubated for 1 h with vehicle or 50 μM zVAD-fmk, a broad spectrum caspase inhibitor. PC-3 cells were then treated with 2 μg/ml TRAIL for 8 h and TSU-Pr1 cells with 50 μM etoposide for 24 h.

Transfections, Indirect Immunofluorescence, and Apotosis Assays. PC-3 cells were transiently transfected with 1 μg pEGFP-N1 plasmids using LipofectAMINE PLUS Reagent (Invitrogen). After 24 h, cells were fixed in 4% paraformaldehyde for 10 min at room temperature, washed, and incubated with the DNA fluorochrome Hoescht No. 33258 (10 μg/ml, Sigma) for 30 min at room temperature. GFP-tagged proteins and nuclei were visualized by

fluorescence microscopy using a Nikon Eclipse E400 microscope as described previously (25, 50). For apoptosis assays, ≥200 GFP-positive cells were scored for apoptotic nuclei (*i.e.*, condensed or fragmented); all experiments were performed at least in triplicate.

Results

Identification of MLH1 as a caspase-3 substrate by small pool expression cloning. We have recently described a small pool expression cloning strategy to screen cDNA libraries for cDNAs encoding caspase substrates (25, 48-50). In this report, small pools (48 cDNAs/pool) of a human prostate adenocarcinoma cDNA library (Invitrogen) were transcribed and translated *in vitro* in the presence of ^{35}S-methionine, and the corresponding ^{35}S-labeled protein pools were incubated with recombinant caspases. As shown in Fig. 1A, a ~64-kDa protein (indicated by asterisk) present in ^{35}S-labeled protein pool 10 was specifically cleaved by caspase-3 (C3), but not by the other caspases tested (caspases-1, -2, or -8), into 2 products ~40 and 24 kDa in size (indicated by arrows). The enzymatic activity of each protease was verified with a known substrate (data not shown). To isolate the putative caspase-3 substrate present in protein pool 10, cDNA pool 10 was further subdivided into smaller pools, and the corresponding ^{35}S-labeled protein pools were reincubated with caspase-3. This process was repeated until a single cDNA encoding a ~64-kDa protein cleaved by caspase-3 into the appropriately sized fragments was identified (Fig. 1B). This cDNA was sequenced and found to be a partial MLH1 cDNA (36, 37).

MLH1 is specifically proteolyzed by caspase-3 at Asp^{418} *in vitro*. To determine whether the full-length MLH1 protein is cleaved by caspases *in vitro*, we incubated ^{35}S-labeled full-length human MLH1 with recombinant caspases. As shown in Fig. 2A, ^{35}S-labeled MLH1 was selectively proteolyzed by caspase-3 into 2 major cleavage products ~48 and 40 kDa in size (indicated by arrows). In contrast, none of the other caspases (-1, -2, -6, -7 or -8) examined cleaved MLH1. The activity of each caspase was confirmed using a known substrate (data not shown). To identify the caspase cleavage site in MLH1, we substituted the Asp residue at a potential caspase-3 cleavage site (DKTD^{418}↓I^{419}) with a Glu residue. Unlike WT MLH1 (left panel, Fig. 2B), the ^{35}S-labeled D418E MLH1 protein was not cleaved by caspase-3 (right panel), indicating that Asp^{418} is the caspase-3 cleavage site *in vitro*.

MLH1 is cleaved by caspase-3 in cancer cells undergoing apoptosis. To determine whether MLH1 is cleaved in cancer cells during the induction of apoptosis, we treated human PC-3 prostate carcinoma cells with 2 μg/ml TRAIL for 0-16 h or human TSU-1 bladder carcinoma cells with 50 μM etoposide for 0-36 h. As demonstrated in Fig. 3A, MLH1 was rapidly proteolyzed into a ~48-kDa product in cells treated with TRAIL (within 4 h) or with etoposide (within 12 h). The caspase substrate PKCδ (54) was used as a positive control in these studies and was cleaved into its characteristic fragment (indicated by arrow) in apoptotic cells. Importantly, the size of the apoptotic MLH1 cleavage product was similar to the larger of the two products generated by caspase-3 *in vitro*. Furthermore, MLH1 proteolysis occurred at a similar time after exposure to apoptotic stimuli as caspase-3 activation (seen as a reduction in procaspase-3 levels due to proteolytic processing). Taken together, these findings suggest that MLH1 might be cleaved by caspase-3 in apoptotic cells. Consistent with this notion, the broad spectrum caspase inhibitor zVAD-fmk potently suppressed MLH1 cleavage in PC-3 cells treated with TRAIL (Fig. 3B, left panel) or TSU-Pr1 cells treated with etoposide (right panel). To specifically evaluate the role of caspase-3 in the apoptotic proteolysis of MLH1, we treated caspase-3 deficient MCF-7 breast carcinoma cells (55) with 10 ng/ml TNF-α and 1 μg/ml cycloheximide for 0-12 h. As shown in Fig. 3C, MLH1 was not cleaved in caspase-3 deficient MCF-7 cells treated with TNF-α, while RAD21, a known substrate of multiple caspases (25), was proteolyzed in these cells. These results indicate that MLH1 is a specific proteolytic target of caspase-3 that is cleaved in cancer cells in response to diverse apoptotic stimuli.

Caspase proteolysis of MLH1 triggers its partial relocalization from the nucleus to the cytoplasm but is not sufficient to induce apoptosis. To begin to assess the functional consequences of MLH1 proteolysis by caspase-3, we transiently transfected PC-3 prostate carcinoma cells with GFP-tagged constructs encoding WT MLH1, the amino-terminal (amino acids 1-418, N-MLH1) or carboxyl-terminal (amino acids 419-756, C-MLH1) caspase cleavage products. As shown in Fig. 4 (upper panels), WT MLH1 and C-MLH1 were expressed in the nuclei of transfected cells, while N-MLH1 was found in both the nucleus and cytoplasm. In all

cases, the nuclei of transfected cells (lower panels) were intact (i.e., non-apoptotic). Indeed, WT MLH1 and each of the caspase cleavage products were unable to induce apoptosis in PC-3 cells in transient transfection experiments (Fig. 5). However, these cells were sensitive to apoptosis induction by the carboxyl-terminal caspase cleavage product of RAD21 (C-RAD21), a proteolytic product we have previously shown to be sufficient to trigger apoptotic cell death (25). The latter findings indicate that the apoptotic cell death machinery is intact in PC-3 cells. Overall, these results indicate that caspase cleavage of MLH1 alters its subcellular localization, triggering a partial redistribution of N-MLH1 from the nucleus to the cytoplasm, but is not sufficient to induce apoptosis.

A caspase cleavage-resistant MLH1 mutant protects against apoptosis induced by DNA DSBs. To examine whether the proteolytic cleavage of MLH1 by caspase-3 is necessary for the execution of apoptosis, we transiently transfected PC-3 cells with GFP-vector or cDNAs encoding GFP-tagged WT or D418E mutant MLH1. After 24 h, transfected PC-3 cells were treated with 2 μg/ml TRAIL for 1 h or 50 μM etoposide for 6 h, and GFP-positive cells were scored for apoptotic nuclei. As shown in Fig. 6, vector- and WT MLH1-transfected cells were sensitive to apoptosis induction by TRAIL or etoposide. In contrast, mutant D418E MLH1-expressing cells were protected against etoposide-induced apoptosis, while their apoptotic response to TRAIL was largely unaffected. These results suggest that MLH1 proteolysis is a functionally important event in the execution of apoptosis by DNA DSBs.

Discussion

We have identified the mismatch repair protein MLH1 as a novel, functionally relevant substrate of caspase-3 that is rapidly proteolyzed in multiple cell types induced to undergo apoptosis by stimuli which engage the extrinsic (TRAIL) or the intrinsic apoptotic pathways (etoposide). MLH1 is selectively cleaved by caspase-3 (but not by other caspases tested) *in vitro*, and is not cleaved in apoptotic caspase-3-deficient MCF-7 cells. These results indicate that MLH1 is a specific substrate of caspase-3, one of the major downstream executioner caspases (1, 2). Intriguingly, experiments performed with cells derived from caspase-3 knockout mice or with caspase-3-deficient MCF-7 cells have revealed that caspase-3 is required for apoptotic chromatin condensation and DNA fragmentation, perhaps because ICAD proteolysis, and therefore CAD activation, is impaired in the absence of caspase-3 (16, 55, 56). MLH1, then, can be added to a short list of caspase-3-specific substrates, which also includes other proteins involved in DNA repair such as RAD51, BLM, and topoisomerase I (27, 30, 57). Human MLH1 is cleaved at a DXXD consensus caspase-3 cleavage motif (58, 59) ($DKTD^{418}\downarrow I^{419}$) near the mid region of the protein. To our surprise, the caspase-3 cleavage site (Asp^{418}) in human MLH1 is not conserved in non-human species; the corresponding residue in rodents is Glu. Hence, the murine and rat MLH1 proteins are similar to the human D418E mutant that we have demonstrated to be resistant to caspase-3 cleavage. Although we have not excluded the possibility that non-human MLH1 proteins may be cleaved at another site(s), these findings suggest that Asp^{418} may have evolved later in evolution, thereby providing humans with a novel mechanism for modifying MLH1 function during apoptosis.

Furthermore, our observation that the caspase cleavage-resistant D418E MLH1 mutant inhibited apoptosis induced by etoposide, which selectively induces DNA DSBs (47), suggests that MLH1 proteolysis is a functionally important event in the apoptotic response to DSBs. Although MLH1 is cleaved in response to diverse apoptotic stimuli, the cleavage-resistant MLH1 mutant had little effect on TRAIL-induced apoptosis, thereby underscoring the specificity

of our observations. How, then, might MLH1 proteolysis promote apoptosis initiated by DSBs? In general, caspase cleavage of a protein can promote apoptosis by activating a latent pro-apoptotic function or by disrupting an anti-apoptotic or pro-survival function (1, 2). In the case of MLH1, neither full-length MLH1 nor its caspase cleavage products was sufficient to induce apoptosis in transiently transfected PC-3 cells. In contrast, the carboxyl-terminal caspase cleavage product of RAD21 (C-RAD21) induced apoptosis in these cells, consistent with our previous work indicating that caspase cleavage of RAD21 unmasks its pro-apoptotic function (25). Unlike RAD21, MLH1 proteolysis does not generate a pro-apoptotic cleavage product that is sufficient to induce apoptosis.

Instead, our results suggest that MLH1 may negatively regulate the apoptotic response to DNA DSBs. Consistent with this notion, cells lacking MLH1 or MSH2 have been shown to be hypersensitive to etoposide or camptothecin (60, 61); the latter drug is a topoisomerase I inhibitor that initiates DNA single-strand breaks, which are subsequently converted to DSBs at stalled replication forks arrested by drug-stabilized topoisomerase I-DNA cleavage complexes (62). Indeed, components of the MMR complex, particularly MSH2, play an active role in homologous recombination repair of DSBs (39, 40, 61), a highly accurate, homology-dependent repair mechanism that utilizes the intact sister chromatid as a template (63). Moreover, MLH1 is a component of the BRCA1-associaated genome surveillance complex (which also includes MSH2, MSH6, ATM, BLM, RAD50 and other components) that has also been implicated in the repair of DSBs by homologous recombination (64, 65). Interestingly, several of the components of this complex (BRCA1, BLM, ATM and MLH1) are cleaved by caspases (28, 30, 31), suggesting that the BRCA1 complex has been systematically targeted for destruction during apoptosis. Given the role of MMR proteins in homologous recombination repair of DSBs, proteolysis of MLH1 may sensitize cells to DSB-induced apoptosis by disrupting its interaction with other MMR proteins or components of the BRCA1 complex, thereby deregulating homologous recombination. Moreover, the relocalization of MLH1 induced by caspase-3 proteolysis partly removes the amino-terminal (N-MLH1) portion of MLH1, along with any

proteins bound to this domain, from the sites of DNA damage. Alternatively, because MLH1 is required for DNA damage-induced S-phase checkpoint activation via its interaction with ATM (42), proteolysis of MLH1 might inactivate its checkpoint function and promote genome instability, ultimately culminating in apoptosis. Regardless of the mechanism(s), the observation that the caspase cleavage-resistant MLH1 anatagonizes DSB-induced apoptosis provides strong support for the notion that proteolysis of MLH1 actively participates in the cytotoxic response to DSBs.

Although our results suggest an anti-apoptotic function for MLH1 in the response to DNA DSBs that is inactivated by proteolysis, MLH1 has been previously demonstrated to mediate the apoptotic response to other types of DNA damage, particularly damage induced by alkylating agents, base analogues and adduct-forming drugs such as cisplatin (each of which generate modified base pairs) (44, 46, 66). Indeed, cells deficient in MLH1 or its interacting protein PMS2 are resistant to apoptosis induced by cisplatin and have a defective p73 response to this drug (46, 67). The tolerance of MMR-deficient cells to these DNA damaging agents, which introduce modified, irreparable base pairs in the template DNA strand, has been attributed to futile attempts of the MMR system acting on the newly synthesized strand to correct these defects (43, 44). These futile cycles of MMR-mediated excision and DNA re-synthesis ultimately trigger apoptosis, at least in part, by activating pro-apoptotic signals such as p73 and/or p53 (41, 46, 67, 68). The results reported here suggest an additional layer of complexity whereby MLH1 may play distinct roles in the apoptotic response to different types of DNA damage, *viz.*, a pro-apoptotic function in the response to alkylating agents and an anti-apoptotic function in the response to DSBs that is disabled by caspase-3. Given the emerging evidence that MMR proteins participate in a growing number of processes (*e.g.,* homologous recombination, nucleotide excision repair, checkpoint activation) (34), such complexity is perhaps not unexpected and suggests that MLH1 can function as either an executioner or inhibitor of the apoptotic response to distinct DNA lesions.

Acknowledgements

We are indebted to Dr. R. Talanian for providing recombinant caspases. This work was supported in part by grant DAMD 17-00-1-0096 from the Department of Defense Prostate Cancer Research Program (to VLC) and by the Elizabeth Boughton Trust (to VLC).

References

1. Cryns, V. L. & Yuan, J. (1998) *Genes & Dev* **12,** 1551-1570.
2. Thornberry, N. A. & Lazebnik, Y. (1998) *Science* **281,** 1312-1316.
3. Muzio, M., Chinnaiyan, A. M., Kischkel, F. C., O'Rourke, K., Shevchenko, A., Ni, J., Scaffidi, C., Bretz, J. D., Zhang, M., Gentz, R., Mann, M., Kreammer, P. H., Peter, M. E. & Dixit, V. M. (1996) *Cell* **85,** 817-827.
4. Boldin, M. P., Goncharov, T. M., Goltsev, Y. V. & Wallach, D. (1996) *Cell* **85,** 803-815.
5. Wang, J., Chun, H. J., Wong, W., Spencer, D. M. & Lenardo, M. J. (2001) *Proc Natl Acad Sci U S A* **98,** 13884-8.
6. Lassus, P., Opitz-Araya, X. & Lazebnik, Y. (2002) *Science* **297,** 1352-4.
7. Guo, Y., Srinivasula, S. M., Druilhe, A., Fernandes-Alnemri, T. & Alnemri, E. S. (2002) *J Biol Chem* **277,** 13430-7.
8. Read, S. H., Baliga, B. C., Ekert, P. G., Vaux, D. L. & Kumar, S. (2002) *J Cell Biol* **159,** 739-45.
9. Li, H., Zhu, H., Xu, C. J. & Yuan, J. (1998) *Cell* **94,** 491-501.
10. Luo, X., Budihardjo, I., Zou, H., Slaughter, C. & Wang, X. (1998) *Cell* **94,** 481-90.
11. Du, C., Fang, M., Li, Y., Li, L. & Wang, X. (2000) *Cell* **102,** 33-42.
12. Verhagen, A. M., Ekert, P. G., Pakusch, M., Silke, J., Connolly, L. M., Reid, G. E., Moritz, R. L., Simpson, R. J. & Vaux, D. L. (2000) *Cell* **102,** 43-53.
13. Zou, H., Henzel, W., Liu, X., Lutschg, A. & Wang, X. (1997) *Cell* **90,** 405-413.
14. Srinivasula, S. M., Ahmad, M., Fernandes-Alnemri, T. & Alnemri, E. S. (1998) *Mol Cell* **1,** 949-57.
15. Muzio, M., Salvesen, G. S. & Dixit, V. M. (1997) *J Biol Chem* **272,** 2952-2956.
16. Slee, E. A., Harte, M. T., Kluck, R. M., Wolf, B. B., Casiano, C. A., Newmeyer, D. D., Wang, H. G., Reed, J. C., Nicholson, D. W., Alnemri, E. S., Green, D. R. & Martin, S. J. (1999) *J Cell Biol* **144,** 281-92.
17. Steller, H. (1995) *Science* **267,** 1445-1449.
18. Li, L. Y., Luo, X. & Wang, X. (2001) *Nature* **412,** 95-9.

19. Arnoult, D., Parone, P., Martinou, J. C., Antonsson, B., Estaquier, J. & Ameisen, J. C. (2002) *J Cell Biol* **159,** 923-9.

20. Wang, X., Yang, C., Chai, J., Shi, Y. & Xue, D. (2002) *Science* **298,** 1587-92.

21. Sakahira, H., Enari, M. & Nagata, S. (1998) *Nature* **391,** 96-99.

22. Liu, X., Zou, H., Slaughter, C. & Wang, X. (1997) *Cell* **89,** 175-184.

23. Enari, M., Sakahira, H., Yokoyama, H., okawa, K., Iwamatsu, A. & Nagata, S. (1998) *Nature* **391,** 43-50.

24. Lazebnik, Y. A., Kaufmann, S. H., Desnoyers, S., Poirier, G. G. & Earnshaw, W. C. (1994) *Nature* **371,** 346-347.

25. Chen, F., Kamradt, M., Mulcahy, M., Byun, Y., Xu, H., McKay, M. J. & Cryns, V. L. (2002) *J Biol Chem* **277,** 16775-81.

26. Pati, D., Zhang, N. & Plon, S. E. (2002) *Mol Cell Biol* **22,** 8267-77.

27. Huang, Y., Nakada, S., Ishiko, T., Utsugisawa, T., Datta, R., Kharbanda, S., Yoshida, K., Talanian, R., Weichselbaum, R., Kuffe, D. & Yuan, Z.-M. (1999) *Mol Cell Biol* **19,** 2986-2997.

28. Smith, G., di Fagagna, F., Lakin, N. & Jackson, S. (1999) *Mol Cell Biol* **19,** 6076-6084.

29. Casciola-Rosen, L., Nicholson, D. W., Chong, T., Rowan, K. R., Thornberry, N. A., Miller, D. K. & Rosen, A. (1996) *J Exp Med* **183,** 1957-1964.

30. Bischof, O., Galande, S., Farzaneh, F., Kohwi-Shigematsu, T. & Campisi, J. (2001) *J Biol Chem* **276,** 12068-75.

31. Zhan, Q., Jin, S., Ng, B., Plisket, J., Shangary, S., Rathi, A., Brown, K. D. & Baskaran, R. (2002) *Oncogene* **21,** 5335-45.

32. Kolodner, R. D. (2000) *Nature* **407,** 687, 689.

33. Heinen, C. D., Schmutte, C. & Fishel, R. (2002) *Cancer Biol Ther* **1,** 477-85.

34. Bellacosa, A. (2001) *Cell Death Differ* **8,** 1076-92.

35. Fishel, R., Lescoe, M. K., Rao, M. R., Copeland, N. G., Jenkins, N. A., Garber, J., Kane, M. & Kolodner, R. (1993) *Cell* **75,** 1027-38.

36. Bronner, C. E., Baker, S. M., Morrison, P. T., Warren, G., Smith, L. G., Lescoe, M. K., Kane, M., Earabino, C., Lipford, J., Lindblom, A. & et al. (1994) *Nature* **368,** 258-61.

37. Papadopoulos, N., Nicolaides, N. C., Wei, Y. F., Ruben, S. M., Carter, K. C., Rosen, C. A., Haseltine, W. A., Fleischmann, R. D., Fraser, C. M., Adams, M. D. & et al. (1994) *Science* **263,** 1625-9.

38. Peltomaki, P. (2003) *J Clin Oncol* **21,** 1174-9.

39. de Wind, N., Dekker, M., Berns, A., Radman, M. & te Riele, H. (1995) *Cell* **82,** 321-30.

40. Elliott, B. & Jasin, M. (2001) *Mol Cell Biol* **21,** 2671-82.

41. Davis, T. W., Wilson-Van Patten, C., Meyers, M., Kunugi, K. A., Cuthill, S., Reznikoff, C., Garces, C., Boland, C. R., Kinsella, T. J., Fishel, R. & Boothman, D. A. (1998) *Cancer Res* **58,** 767-78.

42. Brown, K. D., Rathi, A., Kamath, R., Beardsley, D. I., Zhan, Q., Mannino, J. L. & Baskaran, R. (2003) *Nat Genet* **33,** 80-4.

43. Kat, A., Thilly, W. G., Fang, W. H., Longley, M. J., Li, G. M. & Modrich, P. (1993) *Proc Natl Acad Sci U S A* **90,** 6424-8.

44. Koi, M., Umar, A., Chauhan, D. P., Cherian, S. P., Carethers, J. M., Kunkel, T. A. & Boland, C. R. (1994) *Cancer Res* **54,** 4308-12.

45. Hickman, M. J. & Samson, L. D. (1999) *Proc Natl Acad Sci U S A* **96,** 10764-9.

46. Gong, J. G., Costanzo, A., Yang, H. Q., Melino, G., Kaelin, W. G., Jr., Levrero, M. & Wang, J. Y. (1999) *Nature* **399,** 806-9.

47. Froelich-Ammon, S. & Osheroff, N. (1995) *J Biol Chem* **270,** 21429-21432.

48. Lustig, K. D., Stukenberg, T., McGarry, T., King, R. W., Cryns, V. L., Mead, P., Zon, L., Yuan, J. & Kirschner, M. W. (1997) *Methods Enzymol* **283,** 83-99.

49. Cryns, V., Byun, Y., Rana, A., Mellor, H., Lustig, K., Ghanem, L., Parker, P., Kirschner, M. & Yuan, J. (1997) *J Biol Chem* **272,** 29449-29453.

50. Byun, Y., Chen, F., Chang, R., Trivedi, M., Green, K. & Cryns, V. (2001) *Cell Death Differ* **8,** 443-450.

51. Cryns, V. L., Bergeron, L., Zhu, H., Li, H. & Yuan, J. (1996) *J Biol Chem* **271,** 31277-31282.

52. Pan, G., O'Rourke, K., Chinnaiyan, A. M., Gentz, R., Ebner, R., Ni, J. & Dixit, V. M. (1997) *Science* **276,** 111-113.

53. Kamradt, M., Chen, F. & Cryns, V. (2001) *J Biol Chem* **276,** 16059-16063.

54. Emoto, Y., Manome, Y., Meinhardt, G., Kisaki, H., Kharbanda, S., Robertson, M., Ghayur, T., Wong, W. W., Kamen, R., Weichselbaum, R. & Kufe, D. (1995) *EMBO J* **14,** 6148-6156.

55. Janicke, R. U., Sprengart, M. L., Wati, M. R. & Porter, A. G. (1998) *J Biol Chem* **273,** 9357-60.

56. Zheng, T. S., Schlosser, S. F., Dao, T., Hingorani, R., Crispe, I. N., Boyer, J. L. & Flavell, R. A. (1998) *Proc Natl Acad Sci U S A* **95,** 13618-23.

57. Samejima, K., Svingen, P. A., Basi, G. S., Kottke, T., Mesner, P. W., Jr., Stewart, L., Durrieu, F., Poirier, G. G., Alnemri, E. S., Champoux, J. J., Kaufmann, S. H. & Earnshaw, W. C. (1999) *J Biol Chem* **274,** 4335-40.

58. Thornberry, N., Rano, T., Peterson, E., Rasper, D., Timkey, T., Garcia-Calvo, M., Houtzager, V., Nordstrom, P., Roy, S., Vaillancourt, J., Chapman, K. & Nicholson, D. (1997) *J Biol Chem* **272,** 17907-17911.

59. Talanian, R. V., Quinlan, C., Trautz, S., Hackett, M. C., Mankovich, J. A., Banach, D., Ghayur, T., Brady, K. D. & Wong, W. W. (1997) *J Biol Chem* **272,** 9677-9682.

60. Jacob, S., Aguado, M., Fallik, D. & Praz, F. (2001) *Cancer Res* **61,** 6555-62.

61. Pichierri, P., Franchitto, A., Piergentili, R., Colussi, C. & Palitti, F. (2001) *Carcinogenesis* **22,** 1781-7.

62. Hsiang, Y. H., Liu, L. F., Wall, M. E., Wani, M. C., Nicholas, A. W., Manikumar, G., Kirschenbaum, S., Silber, R. & Potmesil, M. (1989) *Cancer Res* **49,** 4385-9.

63. van Gent, D. C., Hoeijmakers, J. H. & Kanaar, R. (2001) *Nat Rev Genet* **2,** 196-206.

64. Wang, Y., Cortez, D., Yazdi, P., Neff, N., Elledge, S. J. & Qin, J. (2000) *Genes Dev* **14,** 927-39.

65. Jasin, M. (2002) *Oncogene* **21,** 8981-8993.

66. Buermeyer, A. B., Wilson-Van Patten, C., Baker, S. M. & Liskay, R. M. (1999) *Cancer Res* **59,** 538-41.

67. Shimodaira, H., Yoshioka-Yamashita, A., Kolodner, R. D. & Wang, J. Y. (2003) *Proc Natl Acad Sci U S A* **100,** 2420-5.

68. Lin, X., Ramamurthi, K., Mishima, M., Kondo, A., Christen, R. D. & Howell, S. B. (2001) *Cancer Res* **61,** 1508-16.

Footnotes

[1]The abbreviations used are: CAD, caspase-activated DNase; MMR, mismatch repair; TNF, tumor necrosis factor; TRAIL, TNF-related apoptosis-inducing ligand; DSBs, double-strand breaks.

Figure Legends

Fig. 1: Identification of MLH1 as a putative caspase-3 substrate by small pool expression cloning. (A) Presence of 64 kDa protein (indicated by asterisk) in ^{35}S-labeled protein pool 10 that is selectively cleaved by caspase-3 (C3), but not by buffer control (C) or caspases-1, -2, or -8 (C1, C2, or C8), into 2 proteolytic fragments ~ 40 and 24 kDa in size (indicated by arrows). ^{35}S-labeled protein pools were made from small pools of a human prostate adenocarcinoma cDNA library by coupled transcription/translation *in vitro*, and these ^{35}S-labeled protein pools were screened for caspase substrates as described in *Materials and Methods*. **(B)** A single cDNA encoding the putative caspase-3 substrate was isolated from cDNA pool 10 by subdividing the pool and incubating the corresponding ^{35}S-labeled protein pools with caspase-3. Clone 10 4G encodes a 64 kDa protein that is proteolyzed by caspase-3 into cleavage products (indicated by arrows) of similar size to those observed in **(A).** Sequence analysis indicated that this clone is a partial MLH1 cDNA.

Fig. 2: Human MLH1 is selectively proteolyzed by caspase-3 at Asp^{418} *in vitro*. (A) ^{35}S-labeled full-length human MLH1 is specifically cleaved into two products of ~ 48 and 40 kDa (indicated by arrows) by caspase-3 *in vitro*. ^{35}S-labeled MLH1 was incubated with buffer control (C), 2.5 or 25 ng of caspase-1, -2, -3, -6, -7, or -8 (C1-C8) for 1 h at 37°C. **(B)** Substitution of Asp^{418} in MLH1 with a Glu residue produces a mutant MLH1 protein (D418E) which is resistant to cleavage by caspase-3 *in vitro*. ^{35}S-labeled wild-type (WT) or mutant D418E MLH1 were incubated with buffer control (C) or caspase-3 (2.5 or 25 ng) for 1 h at 37°C.

Fig. 3: MLH1 is specifically cleaved by caspase-3 in cancer cells treated with TRAIL or etoposide. (A) MLH1 is rapidly cleaved into a 48 kDa product in PC-3 cells treated with TRAIL (left panel) or in TSU-Pr1 cells treated with 50 μM etoposide (right panel). PC-3 cells were treated with 2 μg/ml TRAIL and TSU-Pr1 cells were treated with 50 μM etoposide for the indicated number of hours. Whole cell lysates were analyzed by immunoblotting with antibodies

recognizing MLH1, PKCδ, procaspase-3 or tubulin; the cleavage products are indicated by arrows. **(B)** The apoptotic proteolysis of MLH1 is antagonized by zVAD-fmk, a broad spectrum caspase inhibitor. PC-3 or TSU-Pr1 cells were untreated or pre-incubated with vehicle or 50 μM zVAD-fmk for 1 h, and then treated with 2 μg/ml TRAIL (PC-3 cells, left panel) for 8 h or 50 μM etoposide (TSU-Pr1 cells, right panel) for 24 h. **(C)** Caspase-3 is required for the apoptotic proteolysis of MLH1. Caspase-3-deficient MCF-7 cells were treated with 10 ng/ml TNF-α and 1 μg/ml cycloheximide for 0-12 h, and the lysates were then examined by immunoblotting with an MLH1 mAb (upper panel) or a RAD21 polyclonal Ab (lower panel).

Fig. 4: Caspase cleavage of MLH1 leads to its partial redistribution from the nucleus to the cytoplasm. PC-3 cells were transiently transfected with pEGFPN1 plasmids encoding full-length WT MLH1, the amino-terminal (N-MLH1) or carboxyl-terminal (C-MLH1) caspase cleavage products. GFP-fluorescence (upper panels) and nuclei (lower panels) were visualized as described in *Materials and Methods*.

Fig. 5: Caspase proteolysis of MLH1 is not sufficient to induce apoptosis. PC-3 cells were transiently transfected with GFP vector or GFP-tagged cDNAs encoding WT MLH1, the amino-terminal (N-MLH1) or carboxyl-terminal (C-MLH1) MLH1 caspase cleavage products, or the pro-apoptotic carboxyl-terminal RAD21 (C-RAD21) caspase cleavage product. GFP-positive cells were scored for apoptotic nuclei as detailed in Materials and Methods. The data are presented as the mean ± S.D. of at least three independent experiments.

Fig. 6: A caspase cleavage-resistant MLH1 confers protection against etoposide-induced apoptosis. PC-3 prostate carcinoma cells were transiently transfected with GFP vector, or GFP-tagged cDNAs encoding WT MLH1 or the caspase cleavage-resistant mutant D418E MLH1. 24 h later, cells were treated with vehicle control (C), 2 μg/ml TRAIL for 1 h or 50 μM etoposide for 6 h, and GFP-positive cells were scored for apoptotic nuclei. The data are presented as the mean ± S.D. of at least three independent experiments.

This page contains unpublished data; do not releases.

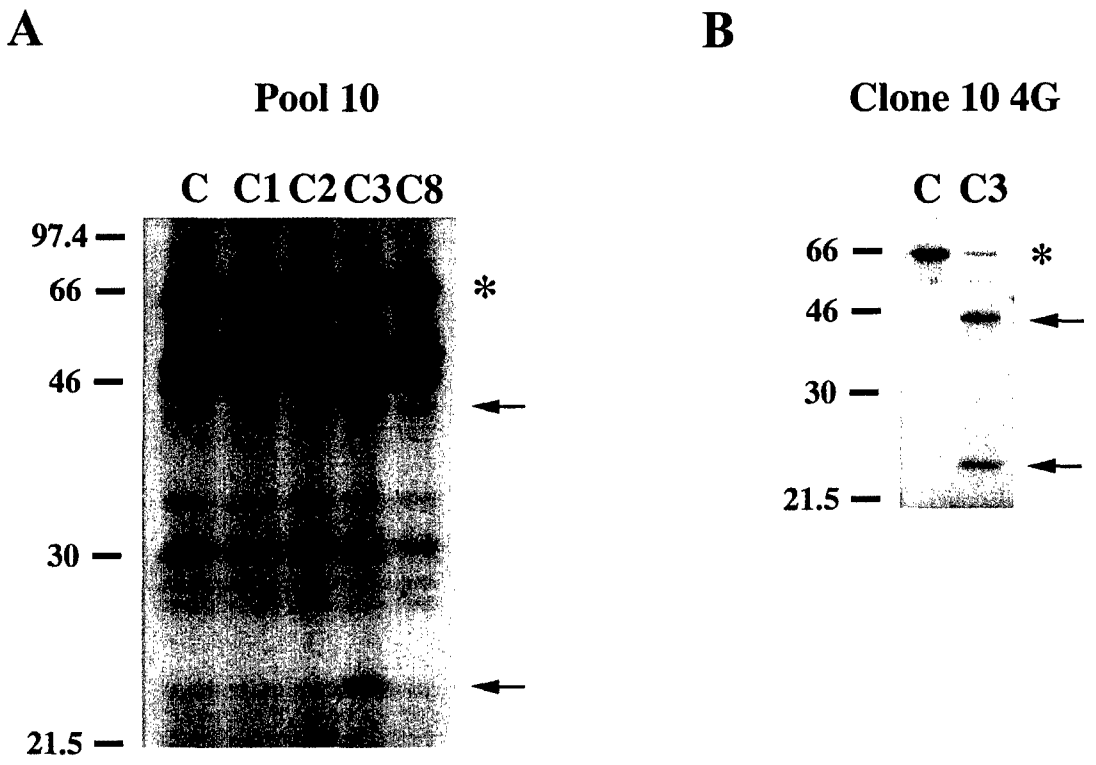

Fig. 1A & 1B

A

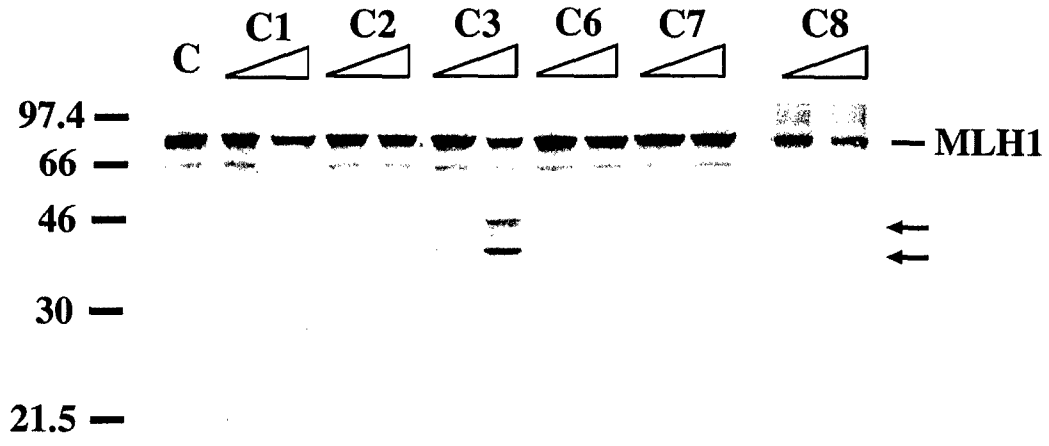

B

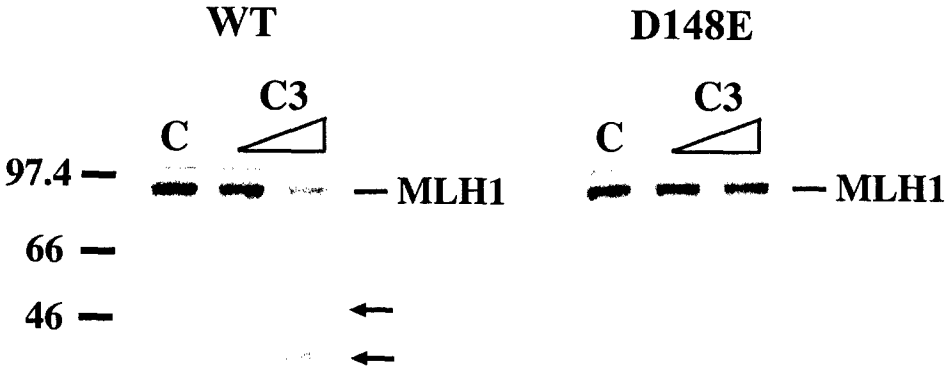

Fig. 2A & 2B

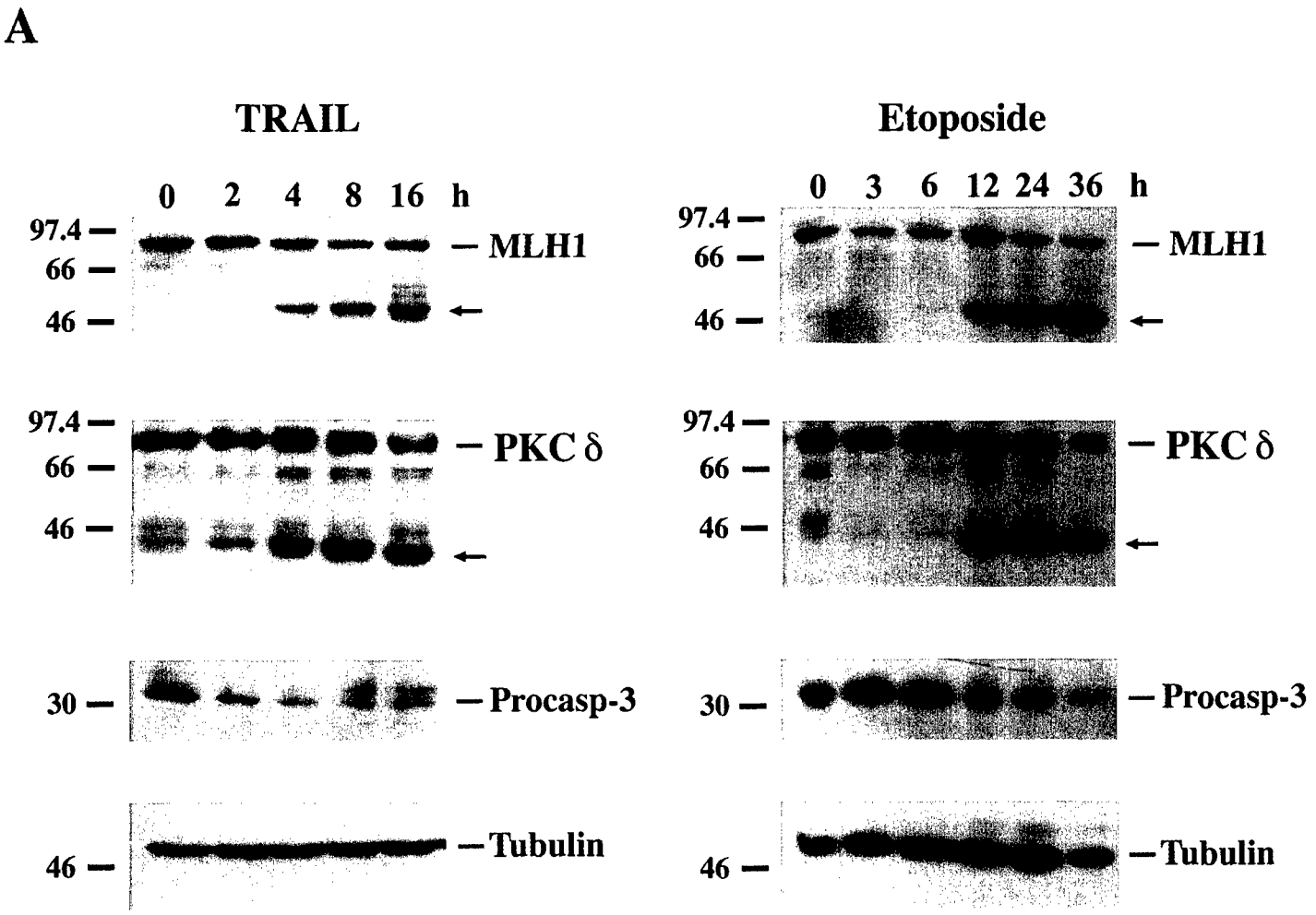

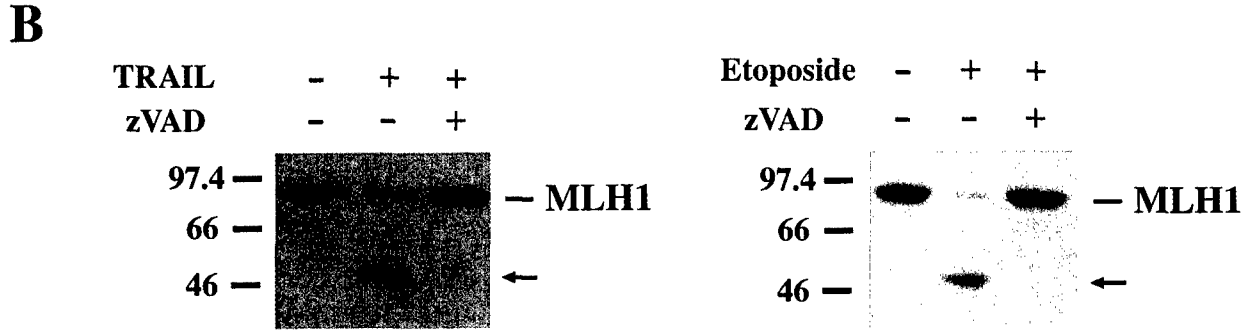

Fig. 3A & 3B

This page contains unpublished data; do not release.

C

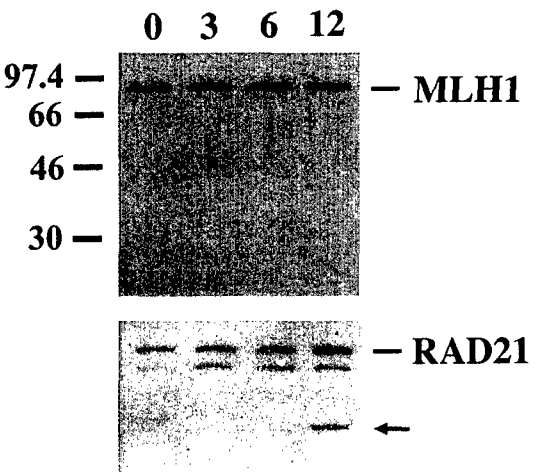

Fig. 3C

This page contains unpublished data; do not release.

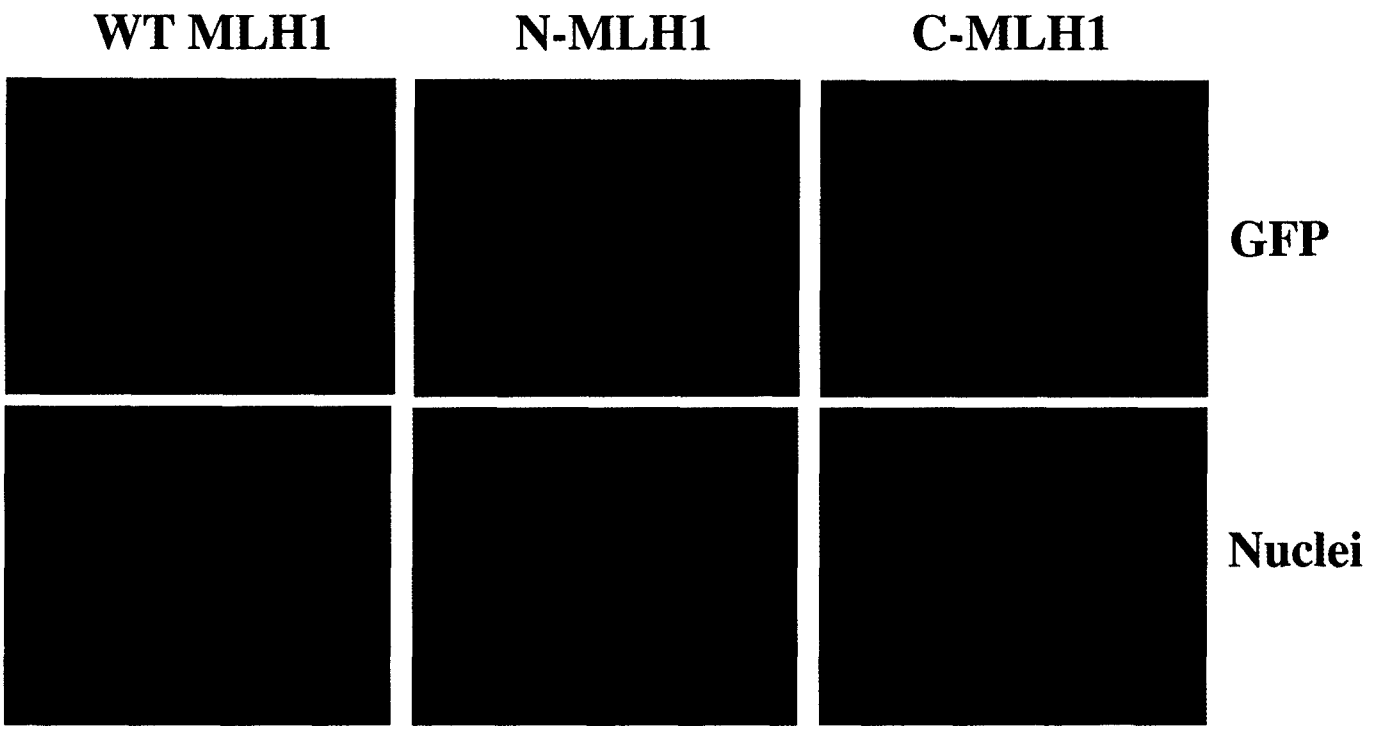

Fig. 4

This page contains unpublished data; do not release.

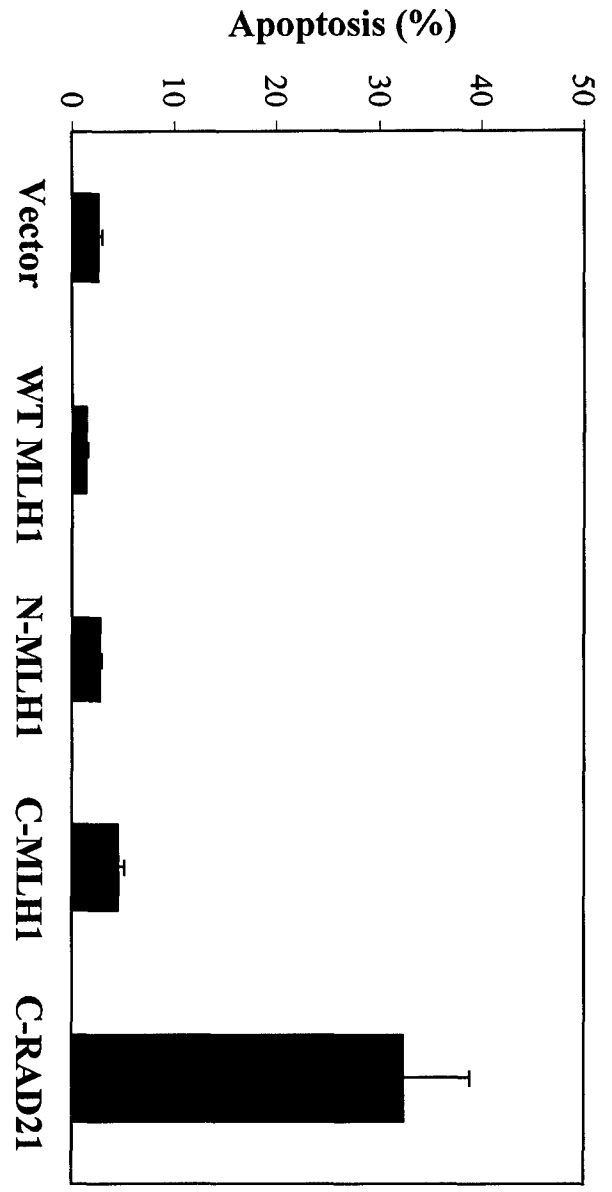

Fig. 5, F. Chen et al.

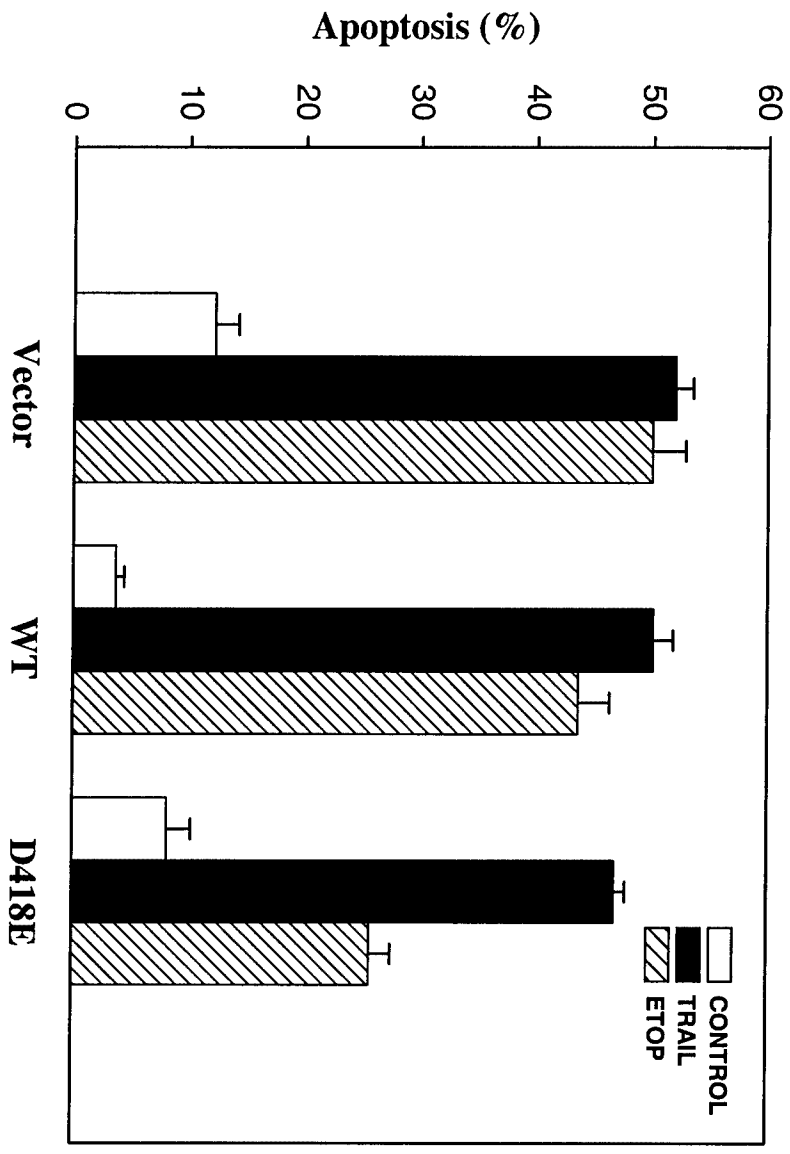

Fig. 6, F. Chen et al.

THE JOURNAL OF BIOLOGICAL CHEMISTRY
Vol. 277, No. 19, Issue of May 10, pp. 16775–16781, 2002
Printed in U.S.A.

Caspase Proteolysis of the Cohesin Component RAD21 Promotes Apoptosis*

Received for publication, February 2, 2002, and in revised form, February 28, 2002
Published, JBC Papers in Press, March 1, 2002, 2002, DOI 10.1074/jbc.M201322200

Feng Chen‡, Merideth Kamradt‡, Mary Mulcahy‡, Young Byun‡, Huiling Xu§, Michael J. McKay§, and Vincent L. Cryns‡¶

From the ‡Robert H. Lurie Comprehensive Cancer Center and the Department of Medicine, Northwestern University Medical School, Chicago, IL 60611 and the §Peter MacCallum Cancer Institute, Melbourne 8006, Australia

Caspases are a conserved family of proteases that play a critical role in the execution of apoptosis by cleaving key cellular proteins at Asp residues and modifying their function. Using an expression cloning strategy we recently developed, we isolated human RAD21/SCC1/MCD1 as a novel caspase substrate. RAD21 is a component of the cohesin complex that holds sister chromatids together during mitosis and repairs double-strand DNA breaks. Interestingly, RAD21 is cleaved by a caspase-like Esp1/separase at the onset of anaphase to trigger sister chromatid separation. Here, we demonstrate that human RAD21 is preferentially cleaved at Asp^{279} by caspases-3 and -7 *in vitro* to generate two major proteolytic products of ~65 and 48 kDa. Moreover, we show that RAD21 is specifically proteolyzed by caspases into a similarly sized 65-kDa carboxyl-terminal product in cells undergoing apoptosis in response to diverse stimuli. We also demonstrate that caspase proteolysis of RAD21 precedes apoptotic chromatin condensation and has important functional consequences, *viz.* the partial removal of RAD21 from chromatin and the production of a proapoptotic carboxyl-terminal cleavage product that amplifies the cell death signal. Taken together, these findings point to an entirely novel function of RAD21 in the execution of apoptosis.

During development and in response to homeostatic challenges, cells are selectively eliminated by a genetically regulated suicide mechanism known as apoptosis or programmed cell death. Activation of this intrinsic cell death apparatus leads to a series of dramatic nuclear events, including chromatin condensation, degradation of chromosomal DNA into internucleosomal fragments, and disassembly of the nuclear membrane (1). Caspases are a conserved family of cysteine proteases that play a critical role in the execution of apoptosis by cleaving a subset of cellular proteins at aspartic acid residues and altering their function (2). Indeed, caspases have been directly linked to many of the nuclear (and other) manifestations of apoptosis. For instance, caspase-3 proteolyzes and activates acinus, a nuclear protein whose caspase cleavage product directly induces chromatin condensation (3). Caspases also activate caspase-activated DNase (CAD),[1] an endonuclease normally present in the nucleus as an inactive heterodimer bound to its inhibitor ICAD/DFF-45. Caspase-3 cleaves and displaces ICAD/DFF-45 from CAD, thereby enabling CAD to degrade chromosomal DNA (4–6). In addition, proteolytic cleavage of the nuclear lamins by caspase-6 promotes the dismantling of the nuclear envelope (7–9). Importantly, caspase-9 proteolysis of yet to be identified proteins increases the permeability of nuclear pores, thereby allowing caspases to enter the nucleus and cleave these critical nuclear targets (10). Clearly, the nuclear manifestations of apoptosis reflect the concerted action of caspases on multiple proteolytic targets, only a subset of which have been identified and characterized.

Using an expression cloning strategy we have described recently to systematically identify cDNAs encoding caspase substrates (11–13), we report here the isolation of human RAD21/SCC1/MCD1 (14–16) (hereafter referred to as RAD21) as a novel nuclear caspase target. RAD21 was first identified as a nuclear phosphoprotein that repairs double-strand DNA breaks and is essential for viability in fission yeast (14, 17). More recently, RAD21 has been demonstrated to be a component of the conserved mitotic cohesin complex that holds sister chromatids together and ensures the faithful segregation of duplicated chromosomes to daughter cells; defects in this process lead to aneuploidy (18, 19). During mitosis, the separation of sister chromatids requires the removal of the cohesin "glue," which holds sister chromatids together from S phase until the beginning of anaphase. In yeast, RAD21 is specifically cleaved during the onset of anaphase by Esp1/separase, a cysteine protease distantly related to caspases, thereby allowing sister chromatid separation and the segregation of chromosomes to opposite poles (20–22). Interestingly, separase proteolysis of budding yeast RAD21 generates a short-lived carboxyl-terminal product that is rapidly degraded by the ubiquitin-proteasome pathway; stabilization of this cleavage product by a variety of methods leads to chromosome loss and is lethal (23). In metazoans, cohesin is removed from chromatin by two distinct processes. During prophase, the vast majority of cohesin is removed from chromosome arms by a cleavage-independent mechanism that likely contributes to the condensation of DNA into discrete chromatid arms, leaving only a small amount of cohesin bound to chromatids at the centromere (24–27). At the onset of anaphase, centromeric cohesin is cleaved by separase

* This work was supported in part by Grant DAMD 17-00-1-0096 from the Department of Defense Prostate Cancer Research Program, by National Institutes of Health grants NS31957 (to V. L. C.), T32-CA79447 (to M. M.), and 5T32-CA70085 (to M. K.), by a grant from the National Health and Medical Research Council Australia (to M. J. M.), by institutional research grants to Northwestern University from the Howard Hughes Medical Institute and the American Cancer Society (to V. L. C.), and by the Elizabeth Boughton Trust (to V. L. C.). The costs of publication of this article were defrayed in part by the payment of page charges. This article must therefore be hereby marked "*advertisement*" in accordance with 18 U.S.C. Section 1734 solely to indicate this fact.

¶ To whom correspondence should be addressed: Tarry 15-755, Northwestern University Medical School, 303 E. Chicago Ave., Chicago, IL 60611. Tel.: 312-503-0644; Fax: 312-908-9032; E-mail: v-cryns@northwestern.edu.

[1] The abbreviations used are: CAD, caspase-activated DNase; ICAD, inhibitor of CAD; TNF, tumor necrosis factor; GFP, green fluorescent protein; WT, wild-type; PARP, poly(ADP-ribose) polymerase.

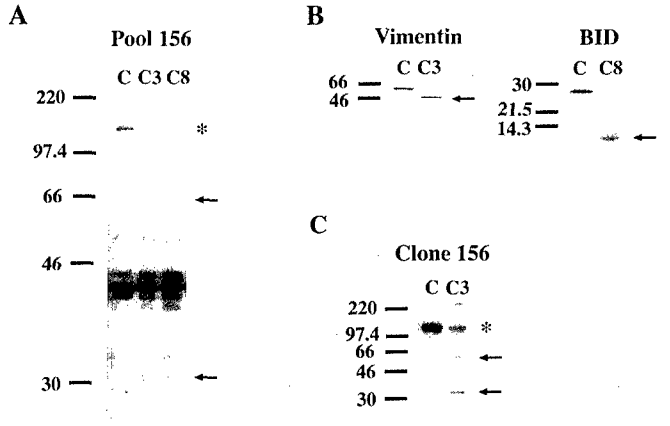

FIG. 1. **Isolation of RAD21 as a caspase-3 substrate *in vitro* by small pool expression cloning.** *A*, ^{35}S-labeled protein pool 156 contains a 125-kDa protein (indicated by the *asterisk*) that is specifically proteolyzed into two products of ~65 and 32 kDa (indicated by *arrows*) by caspase-3 (*C3*) but not by control (*C*) buffer or caspase-8 (*C8*). *B*, selective proteolysis of ^{35}S-labeled vimentin by caspase-3 (*C3*) and ^{35}S-labeled BID by caspase-8 (*C8*) into their signature cleavage fragments (indicated by *arrows*). *C*, identification of a single cDNA from pool 156 that encodes a 125-kDa protein (indicated by the *asterisk*) that is cleaved by caspase-3 (*C3*) into the appropriately sized products (indicated by *arrows*). cDNA pool 156 was subdivided, and the corresponding ^{35}S-labeled protein pools were re-examined as above until a single cDNA encoding the caspase-3 substrate was isolated. Sequencing of this clone revealed that it is a partial human rad21 cDNA. Small pool expression cloning, cleavage reactions, and analysis of proteolytic products were performed as detailed under "Experimental Procedures" and elsewhere (11–13). The molecular mass of markers in kDa is indicated at the *left* of each panel.

to trigger sister chromatid separation (25, 28). In both yeast and metazoans, the introduction of a mutant RAD21 that is resistant to separase cleavage inhibits sister chromatid separation (20, 28). Hence, the mitotic proteolysis of RAD21 by a caspase-like protease is essential for proper chromosome segregation in organisms as diverse as yeast and humans.

In contrast to its critical role in mitosis, RAD21 has not been implicated previously in apoptosis. In the present study, we report that RAD21 is specifically cleaved by caspases at Asp^{279} *in vitro* and in cells undergoing apoptosis in response to diverse stimuli. We also demonstrate that caspase proteolysis of RAD21 precedes apoptotic chromatin condensation and has important functional consequences, *viz.* the partial removal of RAD21 from chromatin and the production of a proapoptotic carboxyl-terminal cleavage product that amplifies the cell death signal. Overall, these findings point to an entirely novel function of RAD21 in the execution of apoptosis.

EXPERIMENTAL PROCEDURES

Cell Culture—HeLa and MCF-7 cells were maintained in DMEM (Mediatech) supplemented with 10% fetal calf serum (Invitrogen).

Small Pool Expression Cloning—^{35}S-labeled protein pools were prepared from small pools (48 cDNAs/pool) of a human heart cDNA library (Invitrogen) using the TNT T7 Quick Coupled Transcription/Translation System (Promega) as described previously (11, 12). These ^{35}S-labeled protein pools were then incubated with control buffer, 25 ng of caspase-3, or 25 ng of caspase-8, and individual cDNAs encoding caspase substrates *in vitro* were isolated as we have detailed elsewhere (11–13).

Proteolytic Cleavage Reactions in Vitro—^{35}S-labeled full-length human RAD21 was prepared using the TNT T7 Quick Coupled Transcription/Translation System (Promega) according to the manufacturer's instructions. ^{35}S-labeled human RAD21 was then incubated with buffer, 2.5 or 25 ng of caspases-1, -2, -3, -6, -7, or -8 for 1 h at 37 °C, and the reaction products were resolved by SDS-PAGE and visualized by autoradiography as described elsewhere (12, 29). To identify the major caspase cleavage site of RAD21 *in vitro*, we selectively altered the Asp residue at a potential cleavage site to a Glu residue (D279E) using the QuikChange site-directed mutagenesis kit (Stratagene) with the following oligonucleotide primers: 5′-GGCCTGATAGTCCTGAGTCAGTGGATCCCGTTG-3′ and 5′-CAACGGGATCCACTGACTCAGGACTATCAGGCC-3′. The resulting RAD21 D279E construct was verified by DNA sequencing. ^{35}S-labeled wild-type and mutant D279E RAD21 were then incubated with buffer or 10 or 25 ng of caspases-3 or -7 as above to determine whether the D279E RAD21 mutant was resistant to caspase proteolysis. In parallel experiments, ^{35}S-labeled human REC8, a meiotic cohesin structurally related to RAD21, was incubated with buffer or 2.5 or 25 ng of caspases-3 or -7, and the reaction products were analyzed as above.

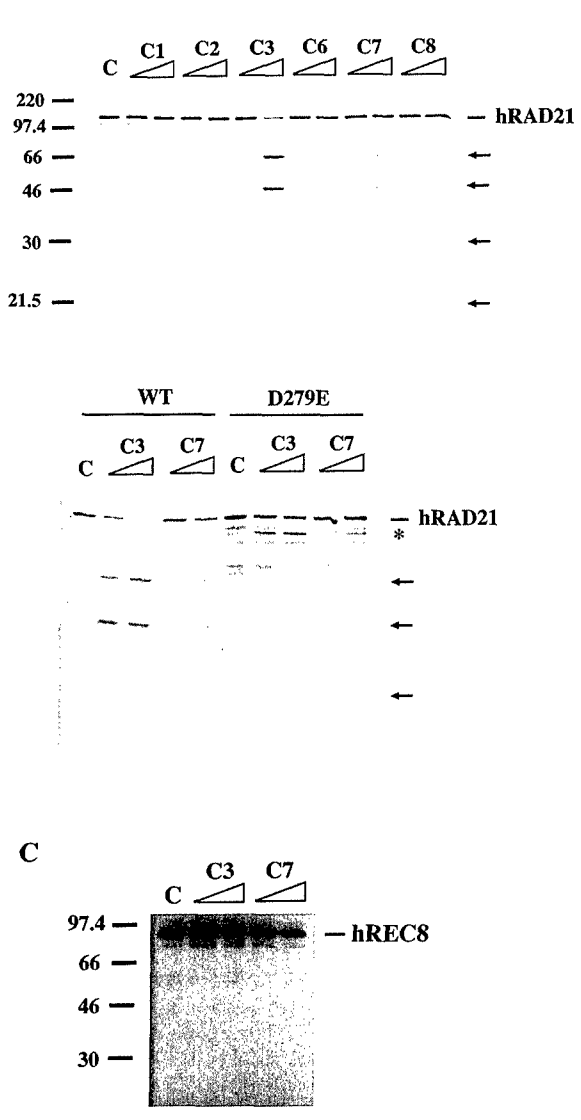

FIG. 2. **Human RAD21 is specifically cleaved by caspases-3 and -7 at multiple sites, including Asp^{279}, to yield several proteolytic products *in vitro*.** *A*, ^{35}S-labeled full-length human RAD21 was incubated with control (*C*) buffer or 2.5 or 25 ng of caspase-1, -2, -3, -6, -7, or -8 (*C1–C8*) for 1 h at 37 °C, and the reaction products were resolved by SDS-PAGE. The cleavage fragments are indicated by *arrows*. *B*, RAD21 mutant D279E is resistant to proteolysis at Asp^{279} by caspases-3 and -7 *in vitro*. ^{35}S-labeled WT or mutant D279E RAD21 were incubated with control (*C*) buffer or 10 or 25 ng of caspases-3 (*C3*) or -7 (*C7*) for 1 h at 37 °C. WT RAD21, but not the D279E mutant, was proteolyzed into major fragments of 65 and 48 kDa (indicated by *arrows*). The D279E mutant was cleaved into a single larger product (indicated by the *asterisk*) that was not observed when WT RAD21 was incubated with caspases-3 or -7 *in vitro*. *C*, Human REC8, a homologue of RAD21, is not cleaved by caspases-3 or -7 *in vitro*. ^{35}S-labeled human REC8 was incubated with control (C) buffer or 2.5 or 25 ng of caspase-3 (*C3*) or caspase-7 (*C7*) for 1 h at 37 °C. The molecular mass of markers in kDa is indicated at the *left* of each panel.

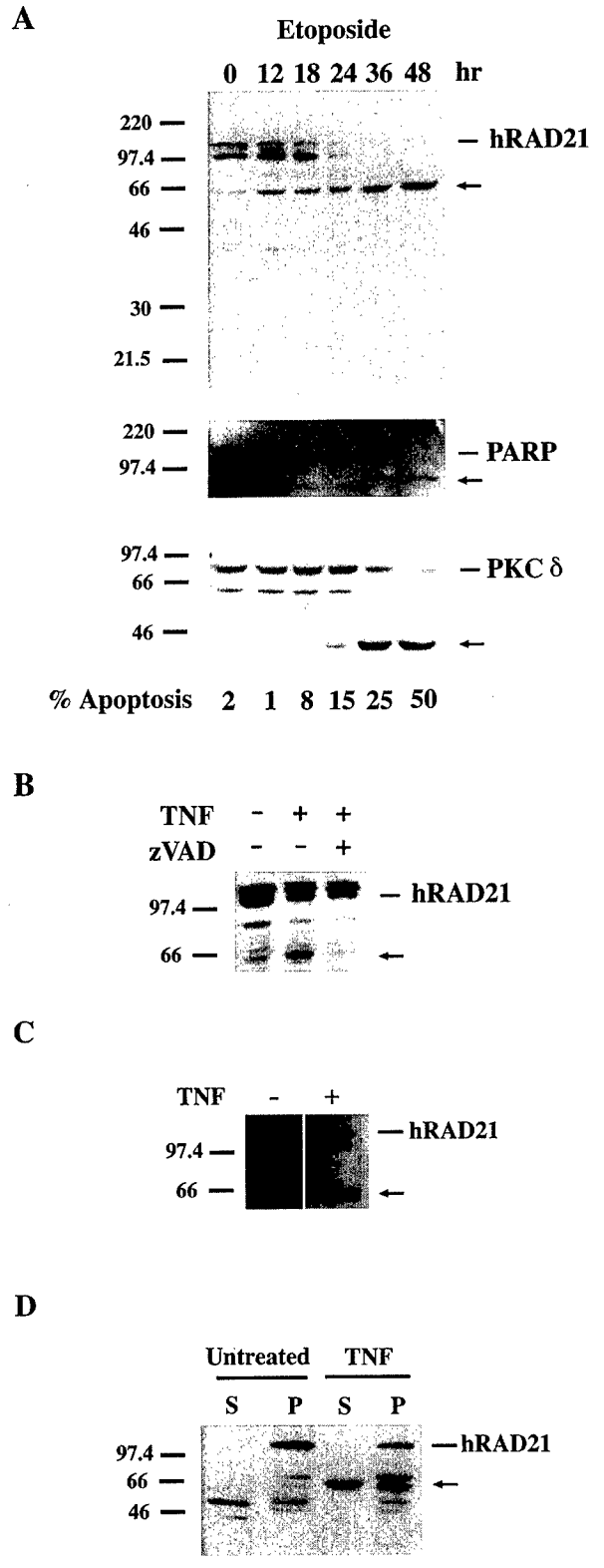

FIG. 3. **Human RAD21 is rapidly proteolyzed by caspases during the induction of apoptosis, leading to its partial dissociation from chromatin.** *A*, time course for proteolysis of RAD21, PARP, and protein kinase Cδ during etoposide-induced apoptosis. HeLa cells were treated with 50 μM etoposide for the indicated amounts of time. The percentage of cells with apoptotic nuclear morphology was determined for each treatment condition in parallel experiments as detailed under "Experimental Procedures" and is indicated at the *bottom*. *B*, the caspase inhibitor zVAD-fmk blocks the apoptotic proteolysis of RAD21. HeLa cells were untreated or preincubated with vehicle or 100 μM zVAD-fmk for 1 h, and then they were treated with 10 ng/ml TNF-α and 1 μg/ml cycloheximide for 18 h. *C*, RAD21 is specifically cleaved in caspase-3-deficient MCF-7 cells undergoing TNF-α-induced apoptosis. MCF-7 breast carcinoma cells were untreated or treated with 10 ng/ml TNF-α and 1 μg/ml cycloheximide for 24 h. *D*, caspase cleavage of RAD21 partially releases it from chromatin into the soluble fraction. Chromatin-enriched pellet (*P*) and supernatant (*S*) fractions were prepared from untreated HeLa cells and HeLa cells incubated with 10 ng/ml TNF-α and 1 μg/ml cycloheximide as described under "Experimental Procedures" and elsewhere (25). In *panels A–D*, immunoblotting was performed as described under "Experimental Procedures." The molecular mass of markers in kDa is indicated at the *left* of each panel.

Induction of Apoptosis and Immunoblotting—HeLa cells were treated with 50 μM etoposide for 0–48 h. Whole cell lysates were then prepared and analyzed by immunoblotting as described previously (29) using a polyclonal antibody that recognizes the carboxyl terminus of human RAD21 (1:400 dilution), PARP monoclonal antibody (BD PharMingen) (1:1000 dilution), or protein kinase Cδ polyclonal antibody (Santa Cruz Biotechnology) (1:1000 dilution). The percentage of cells in each treatment condition that had apoptotic (condensed or fragmented) nuclei was determined in parallel experiments by fixing cells grown on glass coverslips with 100% methanol at −20 °C for 2 min and staining nuclei with 10 μg/ml Hoescht No. 33258 (Sigma) for 30 min. Nuclei were visualized by fluorescence microscopy using a Nikon Eclipse E400 microscope, and the percentage of apoptotic nuclei was determined in three independent experiments (at least 200 nuclei/experiment were scored) as described previously (13, 30). In the caspase inhibitor experiments, HeLa cells were untreated or were preincubated with 100 μM zVAD-fmk (Enzymes Systems Products) for 1 h prior to treatment with 10 ng/ml tumor necrosis factor (TNF)-α and 1 μg/ml cycloheximide for 18 h. RAD21 was then analyzed by immunoblotting as above. Chromatin-enriched pellets and supernatant fractions were obtained by centrifugation of whole cell lysates at 15,000 × *g* as described elsewhere (25).

Construction of GFP-tagged Rad21 cDNAs—GFP-tagged Rad21 cDNAs encoding full-length RAD21, the amino-terminal (N-RAD21), and carboxyl-terminal (C-RAD21) caspase cleavage products were constructed by PCR amplifying human wild-type Rad21 with the following primers: 5′-GGCCCTCGAGCCAGCCAGAACAATGTTC-3′ and 5′-GGCCCCGCGGTATAATATGGAACCTTGG-3′ (full-length Rad21), 5′-GGCCCTCGAGCCAGCCAGAACAATGTTC-3′ and 5′-GGCCCCGCGGTTAATCAGGACTATCAGGCCC-3′ (N-RAD21 encoding amino acids 1–279), 5′-GGCCCTCGAGATGTCAGTGGATCCCGTTGAA-3′ and 5′-GGCCCCGCGGTATAATATGGAACCTTGG-3′ (C-RAD21 encoding amino acids 280–631). The PCR products were then digested with *Xho*I and *Sac*II and cloned into the corresponding sites in pEGFP-N1 (CLONTECH). The sequence of each construct fused at its carboxyl terminus with GFP was confirmed by automated DNA sequencing.

Transient Transfections and Quantitation of Apoptosis—HeLa cells were plated at ~50% confluence on glass coverslips and transiently transfected with 1.2 μg of pEGFP-N1 plasmid containing empty vector, full-length RAD21, the amino-terminal caspase cleavage product (N-RAD21), or the carboxyl-terminal caspase cleavage product (C-RAD21). Transfections were performed using LipofectAMINE reagent (Invitrogen) according to the manufacturer's instructions. Twenty-four h later, cells were fixed in 4% paraformaldehyde for 10 min at room temperature. Nuclei were then stained with 10 μg/ml Hoescht No. 33258 (Sigma) for 30 min. GFP-positive cells were scored for apoptotic (condensed/fragmented) nuclei by fluorescence microscopy as described previously (13). The percentage of GFP-positive cells with apoptotic nuclei was determined in three independent experiments (at least 200 nuclei/experiment were scored). In the co-transfection experiments, HeLa cells were transiently transfected with 0.4 μg of pEGFP-N1 plasmid containing C-RAD21 and 0.8 μg of pcDNA3 plasmid containing empty vector, p35, survivin, Bcl-x_L, or wild-type RAD21. Twenty-four h later, GFP-positive cells were scored for apoptosis as above. In all experiments, the statistical significance of inter-group differences was assessed by a two-tailed paired Student's *t* test.

Cell Cycle Analyses—HeLa cells were transiently transfected as above and subjected to a double thymidine block as follows. HeLa cells were plated at ~50% confluence and treated overnight with 2 mM thymidine. On the next day, cells were transiently transfected with GFP-tagged constructs, returned to normal growth media for the duration of the day, and then subjected to a second overnight incubation with 2 mM thymidine. On the following day, cells were washed in phosphate-buffered saline (PBS) and returned to normal growth media for 16 h. Cells were then trypsinized and incubated with 0.5% paraformaldehyde for 15 min at 37 °C. Next, cells were washed in PBS supple-

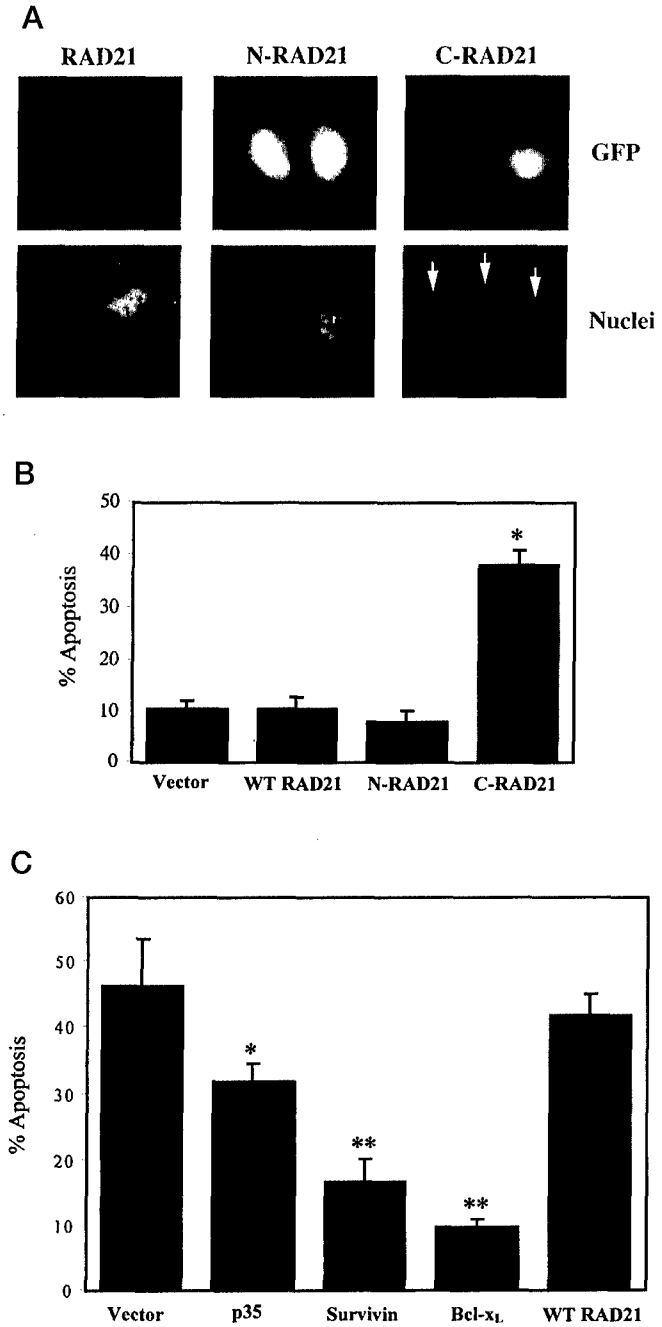

FIG. 4. **Caspase cleavage of RAD21 promotes apoptosis.** In *panels A* and *B*, HeLa cells were transiently transfected with GFP-tagged cDNAs encoding full-length Rad21 (RAD21), the amino-terminal (N-RAD21), or the carboxyl-terminal (C-RAD21) caspase cleavage products, and GFP-positive cells were scored for apoptotic nuclei as described under "Experimental Procedures." *A*, representative photomicrographs showing GFP fluorescence (*upper panels*) and nuclear morphology (*lower panels*). Apoptotic nuclei are indicated by *arrows*. *B*, the data from the three independent experiments (mean ± S.D.) (*, $p < 0.0005$). *C*, C-RAD21-induced apoptosis is inhibited by several anti-apoptotic proteins but not by wild-type RAD21. HeLa cells were transiently co-transfected with GFP-tagged C-RAD21 and a pcDNA3 plasmid containing empty vector, p35, survivin, Bcl-x_L, or WT Rad21 as described under "Experimental Procedures," and GFP-positive cells were scored for apoptotic nuclei. The data are presented as the mean ± S.D. of three independent experiments (*, $p < 0.05$ and **, $p < 0.005$).

mented with 0.05% Tween 20 and resuspended in 70% ethanol for 15 min at 4 °C. After washing in PBS, cells were incubated with propidium iodide (50 μg/ml) and RNase (100 μg/ml) for 1 h at 37 °C. Washed cells were then analyzed by fluorescence-activated cell sorting; the cell cycle distribution of GFP-fluorescent cells was determined by DNA content.

RESULTS

Identification of RAD21 as a Caspase-3 Substrate in Vitro by Small Pool Expression Cloning—We have recently described an expression cloning strategy to systematically identify cDNAs encoding caspase substrates (11–13). In the present study, we prepared ^{35}S-labeled protein pools from small pools (48 cDNAs/pool) of a human heart cDNA library by coupled transcription and translation *in vitro*. These ^{35}S-labeled protein pools were then incubated with control buffer, caspase-3, or caspase-8, and the cleavage products were analyzed by SDS-PAGE. As demonstrated in Fig. 1*A*, ^{35}S-labeled protein pool 156 contained an ~125-kDa protein (indicated by the *asterisk*) that was specifically cleaved by caspase-3 (*C3*) but not by caspase-8 (*C8*) into proteolytic products of ~65 and 32 kDa (indicated by *arrows*). As shown in Fig. 1*B*, the proteolytic activity of caspase-3 and -8 was confirmed by demonstrating their ability to cleave ^{35}S-labeled vimentin (a known caspase-3 substrate) (13, 31) or ^{35}S-labeled BID (a well characterized caspase-8 substrate) (32, 33). cDNA pool 156 was then subdivided into smaller pools, and the ^{35}S-labeled protein pools were retested for their sensitivity to caspase-3 cleavage until a single cDNA encoding the putative caspase substrate was isolated (Fig. 1*C*). Sequencing of clone 156 revealed that it was a partial cDNA encoding the human mitotic cohesin component RAD21 (14–16). The protein encoded by clone 156 lacked the amino-terminal 34 amino acids of the full-length human RAD21 protein.

Human RAD21 Is Specifically Cleaved by Caspases-3 and -7 at Multiple Sites, Including Asp^{279}, to Yield Several Proteolytic Products in Vitro—Because clone 156 was a partial Rad21 cDNA, we next examined the sensitivity of full-length human RAD21 to proteolysis *in vitro* by a panel of recombinant caspases. As shown in Fig. 2*A*, ^{35}S-labeled full-length human RAD21 was preferentially cleaved by caspase-3 (*C3*) and to a lesser extent by caspase-7 (*C7*) into two abundant proteolytic products of ~65 and 48 kDa and two fainter products of 32 and 22 kDa (indicated by *arrows*). Prolonged exposure also revealed a few additional faint products between 25 and 60 kDa (data not shown). In addition, caspases-6 (*C6*) and -8 (*C8*) weakly cleaved RAD21 to generate faint 65- and 48-kDa products. Importantly, the catalytic activity of each caspase was verified by incubation with a known substrate (data not shown). To identify the major caspase cleavage site in RAD21 responsible for producing the observed 65- and 48-kDa fragments, we examined its sequence for consensus caspase-3 cleavage (D*XX*D) motifs (34, 35) and found two adjacent, potential cleavage sites (DSPD ↓ S^{280} and DSVD ↓ P^{283}) that would generate cleavage products of the observed size. Each of the critical Asp residues (Asp^{279} and Asp^{282}) at these potential cleavage sites was individually altered to a Glu residue by site-directed mutagenesis. As shown in Fig. 2*B*, ^{35}S-labeled wild-type (WT) RAD21, but not mutant D279E RAD21, was cleaved into its signature 65- and 48-kDa products by caspases-3 and -7 *in vitro* (indicated by *arrows*). Instead, the D279E mutant was cleaved into a much larger size product (indicated by the *asterisk*) that was not observed when wild-type RAD21 was incubated with caspases-3 or -7. In contrast, ^{35}S-labeled mutant D282E RAD21 was readily proteolyzed by caspases-3 and -7 into the expected size products (data not shown). Interestingly, as demonstrated in Fig. 2*C*, ^{35}S-labeled full-length human REC8, a meiotic cohesin structurally related to RAD21 that is also cleaved by separase (36, 37, 42), was not proteolyzed by caspases-3 (*C3*) or -7 (*C7*) *in vitro*. Although the identity of the minor cleavage site(s) of RAD21 *in vitro* has not been delineated, these findings indicate unambiguously that RAD21 is preferentially cleaved at Asp^{279} by caspases-3 and -7 *in vitro*.

Human RAD21 Is Rapidly Proteolyzed by Caspases during

the Induction of Apoptosis, Leading to Its Partial Dissociation from Chromatin—Having demonstrated that RAD21 is cleaved by caspases *in vitro*, we wanted to determine whether it is also cleaved by caspases in cells undergoing apoptosis *in vivo*. To this end, HeLa cells were treated with 50 μM etoposide for varying time periods, and RAD21 was detected by immunoblotting with a carboxyl-terminal polyclonal antibody. As shown in Fig. 3*A*, RAD21 was rapidly proteolyzed into a 65-kDa fragment (indicated by *arrows*) within 12 h of treatment with etoposide. By 36 h, all of the full-length RAD21 had been cleaved into the 65-kDa product. Of note, the observed RAD21 apoptotic cleavage product was the same size as that generated by RAD21 proteolysis by caspase-3 *in vitro*, suggesting that the apoptotic proteolysis of RAD21 is also mediated by caspases. Interestingly, RAD21 was cleaved more rapidly during etoposide-induced apoptosis than the well characterized nuclear caspase-3 substrate PARP (38); PARP proteolysis was detected only after 36 h of etoposide treatment. Instead, the time course of RAD21 proteolysis during apoptosis more closely resembled that of the cytosolic caspase-3 substrate protein kinase Cδ (39). Indeed, RAD21 proteolysis could be detected after 12 h of etoposide treatment when only 1% of HeLa cells had apoptotic nuclear morphology, and RAD21 was completely cleaved into its 65-kDa product after 36 h of treatment when only 25% of cells had apoptotic nuclei. Hence, the specific proteolysis of RAD21 into its signature 65-kDa product precedes apoptotic chromatin condensation/fragmentation.

To determine whether the specific proteolysis of RAD21 during apoptosis is, indeed, mediated by caspases, HeLa cells were untreated or preincubated with the broad spectrum caspase inhibitor zVAD-fmk (100 μM) for 1 h, and the cells were then treated with 10 ng/ml TNF-α and 1 μg/ml cycloheximide for 18 h. As shown in Fig. 3*B*, the apoptotic cleavage of RAD21 induced by TNF-α (indicated by the *arrow*) was completely inhibited by zVAD-fmk, thereby indicating that caspases are responsible for the proteolysis of RAD21 during apoptosis *in vivo*. zVAD-fmk also inhibited RAD21 proteolysis induced by etoposide (data not shown). To determine whether caspase-3 was necessary for the apoptotic proteolysis of RAD21, we treated MCF-7 breast carcinoma cells, which lack caspase-3 (40), with 10 ng/ml TNF-α and 1 μg/ml cycloheximide for 24 h. As shown in Fig. 3*C*, RAD21 was proteolyzed into its characteristic 65-kDA cleavage product in MCF-7 undergoing TNF-α-induced apoptosis, indicating that caspase-3 is not essential for the apoptotic proteolysis of RAD21 and that other caspases (such as caspase-7) can cleave RAD21 *in vivo*. Taken together, our results demonstrate unequivocally that RAD21 is rapidly and specifically cleaved by caspases during the induction of apoptosis triggered by a broad spectrum of stimuli.

We next examined whether caspase cleavage of RAD21 altered its association with chromatin. To this end, we prepared low speed chromatin-enriched pellet and supernatant fractions from untreated HeLa cells or HeLa cells incubated with TNF-α and cycloheximide for 48 h. As demonstrated in Fig. 3*D*, full-length RAD21 bound to chromatin and was found exclusively in the chromatin-enriched pellet (*P*) in both untreated and TNF-α-treated HeLa cells. In contrast, the 65-kDa RAD21 caspase cleavage product (indicated by the *arrow*) partly dissociated from chromatin and was found in both the supernatant (*S*) and pellet (*P*) fractions in TNF-α-treated cells. These findings were consistent with our observations that GFP-tagged full-length RAD21 was present in the nucleus of interphase cells, whereas its carboxyl-terminal cleavage product was present in both the cytosol and nucleus (Fig. 4*A*). Taken together, these results indicate that caspase cleavage of RAD21 leads to its partial removal from chromatin and relocalization to the cytoplasm.

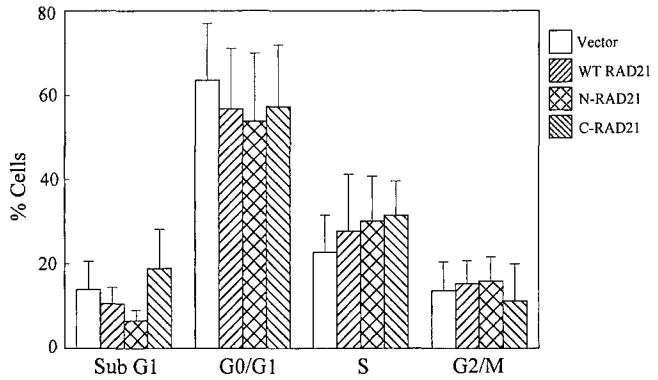

FIG. 5. **Caspase cleavage of RAD21 does not inhibit cell cycle progression.** HeLa cells were transiently transfected with GFP vector or GFP-tagged cDNAs encoding WT Rad21, the amino-terminal (N-RAD21), or the carboxyl-terminal (C-RAD21) caspase cleavage products, and cells were released from a double thymidine block for 16 h as described under "Experimental Procedures." GFP-positive cells were sorted by flow cytometry, and their cell cycle phase was determined as detailed under "Experimental Procedures." The data are presented as the mean ± S.D. of three independent experiments.

Caspase Cleavage of RAD21 Promotes Apoptosis—To determine whether caspase cleavage of RAD21 promotes apoptosis, we transiently transfected HeLa cells with GFP-tagged full-length RAD21 or with cDNAs encoding RAD21's amino-terminal (amino acids 1–279 labeled N-RAD21) or carboxyl-terminal (amino acids 280–631 labeled C-RAD21) caspase cleavage products resulting from cleavage at Asp^{279}. As demonstrated in Fig. 4*A*, neither full-length RAD21 (present in the nucleus of interphase cells) nor N-RAD21 (present in both the nucleus and cytoplasm) induced apoptotic nuclear alterations. In contrast, transient expression of C-RAD21 induced cellular rounding, a reduction in cytosolic volume (*upper panel*) and fragmentation of the nucleus (*lower panel*, apoptotic nuclei indicated by *arrows*) that typify apoptotic cell death. These data are presented quantitatively in Fig. 4*B*. Similar results were obtained in MCF-7 breast carcinoma cells (data not presented). To begin to delineate the mechanisms by which C-RAD21 induces apoptosis, we examined whether co-transfecting HeLa cells with a variety of antiapoptotic cDNAs could inhibit C-RAD21-induced apoptosis. As shown in Fig. 4*C*, both Bcl-x_L and survivin potently inhibited C-RAD21-induced apoptosis, whereas p35, a broad spectrum caspase inhibitor, partially inhibited C-RAD21-induced cell death. In contrast, wild-type RAD21 did not antagonize C-RAD21-induced apoptosis, thereby suggesting that C-RAD21 does not induce apoptosis by inhibiting the function of the full-length protein. Taken together, our findings indicate that caspase cleavage of RAD21 plays an active role in the execution of apoptosis by specifically generating a proapoptotic carboxyl-terminal cleavage product.

Caspase Cleavage of RAD21 Does Not Inhibit Cell Cycle Progression—Because inhibition of RAD21 has recently been shown to cause mitotic arrest as a consequence of misaligned chromosomes at metaphase (41), we examined the effect of RAD21 and each of its caspase cleavage products on cell cycle progression. To this end, HeLa cells were transiently transfected with GFP vector, GFP-tagged RAD21, N-RAD21, or C-RAD21 and released from a double thymidine (G_1/S) block for 16 h. As shown in Fig. 5, none of these RAD21 constructs inhibited cell cycle progression. Similar results were obtained at 28 h after release from a double thymidine block except that the sub-G_1 population of C-RAD21-transfected cells increased, consistent with the induction of apoptosis (data not presented). These findings indicate that caspase cleavage of RAD21 does not induce mitotic arrest under these conditions.

DISCUSSION

We have identified the mitotic cohesin component RAD21 as a novel nuclear caspase substrate using a small pool expression cloning strategy we have described previously (11–13). RAD21 is rapidly cleaved by caspases-3 and -7 at DSPD ↓ S^{280} during the induction of apoptosis by diverse stimuli. Interestingly, the cleavage site Asp^{279} has been remarkably conserved in RAD21 from *Caenorhabditis elegans* to humans (15), suggesting that the apoptotic proteolysis of RAD21 at Asp^{279} may occur in diverse species. In contrast, the structurally related meiotic cohesin REC8 that is also cleaved by separase (42) is not cleaved by caspases, underscoring the specificity of the proteolysis of RAD21 during apoptosis. Moreover, caspase cleavage of RAD21 precedes apoptotic chromatin condensation; we observed RAD21 proteolysis into its characteristic 65-kDa product when 99% of nuclei were intact. We have also demonstrated that caspase cleavage of RAD21 has important functional consequences; caspase-cleaved RAD21 partially dissociates from chromatin and redistributes to the cytosol. Because RAD21 proteolysis precedes apoptotic chromatin condensation, our findings suggest that caspase cleavage of RAD21 and its subsequent removal from chromatin could contribute to this process.

Indeed, we have demonstrated that caspase proteolysis of RAD21 at Asp^{279} actively participates in the apoptotic destruction of the nucleus by specifically generating a proapoptotic carboxyl-terminal cleavage product (C-RAD21). Strikingly, neither full-length RAD21 nor its amino-terminal cleavage product induces apoptosis, thereby underscoring the specificity of our findings and providing additional support for the notion that caspase cleavage of RAD21 activates a latent proapoptotic function. Our first hypothesis as to the proapoptotic mechanism of C-RAD21 was that it might function as an inhibitor of wild-type RAD21; however, our results do not support this mechanism. First, co-transfection of excess wild-type RAD21 does not suppress C-RAD21-induced apoptosis. Second, RAD21-deficient chicken cells undergo mitotic arrest; cohesion defects lead to chromosome misalignment at metaphase, thereby blocking entry into anaphase and subsequent mitotic exit (41). However, C-RAD21 does not induce mitotic arrest under the conditions we examined, suggesting that it does not disrupt the function of wild-type RAD21. Third, disruption of separase cleavage of RAD21 by a variety of approaches leads to aneuploidy as a result of chromosome segregation defects coupled with DNA re-replication (23, 28, 43). In contrast, C-RAD21 transfected cells show little evidence of aneuploidy even 72 h after transfection when the vast majority of transfected cells are apoptotic (data not shown). Taken together, these findings indicate that C-RAD21-induced apoptosis is not mediated by mitotic arrest or by chromosome segregation defects.

How, then, might RAD21 cleavage promote apoptosis? One possibility is that caspase proteolysis of RAD21, as well as its partial removal from chromatin, might render chromosomal DNA more vulnerable to attack by acinus, CAD, or other factors capable of inducing apoptotic DNA fragmentation, such as endonuclease G or apoptosis-inducing factor (AIF) (44–46). Although we observed that the RAD21 D279E mutant did not inhibit etoposide-induced chromatin condensation/fragmentation (data not shown), the interpretation of this finding is complicated by the presence of the endogenous cleavage-sensitive wild-type RAD21 in all the cancer cell lines we examined. Alternatively, C-RAD21 (which remains partly associated with chromatin) might directly alter chromatin structure through dysregulated interactions with its known binding proteins SMC1 and SMC3, which play a key role in maintaining chromatin structure (18, 19). Caspase cleavage of RAD21 might also contribute to the execution of apoptotic cell death by disrupting the DNA repair function of RAD21. RAD21 repairs double-strand DNA breaks induced by ionizing radiation and/or other DNA damaging agents in fission yeast and chicken cells, and it is essential for viability in fission yeast (14, 17, 41). These findings suggest that the close proximity of sister chromatids resulting from their cohesion facilitates homologous recombination repair of double-strand DNA breaks (41). In addition, mutations in RAD21 sensitize yeast to cell death induced by DNA damage or microtubule-disrupting agents (47). Caspase cleavage of RAD21 at Asp^{279} separates the conserved amino-terminal domain necessary for DNA repair from other functional domains, including the putative nuclear localization motifs (^{317}KRKRK and ^{401}RKRRK) (15). Consequently, caspase proteolysis of RAD21 likely impairs its DNA repair capabilities by directly inactivating its repair activity and/or by triggering its partial dissociation from chromatin. RAD21, thus, can be added to a growing list of DNA repair enzymes that are cleaved by caspases, including PARP, the catalytic subunit of the DNA-dependent protein kinase (DNA-PK_{CS}), the ataxia telangiectasia gene product, and RAD51 (38, 48–53). Hence, the coordinated destruction of the cellular DNA repair machinery by caspases is a central theme in apoptosis that likely expedites apoptotic cell death by allowing CAD-mediated DNA fragmentation to proceed unimpeded by repair processes.

Furthermore, caspase proteolysis of RAD21 likely amplifies the apoptotic signal. Indeed, apoptosis induced by C-RAD21 is partially suppressed by the baculoviral p35 gene product, a broad spectrum caspase inhibitor (54). Hence, caspase proteolysis of RAD21 amplifies the cell death signal by generating a carboxyl-terminal cleavage product that activates more caspases, creating a positive feedback loop. This mechanism for amplifying the apoptotic cell death signal has been described for other caspase substrates such as MEKK-1 and vimentin (13, 55). In addition, we observed that the antiapoptotic protein survivin, an inhibitor of apoptosis (IAP) family member frequently overexpressed in cancer (56), inhibits C-RAD21-induced apoptosis. Although the antiapoptotic mechanism of survivin is unclear, it may directly inhibit caspases (57, 58). Intriguingly, survivin is a chromosomal passenger protein that forms a multimeric complex with other such proteins including inner centromere protein (INCENP) and Aurora-B; these proteins play important roles in chromosome segregation and cytokinesis (59, 60). Recent evidence suggests that RAD21 also behaves like a chromosomal passenger protein; it moves from the centromere to the spindle midzone during anaphase and to the midbody during telophase, and it is necessary for INCENP localization to centromeres (27, 41). Taken together, these studies suggest an intimate relationship between RAD21 and survivin that might account for the ability of survivin to antagonize C-RAD21-induced apoptosis. Clearly, the elucidation of the precise mechanism(s) by which caspase cleavage of RAD21 promotes apoptosis will require further study.

Another intriguing aspect of our findings is the striking parallel between the actions of RAD21 during apoptosis and mitosis. In mammalian cells, the vast majority of RAD21/cohesin is removed from sister chromatid arms prior to their condensation by a poorly understood cleavage-independent mechanism during prophase (25, 27, 61). Indeed, the observation that chromatin arm condensation begins immediately after cohesin removal has led to the speculation that chromatin-associated cohesin may inhibit condensation. During the onset of anaphase, the remaining centromeric cohesin is subsequently removed by the proteolysis of RAD21 by a caspase-like separase that triggers sister separation to opposite poles (25, 28). Moreover, the cleavage of RAD21/SCC1 is necessary for

sister chromatid separation; the introduction of a cleavage-resistant RAD21/SCC1 into budding yeast or human HeLa cells blocks sister separation (20, 21, 28). As in mitosis, the apoptotic removal of RAD21 precedes chromatin condensation, although in apoptosis (but not mitosis), the dissociation of RAD21 from chromatin is initiated by proteolysis. Furthermore, in both apoptosis and mitosis, RAD21 is cleaved by distantly related proteases. Taken together, these striking similarities suggest that components of the apoptotic and mitotic machinery have been shared during the course of evolution.

Acknowledgments—We are indebted to Dr. R. Talanian for providing the recombinant caspases used in this study and to Drs. H. Li and H. Perlman for the critical reading of the manuscript.

REFERENCES

1. Steller, H. (1995) *Science* **267,** 1445–1449
2. Cryns, V. L., and Yuan, J. (1998) *Genes Dev.* **12,** 1551–1570
3. Sahara, S., Aoto, M., Eguchi, Y., Imamota, N., Yoneda, Y., and Tsujimoto, Y. (1999) *Nature* **401,** 168–173
4. Enari, M., Sakahira, H., Yokoyama, H., Okawa, K., Iwamatsu, A., and Nagata, S. (1998) *Nature* **391,** 43–50
5. Liu, X., Zou, H., Slaughter, C., and Wang, X. (1997) *Cell* **89,** 175–184
6. Sakahira, H., Enari, M., and Nagata, S. (1998) *Nature* **391,** 96–99
7. Lazebnik, Y. A., Takahashi, A., Moir, R. D., Goldman, R. D., Poirier, G. G., Kaufmann, S. H., and Earnshaw, W. C. (1995) *Proc. Natl. Acad. Sci. U. S. A.* **92,** 9042–9046
8. Rao, L., Perez, D., and White, E. (1996) *J. Cell Biol.* **135,** 1441–1455
9. Takahashi, A., Alnemri, E. S., Lazebnik, Y. A., Fernandes-Alnemri, T., Litwack, G., Moir, R. D., Goldman, R. D., Poirier, G. G., Kaufmann, S. H., and Earnshaw, W. C. (1996) *Proc. Natl. Acad. Sci. U. S. A.* **93,** 8395–8400
10. Faleiro, L., and Lazebnik, Y. (2000) *J. Cell Biol.* **151,** 951–960
11. Lustig, K. D., Stukenberg, T., McGarry, T., King, R. W., Cryns, V. L., Mead, P., Zon, L., Yuan, J., and Kirschner, M. W. (1997) *Methods Enzymol.* **283,** 83–99
12. Cryns, V. L., Byun, Y., Rana, A., Mellor, H., Lustig, K., Ghanem, L., Parker, P. J., Kirschner, M. W., and Yuan, J. (1997) *J. Biol. Chem.* **272,** 29449–29453
13. Byun, Y., Chen, F., Chang, R., Trivedi, M., Green, K., and Cryns, V. L. (2001) *Cell Death Differ.* **8,** 443–450
14. Birkenbihl, R. P., and Subramani, S. (1992) *Nucleic Acids Res.* **20,** 6605–6611
15. McKay, M. J., Troelstra, C., van der Spek, P., Kanaar, R., Smit, B., Hagemeijer, A., Bootsma, D., and Hoeijmakers, J. H. (1996) *Genomics* **36,** 305–315
16. Guacci, V., Koshland, D., and Strunnikov, A. (1997) *Cell* **91,** 47–57
17. Birkenbihl, R. P., and Subramani, S. (1995) *J. Biol. Chem.* **270,** 7703–7711
18. Nasmyth, K., Peters, J. M., and Uhlmann, F. (2000) *Science* **288,** 1379–1385
19. Hirano, T. (2000) *Annu. Rev. Biochem.* **69,** 115–144
20. Uhlmann, F., Lottspeich, F., and Nasmyth, K. (1999) *Nature* **400,** 37–42
21. Uhlmann, F., Wernic, D., Poupart, M.-A., Koonin, E., and Nasmyth, K. (2000) *Cell* **103,** 375–386
22. Tomonaga, T., Nagao, K., Kawasaki, Y., Furuya, K., Murakami, A., Morishita, J., Yuasa, T., Sutani, T., Kearsey, S. E., Uhlmann, F., Nasmyth, K., and Yanagida, M. (2000) *Genes Dev.* **14,** 2757–2770
23. Rao, H., Uhlmann, F., Nasmyth, K., and Varshavsky, A. (2001) *Nature* **410,** 955–959
24. Losada, A., Hirano, M., and Hirano, T. (1998) *Genes Dev.* **12,** 1986–1997
25. Waizenegger, I. C., Hauf, S., Meinke, A., and Peters, J. M. (2000) *Cell* **103,** 399–410
26. Warren, W. D., Steffensen, S., Lin, E., Coelho, P., Loupart, M., Cobbe, N., Lee, J. Y., McKay, M. J., Orr-Weaver, T., Heck, M. M., and Sunkel, C. E. (2000) *Curr. Biol.* **10,** 1463–1466
27. Hoque, M. T., and Ishikawa, F. (2001) *J. Biol. Chem.* **276,** 5059–5067
28. Hauf, S., Waizenegger, I. C., and Peters, J. M. (2001) *Science* **293,** 1320–1323
29. Cryns, V. L., Bergeron, L., Zhu, H., Li, H., and Yuan, J. (1996) *J. Biol. Chem.* **271,** 31277–31282
30. Kamradt, M., Chen, F., and Cryns, V. L. (2001) *J. Biol. Chem.* **276,** 16059–16063
31. Morishima, N. (1999) *Genes Cells* **4,** 401–414
32. Li, H., Zhu, H., Xu, C. J., and Yuan, J. (1998) *Cell* **94,** 491–501
33. Luo, X., Budihardjo, I., Zou, H., Slaughter, C., and Wang, X. (1998) *Cell* **94,** 481–490
34. Talanian, R. V., Quinlan, C., Trautz, S., Hackett, M. C., Mankovich, J. A., Banach, D., Ghayur, T., Brady, K. D., and Wong, W. W. (1997) *J. Biol. Chem.* **272,** 9677–9682
35. Thornberry, N., Rano, T., Peterson, E., Rasper, D., Timkey, T., Garcia-Calvo, M., Houtzager, V., Nordstrom, P., Roy, S., Vaillancourt, J., Chapman, K., and Nicholson, D. (1997) *J. Biol. Chem.* **272,** 17907–17911
36. Watanabe, Y., and Nurse, P. (1999) *Nature* **400,** 461–464
37. Parisi, S., McKay, M. J., Molnar, M., Thompson, M. A., van der Spek, P. J., van Drunen-Schoenmaker, E., Kanaar, R., Lehmann, E., Hoeijmakers, J. H., and Kohli, J. (1999) *Mol. Cell. Biol.* **19,** 3515–3528
38. Lazebnik, Y. A., Kaufmann, S. H., Desnoyers, S., Poirier, G. G., and Earnshaw, W. C. (1994) *Nature* **371,** 346–347
39. Emoto, Y., Manome, Y., Meinhardt, G., Kisaki, H., Kharbanda, S., Robertson, M., Ghayur, T., Wong, W. W., Kamen, R., Weichselbaum, R., and Kufe, D. (1995) *EMBO J.* **14,** 6148–6156
40. Janicke, R. U., Sprengart, M. L., Wati, M. R., and Porter, A. G. (1998) *J. Biol. Chem.* **273,** 9357–9360
41. Sonoda, E., Matsusaka, T., Morrison, C., Vagnarelli, P., Hoshi, O., Ushiki, T., Nojima, K., Fukagawa, T., Waizenegger, I. C., Peters, J. M., Earnshaw, W. C., and Takeda, S. (2001) *Dev. Cell* **1,** 759–770
42. Buonomo, S. B., Clyne, R. K., Fuchs, J., Loidl, J., Uhlmann, F., and Nasmyth, K. (2000) *Cell* **103,** 387–398
43. Jallepalli, P. V., Waizenegger, I. C., Bunz, F., Langer, S., Speicher, M. R., Peters, J. M., Kinzler, K. W., Vogelstein, B., and Lengauer, C. (2001) *Cell* **105,** 445–457
44. Li, L. Y., Luo, X., and Wang, X. (2001) *Nature* **412,** 95–99
45. Parrish, J., Li, L., Klotz, K., Ledwich, D., Wang, X., Xue, D. (2001) *Nature* **412,** 90–94
46. Susin, S. A., Daugas, E., Ravagnan, L., Samejima, K., Zamzami, N., Loeffler, M., Costantini, P., Ferri, K. F., Irinopoulou, T., Prevost, M. C., Brothers, G., Mak, T. W., Penninger, J., Earnshaw, W. C., and Kroemer, G. (2000) *J. Exp. Med.* **192,** 571–580
47. Tatebayashi, K., Kato, J., and Ikeda, H. (1998) *Genetics* **148,** 49–57
48. Casciola-Rosen, L. A., Anhalt, G. J., and Rosen, A. (1995) *J. Exp. Med.* **182,** 1625–1634
49. Han, Z., Malik, N., Carter, T., Reeves, W. H., Wyche, J. H., and Hendrickson, E. A. (1996) *J. Biol. Chem.* **271,** 25035–25040
50. Song, Q., Lees-Miller, S. P., Kumar, S., Zhang, Z., Chan, D. W., Smith, G. C., Jackson, S. P., Alnemri, E. S., Litwack, G., Khanna, K. K., and Lavin, M. F. (1996) *EMBO J.* **15,** 3238–3246
51. Smith, G., di Fagagna, F., Lakin, N., and Jackson, S. (1999) *Mol. Cell. Biol.* **19,** 6076–6084
52. Huang, Y., Nakada, S., Ishiko, T., Utsugisawa, T., Datta, R., Kharbanda, S., Yoshida, K., Talanian, R., Weichselbaum, R., Kufe, D., and Yuan, Z.-M. (1999) *Mol. Cell. Biol.* **19,** 2986–2997
53. Hotti, A., Jarvinen, K., Siivola, P., and Holtta, E. (2000) *Oncogene* **19,** 2354–2362
54. Bump, N. J., Hackett, M., Hugunin, M., Seshagiri, S., Brady, K., Chen, P., Ferenz, C., Franklin, S., Ghayur, T., Li, P., Licari, P., Mankovich, J., Shi, L., Greenberg, A. H., Miller, L. K., and Wong, W. W. (1995) *Science* **269,** 1885–1888
55. Cardone, M. H., Salvesen, G. S., Widmann, C., Johnson, G., and Frisch, S. M. (1997) *Cell* **90,** 315–323
56. Ambrosini, G., Adida, C., and Altieri, D. C. (1997) *Nat. Med.* **3,** 917–921
57. Tamm, I., Wang, Y., Sausville, E., Scudiero, D. A., Vigna, N., Oltersdorf, T., and Reed, J. C. (1998) *Cancer Res.* **58,** 5315–5320
58. Shin, S., Sung, B. J., Cho, Y. S., Kim, H. J., Ha, N. C., Hwang, J. I., Chung, C. W., Jung, Y. K., and Oh, B. H. (2001) *Biochemistry* **40,** 1117–1123
59. Skoufias, D. A., Mollinari, C., Lacroix, F. B., and Margolis, R. L. (2000) *J. Cell Biol.* **151,** 1575–1581
60. Uren, A. G., Wong, L., Pakusch, M., Fowler, K. J., Burrows, F. J., Vaux, D. L., and Choo, K. H. A. (2000) *Curr. Biol.* **10,** 1319–1328
61. Sumara, I., Vorlaufer, E., Gieffers, C., Peters, B. H., and Peters, J. M. (2000) *J. Cell Biol.* **151,** 749–762

REPORT DOCUMENTATION PAGE

Form Approved
OMB No. 074-0188

1. AGENCY USE ONLY (Leave blank)	2. REPORT DATE	3. REPORT TYPE AND DATES COVERED
	October 2002	Final (1 Sep 98 -31 Aug 02)

4. TITLE AND SUBTITLE
Bone-97 Alcohol and Skeletal Adaptation to Mechanical Usage

5. FUNDING NUMBERS
DAMD17-98-1-8517

6. AUTHOR(S):
Russell Turner, Ph.D.

7. PERFORMING ORGANIZATION NAME(S) AND ADDRESS(ES)
Mayo Clinic and Foundation
Rochester, Minnesota 55905

E-Mail: turner.russell@mayo.edu

8. PERFORMING ORGANIZATION REPORT NUMBER

9. SPONSORING / MONITORING AGENCY NAME(S) AND ADDRESS(ES)
U.S. Army Medical Research and Materiel Command
Fort Detrick, Maryland 21702-5012

10. SPONSORING / MONITORING AGENCY REPORT NUMBER

11. SUPPLEMENTARY NOTES

12a. DISTRIBUTION / AVAILABILITY STATEMENT
Approved for Public Release; Distribution Unlimited

12b. DISTRIBUTION CODE

13. Abstract ***(Maximum 200 Words)*** *(abstract should contain no proprietary or confidential information)*

These studies were designed to determine whether alcohol antagonizes the ability of the skeleton to adapt to increased mechanical usage. This report summarizes our progress from the award date (Nov 1998) through September 2002. We have essentially completed all of the tasks outlined in the original proposal. The results clearly demonstrate that alcohol results in: 1) dose dependent decreases in bone turnover and bone mass; 2) disturbed gene expression for selected cytokines (e.g., mRNA levels for Insulin-like growth factor 1 were decreased and Tumor necrosis factor-alpha were increased) that influence bone metabolism. The effects of alcohol were observed in the presence and absence of weight bearing exercise. Taken together, these findings support the hypothesis that alcohol abuse could contribute to the high incidence of stress fractures that occur during rigorous military training.

14. SUBJECT TERMS	15. NUMBER OF PAGES
alcohol abuse, bone metabolism, fracture risk, osteoporosis	126
	16. PRICE CODE

17. SECURITY CLASSIFICATION OF REPORT	18. SECURITY CLASSIFICATION OF THIS PAGE	19. SECURITY CLASSIFICATION OF ABSTRACT	20. LIMITATION OF ABSTRACT
Unclassified	Unclassified	Unclassified	Unlimited

Table of Contents

Cover	1
SF 298	2
Table of Contents	3
Introduction	4
Body	4
Key Research Accomplishments	9
Reportable Outcomes	10
Conclusions	11
References	12
Appendices	13

INTRODUCTION

Chronic alcohol abuse is an important risk factor for osteoporosis. The ultimate goal of this research is to identify the cellular and molecular mechanisms responsible for mediating ethanol's dose- and time-dependent actions on bone turnover, mass, architecture, and strength. It is well established that ethanol reversibly alters the biophysical properties of cell membranes and in doing so disturbs normal membrane function. The proposed studies in young adult rats were designed to test our working hypothesis that these membrane changes disrupt essential cell signaling pathways for one or more bone cells "coupling" factors and/or polypeptide hormones that regulate bone modeling and remodeling. These changes are postulated to lead to the bone loss associated with chronic alcohol abuse. If our hypothesis is correct, then ethanol antagonizes the ability of the skeleton to respond to weight bearing because the signal transduction pathways for mechanical signals require peptide signaling molecules as intermediates. This latter effect of ethanol to reduce the ability of the skeleton to adapt to increased mechanical stress would be especially detrimental during rigorous military training.

BODY

Introduction

We have performed all of the proposed tasks.

We will discuss the progress for each task separately. Table 1 lists experiment number, title, and task(s).

Task 1

The goal of this Task was to determine the dose response effects of administered ethanol on serum chemistry and gene expression in bone. Four rat studies (Experiments 1-4) have been completed as outlined in Table 1 (Appendix 1).

The dose response effects of administered ethanol on serum ethanol concentration was determined one hour later. The lower doses of ethanol (0 to .3 mg/kg) resulted in blood alcohol concentration below the detection limit. Further increases in the dose led to a rapid rise in blood alcohol. Doses greater than 1.2 mg/kg led to blood alcohol levels (>0.01%) which would be considered to lead to functional impairment. Blood alcohol was below the detection limit at all doses when assayed at 6 hours.

Ethanol did not induce the expression of either c-*fos* or c-*jun* (negative data not shown). In contrast, 1 hour treatment with either estrogen (1) or PTH (unpublished data) induced mRNAs for these two immediate response genes.

Ethanol resulted in dose dependent increases in mRNA levels for osteocalcin, type 1 collagen and osteonectin at the proximal tibial metaphysis. The mRNA levels for all three bone matrix proteins were significantly elevated at the 1.2 g/kg dose. Similar increases were observed in vertebrae. The dose response effects of ethanol on mRNA levels for several cytokines and

growth factors was determined. Ethanol resulted in a dose dependent increase in the RNA levels for TNF-α (significantly elevated at the two highest doses) and a dose dependent decrease in the mRNA for IGF-I (significantly reduced at the highest dose). The details of the experimental design, results and interpretation of results for Task 1 are published (Appendix 2).

Task 2

The goal of this Task was to establish the time course effects of ethanol on the gene expression of bone matrix proteins and signaling peptides. Three studies were performed (Table 1).

The time course effects of ethanol (1.2 g/kg) on serum chemistry were determined. Ethanol resulted in a transient increase in blood alcohol (detected at 1 and 2 hours), mild hypocalcemia (significant at 4, 8, 12, and 16 hours), and no change in serum immunoreactive parathyroid hormone (*i*PTH) (Appendix 1).

The maximum induction of mRNA for each of the three bone matrix proteins occurred 6 hours following administration of ethanol. There were transient decreases in mRNA levels for IL-1, IFN-γ, and MIF prior to the increase in mRNA levels for the bone matrix proteins. In contrast, the restoration of normal mRNA levels for the bone matrix proteins corresponded to a significant decrease in the mRNA levels for IGF-I (Appendix 2). Ethanol treatment had minimal effects on mRNA levels for pro- and anti-apoptotic genes (Table 2), suggesting that ethanol is not toxic to bone cells. These findings were verified by studying the effects of alcohol on cultured bone cells (Appendix 3).

The transient rise in mRNA levels for bone matrix proteins did not lead to a corresponding increase in bone matrix synthesis. There was no significant difference ($p=0.50$; n=5-6/group) in ^{3}H-proline incorporation into proximal tibial metaphysis between ethanol-treated (297 ± 61 CPM/mg) and solvent-treated (253 ± 28 CPM/mg) rats when the labeled amino acid was administered 6 hours after ethanol treatment (Table 1; Experiment 6). These data are published (Appendix 2).

To determine whether the ethanol-induced transient increases in mRNA levels for bone matrix proteins requires protein synthesis, rats were administered cycloheximide 2 hours prior to ethanol (Table 3). Cycloheximide had no effect on mRNA levels in solvent-treated or ethanol-treated rats. However, the results are not definitive because the expected ethanol-induced significant increase in mRNA levels was not observed. They do show, however, that the normal "half life" of the message for these genes is quite long. The original goal of Task 2 was accomplished by the end of year 1. However, we continued to investigate mRNA isolated during the course of performing these studies using cDNA microarrays. This technology was not available when the proposal was submitted and results of this analysis provided additional insight into the mechanism for the detrimental actions of alcohol on bone metabolism. Using this method we have shown that alcohol results in tissue specific effects on gene expression. Furthermore, alcohol influences the expression of many more genes and signaling pathways in bone than formally suspected. The details of the experimental design, results and interpretation can be found in Appendices 4 and 5. The data is undergoing additional analysis because of the complexities involved in interpreting data from over 5000 genes.

Task 3

The goal of Task 3 was to determine which induces a more detrimental skeletal response: peak blood concentrations of ethanol or chronic elevation of blood alcohol.

We have completed two studies investigating the effects of ip injection and gavage (Table 1; Experiments 7 and 8).

The comparative effects of administration of ethanol by daily ip injection (Table 1; Experiment 7) with gavage (Experiment 8) on mRNA levels for bone matrix protein and bone histomorphometry are shown in Tables 4 and 5, respectively. Gavage has no effects on steady-state mRNA levels for bone matrix proteins or bone histomorphometry. In contrast, ip injection significantly reduced mRNA levels for Type 1 collagen, osteocalcin and osteonectin, and decreased cancellous bone formation. Similarly, gavage had no effect on mRNA levels for cytokines. Ip injection, however, decreased mRNA levels for IGF-1 and IL-6. The influence of ethanol exposure kinetics needs further investigation. However, this was beyond the scope of the proposed research. We, therefore, chose to proceed with the remainder of our investigations using a model in which ethanol is incorporated into the diet. This is a good model for chronic alcohol abuse but may give different results than binge drinking.

Task 4

The goal of this task is to evaluate the long-term skeletal effects of ethanol. We have completed the animal studies (Table 1; Experiment 9) and have performed bone histomorphometry and RNA analysis. The long-term effects of administration of ethanol on serum chemistry, body weight, bone histomorphometry, and gene expression are published (Appendix 6).

Pair-feeding had no effect on any measured value. For this reason, the pair-fed and ad lib controls groups were combined.

We determined the dose effects of ethanol on body weight, food and alcohol consumption. The initial body weights did not differ between the treatment groups. Ethanol had minor effects on body weight and food consumption. The lowest concentration of ethanol (3% caloric intake) increased final body weight as well as consumption of the diet, whereas the highest concentration (35% of caloric intake) tended to reduce final weight gain ($p<.06$) and significantly decreased consumption. There was a near linear increase in total ethanol consumed/day as the concentration of ethanol was increased in the diet.

We determined the dose effects of ethanol on serum chemistry. Ethanol had either no effect or mildly increased total calcium (6% of caloric intake), had no effect on cholesterol and creatinine, and significantly reduced osteocalcin at all but one dose rate (6% of caloric intake).

We determined the dose effects of ethanol on static bone histomorphometry. Bone volume (BV/TV) was significantly decreased at 13% and 35% of caloric intake and trabecular thickness (Tb.Th) was decreased at intake levels at and above 6%. Trabecular number and separation (Tb.N and Tb.S) were not influenced by ethanol. Ethanol treatment resulted in a significant

($p<0.0001$) dose dependent decrease ($r = .31$) in BV/TV as determined by linear regression analysis.

We determined the dose effects of ethanol on cancellous bone dynamic and cellular histomorphometry indices on bone formation. Ethanol-treatment resulted in progressive dose dependent decreases in MS/BS, BFR/BS and BFR/BS. Ethanol had no effect on MAR or osteoblast perimeter. Ethanol-treatment reduced osteoclast number at all concentrations but the magnitude of the inhibition did not depend upon dose.

We determined the dose effects of ethanol on steady-state mRNA levels for bone matrix proteins. The highest concentration of ethanol (35% of caloric intake) uniformly reduced mRNA levels for type 1 collagen, osteonectin and osteocalcin. There were no other significant differences.

The effects of ethanol (6% and 35% of caloric intake) on steady-state mRNA levels for cytokines and growth factors were determined. The mRNAs for TNF-ß, IL-1 receptor antagonist, IL-10, or IFN-ß were not detected in extracts from rat bone from either control or ethanol-treated rats. The mRNAs for IL-1α, IL-12, IFN-γ, MIF, TGF-$ß_1$, TGF-$ß_2$, and TNF-α were detected but were not influenced by the treatment. Steady-state mRNA levels for IGF-I and IL-6 were reduced by ethanol treatment.

The long-term effects of ethanol on mRNA levels for pro- and anti-apoptotic genes (Experiment 9) are shown in Table 6. Ethanol resulted in dose dependent decreases in mRNA levels for bcl-x, bax, bcl-2, FAF and RIP. mRNA levels for bcl-x, bax, bcl-2 were decreased in rats fed 6% of their caloric intake as ethanol, whereas, FAF and RIP were decreased at 35%. These results are in agreement with the short-term animal studies and cell culture studies in that they suggest that ethanol is not toxic to bone cells.

We performed an additional study investigating the long-term effects of very low doses of ethanol (< 3% caloric intake) on bone histomorphometry. Initial analysis has not detected consistent dose-related changes suggesting that there is a threshold dose. Further investigation is warranted (data not shown).

Task 5

The goal of this task was to determine the effects of ethanol on the skeletal adaptation to resistance exercise training. We performed a long-term (2 month) study using a published protocol (14). The results are shown in Table 7. As expected, ethanol (35% caloric intake) had detrimental effects on bone histomorphometry. Ethanol clearly antagonized the beneficial effects of resistance exercise (weight training) on cancellous bone. This study was recently completed and the results are undergoing additional analysis prior to submission for publication.

Task 6

The goal of this Task was to determine the effects of ethanol on skeletal adaptation to normal weight bearing following unloading. Members of Dr. Turner's laboratory performed a hindlimb

unloading study in Dr. Emily Morey-Holton's laboratory at NASA-Moffett Field in order to transfer expertise in using this model system to Mayo. Mayo engineering has constructed a prototype hindlimb unloading cage. The design has received approval and 30 cages were manufactured.

We performed a preliminary study to validate the method in our laboratory. As anticipated, hindlimb unloading for two weeks resulted in decreased bone formation and bone loss (Table 1, Experiment 15). We completed a second study to determine the combined effects of ethanol and hind limb unloading on bone metabolism in 6-month-old male rats (Table 1, Experiment 16). We have performed the two week long unloading portion of the study and have analyzed cortical bone histomorphometry. These studies show that alcohol and disuse have independent additive detrimental effects on the skeleton and have been accepted for publication. The details of these studies are described in Appendix 7.

Task 7

The goal of this Task was to determine the effects of ethanol on the skeletal adaptation to treadmill running. The treadmill running equipment was procured and tested.

We have completed a 4-month-long animal study and have performed histomorphometry and biochemical measurements (Table 1 Experiment 11). Briefly, we have found that ethanol results in highly detrimental effects on the skeleton of exercising rats. The experimental design and results are described in detail in Appendix 8 which is now published. These findings suggest that the risk for fracture attributable to vigorous exercise is greatly enhanced by ethanol.

Task 8

The goal of Task 8 was to determine the effects of prior consumption of ethanol on PTH-induced increases in mRNA levels for bone matrix proteins. We have performed three studies (Table 1; Experiment 10, 12, and 13).

The effects of administration of ethanol (1.2 g/kg) or water 6 hr prior to administration of PTH or vehicle on steady state mRNA levels for bone matrix proteins (Experiment 10) are shown in Table 8. Shown also is the effect of simultaneous administration of ethanol and PTH. Ethanol followed by PTH resulted in a decrease in mRNA levels for Type 1 collagen. Ethanol alone and simultaneous administration of ethanol and PTH resulted in significant decreases in mRNA levels for osteonectin. Simultaneous administration of ethanol and PTH also reduced mRNA levels for osteocalcin.

One study (Experiment 12) investigated the effects of concurrent daily administration of alcohol and PTH. Alcohol was administered orally to simulate moderate drinking (1 g/alcohol/kg body weight). Moderate alcohol did not antagonize the stimulatory effects of PTH on steady-state mRNA levels for bone matrix proteins.

Another study (Experiment 13) investigated the effects of prior consumption of ethanol on PTH-induced increases in bone matrix proteins. Alcohol was administered to rats in their diet (36%

caloric intake) for one week prior to administration of alcohol (80 μg/kg/d for one week). Alcohol feeding was continued during the PTH treatment interval. Alcohol treatment significantly reduced the anabolic effects of PTH on osteoblast number and bone formation (see Appendix 5 for details).

Task 8 was accomplished in Year 2. However, we performed an additional 1 week study to compare the effects of pulsatile PTH, continuous infusion of PTH and alcohol on gene expression in the skeleton. Pulsatile PTH increases bone formation and bone mass, and is being investigated as a treatment for osteoporosis. Continuous PTH is a model for chronic hyperparathyroidism which causes severe bone disease. Using micro gene arrays, a technology that was not available when this proposal was submitted, we identified genes that were differentially expressed by the 3 treatments. By performing subtractive hybridixation of RNA from rats treated with continuous and pulsatile PTH we hope to determine the genes responsible for the anabolic and catabolic effects of PTH. Similarly, by performing subtractive hybridization of RNA from rats treated with ethanol alone, pulsatile PTH alone and a combination of PTH and ethanol we hope to identify the genes responsible for the detrimental effects of alcohol. Using this approach, we have identified that the probable causative factor for osteitis fibrosa is over-expression of platelet derived growth factor-A (PDGF-A) (see Appendix 9 for details). This finding is relevant to this project because PDGF may also play a role in the etiology of alcohol-induced liver disease.

Task 9

The goal of this task was to determine the effects of PTH-induced increases in osteoblast number and bone formation. Moderate alcohol consumption had not effect on PTH-induced increases in bone formation and osteoblast number. In contrast, chronic alcohol abuse reduced bone formation and osteoblast number and antagonized the PTH induced increases in bone formation and osteoblast number. The details of the experimental design, results and interpretation of these studies can be found in Appendix 5.

An additional *in vitro* study was performed to determine whether the inhibitory effects of alcohol on bone cell number and activity is due to a direct toxic action on the osteoblast. These results demonstrate that relevant concentrations of alcohol have little or no direct effects on osteoblast proliferation or expression of differentiated function. The details of these studies can be found in Appendix 3.

Task 10

The goal of this task was the submission of a final report. This document completes that task.

KEY RESEARCH ACCOMPLISHMENTS

The detrimental effects of chronic alcohol abuse on the skeleton of humans and laboratory animals are well established (2-10). The present studies demonstrate that even low dose rates of ethanol inhibit bone turnover. A daily caloric intake of ethanol as little as 3% (equivalent to ~1/2

drink/day) significantly inhibited indices of bone turnover. The inhibitory effects of ethanol do not appear to be due to toxicity and thus may be reversible.

The inhibitory effects of ethanol on bone metabolism are associated with transient changes in mRNA levels for bone matrix proteins and cytokines and growth factors. Although acute ethanol treatment results in a transient rise in mRNA levels for bone matrix proteins, this effect is not accompanied by an increase in bone matrix synthesis. Indeed, chronic daily treatment with ethanol results in decreased mRNA levels for these proteins and reduced bone formation. This inhibition in bone formation is associated with decreased mRNA levels for IGF-I, an important osteoblast growth factor.

The present studies demonstrate that concurrent moderate alcohol consumption has no effect on PTH-induced bone formation, whereas chronic alcohol abuse significantly impairs the beneficial skeletal response to PTH. The PTH response, although impaired by alcohol abuse, was sufficiently robust to effectively counteract the detrimental effects of alcohol. Thus, PTH treatment may be effective in reversing alcohol-induced bone loss.

Skeletal disuse such as which occurs following an injury has highly detrimental effects on bone metabolism which result in rapid bone loss. These detrimental effects were accentuated by ethanol. In contrast, ethanol continued to have adverse effects on bone metabolism when mechanical usage was increased. We investigated two models of increased physical activity; treadmill running and weight training.

In summary, we have now shown that ethanol: 1) blunts the skeletal response to PTH, a key physiological regulator of mineral homeostasis; 2) may increase the risk of injury during rigorous exercise by inhibiting bone remodeling and reducing bone mass; and 3) accentuates the detrimental skeletal response to disuse.

REPORTABLE OUTCOMES

1. Turner RT, Wronski TJ, Zhang M, Bloomfield SA, Sibonga JD: Effects of ethanol on gene expression in rat bone: Transient dose dependent changes in mRNA levels for matrix proteins, skeletal growth factors and cytokines are followed by reductions in bone formation. Alcoholism: Clin Exp Res, 22:1591-1599, 1998.
2. Turner RT: Skeletal response to alcohol. Alcohol Clin Exp Res, 24:1693-1701, 2000.
3. Turner RT, Kidder LS, Kennedy A, Evans GL, Sibonga JD: Moderate alcohol consumption suppresses bone turnover in adult female rats. J Bone Miner Res, 16:589-594, 2001.
4. Turner RT, Maran A, Lotinun S, Hefferan T, Evans GL, Zhang M, Sibonga JD: Animal models for osteoporosis. Reviews in Endocrine and Metabolic Disorders, 2:117-127, 2001.
5. Maran A, Zhang M, Spelsberg TC, Turner RT: The dose-response effects of ethanol on the human fetal osteoblastic cell line. J Bone Miner Res 16:270-276, 2001.

6. Turner RT, Evans GL, Zhang M, Sibonga JD: Effects of parathyroid hormone on bone formation in a rat model for chronic alcohol abuse. Alcohol Clin Exp Res, 25:667-671, 2001.
7. Martin EA, Ritman EL, Turner RT: Time course and pattern of epiphyseal growth plate fusion in rat tibia. Bone, In revision.
8. Turner RT, Bolander ME, Sarkar G, An KN, Maran A, Ritman EL: Editorial: An integrated approach to assess structure to function relationships in the skeleton. J Musculoskeletal Neuronal Interactions, 2:3-8, 2001.
9. Turner RT, Sibonga JD: Effects of alcohol and estrogen on bone metabolism. Alcohol Research and Health, 25:276-281, 2001.
10. Lotinun S, Turner RT: Triazolopyrimidine (trapidil) inhibits the detrimental effects of parathyroid hormone in an animal model for chronic hyperparathyroidism Endocrinology, Submitted.
11. Lotinun S, Sibonga JD, Turner RT: Differential effects of intermittent and continuous administration of parathyroid hormone on bone histomorphometry and gene expression. Endocrine 17:29-36, 2002.
12. Hefferan T, Kennedy AM, Evans GL, Turner RT: Disuse exaggerates the detrimental effects of alcohol on cortical bone. Alcohol Clin Exp Res, In press.
13. Reed AH, McCarty HL, Evans GL, Turner RT, Westerlind KC: The effects of chronic alcohol consumption and exercise on the skeleton of adult male rats. Alcoholism: Clin Exp Res 26:1269-1274, 2002.

CONCLUSIONS

The data obtained during the project is consistent with the concept that ethanol has profound effects on bone metabolism. Furthermore, these actions occur at lower dose rates than anticipated. Importantly, the data strongly suggests that ethanol antagonizes osteoblast function but does not appear to be toxic. This finding supports the concept that ethanol interferes with the response of bone cells to extracellular signals such as hormones and mechanical loading. These changes appear to be specific because we do not observe a uniform decrease in expression of cytokines and growth factors. We have identified two putative factors which are consistently altered by ethanol; IGF-I and TNF-α. TNF-α is increased in a dose- and time-dependent manner whereas IGF-I is decreased. These findings are of great interest because TNF-α is positively associated with bone resorption whereas IGF-I is associated with bone formation (11-13). Furthermore, IGF-I is believed to be an important intermediate in PTH as well as mechanical loading induced stimulation of bone formation. Thus, we may have identified a potential molecular mechanism for the detrimental effects of ethanol on bone remodeling.

Ethanol had negative effects on bone metabolism regardless of the level of physical activity. This disturbing result suggests that alcohol abuse, and perhaps even moderate drinking, will increase fracture risk during vigorous physical training because of a reduced capability of the skeleton to adapt to increased mechanical usage.

We have clearly shown that alcohol abuse antagonizes the skeletal response to PTH. Nevertheless, PTH was effective in increasing bone formation in alcoholic rats to values which exceeded normal. Thus, an important unanticipated finding of our research is that PTH treatment may be effective in treatment of alcohol-induced osteoporosis.

REFERENCES

1. R.T. Turner, L.S. Kidder, M. Zhang, S.A. Harris, K.C. Westerlind, A. Maran, T.J. Wronski: Estrogen has rapid tissue-specific effects on rat bone. J Appl Physiol 86:1950-1958, 1999.
2. S.R. Cummings, J.L. Kelsey, M.C. Nevitt, K.J. O'Dowd, *Epidemiol. Rev.* **7**, 178 (1985).
3. H. Spencer, N. Rubio, E. Rubio, M. Indreika, A. Seitam, *Am. J. Med.* **80**, 393 (1986).
4. D.D. Bikle, H.K. Genant, C. Cann, R.R. Recker, B.P. Halloran, G.J. Strewler, *Ann. Intern. Med.* **103**, 42 (1985).
5. B.C. Lalor, M.W. France, D. Powell, P.H. Adams, T.B. Counihan, *Q. J. Med.* **59**, 497 (1986).
6. T.C. Peng, C.W. Cooper, P.L. Munson, *Endocrinology* **91**, 586 (1972).
7. R.T. Turner, R.C. Aloia, L.D. Segel, K.S. Hannon, N.H. Bell, *Alcohol Clin. Exp. Res.* **12**, 151 (1988).
8. R.T. Turner, M. Spector, N.H. Bell, *Cell Mater.* **Suppl 1**, 167 (1991).
9. R.T. Turner, V.S. Greene, N.H. Bell, *J. Bone Miner. Res.* **2**, 61 (1987).
10. H.W. Sampson, N. Perks, T.H. Champney, B. DeFee II, *Alcohol Clin. Exp. Res.* **20**, 1375 (1996).
11. E.M. Spencer, C.C. Liu, C.C. Si, G.A. Howard, *Bone* **12**, 21 (1991).
12. E. Canalis, In Osteoporosis, R. Marcus, D. Feldman, J. Kelsey, Eds. (Academic Press, New York, 1996), pp 261-280.
13. G.R. Mundy, B.F. Boyce, T. Yoneda, L.F. Bonewald, G.D. Roodman, In Osteoporosis, R. Marcus, D. Feldman, J. Kelsey, Eds. (Academic Press, New York, 1996), pp 302-314.
14. K.C. Westerlind, J.D. Fluckey, SE Gordon, W.J. Kraemer, P.A. Farrell, R.T. Turner: *J Appl Physiol* **84**, 459 (1998).

APPENDICES

Appendix 1: Tables

Appendix 2: Turner RT, Wronski TJ, Zhang M, Bloomfield SA, Sibonga JD: Effects of ethanol on gene expression in rat bone: Transient dose dependent changes in mRNA levels for matrix proteins, skeletal growth factors and cytokines are followed by reductions in bone formation. Alcoholism: Clin Exp Res, 22:1591-1599, 1998.

Appendix 3: Maran A, Zhang M, Spelsberg TC, Turner RT: The dose-response effects of ethanol on the human fetal osteoblastic cell line. J Bone Miner Res 16:270-276, 2001.

Appendix 4: Maran A, Zhang M, Turner RT: Organ-specific effects of alcohol on gene expression. (Draft manuscript)

Appendix 5: Turner RT, Evans GL, Zhang M, Sibonga JD: Effects of parathyroid hormone on bone formation in a rat model for chronic alcohol abuse. Alcohol Clin Exp Res 25:667-671, 2001.

Appendix 6: Turner RT, Kidder LS, Kennedy A, Evans GL, Sibonga JD: Moderate alcohol consumption suppresses bone turnover in adult female rats. J Bone Miner Res 16:589-594, 2001.

Appendix 7: Hefferan T, Kennedy AM, Evans GL, Turner RT: Disuse exaggerates the detrimental effects of alcohol on cortical bone. Alcohol Clin Exp Res, In press.

Appendix 8: Reed AH, McCarty HL, Evans GL, Turner RT, Westerlind KC: The effects of chronic alcohol consumption and exercise on the skeleton of adult male rats. Alcoholism: Clin Exp Res 26:1269-1274, 2002.

Appendix 9: Lotinun S, Turner RT: Triazolopyrimidine (trapidil) inhibits the detrimental effects of parathyroid hormone in an animal model for chronic hyperparathyroidism Endocrinology, Submitted.

Appendix 1: Tables 1-8

Table 1: Summary of Experiments Performed		
Experiment #	Title	Task Number(s)
1	Dose response effects of ethanol on blood alcohol	1
2	Dose response effects of ethanol on gene expression	1
3	Effect of ethanol on proto-oncogene expression	1
4	Time course effects of ethanol on blood alcohol and gene expression	1,2
5	Effect of cyclohexamide on ethanol-induced changes in gene expression	2
6	Short-term effects of ethanol on bone matrix synthesis	2
7	Time course effects of ip delivery of ethanol on bone histomorphometry and gene expression	3
8	Effect of gavage delivery of ethanol on bone histomorphometry and gene expression	3
9	Long-term dose response effects of ethanol on bone histomorphometry and gene expression	4
10	Effect of prior consumption of ethanol on PTH-induced increases in mRNA levels for bone matrix proteins	8
11	Effects of Alcohol on Skeletal Adaptation to Treadmill Running	7
12	Effects of Concurrent Daily Administration of Moderate Alcohol and PTH on Bone Metabolism	8,9
13	Effects of Prior Consumption of Ethanol on PTH-induced Increase in Bone Matrix Proteins	8,9
14	Effects of Alcohol on Growth and Differentiation of Human Osteoblasts	9
15	Effects of Hindlimb Unloading on Bone Histomorphometry	6
16	Effect of Alcohol on the Skeletal Response to Hindlimb Unloading	6
17	Differential Effects of Pulsatile PTH, Continuous PTH and Alcohol on Gene Expression in Rat Bone	8
18	Effects of Alcohol on Resistance Training	5
19	Long-term Dose Response Effects of Very Low Doses of Ethanol on Bone Histomorphometry	4

Table 2: Time Course Effects of Ethanol on Expression of Pro- and Anti-Apoptotic Genes						
Gene	bcl-w	bcl-x	bak	bax	bcl-2	bad
Control	.007±.001	.050±.005	.040±.004	.278±.024	.186±.011	.064±.003
2 hr	.009±.001*	.052±.006	.038±.004	.280±.021	.193±.016	.057±.002
4 hr	.012±.001*	.052±.006	.038±.003	.321±.017	.213±.009	.063±.003
6 hr	.009±.001	.055±.009	.044±.005	.261±.054	.203±.014	.059±.003
8 hr	.011±.001*	.221±.163	.045±.004	.426±.106	.279±.046	.073±.011
12 hr	.009±.001	.048±.007	.037±.005	.259±.015	.193±.008	.056±.002
16 hr	.009±.001*	.041±.005	.031±.003	.295±.025	.193±.001	.068±.012
24 hr	.004±.001	.038±.005	.028±.003	.347±.041	.215±.018	.055±.006
Values are mean ± SE; n=4. *p<0.05 compared to control.						

Table 3: Lack of an Acute Effect of Ethanol and/or Cycloheximide on mRNA Levels for Bone Matrix Proteins			
Gene	Type 1 Collagen	Osteocalcin	Osteonectin
Control	.98±.13	1.16±.47	1.11±.21
Ethanol	.72±.11	1.70±.54	1.30±.31
CHX+Ethanol	1.12±.20	1.49±.48	1.34±.35
CHX	1.34±.22	1.29±.38	1.28±.30
Values are means ± SE; n=6. CHX is cycloheximide.			

Table 4: Comparative Effects of Ethanol Administered by ip Injection with Gavage on mRNA Levels for Bone Matrix Proteins, Cytokines and Growth Factors		
mRNA	i.p.	Gavage
Bone Matrix Proteins		
Osteonectin	↓ ($p < .002$)	NC
Osteocalcin	↓ ($p < .0001$)	NC
Type 1 Collagen	↓ ($p < .0002$)	NC
Cytokines and Growth Factors		
IGF-I	↓ ($p < .015$)	NC
TNF-α	NC	NC
TGF-β_1	NC	NC
TGF-β_2	NC	NC
IL-12	NC	NC
IL-1β	NC	NC
IL-Ra	NC	NC
IFN-γ	NC	NC
MIF	NC	NC
IL-6	↓ ($p < .03$)	NC
Arrow points in direction of change. NC = no change.		

Table 5: Comparative Effects of Daily Ethanol Administration for 1 Week by ip Injection with Gavage on Bone Histomorphometry		
Measurement	i.p.	Gavage
Cortical Bone		
Cross-sectional area	NC	NC
Medullary area	NC	NC
Cortical area	↓ ($p < .07$)	NC
Periosteal BFR	↓ ($p < .0003$)	NC
Periosteal MAR	↓ ($p < .001$)	NC
Periosteal MS	↓ ($p < .0002$)	NC
Cancellous Bone		
BV/TV	NC	NC
MS/BS	NC	NC
MAR	↓ ($p < .025$)	NC
BFR/BS	↓ ($p < .0025$)	NC
Cortical measurements were performed at the tibia fibula junction. Cancellous bone measurements were performed in the secondary spongiosa of the proximal tibia metaphysis. Bone formation rate (BFR), mineral apposition rate (MAR), mineralizing surface (MS), bone volume (BV), tissue volume (TV), arrow points toward direction of change. NC = no change.		

Table 6: Dose Response Effects of Long-Term (4 months) Ethanol Treatment on mRNA Levels for Pro- and Anti-apoptotic Genes		
Gene	6% Caloric Intake	35% Caloric Intake
bcl-w	NC	NC
bcl-x	↓ ($p < .025$)	NC
bak	NC	NC
bax	↓ ($p < .002$)	NC
Bcl-2	NC	NC
Bad	NC	NC
FAP	NC	↓ ($p < .015$)
RIP	NC	↓ ($p < .05$)
Arrow points in direction of change. NC = no change.		

Table 7: Effect of Ethanol on Bone Histomorphometry in Weight-Trained Rats							
					2-Way ANOVA		
Measurement	Ethanol + Exercise	Ethanol	Exercise	Control	Ethanol	Exercise	Interaction
Cancellous Bone							
BV/TV (%)	17.3±1.9	16.2±1.4	20.4±1.5	10.9±1.7	NS	P=0.005	P=0.026
Tb.Th (μm)	71.6±3.8	71.7±2.8	82.5±4.1	65.1±4.6	NS	P=0.044	P=0.044
Tb.Sp (μm)	378±38	393±49	337±25	574±57	NS	P=0.005	P=0.012
Tb.N (mm^{-1})	2.36±0.17	2.26±0.18	2.47±0.15	1.64±0.16	NS	P=0.012	P=0.044
LS/BS (%)	2.19±0.6	0.5±0.3	3.6±1.3	6.2±1.8	P=0.004	NS	NS (P=0.07)
MAR (μm/d)	0.65±0.10	0.38±0.14	0.99±0.12	1.04±0.06	P<0.001	NS	NS
BFR/BS ($\mu m^3/\mu m^2/d$)	0.017±0.005	0.003±0.002	0.042±0.015	0.064±0.020	P=0.001	NS	NS
Cortical Bone							
Cross-sectional area (mm^2)	6.90±0.15	6.69±0.11	6.70±0.11	6.56±0.17	NS	NS	NS
Medullary area (mm^2)	1.23±0.05	1.29±0.05	1.14±0.03	1.10±0.05	P=0.016	NS	NS
Cortical area (mm^2)	5.67±0.14	5.40±0.06	5.56±0.11	5.45±0.15	NS	NS	NS
LS (mm)	7.50±0.42	4.42±0.68	6.50±0.42	5.36±0.60	NS	P<0.001	NS
MAR (μm/d)	3.97±0.28	3.98±0.23	5.23±0.29	4.44±0.34	P<0.006	NS	NS
BFR (mm^2x10^{-3}/d)	30.4±3.3	18.3±3.4	34.7±3.6	24.5±4.2	NS	P=0.004	NS

Values are mean ± SE (N=7-8, non-exercised or 11-12, exercised).
Bone volume (BV); Tissue volume (TV); Trabecular (Tb); thickness (Th); Separation (Sp); Number (N); Labeled surface (LS); Bone surface (BS); Mineral apposition rate (MAR); Bone formation rate (BFR)

Table 8: The Effects of Prior and Simultaneous Ethanol Treatment on mRNA Levels for Bone Matrix Proteins in PTH-Treated Rats			
Gene	Type 1 Collagen	Osteonectin	Osteocalcin
Control	4.3±0.7	0.94±0.08	0.90±0.10
Ethanol followed by PTH	2.4±0.2*	0.73±0.09	0.59±0.09
Ethanol	2.8±0.4	0.66±0.07*	0.79±0.19
PTH	3.1±0.2	0.78±0.06	0.64±0.06
Ethanol and PTH	2.5±0.6	0.51±0.10*	0.51±0.10*
Values are mean ± SE; n = 4 *p < 0.05 compared to control			

0145-6008/98/2207-1591$03.00/0
ALCOHOLISM: CLINICAL AND EXPERIMENTAL RESEARCH

Vol. 22, No. 7
October 1998

Effects of Ethanol on Gene Expression in Rat Bone: Transient Dose-Dependent Changes in mRNA Levels for Matrix Proteins, Skeletal Growth Factors, and Cytokines Are Followed by Reductions in Bone Formation

Russell T. Turner, Thomas J. Wronski, Minzhi Zhang, Louis S. Kidder, Susan A. Bloomfield, and Jean D. Sibonga

Several studies were performed in female rats to determine dose and time course changes in mRNA levels for matrix proteins in bone after a single administration of ethanol. As expected, dose-dependent transient increases in blood ethanol were measured. Additionally, there was mild hypocalcemia with no change in immunoreactive parathyroid hormone. Coordinated dose-dependent increases in mRNA for type 1 collagen, osteonectin, and osteocalcin were noted in the proximal tibial metaphysis 6 hr after ethanol was given, with the peak values occurring at a dose of 1.2 g/kg (0.4 ml). Similar increases in mRNA levels for matrix proteins were noted in lumbar vertebrae after ethanol treatment. The changes were specific for bone; ethanol had no effect on mRNA levels for matrix proteins in the uterus or liver, although the mRNA concentrations tended to be reduced in uterus. Message levels for several cytokines implicated in the regulation of bone turnover were also assayed; mRNA levels for transforming growth factor-β_1, transforming growth factor-β_2, interferon-γ, and interleukin-6 were unchanged at doses ranging from 0.14 to 1.7 g/kg. At the highest dose of ethanol, the mRNA level for tumor necrosis factor-α was elevated while the level for insulin-like growth factor-1 was reduced. The time course effects of ethanol (0.4 ml dose) were determined in a separate experiment. Ethanol resulted in a transient increase in mRNA levels for the three bone matrix proteins assayed. However, matrix protein synthesis, as determined by incorporation of ^{3}H-proline into the proximal tibial metaphysis, was not changed after 6 hr. The changes in mRNA levels for the matrix proteins were preceded by brief, transient decreases in mRNA levels for interleukin-1β, interferon-γ, and migration inhibitory factor, and followed by a more prolonged decrease in the mRNA level for insulin-like growth factor-1. A subsequent study was performed to determine the effects of repetitive daily treatment with ethanol on rat bone. After 7 days, there were highly significant decreases in the mRNA level for type 1 collagen, as well as decreased bone formation. These results suggest that ethanol may alter bone metabolism by disturbing signal transduction pathways that regulate the expression of genes for bone matrix proteins, skeletal growth factors, and cytokines.

From the Department of Orthopedics (R.T.T., M.Z., L.S.K., J.D.S.), Mayo Clinic, Rochester, Minnesota; Department of Physiological Sciences (T.J.W.), University of Florida, Gainesville, Florida; and the Department of Health and Kinesiology (S.A.B.), Texas A&M, College Station, Texas.

Received for publication December 9, 1997; accepted June 15, 1998

This study was supported by the National Institutes of Health Grant AA11140 and by the Mayo Foundation.

Reprint requests: Russell T. Turner, Ph.D., Orthopedic Research, Room 3-69, Medical Science Building, Mayo Clinic, 200 First Street, S.W., Rochester, MN 55905.

Alcohol Clin Exp Res, Vol 22, No 7, 1998: pp 1591–1599

Key Words: Rat Bone, Matrix Proteins, Northern Analysis, RNase Protection, Osteoporosis.

BONE LOSS resulting in atraumatic fractures is a problem most commonly associated with gonadal hormone deficiency in women.[1] The development of osteoporosis in men is less frequent and is often associated with alcoholism.[2–8] Histological studies suggest that the skeletal effects of long-term alcohol abuse are characterized by decreased osteoblast activity, as well as reductions in cancellous bone volume and thickness of individual trabeculae.[5–8]

The histological evidence for disturbed bone formation is supported by consistent findings of reduced serum osteocalcin, a marker of global bone formation.[4,9–14] In contrast, the reported effects of alcohol on histological and serum measurements related to bone resorption are contradictory with evidence for no change, and decreased and increased bone resorption.[3,5–8,12,14,15] The inconsistent results may reflect differences in study populations. Also, the biochemical markers and histological indices provide an indirect assessment of bone resorption and do not reveal quantitative rate changes. In some cases, resorption markers can be influenced by changes in bone formation.[16]

The long-term detrimental effects of alcohol abuse on the skeleton have been reasonably well established. Although relevant to greater numbers of people, the possible skeletal effects of moderate alcohol consumption on bone turnover and balance are much less certain. Reports of increased bone mass in moderate drinkers, especially among postmenopausal women, are especially intriguing.[17,18]

Human studies are often difficult to interpret because the minimally invasive measurements available provide ambiguous results, as do the relatively small number of patients studied and the wide variations in age, duration, and patterns of alcohol consumption and other contributing factors within the study population. The precise skeletal effects are not known because it is difficult to distinguish the specific effects of ethanol from contributing factors, such as poor nutrition, magnesium and zinc deficiency,

reduced exercise, weight reduction, malabsorption associated with chronic pancreatitis, abnormal liver function, higher rate of cigarette smoking, and excessive use of aluminum-containing antacids.[2]

Many of the limitations of human studies can be circumvented by the use of an appropriate laboratory animal model. Alcohol intake and diet can be carefully controlled within a homogeneous laboratory animal population, and much more specific and sensitive invasive assays of bone metabolism can be performed in the laboratory animals than can be accommodated in humans. The detrimental effects of chronic high dose alcohol on mineral homeostasis and bone histomorphometry reported in rats[19–25] have been identified in alcoholics.[3–6,8,15,26–29] The commonality in the skeletal response of the two species to ethanol suggests that the rat is an appropriate model to investigate the cellular and biochemical mechanisms of action. To characterize the initial effects of ethanol on bone metabolism, we determined the dose, tissue specificity, and time-dependent changes in mRNA levels for bone matrix proteins, cytokines, and skeletal growth factors in tibial metaphysis from normal female rats. We determined the acute effects of ethanol treatment on bone matrix synthesis by measuring the incorporation of ^{3}H-proline into cancellous bone and the chronic effects of repetitive treatment by performing dynamic bone histomorphometry.

MATERIALS AND METHODS

Experiment 1—This study determined the dose-response effects of ethanol on blood alcohol. Forty-two 4-month-old female Sprague-Dawley rats were obtained from Harlan (Madison, WI) and divided randomly into 1 control and 5 treatment groups (n = 5 to 6 animals/group). The control rats were treated with saline intraperitoneally. The treatment groups received ethanol intraperitoneally at doses of 0.05, 0.1, 0.2, 0.4, and 0.6 ml (0.14 to 1.7 g/kg body weight) diluted with saline to make a total volume of 1 ml. One hour later, the rats were anesthetized with CO_2 gas, bled by cardiac puncture, and sacrificed by decapitation.

Experiment 2—This study determined the dose-response effects of ethanol on mRNA levels for matrix proteins and cytokines. The experiment was identical to experiment 1, except that the rats were sacrificed 6 hr after treatment; and, after sacrifice, the uteri, liver, and tibias were quickly excised, cleaned of adherent tissues, and frozen in liquid N_2. Tissues were stored frozen at −84°C until processed for RNA isolation.

Experiment 3—This study determined the time course for the effects of ethanol on gene expression in bone. Rats were randomly divided into 1 saline-treated control and six ethanol-treated groups; the latter received 0.4 ml (1.2 g/kg) of ethanol and were sacrificed 2, 4, 6, 8, 12, and 16 hr later (n = 5 to 6, except at 12 hr where n = 10). Before sacrifice, the rats were bled for measurement of ethanol, immunoreactive parathyroid hormone (*i*PTH), and total serum calcium. Uteri, tibias, and liver were excised and stored as described for RNA analysis. In addition, the first and second lumbar vertebrae were excised from the control and 6 hr time points, cleaned, and frozen in liquid N_2, and stored frozen at −84°C until processed for RNA isolation.

Experiment 4—This study determined whether the transient increases in mRNA levels for matrix proteins are associated with a corresponding increase in bone matrix synthesis. Twelve rats were randomly divided between saline-treated control and ethanol-treated groups [n = 6/group; the latter received 0.4 ml (1.2 g/kg) of the ethanol]. Six hours later, the rats were given ^{3}H-proline (L-[4,5-^{3}H]proline; 1.81 terabecquerel/mmol; Amersham Life Sciences, Arlington Heights, IL) at 50 μCi/rat in 0.05 ml (0.5% ethanol). Rats were killed 6 hr later with CO_2 gas. Tibiae were excised, and the proximal epiphysis was separated from the metaphysis by blunt dissection. Cancellous bone was isolated and ^{3}H-proline measured as described.[30]

Experiment 5—This study was performed to determine the chronic effects of daily treatment with ethanol on mRNA levels for bone matrix proteins and bone matrix synthesis. Twenty rats were randomly divided between saline-treated and ethanol-treated groups (n = 10/group). The experiment was similar to experiment 4, with the following changes: the rats received daily treatments for 7 days; the rats were given fluorochromes to label mineralizing bone surfaces on the day of treatment (calcein, 20 mg/kg) and 2 days before sacrifice (tetracycline, 20 mg/kg) by tail vein; and, after necropsy, the tibiae were placed immediately in 70% ethanol for fixation before histomorphometric analyses, whereas the femora were frozen in liquid N_2 and stored at −84°C before RNA analyses.

Serum Measurements

Serum alcohol was determined spectrophotometrically using a kit from Sigma Diagnostics (St. Louis, MO).

Serum PTH was determined using an immunoradiometric assay kit (Nichols Institute Diagnostics, San Clemente, CA).

Total serum calcium was measured by the Mayo Immunochemical Core Facility using a colorimetric assay (Catachem, Bridgeport, CT).

Isolation of RNA

The frozen proximal tibial metaphysis and lumbar vertebral body were individually homogenized in guanidine isothiocyanate using a Spex freezer mill (Edison, NJ). Total cellular RNA was extracted and isolated using a modified organic solvent method and the yields determined spectrophotometrically at 260 nM.[31] Uterus and liver were homogenized using a Tekmar (Cincinnati, OH) homogenizer and the RNA isolated as described for bone.

Northern Analysis

Ten micrograms of each sample were denatured by incubation at 52°C in a solution of 1 M glyoxal, 50% dimethyl sulfoxide, and 0.01 M NaH_2PO_4, and then separated electrophoretically in a 1% agarose gel. The amounts of RNA loaded and transferred were assessed by methylene blue staining of the membranes and hybridization with a ^{32}P-labeled cDNA for 18S ribosomal RNA.

RNA was transferred overnight via capillary action in 20× standard saline citrate (SSC) (1× SSC = 0.15 M NaCl and 0.015 M sodium citrate, pH 7.0), sodium citrate buffer to an Amersham Hybond nylon membrane (Arlington Heights, IL) and at 80°C vacuum oven for 2 hr before hybridization. Membranes were prehybridized for 1 to 2 hr at 65°C in a buffer containing 50% deionized formamide, 10% dextran sulfate, 5× SSC, 100 μg/ml of heat-denatured single-strand salmon sperm DNA, and 2× Denhardts solution. Hybridization was conducted for 80 min in a buffer containing the above ingredients in addition to a minimum of 4×10^6 cpm/ml ^{32}P-labeled cDNA for osteonectin, osteocalcin, and prepro-α2 (1) subunit of type 1 collagen (collagen).

cDNA probes were labeled by random sequence hexanucleotide primer extension using the Megaprime DNA labeling kit from Amersham (Arlington Heights, IL). Membranes were washed for 30 min at 45°C in 2× SSC and for 15 to 60 min in 0.1× SSC at 45°C. The mRNA bands on the Northern blots were quantitated by densitometric scanning using a Molecular Dynamics Phosphor Imager (Sunnyvale, CA).

The cDNA probes were: (1) rat transforming growth factor (TGF)-β, cloned in pBluescript II ks$^+$ vector (this fragment is excisable with *Hind*III and *Xba*I, and was from Lofstrand Labs., Ltd.); (2) rat osteocalcin, a gift from Dr. S. Rossi-Langen (Genetics Institute, Cambridge, MA)[32]; (3) rat collagen obtained from Lofstrand Labs., Ltd.[33]; (4) rat osteonectin[34] (a gift from Dr. G. Long, University of Vermont, Burlington, CT); and (5) rat

glyceraldehyde-3-phosphate dehydrogenase (GAP), a gift from Dr. P. Fort (Laboratorie de Biologie Moleculaire, Montpeller, France).[35]

RNase Protection Assay for Insulin-Like Growth Factor-1 (IGF-1) mRNA

IGF-1 is an important osteoblast growth factor. The RNAse protection procedure to measure IGF-1 mRNA levels was performed using the RPA II kit (Ambion, Austin, TX) as recommended by the manufacturer. Briefly, a 226 bp fragment of rat IGF-I cDNA was synthesized by reverse transcriptase-polymerase chain reaction from rat liver RNA using oligonucleotide primers with the following sequences: CAGAATTCGCCGGACCAGAGACCCTTTG and CAGGATCCCCCGGATGGAACGAGCTGAC. These primers contain *Eco*RI and *Bam*HI sites and 20 bp sequences from exons 3 and 4 of the rat IGF-I gene, respectively. The resultant cDNA fragment was cloned into the *Eco*RI and *Bam* HI sites of the SK Bluescript vector (Stratagene). A 293 nucleotide antisense RNA probe was synthesized and labeled with ^{32}P-UTP by in vitro transcription using 100 ng of IGF/SK vector (linearized with *Eco*RI) and T3 polymerase. Similarly, a GAP antisense probe was synthesized using the provided template (Ambion). The antisense RNA probes were purified by DNase digestion of the template, followed by G-50 gel filtration. The purified antisense RNA probes (6×10^4 cpm) were hybridized for 18 hr at 43°C in 20 μl of hybridization buffer [80% deionized formamide, 100 mM sodium citrate (pH 6.4), 300 mM sodium acetate (pH 6.4), and 1 mM EDTA] containing bone RNA (10 or 20 μg). The hybridized RNA was digested with 0.5 units of RNase A and 20 units of RNase T1 for 30 min at 37°C, then ethanol-precipitated, and resuspended in 8 μl of gel loading buffer (95% formamide, 0.025% xylene cyanol, 0.025% bromophenol blue, 0.5 mM EDTA, and 0.025% sodium dodecyl sulfate). The RNase-digested samples were then fractionated by urea-polyacrylamide [50% urea (w/v), 7% acrylamide (w/v), 45 mM Tris base, 45 mM boric acid, and 2 mM EDTA, pH 8.0 gel electrophoresis. The polyacrylamide gel was vacuum-dried and placed on a Phosphor Imager screen for 18 hr. Quantitation of protected IGF-I RNA fragments was performed by Phosphor Imager analyses and normalized to GAP.

RNase Protection Assays for Cytokines

We measured mRNA concentrations of cytokines that have been implicated in the regulation of bone formation (TGF-β_1 and TGF-β_2) and bone resorption [interleukin (IL)-1α, IL-6, tumor necrosis factor (TNF)-α, and interferon (IFN)-γ]. We measured mRNA concentrations for additional cytokines, which have not been associated with regulation of bone metabolism, to evaluate the specificity of the skeletal response to ethanol. RNase protection assays (Pharmingen, San Diego, CA) were used to measure steady-state mRNA levels for IL-1α, IL-1β, IL-1 receptor antagonist, IL-6, IL-10, IL-12 (p35 and p40), IFN-β, IFN-γ, macrophage migration inhibitory factor (MIF), TNF-α, TNF-β, lymphotoxin-β, TGF-β_1, TGF-β_2, ribosomal structure protein L32 (L32), and GAP. The tissue specificity of cytokine expression was determined by comparing RNase protection assays of RNA isolated from the bone and uterus of normal rats. Quantitation of protected RNA fragments was performed by Phosphor Imager analyses and normalized to L32 or GAP levels.

Bone Histomorphometry

Histomorphometric measurements were performed with a semiautomatic image-analysis system that has been described in detail.[36] The metaphysis was dehydrated, embedded without demineralization, and sectioned as described.[30] Measurements were performed at a standard sampling site[30] using unstained 5-μm-thick sections. Measurements have been described[30] and consisted of total cancellous bone perimeter, double-labeled perimeter, and mean distance between the two fluorochrome labels. The bone formation rate (perimeter referent) was calculated as the double-labeled perimeter multiplied by the mineral apposition rate and divided by the total bone perimeter. Mineral apposition rate was calculated as the mean distance between the two fluorochrome labels divided by the labeling interval, which was 5 days.

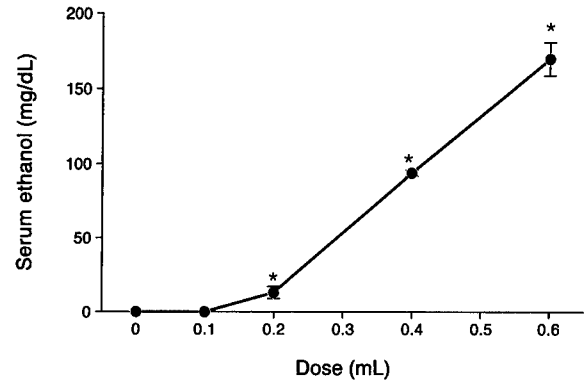

Fig. 1. Dose-response effects of administered ethanol on serum ethanol 1 hr later. Values are means ± SE; n = 4–5/group. *$p < 0.01$, compared with saline-treated control.

Table 1. Time Course for Effects of Ethanol (0.4 ml) on Serum Chemistry

Time (hr)	Ethanol (mg/dl)	Calcium (mg/dl)	*i*PTH (ng/ml)
0	—	11.6 ± 0.2	198 ± 44
1	94 ± 2*	11.0 ± 0.1	175 ± 65
2	55 ± 14*	11.1 ± 0.2	115 ± 20
4	—	10.7 ± 0.2*	167 ± 39
6	—	11.3 ± 0.1	214 ± 74
8	—	10.9 ± 0.2*	288 ± 30
12	—	10.2 ± 0.3*	210 ± 43
16	—	10.6 ± 0.2*	196 ± 29

Values are means ± SE; n = 5–6, except 12-hr time point where n = 10.
—, values below the detection limit.
*$p < 0.05$ vs. 0 time.

Statistical Analysis

To establish significance, we performed a one-way ANOVA with Fisher's protected least significant difference post-hoc multiple comparison. Treatment groups were compared with the saline-treated group.

RESULTS

The dose-response and time-course changes in serum ethanol are shown in Fig. 1 and Table 1, respectively. Blood alcohol was not detected 1 hr after administration of 0.05 ml and 0.1 ml of ethanol. Higher doses of ethanol resulted in a progressive increase in blood alcohol to 170 mg/dl at the 0.6 ml (1.7 g/kg) dose. Administration of 0.4 ml (1.2 g/kg) of ethanol resulted in a blood alcohol value of 94 mg/ml at 1 hr; blood alcohol was not detected at this dose after 2 hr.

The time course for changes in total serum calcium and *i*PTH after a dose of 0.4 ml of ethanol are shown in Table 1. Administration of this dose resulted in mild hypocalcemia; blood calciums were significantly decreased at 4, 8, 12, and 16 hr posttreatment. Ethanol did not result in significant changes in serum *i*PTH at any time point sampled.

Representative Northern analyses for type 1 collagen and 18S RNA, as well as RNase protection assays for selected cytokines and growth factors, are shown in Fig. 2. Northern and RNase protection analyses revealed that ethanol treatment had no effect on mRNA levels for GAP, L32, and 18S RNA in the bone or uterus (data not shown). Northern analyses detected high levels of expression of

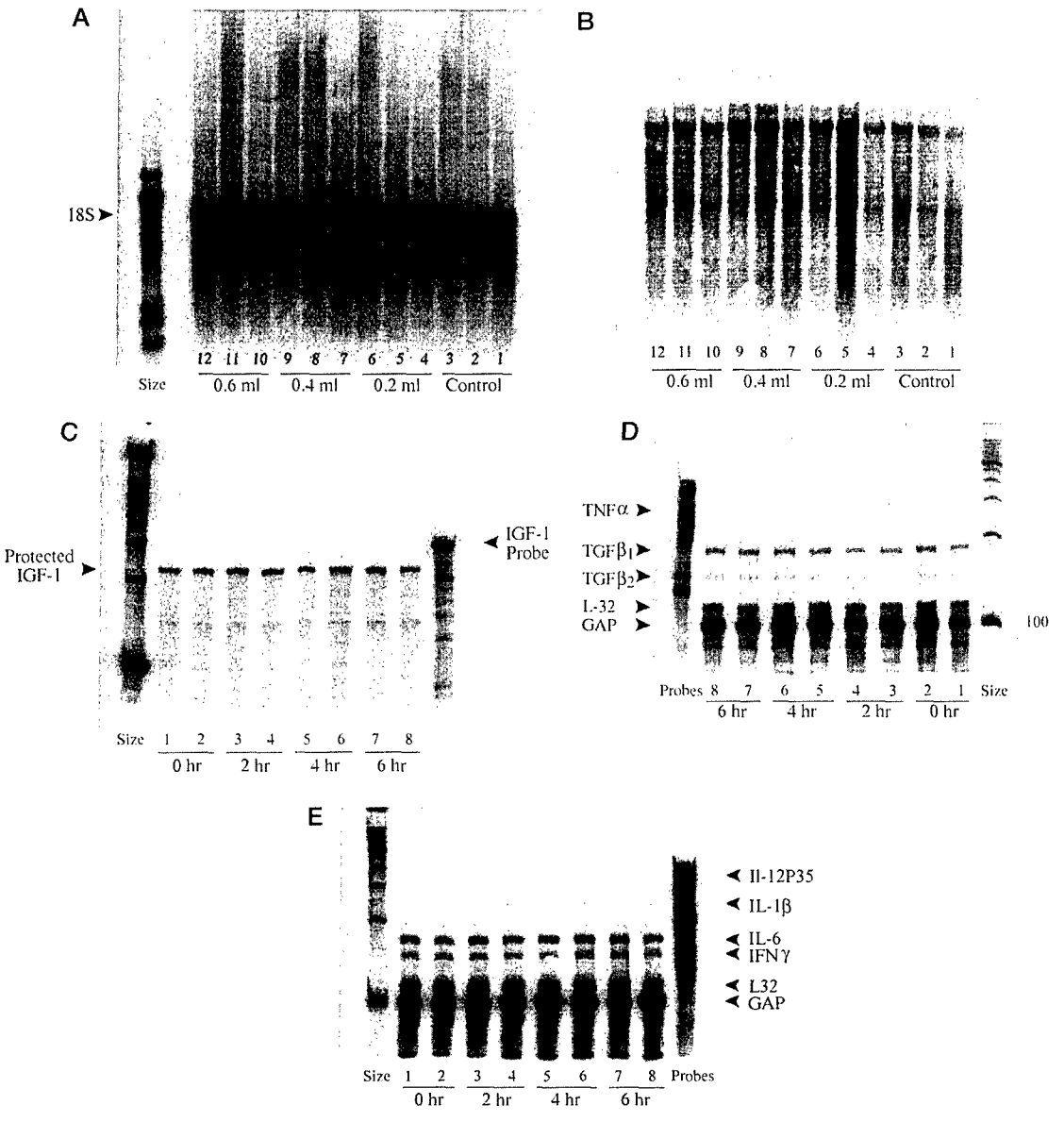

Fig. 2. Representative phosphor images of Northern blot analyses as well as RNase protection assays. (A) Representative Northern analyses for 18S ribosomal RNA. Ten micrograms of total cellular RNA were added to each lane and separated electrophoretically before transfer to a membrane and hybridization with a cDNA probe for 18S. The RNA in each lane was from a different animal. The results contribute to the data showing no effect of increasing doses of alcohol on 18S. (B) Northern analyses for collagen. The same membrane as in (A) was hybridized with a cDNA probe for collagen. Quantitative results from multiple similar assays are summarized in Figs. 3–5. (C) RNase protection assay for IGF-1. Ten micrograms of total cellular RNA were hybridized with a riboprobe for IGF-1 and treated with RNase before electrophoresis. Size refers to size markers. The last lane to the right shows the size of the undigested probe. Results from multiple quantitative similar assays are summarized in Figs. 6 and 7. (D) RNase protection assay showing GAP, L32, TGF-β_1, TGF-β_2, and TNF-α. Quantitative results of multiple similar assays are summarized in Figs. 6 and 7. (E) RNase protection assays showing GAP, L32, IFN-γ, IL-6, IL-β, and IL-12 P35. Quantitative results of multiple similar assays are shown in Figs. 6 and 7.

collagen and osteonectin in the bone and uterus of normal rats, but we did not detect mRNA for these matrix proteins in the liver. As expected, osteocalcin was detected in bone, but not in the uteri or liver from either control or ethanol-treated rats. We did not measure mRNA levels for cytokines in the liver. TGF-β_1, TGF-β_2, IGF-1, IL-6, and IFN-γ mRNAs were easily detected in extracts of total cellular RNA from tibial metaphysis using RNase protection assays. With the exception of IFN-γ, which was not detected, mRNAs for each of these cytokines were expressed in the uterus. Low message levels of IL-1β, IL-12, MIF, and TNF-α were also detected in extracts from the bone and uterus. We did not detect the mRNAs for TNF-β, IL-1α, IL-1 receptor antagonist, IL-10, or IFN-β in rat bone from either control or ethanol-treated rats. In contrast, mRNAs for TNF-β and IL-1α were detected in the uterus.

The effects of ethanol on mRNA levels for matrix proteins in tibial metaphysis, liver, and uterus were determined 6 hr after administration of alcohol (Fig. 3). The effects of ethanol on matrix protein message levels were tissue-specific. No significant changes in collagen or osteonectin were detected in the uterus, although ethanol treatment

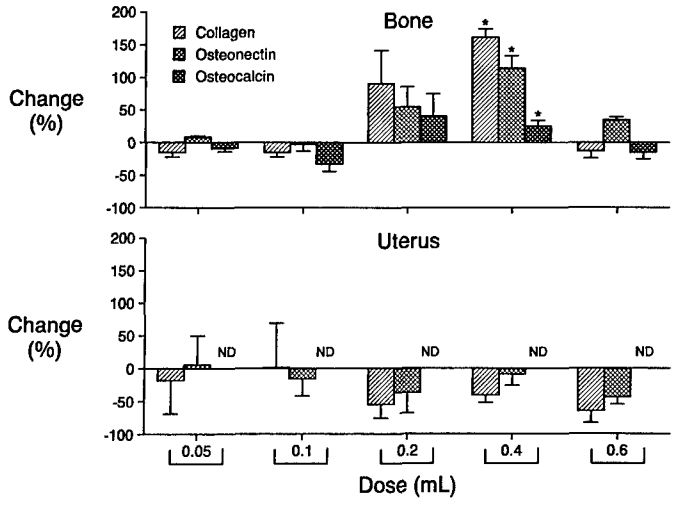

Fig. 3. Dose-response effects of ethanol on steady-state mRNA levels for matrix proteins in the bone and uterus. Tissues were retrieved 6 hr after administration of 0.05 to 0.6 ml (0.15 to 1.7 g/kg) of ethanol. Values are means ± SE; n = 4–5/group. ND, not detected. *$p < 0.005$ vs. 0 dose.

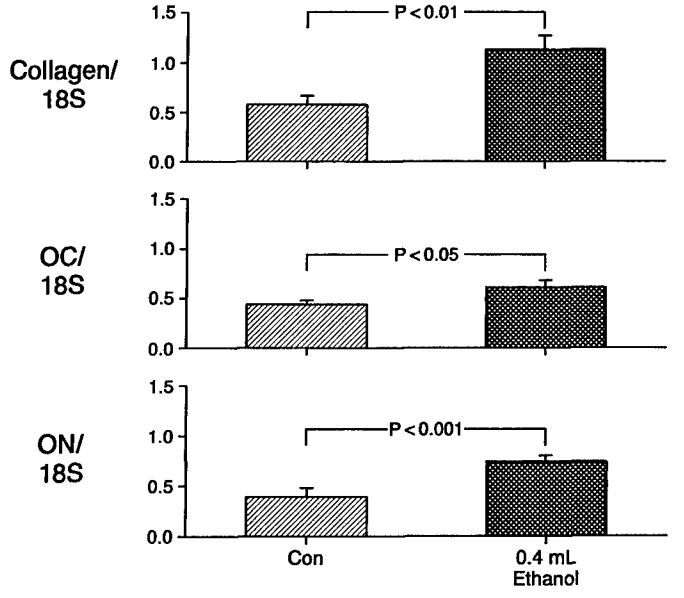

Fig. 4. Ethanol increases steady-state mRNA levels for matrix proteins in vertebrae 6 hr after intraperitoneal administration of 0.4 ml of alcohol. Values are means ± SE; n = 4–5. OC, osteocalcin; ON, osteonectin; Con, control.

tended to reduce the values. mRNA levels for collagen, osteocalcin, and osteonectin were below the detection limits in the liver of all ethanol-treated rats. In contrast, ethanol treatment resulted in coordinated dose-dependent increases in mRNA levels for collagen, osteocalcin, and osteonectin in tibia, the increases in mRNA levels for collagen (maximum increase of 162%), osteocalcin (maximum increase of 41%), and osteonectin (maximum increase of 115%) occurred at doses of 0.2 to 0.4 ml (0.6 to 1.2 g/kg). Ethanol resulted in similar increases in the mRNA levels for bone matrix proteins in lumbar vertebrae (Fig. 4).

The time course for changes in mRNA levels for bone matrix proteins after administration of 0.4 ml (1.2 g/kg) of ethanol are shown in Fig. 5. Ethanol treatment resulted in

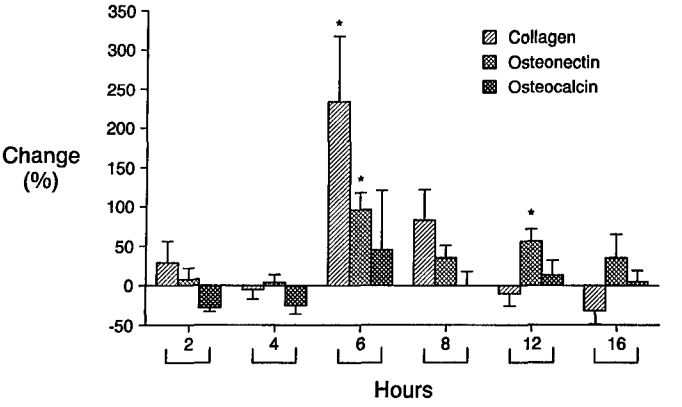

Fig. 5. Time-course effects of intraperitoneal administration of 0.4 ml (1.2 g/kg) of ethanol on steady-state mRNA levels for matrix proteins in bone. Values are means ± SE; n = 4–5/group. *$p < 0.005$ vs 0 time.

a transient increase in the message level for collagen in the tibia with the maximum increase of 234% occurring after 6 hr. The maximum increase in the mRNA level for the osteonectin gene also occurred after 6 hr, but the message level for osteonectin declined more slowly than collagen. The maximum increase in osteocalcin mRNA of 45% was similar in experiment 2, but it just failed to achieve statistical significance. There was no significant difference (p = 0.50; n = 5 to 6/group) in ^{3}H-proline incorporation into proximal tibial metaphysis between ethanol-treated (297 ± 61 cpm/mg) and solvent-treated (253 ± 28 cpm/mg) rats when the labeled amino acid was administered 6 hr after ethanol treatment.

The dose- and time-dependent effects of ethanol treatment on mRNA levels for cytokines and growth factors expressed in the proximal tibial metaphysis are shown in Figs. 6 and 7, respectively. The mRNA level for TNF-α was increased 6 hr after treatment at the highest two doses of ethanol, and the mRNA level for IGF-1 was decreased at the highest dose. No other significant changes were detected. The time course study revealed that the mRNA levels for IL-1β, IFN-γ, and MIF were significantly reduced

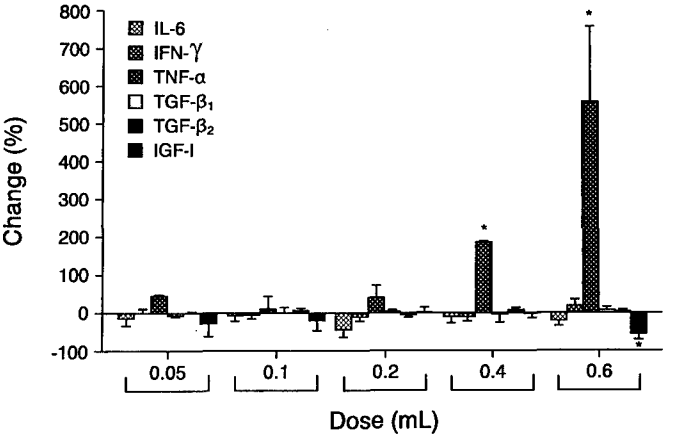

Fig. 6. Dose-response effects of ethanol on steady-state mRNA levels for growth factors and cytokines in bone. Values are means ± SE; n = 4–5/group. *p <0.05 vs 0 dose.

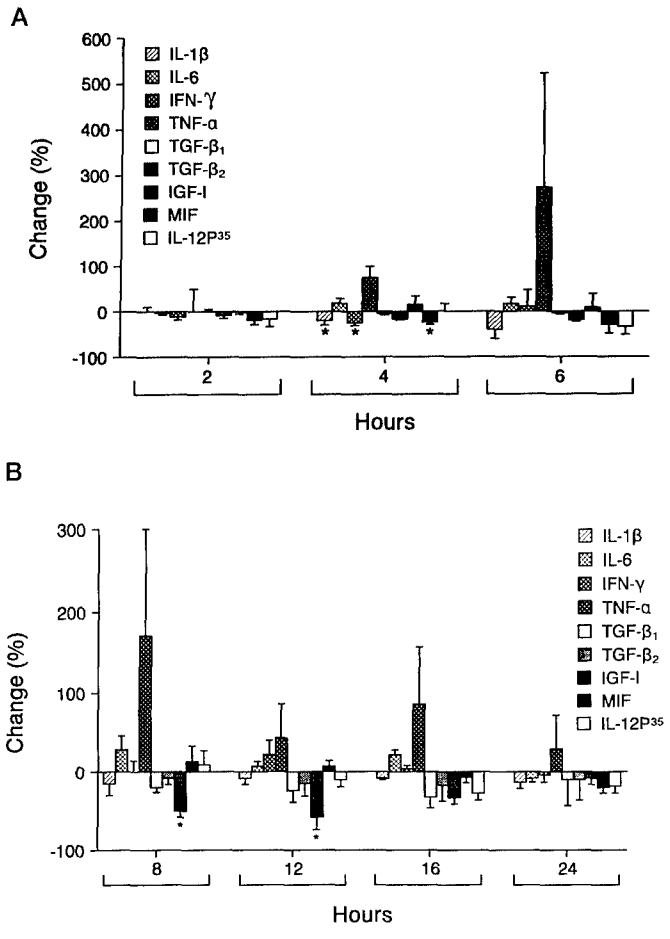

Fig. 7. Time-course effects of ethanol on steady-state mRNA levels for cytokines and growth factors in proximal tibial metaphysis. (A) 2–6 hr. (B) 8–24 hr. Values are means ± SE; n = 4–5/group. *$p < 0.05$ vs 0 time.

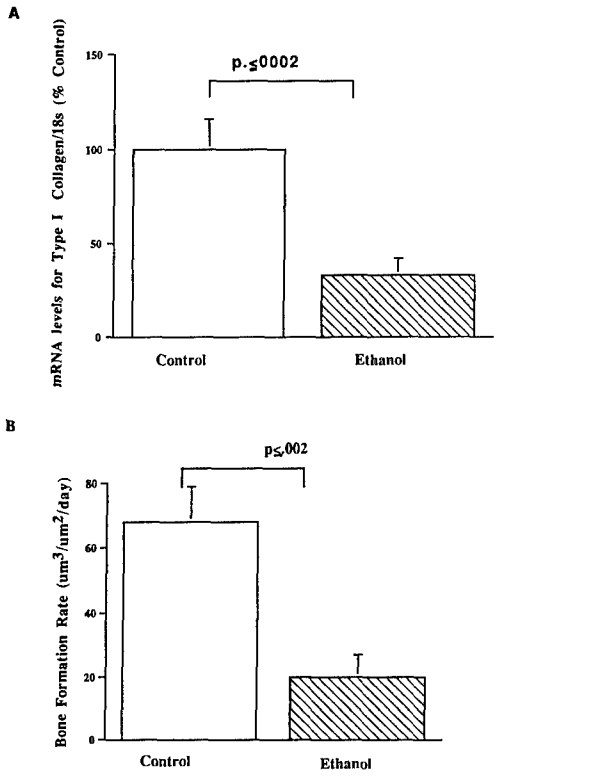

Fig. 8. Effects of chronic daily intraperitoneal administration of 0.4 ml (1.2 g/kg) of ethanol on (A) steady-state mRNA levels for type 1 collagen and (B) calculated bone formation rate. Values are means ± SE; n = 6 for mRNA levels and 8–10 for bone histomorphometry.

4 hr after ethanol treatment (0.4 ml dose). Also, the level of IGF-1 mRNA was significantly reduced at 8 and 12 hr. No other significant changes were detected, although there was a strong tendency for an increase in mRNA levels for TNF-α from 4 to 16 hr after ethanol treatment.

The effects of repetitive daily treatment with ethanol on mRNA levels for type 1 collagen, the major bone matrix protein, and bone matrix deposition are shown in Fig. 8. Ethanol resulted in a significant (−67%) decrease in the steady-state mRNA levels for type 1 collagen and a similar decrease in the calculated bone formation rate (−70%).

DISCUSSION

Acute treatment with ethanol resulted in very rapid, highly coordinated, transient increases in mRNA levels for bone matrix proteins. These findings, which were observed at two different skeletal sites in the rat, contrast with the marked inhibition of biochemical and histological indices of bone formation reported in alcoholics[3–6,9–14] and rats[21–25] fed high concentrations of alcohol in their diet. The large magnitude of this initial response may be better appreciated by comparing the observed changes after ethanol treatment to the response to physiological regulators of bone metabolism. The ethanol-induced changes in mRNA levels for bone matrix proteins are similar or greater in magnitude to changes initiated by PTH, growth hormone, estrogen, and mechanical usage.[30,36–41]

Rats fed diets in which ethanol contributed at least one-third of the caloric intake developed skeletal abnormalities, consisting of depressed bone formation, cortical and cancellous osteopenia, and reduced bone strength.[23–25] Additionally, ethanol-treated rats developed hypocalcemia and hypomagnesia, disturbed vitamin D metabolism,[19,22] and resistance to PTH-induced increases in serum calcium.[20] Each of these alterations in bone and mineral metabolism have subsequently been reported in humans.[26–29] The marked similarities between the laboratory animal model and humans suggest that the present findings may be relevant to people.

There is no universally accepted standard for moderate alcohol consumption. However, rats and humans with blood levels of ethanol in excess of 100 mg/dl are functionally impaired. The blood levels of ethanol (20 to 90 mg/dl), which were associated with increased mRNA levels for bone matrix proteins, are lower and potentially relevant to nonalcohol-dependent drinkers.

There is a very strong correlation in longer term studies in normal growing rats between collagen mRNA levels and bone matrix synthesis.[42,43] The association between the two measurements was maintained after treatments that alter

bone turnover and bone balance, including ovariectomy,[36] spaceflight,[37] estrogen treatment,[38] growth hormone treatment,[39] and PTH treatment.[40,41] The observed changes in mRNA levels in the present acute studies apparently do not reflect acute changes in bone matrix synthesis. In contrast, repetitive daily administration of ethanol at 1.2 g/kg lead to reduced concentrations of the mRNAs for type 1 collagen, the principal bone matrix protein, and depressed bone formation of similar magnitudes.

The observed tissue specificity and coordinated regulation of message levels for three of the major bone matrix proteins suggest that ethanol is activating a osteoblast-specific intracellular regulatory pathway. PTH is recognized as one of the most potent stimulators of bone matrix protein expression and was considered as a candidate for the putative alcohol-regulated systemic factor.[40,41] We did not, however, detect changes in serum *i*PTH, and recent studies performed in our laboratory indicate that ethanol- and PTH-induced increases in mRNA levels for bone matrix proteins follow much different time courses (Turner, unpublished data). Therefore, it is unlikely that ethanol is activating the PTH-mediated signaling pathway.

Alternatively, ethanol may influence the signaling pathway for cytokines and peptide hormones by altering the biophysical properties of the cell membrane. Farley et al.[44] reported that ethanol alters the sensitivity of bone cells to growth factors by increasing cell membrane fluidity. Thus, the observed transient increases in expression of bone matrix proteins may have been due to an increased responsiveness of osteoblasts to prevailing levels of systemic hormones and/or locally produced signaling peptides (cytokines and growth factors). These postulated alterations in cell signaling could disrupt the sensitive regulation of bone cell metabolism and lead to abnormal bone turnover. Further studies should be directed at investigating this hypothesis.

TGF-β and IGF-1 are two of the most important signaling peptides produced by cells of the osteoblast lineage. These growth factors have been shown to stimulate bone formation in vivo[45,46] and increase indices of osteoblast activity in cultured bone cells.[47,48] The present results demonstrate that the ethanol-induced increase in expression of bone matrix proteins is not associated with upregulation of message levels for either of these growth factors. The pronounced decrease in mRNA levels for IGF-1, which corresponds temporally to the transient elevation in mRNA levels for bone matrix proteins, may be relevant to the failure of ethanol to sustain elevated expression of the matrix proteins and may, in point-of-fact, represent a counterregulatory mechanism that leads to an observed decrease in mRNA levels for bone matrix proteins and bone matrix production that follows repetitive treatment with ethanol.

As discussed in recent reviews,[49,50] IL-1β, IL-6, IFN-γ, TNF-α, and IGF-1 have been implicated as important mediators of bone resorption. Although generally associated with bone formation, IGF-1 supports formation and activation of osteoclasts in cell culture.[51] When added to cultured cells or administered to laboratory animals, IL-1β, IL-6, and TNF-α generally increase resorption, whereas IFN-γ decreases resorption in organ culture.[49,50] However, IFN-γ increased resorption in rats and cured osteopetrosis in some children, suggesting that the in vivo effects of the cytokine differ from those reported in cell culture.[50] We are not aware of studies investigating the effects of MIF and IL-12 p35 on bone metabolism. Additionally, we are not aware of studies reporting the expression of these two cytokines in skeletal tissues. No changes were observed with IL-12 p35, but ethanol resulted in a rapid transient decrease in message levels for MIF. Ethanol also resulted in increases (TNF-α), decreases (IFN-γ, IGF-1, and IL-1β), and no change (IL-6) in message levels for the cytokines positively associated with bone turnover. The net effect of the changes on either bone resorption or bone formation is not yet clear.

Ethanol-induced changes in expression of matrix proteins may not be unique to bone. Moderate ethanol tended to decrease message levels for uterine matrix proteins in the current study, and these tendencies have been verified in subsequent studies (Turner, unpublished data). In the current study, mRNA levels for matrix proteins were below detectable levels in the liver. However, high doses of ethanol and acetaldehyde were reported to induce expression of type 1 collagen mRNA and protein in the liver.[52–55] Additionally, a collagen enhancer-promoter construct in transgenic mice was reported to be markedly stimulated by ethanol.[56] These changes in collagen gene expression are likely to be important because increased collagen synthesis is believed to contribute to the pathogenesis of liver fibrosis. We conclude from these comparisons of bone, uterus, and liver that the transient increases in mRNA levels for matrix proteins after acute treatment with ethanol is unique to bone.

In summary, ethanol resulted in rapid, dose-dependent, transient coordinated increases in mRNA levels for bone matrix proteins. Additionally, there were changes in expression of multiple growth factors and cytokines that influence bone turnover. These results suggest that the effects of ethanol on the skeleton are very dose-sensitive and that ethanol may alter bone mass by influencing signal transduction pathways that regulate bone metabolism.

ACKNOWLEDGMENTS

The authors thank Ms. Glenda Evans for technical assistance and Ms. Lori Rolbiecki for editorial assistance.

REFERENCES

1. Cummings SR, Kelsey JL, Nevitt MC, O'Dowd KJ: Epidemiology of osteoporosis and osteoporotic fractures. Epidemiol Rev 7:178–208, 1985

2. Spencer H, Rubio N, Rubio E, Indreika M, Seitam A: Chronic alcoholism: Frequently overlooked cause of osteoporosis in men. Am J

Med 80:393–397, 1986

3. Bikle DD, Genant HK, Cann C, Recker RR, Halloran BP, Strewler GJ: Bone disease in alcohol abuse. Ann Intern Med 103:42–48, 1985

4. Gonzalez-Calvin JL, Garcia-Sanchez A, Bellot V, Munoz-Torres M, Raya-Alvarez E, Salvatierra-Rios D: Mineral metabolism, osteoblastic function and bone mass in chronic alcoholism. Alcohol Alcohol 28:571–579, 1993

5. Lalor BC, France MW, Powell D, Adams PH, Counihan TB: Bone and mineral metabolism and chronic alcohol abuse. Q J Med 59:497–511, 1986

6. Schnitzler CM, Solomon L: Bone changes after alcohol abuse. S African Med J 66:730–734, 1984

7. Diez A, Puig J, Serrano S, Marinoso ML, Bosch J, Marrugat J, Mellibovsky L, Nogues X, Knobel H, Aubia J: Alcohol-induced bone disease in the absence of severe chronic liver damage. J Bone Miner Res 9:825–831, 1994

8. Bikle DD, Stesin A, Halloran B, Steinbach L, Recker R: Alcohol-induced bone disease: Relationship to age and parathyroid hormone levels. Alcohol Clin Exp Res 17:690–695, 1993

9. Nielsen HK, Lundby L, Rasmussen K, Charles P, Hansen C: Alcohol decreases serum osteocalcin in a dose-dependent way in normal subjects. Calcif Tiss Int 46:173–178, 1990

10. Labib M, Abdel-Kader M, Ranganath L, Teale D, Marks V: Bone disease in chronic alcoholism: The value of plasma osteocalcin measurement. Alcohol Alcohol 24:141–144, 1989

11. Rico H, Cabranes JA, Cabello J, Gomez-Castresana F, Hernandez ER: Low serum osteocalcin in acute alcohol intoxication: A direct toxic effect of alcohol on osteoblasts. Bone Miner 2:221–225, 1987

12. Laitinen K, Tahtela R, Luomanmaki K, Valimaki MJ: Mechanisms of hypocalcemia and markers of bone turnover in alcohol-intoxicated drinkers. Bone Miner 24:171–179, 1994

13. Laitinen K, Lamberg-Allardt C, Tunninen R, Harkonen M, Valimaki M: Bone mineral density and abstention-induced changes in bone and mineral metabolism in noncirrhotic male alcoholics. Am J Med 93:642–650, 1992

14. Laitinen K, Lamberg-Allardt C, Tunninen R, Karonen SL, Ylikahri R, Valimaki M: Effects of 3 weeks' moderate alcohol intake on bone and mineral metabolism in normal men. Bone Miner 13:139–151, 1991

15. Crilly RG, Anderson C, Hogan D, Delaquerriere-Richardson L: Bone histomorphometry, bone mass, and related parameters in alcoholic males. Calcif Tiss Int 43:269–276, 1988

16. Turner RT, Evans GL, Wakley GK: Spaceflight results in depressed cancellous bone formation in rat humeri. Aviat Space Environ Med 66:770–774, 1995

17. Laitinen K, Karkkainen M, Lalla M, Lamberg-Allardt C, Tunninen R, Tahtela R, Valimaki M: Is alcohol an osteoporosis-inducing agent for young and middle-aged women? Metab Clin Exp 42:875–881, 1993

18. Laitinen K, Valimaki M, Keto P: Bone mineral density measured by dual-energy x-ray absorptiometry in healthy Finnish women. Calcif Tiss Int 48:224–231, 1991

19. Peng TC, Cooper CW, Munson PL: The hypocalcemic effect of alcohol in rats and dogs. Endocrinology 91:586–593, 1972

20. Peng TC, Gitelman HJ: Ethanol-induced hypocalcemia, hypermagnesemia and inhibition of the serum calcium-raising effect of parathyroid hormone in rats. Endocrinology 94:608–611, 1974

21. Turner RT, Aloia RC, Segel LD, Hannon KS, Bell NH: Chronic alcohol treatment results in disturbed vitamin D metabolism and skeletal abnormalities in rats. Alcohol Clin Exp Res 12:151–155, 1988

22. Peng TC, Kusy RP, Hirsch PF, Hagman JR: Ethanol-induced changes in morphology and strength of femurs of rats. Alcohol Clin Exp Res 12:1655–659, 1988

23. Turner RT, Spector M, Bell NH: Ethanol induced abnormalities in bone formation, turnover, mechanical properties, and mineralization in young adult rats. Cell Mater (Suppl. 1):167–173, 1991

24. Turner RT, Greene VS, Bell NH: Demonstration that ethanol inhibits bone matrix synthesis and mineralization in the rat. J Bone Miner Res 2:61–66, 1987

25. Sampson HW, Perks N, Champney TH, DeFee II B: Alcohol consumption inhibits bone growth and development in young actively growing rats. Alcohol Clin Exp Res 20:1375–1384, 1996

26. Bikle DD, Genant HK, Cann C, Recker RR, Halloran BP, Strewler GJ: Bone disease in alcoholic abuse. Ann Intern Med 103:42–48, 1985

27. Barragry JM, Long RG, France MW, Willis MR, Boucher BJ, Sherlock S: Intestinal absorption of cholecalciferol in alcoholic liver disease and primary biliary cirrhosis. Gut 20:559–564, 1979

28. Hepner GW, Roginsky M, Moo HF: Abnormal vitamin D metabolism in patients with cirrhosis. Dig Dis 21:527–532, 1976

29. Bouillon R, Auwerx J, Dekeyser L, Fevery J, Lissens W, DeMoor P: Serum vitamin D metabolites and their binding protein in patients with liver cirrhosis. J Clin Endocrinol Metab 59:86–89, 1984

30. Westerlind KC, Wakley GK, Evans GL, Turner RT: Estrogen does not increase bone formation in growing rats. Endocrinology 133:2924–2934, 1993

31. Chomczynski P, Sacchi N: Single-step method of RNA isolation by acid guanidinium thiocyanate-phenol-chloroform extraction. Anal Biochem 162:156–159, 1987

32. Celeste AJ, Rosen V, Buecker JL, Kriz R, Wang EA, Wozney JM: Isolation of the human gene for the bone gla protein utilizing the mouse and rat cDNA clones. EMBO J 5:1885–1890, 1986

33. Genovese C, Rowe D, Kream B: Construction of DNA sequences complementary to rat α1 and α2 collagen mRNA and their use in studying the regulation of type 1 collagen synthesis by 1,25-dihydroxyvitamin D. Biochemistry 23:6210–6216, 1984

34. Villarreal XC, Mann KG, Long GL: Structure of human osteonectin based upon analysis of cDNA and genomic sequences. Biochemistry 28:6483–6491, 1989

35. Fort P, Marty L, Piechaczyk M, el Sabrouty S, Dani C, Jeanteur P, Blanchard JM: Various rat adult tissues express only one major mRNA species from the glyceraldehyde-3-phosphate dehydrogenase multigenic family. Nucleic Acids Res 13:1431–1442, 1985

36. Cavolina JM, Evans GL, Harris SA, Zhang M, Westerlind KC, Turner RT: The effects of orbital spaceflight on bone histomorphometry and mRNA levels for bone matrix proteins and skeletal signaling peptides in ovariectomized growing rats. Endocrinology 138:1567–1576, 1997

37. Backup P, Westerlind K, Harris S, Spelsberg TC, Kline B, Turner RT: Spaceflight results in reduced mRNA levels for tissue specific proteins in the musculoskeletal system. Am J Physiol 266:E567–E573, 1994

38. Turner RT, Colvard DS, Spelsberg TC: Estrogen inhibition of periosteal bone formation in rat long bones: Down regulation of gene expression for bone matrix proteins. Endocrinology 127:1346–1351, 1990

39. Kidder LS, Schmidt IU, Evans GL, Turner RT: Effects of growth hormone and low dose estrogen on bone growth and turnover in long bones of hypophysectomized rats. Calcif Tissue Int 61:327–335, 1997

40. Schmidt I, Dobnig H, Turner RT: Intermittent parathyroid hormone treatment increases osteoblast number, steady-state mRNA levels for osteocalcin and bone formation in tibial metaphysis of hypophysectomized female rats. Endocrinology 136:5127–5134, 1995

41. Dobnig H, Turner RT: Evidence that intermittent treatment with parathyroid hormone increases bone formation in adult rats by activation of bone lining cells. Endocrinology 136:3632–3638, 1995

42. Turner RT, Spelsberg TC: Correlation between mRNA levels for bone cell proteins and bone formation in long bones of maturing rats. Am J Physiol 261:E348–E353, 1991

43. Turner RT, Kapelner S, Spelsberg TC: Tissue specific expression of bone proteins in femora of growing rats. Am J Physiol 263:E724–E729, 1992

44. Farley JR, Fitzsimons R, Taylor AK, Jorch UM, Lau KH: Direct effects of ethanol on bone resorption and formation in vitro. Arch Biochem Biophys 238:305–314, 1985

45. Spencer EM, Liu CC, Si CC, Howard GA: In vivo actions of insulin-like growth factor-I (IGF-1) on bone formation and resorption in rats. Bone 12:21–26, 1991

46. Noda M, Camilliere JJ: In vivo stimulation of bone formation by transforming growth factor-β. Endocrinology 124:2991–2994, 1989

47. McCarthy TG, Centrella M, Canalis E: Regulatory effects of insulin-like growth factor I and II on bone collagen synthesis in rat calvarial cultures. Endocrinology 124:301–309, 1989

48. Pfeilschifter J, D'Souza SM, Mundy GR: Effects of transforming growth factor beta on osteoblastic osteosarcoma cells. Endocrinology 121:212–218, 1987

49. Canalis E: Skeletal growth factors, in Marcus R, Feldman D, Kelsey J (eds): Osteoporosis. New York, Academic Press, 1996, pp 261–280

50. Mundy GR, Boyce BF, Yoneda T, Bonewald LF, Roodman GD: Cytokines and bone remodeling, in Marcus R, Feldman D, Kelsey J (eds): Osteoporosis. New York, Academic Press, 1996, pp 302–314

51. Mochizuki H, Hakeda Y, Wakatsuki N, Usui S, Akashi T, Sato T, Tanaka K, Kumegawa M: Insulin-like growth factor-1 supports formation and activation of osteoclasts. Endocrinology 131:1075–1080, 1992

52. Annoni G, Weiner FR, Colombo M, Czaja MJ, Zern MA: Albumin and collagen gene regulation in alcohol- and virus-induced human liver disease. Gastroenterology 98:197–202, 1990

53. Casini A, Cunningham M, Rojkind M, Lieber CS: Acetaldehyde increase procollagen type 1 and fibronectin gene expression in cultured rat fat storing cells through a protein synthesis-dependent mechanism. Hepatology 13:758–765, 1991

54. Frizell E, Abraham A, Doolittle M, Bashey R, Kresina T, Van Thiel D, Zern MA: FK506 enhances fibrogenesis in in vitro and in vivo models of liver fibrosis. Gastroenterology 107:492–498, 1994

55. Lieber CS: Alcohol and fibrogenesis. Alcohol Alcohol 1:339–334, 1991

56. Walton CM, Wu GY, Petruff CA, Clark SH, Lichtler AC, Wu CH: A collagen enhancer-promoter construct in transgenic mice is markedly stimulated by ethanol administration. Hepatology 23:310–315, 1996

JOURNAL OF BONE AND MINERAL RESEARCH
Volume 16, Number 2, 2001

The Dose-Response Effects of Ethanol on the Human Fetal Osteoblastic Cell Line

A. MARAN,[1] M. ZHANG,[1] T.C. SPELSBERG,[2] and R.T. TURNER[1,2]

ABSTRACT

Alcohol is a risk factor for the development of osteoporosis, especially in men. Chronic alcohol abuse decreases bone mass, which contributes to the increased incidence of fractures. To better understand the mechanism of action of ethanol on bone metabolism, we have studied the dose-response effects of ethanol on conditionally immortalized human fetal osteoblasts (hFOB) in culture. Ethanol treatment had no significant effects on osteoblast number after 1 day or 7 days. Ethanol treatment did not reduce type I collagen protein levels at either time point at any dose but slightly reduced alkaline phosphatase activity after 7 days. The messenger RNA (mRNA) levels for alkaline phosphatase, type I collagen, and osteonectin were unaltered by 24 h of ethanol treatment but a high dose (200 mM) reduced mRNA levels for the two bone matrix proteins after 7 days. Ethanol treatment led to dose-dependent increases in transforming growth factor β1 (TGF-β1) mRNA levels and decreases in TGF-β2 mRNA levels. The concentration of ethanol in the medium decreased with time because of evaporation but there was little degradation caused by metabolism. These results, which show that cultured osteoblasts are less sensitive than osteoblasts in vivo, suggest that the pronounced inhibitory effects of ethanol on bone formation are not caused by direct cell toxicity. (J Bone Miner Res 2001;16:270–276)

Key words: alcohol abuse, bone formation, osteoporosis, bone fractures

INTRODUCTION

CHRONIC ALCOHOL abuse is associated with pronounced detrimental effects on the musculoskeletal system. Numerous reports implicate alcohol as a major risk factor for osteoporosis, especially in men. Habitual alcohol abuse clearly results in bone loss while moderate intake of alcohol has been reported to have variable effects on bone mass, depending on age and gender.[1] However, the mechanism for the bone loss induced by alcohol is not understood. There is consensus that alcohol abuse results in decreased bone formation.[2,3] On the other hand, the effects of alcohol on bone resorption are less certain with a number of conflicting reports.[4–9]

Alcohol results in dose-dependent decreases in rat bone formation with dose rates comparable with alcoholics, leading to osteopenia.[10–13] The molecular mechanism(s) that mediates this bone loss is characterized poorly. Some studies suggest that ethanol has a direct toxic effect on osteoblasts.[14] The histological changes to bone are preceded by changes in messenger RNA (mRNA) levels for bone matrix proteins and cytokines.[12] Rapid (within 6 h) transient dose-dependent changes in expression of matrix proteins in bone have been reported in the rat, suggesting that exposure to ethanol results in reversible changes in osteoblast function. Farley et al. have shown that chemicals, including ethanol, modify membrane fluidity and alter the response of bone cells to mitogens.[15] This suggests that some of the actions of ethanol in vivo may be influenced by systemic factors, including gonadal hormones and cytokines. To better understand the mechanism of ethanol action on skeletal development, we have studied the direct effects of ethanol on

[1]Department of Orthopedics, Mayo Clinic, Rochester, Minnesota, USA.
[2]Department of Biochemistry and Molecular Biology, Mayo Clinic, Rochester, Minnesota, USA.

immortalized human fetal osteoblast (hFOB) cells[16] in culture. In these studies, hFOB cells were exposed to ethanol at concentrations corresponding to blood alcohol levels relevant to moderate drinking (10 mM; 0.046% wt/vol) and chronic alcohol abuse (50 mM; 0.23% wt/vol), as well as concentrations incompatible with human life (≧100 mM; 0.46% wt/vol).

MATERIALS AND METHODS

Cell culture and ethanol treatment

The hFOB cell line that contains the temperature-sensitive T-antigen expression vector with the neomycin resistance gene[16] was maintained at 34°C in phenol red–free Dulbecco's modified Eagle's medium (DMEM)/F12 containing 10% charcoal-stripped fetal bovine serum (FBS; Sigma Chemical Co., St. Louis, MO, USA) and supplemented with geneticin (300 μg/ml; Gibco/BRL, Rockville, MD, USA). The cells were plated into T-75 flasks at 1×10^6 cells per flask 24 h before ethanol treatment. The cells were treated with ethanol (10–500 mM) for 1 day and 7 days. During 7-day treatment, the media were changed with fresh media containing ethanol on day 4 and maintained for an additional 3 days. Cells were washed with phosphate-buffered saline (PBS) and harvested at the end of ethanol treatment for RNA analyses. The media were stored and used for type I collagen protein analyses.

Ethanol assay

Ethanol content in media was determined using a kit as per the manufacturer's protocol (Sigma Chemical Co., St. Louis, MO, USA).

RNA isolation

Total cellular RNA was extracted and isolated using a modified organic solvent method and the RNA yields were determined spectrophotometrically at 260 nM.[17]

Northern blot hybridization

Ten micrograms of each sample was denatured by incubation at 52°C in a solution of 1 M glyoxal, 50% dimethyl sulfoxide, and 0.01 M NaH_2PO4 and then separated in a 1% agarose gel. The amounts of RNA loaded and transferred were assessed by methylene blue staining of the membranes and hybridization with a [^{32}P]-labeled complementary DNA (cDNA) for 18S ribosomal RNA (rRNA). RNA that was separated in agarose gels was transferred to an Amersham Hybond nylon membrane (Amersham, Arlington Heights, IL, USA) overnight via capillary action in 20× SSC (1× SSC = 0.15 M NaCl and 0.015 M sodium citrate, pH 7.0) sodium citrate buffer. The membranes were baked in a vacuum oven at 80°C for 2 h before hybridization. Membranes were prehybridized for 2 h at 45°C in buffer containing 50% deionized formamide, 10% dextran sulfate, 5× SSC, 100 μg/ml of heat-denatured single-strand salmon sperm DNA, and 2× Denhardt's solution. Hybridization was conducted for 80 minutes in a buffer containing the previously mentioned ingredients in addition to a minimum of 1×10^6 cpm/ml [^{32}P]-labeled cDNA probe. Labeled cDNAs for alkaline phosphatase, osteocalcin, and type I collagen were used as probes. cDNA probes were labeled by random sequence hexanucleotide primer extension using the Megaprime DNA labeling kit from Amersham. Membranes were washed for 30 minutes at 65°C in 2× SSC and for 15–60 minutes in 0.1× SSC at 45°C. The resulting radioactive mRNA bands on the blots were quantitated by PhosphorImager (Molecular Dynamics, Sunnyvale, CA, USA) and normalized to 18S rRNA.

The cDNA probes were: (1) alkaline phosphatase cDNA (a gift from Dr. Gideon Rodan, Merck, Sharp, and Dohme, West Point, PA, USA); (2) type I collagen cDNA probe obtained from Lofstrand Labs, Ltd. (Gaithersburg, MD, USA)[18]; (3) osteonectin cDNA (a gift from Dr. G. Long, University of Vermont, Burlington, VT, USA)[19]; and (4) cDNA for 18S rRNA was purchased from Ambion (Austin, TX, USA).

RNAse protection assay for cytokines

We measured the mRNA concentrations of transforming growth factor β1 (TGF-β1), TGF-β2, and TGF-β3; tumor necrosis factor α (TNF-α) and TNF-β; interleukin-1α (IL-1α), IL-1β, IL-1Ra, IL-6, IL-10, and IL-12 (p35 and p40); interferon β (IFN-β) and IFN-γ; and lymphotoxin β (LT-β) by RNAse protection assays. Quantitation of protected RNA fragments was performed by PhosphorImager analyses and normalized to glyceraldehyde-3-phosphate dehydrogenase and ribosomal structural protein L32.

Type I collagen protein assay

The medium from ethanol-treated hFOB cells was collected at the end of 24 h and 7 days of ethanol treatment, centrifuged to remove debris before used for type I procollagen assays. The type I procollagen assay, which measures the propeptide portion of the molecule, reflects the synthesis of the mature form of the protein and it was carried out using Prolagen-C kit as described by the manufacturer's protocol (Metra Biosystems, Mountainview, CA, USA). The type I procollagen levels obtained were normalized to total protein concentrations that were determined by bicinchoninic acid (BCA) protein assay (Pierce, Rockford, IL, USA).

Alkaline phosphatase activity

The alkaline phosphatase activity was measured using a kit (Sigma Chemical Co.). The cells treated with ethanol were rinsed with PBS, harvested, and processed for determining the alkaline phosphatase activity. The activity was normalized to total cellular protein, which was determined by BCA protein assay.

Statistical analysis

In each experiment, three to six replicates of each treatment were measured. Unless indicated otherwise, the data represent the mean ± SE of three independent experiments.

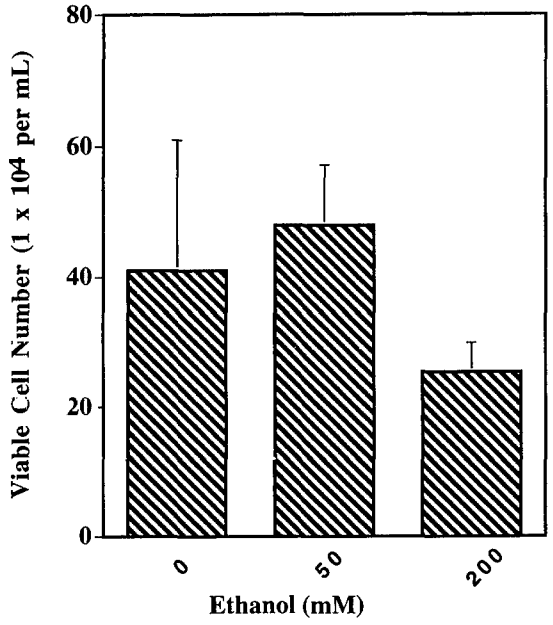

FIG. 1. Effect of 7 days of treatment of ethanol on growth of hFOB cells. Cells were treated with 0, 50, and 200 mM concentrations of ethanol. The data represent the mean ± SE of three independent experiments. No significant changes were detected.

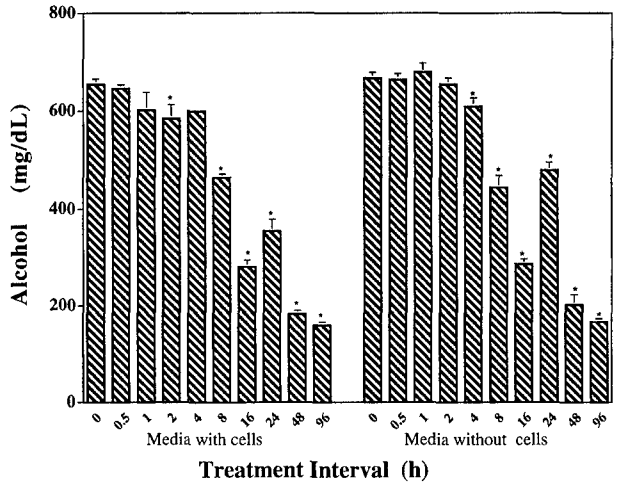

FIG. 2. Time course for ethanol present in the media. Culture dishes containing media in the presence and absence of hFOB cells were treated with 200-mM concentrations of ethanol. The data represent the mean ± SE of three independent experiments. $^*p \leq 0.05$ (compared with untreated control, by one-way ANOVA and Fisher's projected least significant difference [PLSD] analysis).

Significant differences between groups were determined by Fisher's protected least significant difference post hoc test for multiple group comparisons after detection of significance by one-way analysis of variance (ANOVA). Significance was considered at values of $p < 0.05$. Dose-response effects were analyzed by linear regression analysis.

RESULTS

Effect of ethanol on cell growth

The effect of ethanol treatment on hFOB cell growth was determined after 1-day and 1-week treatment with 0, 50, and 200 mM concentrations of ethanol. The viable cell numbers were measured by trypan blue dye exclusion assay in a hemocytometer. There were no changes in cell number after either 1 day (data not shown) or 1 week of treatment (Fig. 1).

Assay for alcohol levels

The amount of ethanol present in the media as a function of time after incubation at 34°C was determined (Fig. 2). The ethanol disappearance curves follow the same pattern in the presence and absence of cells. About 24% of the initial amount was still detectable after 4 days of incubation, the time at which replacement of new media containing ethanol was performed.

Effect of ethanol on bone matrix gene expression in cultured human osteoblasts

The dose (0–200 mM) effects of 24 h of ethanol treatment on alkaline phosphatase, osteonectin, and type 1 collagen mRNA levels studied by Northern analysis in hFOB cells in culture are shown in Fig. 3. Ethanol had no effect on steady-state mRNA levels for these markers of osteoblast differentiation and activity.

The dose (0–200 mM) effects of 7 days of ethanol treatment on alkaline phosphatase, type I collagen, and osteonectin mRNA levels are shown in Fig. 4. Ethanol had no effect on the mRNA levels for alkaline phosphatase. The type I collagen mRNA levels were significantly decreased by 46% at 200 mM. Finally, ethanol decreased the mRNA levels for osteonectin by 31% at 200 mM.

The effects of (0–200 mM) ethanol on type I collagen protein levels after 24 h and 1 week of ethanol treatment are shown in Fig. 5. The type I collagen protein levels did not change significantly after 24 h of ethanol treatment in hFOB cells in culture, whereas after 1 week, it significantly increased by 57% at 50 mM of ethanol (Fig. 5).

To determine whether the alcohol alters alkaline phosphatase activity, we measured the activity at two different doses of ethanol (50 mM and 200 mM) after 24 h and 1 week (Fig. 6.). The alkaline phosphatase activity was not significantly changed at either dose after 24 h. After 1 week of treatment, the alkaline phosphatase activity was decreased at both doses of ethanol.

Effect of ethanol on cytokines and growth factors

We studied the changes in steady-state mRNA levels for selected cytokines that have been implicated in the regulation of bone formation and resorption. We analyzed the mRNA concentrations for members of the IL family, IFNs, TNF, and TGF-β by RNAse protection assay (Table 1). Although many cytokine genes were not detectable by our assay (Table 1), there were changes in the mRNA levels of TGF-β1 and TGF-β2 (Fig. 7). The mRNA levels of TGF-β1 increased whereas that of TGF-β2 decreased with

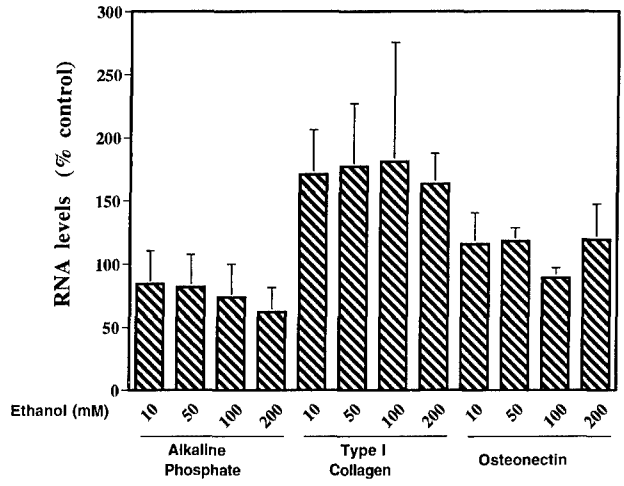

FIG. 3. Effect of ethanol at various doses after 1-day treatment on alkaline phosphatase, type 1 collagen, and osteonectin mRNA levels. Total RNA was isolated from cells treated with 0-, 10-, 50-, 100-, and 200-mM concentrations of ethanol and analyzed by Northern blot hybridization using specific cDNA probes. The radioactive signal measured by PhosphorImager analysis has been expressed as a percentage of the value obtained from untreated controls. The data represent the mean ± SE of three independent experiments. No significant changes were detected.

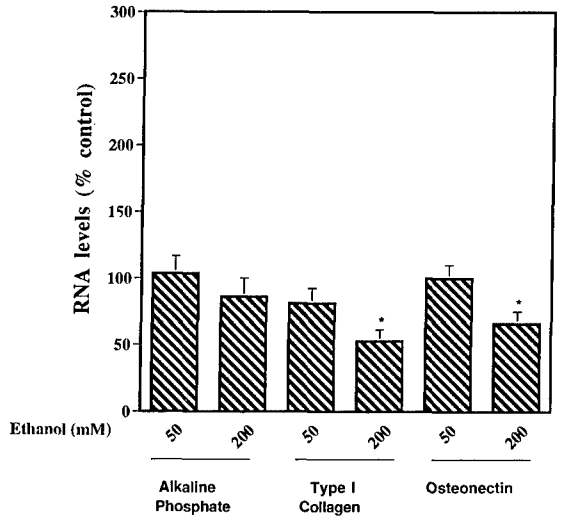

FIG. 4. Effect of ethanol at various doses after 1 week of treatment on alkaline phosphatase, type 1 collagen, and osteonectin mRNA levels. Total RNA was isolated from cells treated with 0-, 50-, and 200-mM concentrations of ethanol and analyzed by Northern blot hybridization using specific cDNA probes. The radioactive signal measured by PhosphorImager analysis has been expressed as a percentage of the value obtained from untreated controls. The data represent the mean ± SE of three independent experiments. $*p \leq 0.05$ (compared with untreated control, by one-way ANOVA and Fisher's projected least significant difference [PLSD] analysis).

increasing ethanol concentrations (Figs. 7B and 7C). Linear regression analysis revealed significant dose relationships for TGF-β1 ($R = 0.81$; $p < 0.05$) and TGF-β2 ($R = -0.50$; $p < 0.05$). TGF-β3 mRNA was not detected by this assay both in control and in ethanol-treated cells.

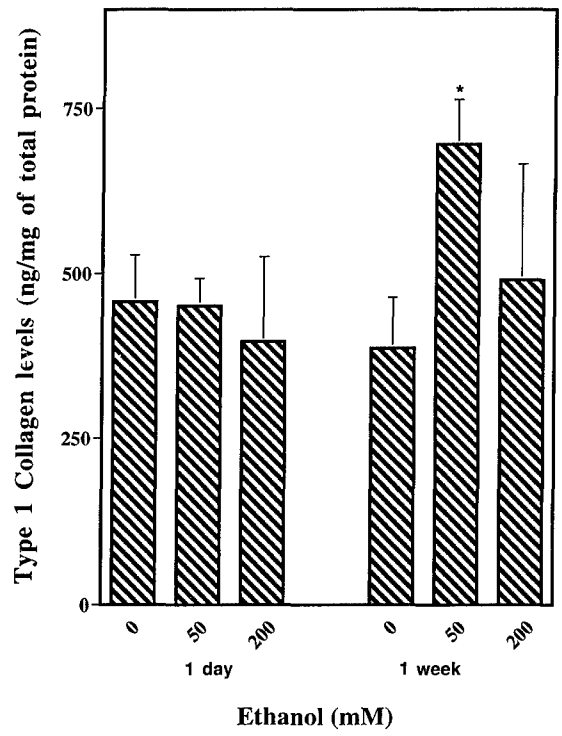

FIG. 5. Effects of 1-day and 1-week treatments of ethanol on type 1 collagen protein levels in hFOB cells. Cells were treated with 0-, 50-, and 200-mM concentrations of ethanol and the type 1 collagen levels in the medium were measured. The results represent the mean ± SE of three independent experiments. $*p \leq 0.05$ (compared with untreated control, by one-way ANOVA and Fisher's projected least significant difference [PLSD] analysis).

DISCUSSION

Although alcohol abuse has been long associated with osteoporosis, uncovering the mechanism of ethanol-mediated bone loss has been a challenging task. Interpretation of human data is difficult because of the uncertainties that arise as a result of the many problems inherent to performing controlled experiments in alcoholics. Nevertheless, a consensus has arisen that alcohol inhibits bone formation in humans.[2] Studies in laboratory animal models for alcohol abuse, which are much easier to control than human studies, have confirmed that ethanol inhibits bone growth, decreases bone formation, and leads to osteopenia.[11,13,20] However, these animal studies cannot distinguish a direct toxic effect of ethanol on osteoblasts from alternative indirect mechanisms such as a detrimental response to more toxic metabolites, changes in circulating levels of hormones and other systemic factors, and local production of cytokines and other signaling molecules. The present dose-response study using cultured normal hFOB[16] was designed to determine whether ethanol has a direct toxic effect on osteoblast growth and gene expression. This hFOB cell line has been well characterized and has been shown to respond to known regulators of osteoblast activity and gene expression.[21–25] The results show that ethanol has

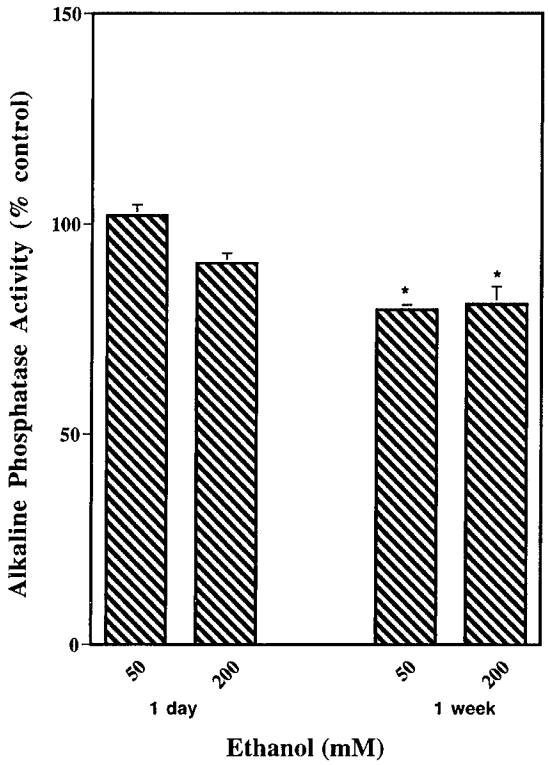

FIG. 6. Effects of ethanol treatment on alkaline phosphatase activity. The hFOB cells treated with 0-, 50-, and 200-mM concentrations of ethanol for 1 day and 1 week were harvested and the alkaline phosphatase activity in the cell pellet was measured. The results represent the mean ± SE of six replicate cultures from a single experiment. *$p \leq 0.05$ (compared with untreated control, by one way ANOVA and Fisher's projected least significant difference [PLSD] analysis).

TABLE 1. LIST OF CYTOKINES ANALYZED BY RNASE PROTECTION ASSAY IN ETHANOL-TREATED hFOB CELLS

IL-12 p35	Not detected
IL-12 p40	Not detected
IL-10	Not detected
IL-6	Not detected
IL-1α	Not detected
IL-1β	Not detected
IL-1Ra	Not detected
IFN-β	Not detected
IFN-γ	Not detected
LT-β	Not detected
TNF-α	Not detected
TNF-β	Not detected
TGF-β1	Increased
TGF-β2	Decreased
TGF-β3	Not detected

mixed effects on indices of osteoblast differentiation and no significant effect on osteoblast number. These generally weak effects contrast to the robust response to alcohol observed in humans and laboratory animals at much lower concentrations of ethanol.

Blood alcohol levels of <20 mM are sufficient to reduce biochemical markers of bone formation in humans rapidly, as well as histological indices of bone formation in rats. Indeed, bone formation was significantly decreased in rats fed alcohol in their diet comprising as little as 3% of total caloric intake resulting in blood alcohol levels below 5 mM (R.T. Turner, unpublished data). On the other hand, our present study shows that a wide range of ethanol concentration (10–200 mM) had no short-term (1 day) effect on indices of osteoblast differentiation (alkaline phosphatase, osteonectin, and collagen mRNA levels). Additionally, alcohol had no detrimental effect on short- or long-term (7 days) accumulation of collagen in the media and the alkaline phosphatase activity was only slightly reduced after a long duration of ethanol treatment. These results provide strong evidence that ethanol has minimal toxic effects on the mature osteoblast. We cannot rule out the possibility that hFOB cells are more resistant to the direct toxic effects of alcohol than osteoblasts in vivo. However, if this were the case, it would represent a general in vitro phenomenon because other osteoblastic cell lines are similarly resistant to ethanol.[26]

The lack of short-term effects of ethanol on expression of bone matrix protein genes in cultured osteoblasts contrasts with the dramatic in vivo response. Ethanol has transient tissue and dose-dependent effects on steady-state mRNA levels for extracellular matrix proteins (collagen, osteocalcin, and osteonectin) in rats.[12] Acute ethanol treatment resulted in a coordinated increase in mRNA levels for all the matrix proteins in bone but not in the uterus and liver. However, continued treatment resulted in a decrease in mRNA levels for the matrix proteins as well as a decrease in bone formation.[12] The results obtained in the present studies suggest that the changes in gene expression observed in vivo are not caused by a direct effect of ethanol on the mature osteoblast. The relatively small inhibitory effects of very high concentrations of ethanol on mRNA levels for matrix proteins after prolonged exposure may have been mediated by the observed changes in TGF-β expression. The physiological significance of this proposed mechanism can be questioned because the changes in matrix protein gene expression were observed only at levels of ethanol unlikely to be observed in humans. Nevertheless, the apparent linear dose responses of TGF-β1 and TGF-β2 steady-state mRNA levels suggest that expression of these cytokines also might be influenced by a lower concentration of ethanol. However, there is no in vivo data to support changes in TGF-β expression in bone with alcohol.

With the exception of TGF-β1 and TGF-β2, we either could not detect or did not observe changes in gene expression of any of the other cytokines analyzed. TGF-β is an important signaling protein produced by osteoblasts that affects both bone formation and bone resorption.[27] It promotes osteoclast apoptosis but inhibits osteoblast apoptosis, thus exerting an influence on bone remodeling. Overexpression of TGF-β2 in transgenic mice deregulates bone remodeling, leading to an age-dependent loss of bone mass that resembles high-turnover osteoporosis in humans.[28] These mice also have an increased rate of bone matrix formation, which is not because of direct action of TGF-β but because of homeostatic response to the increase in bone resorption caused by TGF-β. These observations confirm that TGF-β is a physiological regulator of bone metabolism, suggesting

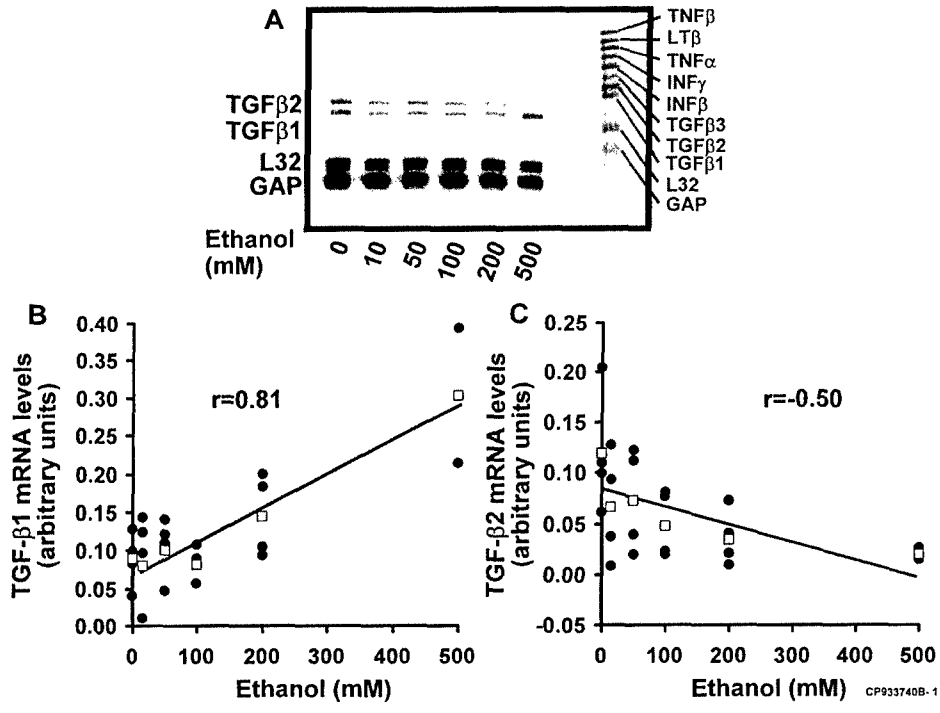

FIG. 7. Effect of 1-day ethanol treatment on TGF-β mRNA levels. Total RNA (10 μg) isolated from ethanol-untreated and -treated cells was analyzed by ribonuclease protection assay. (A) The radioactive signals from the gel were measured by PhosphorImager analysis. The data points in closed circles (●) are mRNA levels per ethanol dose for (B) TGF-β1 and (C) TGF-β2. The open square (□) represents the mean for each dose. The mRNA response of TGF-β1 and TGF-β2 correlate significantly with ethanol doses ($p \leq 0.002$ and $p \leq 0.017$, respectively).

that it may have a role in mediating some of the effects of alcohol. The observed alterations in TGF-β by alcohol are not unique to osteoblasts. Ethanol-mediated induction of TGF-β has been reported in macrophages.[29] Also, ethanol at physiologically relevant concentrations (25 mM) has been shown to induce TGF-β in monocytes.[30]

The cells in our study were not exposed to uniform concentrations of ethanol; there was a gradual decrease with time until the media were replaced, which restored ethanol levels to the previous maximal concentrations. This pulsatile exposure, although imperfect, is likely to model more accurately the changes in blood levels in chronic drinkers than maintenance of constant levels of alcohol. The nearly identical time-course changes in ethanol concentration in culture dishes with and without cells suggest that hFOB cells are unable to metabolize ethanol. This finding is significant because the metabolites of ethanol may be more toxic than the parent compound.[31,32]

A direct inhibition of osteoblast proliferation is supported by the work of Klein et al.[26] who have shown that ethanol decreases [^{3}H]thymidine incorporation and reduces cell growth in cultured TE85 osteosarcoma cells. Our observed tendency for a reduction in cell number generally is consistent with the earlier result, but only at concentrations of ethanol unlikely to be observed in humans (200 mM). Further studies will be necessary to determine the respective mechanisms of the cell-specific ethanol-induced growth arrest in the two cell lines as well as the relevance for this response to the whole organism.

Finally, ethanol may have minimal effects on expression of osteoblasts in their basal state but may alter the response of these cells to external regulatory signals. Bone turnover is regulated by locally produced as well as systemic factors.[27,33–36] Disruption of one or more of these important signaling pathways could have detrimental effects on bone formation. This possibility is supported by Farley et al., who have shown that ethanol disrupts the response of primary cultures on bone cells to several mitogenic agents.[15] hFOB cells have not been shown to express mRNA for either insulin-like growth factor I (IGF-I) or TNF-α. This may be important to the failure to detect large effects of ethanol on these cells because those two cytokines are clearly altered in skeletal tissues in vivo.[12] Whatever the specific mechanism by which alcohol indirectly inhibits bone formation, our finding that ethanol does not have a toxic effect on the osteoblast is important because it increases the likelihood that the detrimental effects of ethanol on osteoblast functions are reversible.

ACKNOWLEDGMENTS

We thank Mr. Larry Pederson and Ms. Angela Kennedy for technical assistance. This investigation was supported by grant AA11140 from the National Institutes of Health and Department of Defense grant DAMD 17-98-1-8517.

REFERENCES

1. Bikle DD 1993 Alcohol-induced bone disease. World Rev Nutr Diet **73:**53–79.
2. Spencer H, Rubio N, Rubio E, Indreika M, Seitam A 1986 Chronic alcoholism. Frequently overlooked cause of osteoporosis in men. Am J Med **80:**393–397.
3. Diamond T, Stiel D, Lunzer M, Wilkinson M, Posen S 1989 Ethanol reduces bone formation and may cause osteoporosis. Am J Med **86:**282–288.
4. Bikle DD, Genant HK, Cann C, Recker RR, Halloran BP, Strewler GJ 1985 Bone disease in alcohol abuse. Ann Intern Med **103:**42–48.

5. Lalor BC, France MW, Powell D, Adams PH, Counihan TB 1986 Bone and mineral metabolism and chronic alcohol abuse. QJ Med **59:**497–511.
6. Schnitzler CM, Solomon L 1984 Bone changes after alcohol abuse. S Afr Med J **66:**730–734.
7. Diez A, Puig J, Serrano S, Marinoso ML, Bosch J, Marrugat J, Mellibovsky L, Nogues X, Knobel H, Aubia J 1994 Alcohol-induced bone disease in the absence of severe chronic liver damage. J Bone Miner Res **9:**825–831.
8. Laitinen K, Valimaki M, Keto P 1991 Bone mineral density measured by dual-energy X-ray absorptiometry in healthy Finnish women. Calcif Tissue Int **48:**224–231.
9. Crilly RG, Anderson C, Hogan D, Delaquerriere-Richardson L 1988 Bone histomorphometry, bone mass, and related parameters in alcoholic males. Calcif Tissue Int **43:**269–276.
10. Turner RT, Greene VS, Bell NH 1987 Demonstration that ethanol inhibits bone matrix synthesis and mineralization in the rat. J Bone Miner Res **2:**61–66.
11. Sampson HW, Perks N, Champney TH, DeFee B II 1996 Alcohol consumption inhibits bone growth and development in young actively growing rats. Alcohol Clin Exp Res **20:** 1375–1384.
12. Turner RT, Wronski TJ, Zhang M, Kidder LS, Bloomfield SA, Sibonga JD 1998 Effects of ethanol on gene expression in rat bone: Transient dose-dependent changes in mRNA levels for matrix proteins, skeletal growth factors, and cytokines are followed by reductions in bone formation. Alcohol Clin Exp Res **22:**1591–1599.
13. Peng TC, Kusy RP, Hirsch PF, Hagaman JR 1988 Ethanol-induced changes in morphology and strength of femurs of rats. Alcohol Clin Exp Res **12:**655–659.
14. Rico H, Cabranes JA, Cabello J, Gomez-Castresana F, Hernandez ER 1987 Low serum osteocalcin in acute alcohol intoxication: A direct toxic effect of alcohol on osteoblasts. Bone Miner **2:**221–225.
15. Farley JR, Fitzsimmons R, Taylor AK, Jorch UM, Lau KH 1985 Direct effects of ethanol on bone resorption and formation in vitro. Arch Biochem Biophys **238:**305–314.
16. Harris SA, Enger RJ, Riggs BL, Spelsberg TC 1995 Development and characterization of a conditionally immortalized human fetal osteoblastic cell line. J Bone Miner Res **10:**178–186.
17. Chomczynski P, Sacchi N 1987 Single-step method of RNA isolation by acid guanidinium thiocyanate-phenol-chloroform extraction. Anal Biochem **162:**156–159.
18. Genovese C, Rowe D, Kream B 1984 Construction of DNA sequences complementary to rat alpha 1 and alpha 2 collagen mRNA and their use in studying the regulation of type I collagen synthesis by 1,25-dihydroxyvitamin D. Biochemistry **23:**6210–6216.
19. Villarreal XC, Mann KG, Long GL 1989 Structure of human osteonectin based upon analysis of cDNA and genomic sequences. Biochemistry **28:**6483–6491.
20. Turner RT, Aloia RC, Segel LD, Hannon KS, Bell NH 1988 Chronic alcohol treatment results in disturbed vitamin D metabolism and skeletal abnormalities in rats. Alcohol Clin Exp Res **12:**159–162.
21. Tau KR, Hefferan TE, Waters KM, Robinson JA, Subramaniam M, Riggs BL, Spelsberg TC 1998 Estrogen regulation of a transforming growth factor-beta inducible early gene that inhibits deoxyribonucleic acid synthesis in human osteoblasts. Endocrinology **139:**1346–1353.
22. Robinson JA, Harris SA, Riggs BL, Spelsberg TC 1997 Estrogen regulation of human osteoblastic cell proliferation and differentiation. Endocrinology **138:**2919–2927.
23. Spelsberg TC, Harris SA, Riggs BL 1995 Immortalized osteoblast cell systems (new human fetal osteoblast systems). Calcif Tissue Int **56**(Suppl 1)**:**S18–S21.
24. Hofbauer LC, Dunstan CR, Spelsberg TC, Riggs BL, Khosla S 1998 Osteoprotegerin production by human osteoblast lineage cells is stimulated by vitamin D, bone morphogenetic protein-2, and cytokines. Biochem Biophys Res Commun **250:** 776–781.
25. Hofbauer LC, Gori F, Riggs BL, Lacey DL, Dunstan CR, Spelsberg TC, Khosla S 1999 Stimulation of osteoprotegerin ligand and inhibition of osteoprotegerin production by glucocorticoids in human osteoblastic lineage cells: Potential paracrine mechanisms of glucocorticoid-induced osteoporosis. Endocrinology **140:**4382–4389.
26. Klein RF, Fausti KA, Carlos AS 1996 Ethanol inhibits human osteoblastic cell proliferation. Alcohol Clin Exp Res **20:**572–578.
27. Turner RT, Riggs BL, Spelsberg TC 1994 Skeletal effects of estrogen. Endocr Rev **15:**275–300.
28. Erlebacher A, Derynck R 1996 Increased expression of TGF-beta 2 in osteoblasts results in an osteoporosis-like phenotype. J Cell Biol **132:**195–210.
29. Singhal PC, Reddy K, Ding G, Kapasi A, Franki N, Ranjan R, Nwakoby IE, Gibbons N 1999 Ethanol-induced macrophage apoptosis: The role of TGF-beta. J Immunol **162:**3031–3036.
30. Szabo G, Mandrekar P, Girouard L, Catalano D 1996 Regulation of human monocyte functions by acute ethanol treatment: Decreased tumor necrosis factor-alpha, interleukin-1 beta and elevated interleukin-10, and transforming growth factor-beta production. Alcohol Clin Exp Res **20:**900–907.
31. Lin RC, Fillenwarth MJ, Du X 1998 Cytotoxic effect of 7alpha-hydroxy-4-cholesten-3-one on HepG2 cells: Hypothetical role of acetaldehyde-modified delta4–3-ketosteroid-5beta-reductase (the 37-kd-liver protein) in the pathogenesis of alcoholic liver injury in the rat. Hepatology **27:**100–107.
32. Diczfalusy MA, Bjorkhem I, Einarsson C, Alexson SE 1999 Formation of fatty acid ethyl esters in rat liver microsomes. Evidence for a key role for acyl-CoA: Ethanol O-acyltransferase. Eur J Biochem **259:**404–411.
33. Oreffo RO, Bonewald L, Kukita A, Garrett IR, Seyedin SM, Rosen D, Mundy GR 1990 Inhibitory effects of the bone-derived growth factors osteoinductive factor and transforming growth factor-beta on isolated osteoclasts. Endocrinology **126:** 3069–3075.
34. Wergedal JE, Mohan S, Taylor AK, Baylink DJ 1986 Skeletal growth factor is produced by human osteoblast-like cells in culture. Biochim Biophys Acta **889:**163–170.
35. Raisz LG 1988 Local and systemic factors in the pathogenesis of osteoporosis. N Engl J Med **318:**818–828.
36. Kimble RB 1997 Alcohol, cytokines, and estrogen in the control of bone remodeling. Alcohol Clin Exp Res **21:**385–391.

Address reprint requests to:
A. Maran, Ph.D.
3–69 Medical Sciences Building
Assistant Professor
Department of Orthopedics
Mayo Clinic
Rochester, MN 55905, USA

Received in original form December 2, 1999; in revised form September 13, 2000; accepted October 6, 2000.

ORGAN-SPECIFIC EFFECTS OF ALCOHOL ON GENE EXPRESSION

A. Maran, M. Zhang, and R.T. Turner

Departments of Orthopedics and
Biochemistry and Molecular Biology
Mayo Clinic, Rochester, MN

Address correspondence to: Russell T. Turner, Ph.D.
Orthopedic Research
Room 3-69 Medical Science Building
Mayo Clinic
200 First Street SW
Rochester, MN 55905
Phone: (507) 284-2267
FAX: (507) 284-5075
E-mail: turner.russell@mayo.edu

Key words: cDNA microarray, pathophysiology, alcohol abuse, gene expression, rat

ABSTRACT

The present study was designed to investigate the effects of a brief exposure to ethanol (1 g/kg) on gene expression in 3 organs in sexually mature female rats. Gene microarrays revealed that ethanol altered mRNA concentrations in an organ specific manner. The number of genes whose expression was altered varied greatly with liver > bone > uterus. Only 1 of 5531 genes assayed was altered in all 3 organs. The results demonstrate that the initial skeletal response to alcohol differs greatly from the response of liver and uterus, suggesting that organ-specific gene alterations play an important role in the development of alcohol-induced pathophysiology.

INTRODUCTION

Chronic alcohol abuse results in a bewildering array of pathological changes affecting numerous organs (1-6). These include brain, liver, heart, bone, bone marrow, digestive system, and pancreas. Not all alcoholics develop organ pathology and the ones who do usually develop serious problems in only one organ.

Drinking is rarely likely to have a direct lethal effect on cells. It is more likely that ethanol disturbs cell signaling and as a consequence disrupts normal function. There has been great interest in the signaling pathways that are disturbed by alcohol and several have been identified, including membrane receptor-mediated stimulation of second messengers, phospholipase C signaling, serine/threonine protein kinases, ion channels, cell adhesion, and gap junctional signaling (7-17). However, it is possible that a common mechanism of action underlies these organ-specific actions of ethanol. According to this view, specific organ pathologies associated with chronic drinking are the result of additional co-morbidity factors.

We tested the possibility that acute exposure to ethanol induces a similar initial response in three representative organs. Ethanol was administered to sexually mature female rats (1 g/kg) resulting in a peak blood alcohol level of ~0.1% 1 h later. Blood alcohol decreased to undetected levels within 4 h (18). As shown in Figure 1, changes in gene expression induced by this brief exposure to alcohol were evaluated after 24 h in liver, bone and uterus by analyzing isolated total cellular RNA samples using a cDNA microarray (19).

Of the genes evaluated (Table 1), ethanol resulted in changes (>2.5-fold increases or decreases) in steady-state mRNA levels for 54 genes in uterus, 497 in proximal tibial metaphysis and 3175 in liver (20). These results demonstrate that alcohol results in profound organ-specific differences in the number of genes whose expression is altered. The genes that changed included

representatives of classes of peptides involved in virtually every aspect of cell function, including infrastructure, extracellular matrix, metabolism, and cell signaling. This finding suggests that even acute exposure to relatively modest concentrations of ethanol influences multiple signaling pathways.

None of the 28 named genes whose expression was altered by alcohol in uterus corresponded to alcohol-regulated genes in bone but all of these genes were also altered in liver. Expression levels of three of the expressed sequence tags (ESTs) were altered by alcohol in uterus and bone. In bone, 45 of the 134 named genes and 50 of the 124 ESTs whose expression was altered by alcohol were also regulated in liver.

The direction of the changes provides an additional indication of organ specificity. All 54 shared genes changed in the same direction in uterus and liver (Table 2), strongly suggesting a common pathway accessed by alcohol. However, comparing the 169 genes shared between bone and liver reveals only 66 that were regulated in the same direction, which suggests activation of different signaling pathways. This conclusion is further supported by the observation that of 5531 genes assayed, only one was altered by alcohol in all 3 organs and the direction of change of this gene differed between bone and the other two organs.

Ethanol induces a variety of pathophysiological changes in the uterus in non-pregnant as well as pregnant laboratory animals, including alterations in the methylation of membrane phospholipids, increased oxygen tension, impaired glucose homeostasis, altered spontaneous motility, prostaglandin production, triglyceride metabolism and tissue atrophy (21-25). Many of these changes are believed to be indirect. Our results suggest that the uterine response to alcohol is associated with a limited number of genes and that these changes in gene expression share a common pathway with a subgroup of changes occurring in the liver.

Alcoholic liver disease is characterized by progressively severe changes. The initial pathology of fatty liver, which is reversible, is followed by fibrosis which may be reversible and cirrhosis which is irreversible (26-28). Although acute administration of alcohol resulted in dramatic changes in gene expression in rat liver, even chronic exposure to high concentrations of alcohol is insufficient to induce irreversible alcoholic liver disease in the animal model (29,30). Co-morbidity factors such as dietary iron, estrogen and endotoxin appear to be needed (31-34). Gene microarrays should provide a useful tool for investigating the interactions between these factors and alcohol.

Alcohol abuse disturbs bone and mineral homeostasis and is an important risk factor for osteoporosis (35-41). Even small amounts of alcohol suppress bone formation (6,38,41-46). The rat skeleton is similarly sensitive to alcohol and the rat model duplicates human pathology with a high degree of fidelity (18,47-58). The results of the current study indicate that the skeletal effects of moderate alcohol consumption on bone metabolism are associated with changes in the expression of a large number of genes. Furthermore, the pattern of changes differs considerably from liver. The regulation of mRNA levels for collagen is especially noteworthy because gene expression occurs in opposite directions. Excess collagen production occurs in the fibrotic liver whereas alcohol-induced osteoporosis is due, at least in part, to decreased collagen synthesis by osteoblasts (6,36,58,59).

In summary, we have shown dramatic organ differences in the numbers of genes whose expression is altered by brief exposure to alcohol. Minimal overlap in gene changes between bone and uterus and a preponderance of changes in the opposite direction for bone and liver suggest these 3 organs exhibit important organ-specific differences in signaling pathways disturbed by alcohol. However, the similarity of the changes between liver and uterus provides

strong evidence for conservation of a limited number of mechanisms of action between organs (60).

REFERENCES

1. Zakhari, S. Recent Dev Alcohol 9:225, 1991.

2. Cook, R. Alcohol Clin Exp Res 22:1927, 1998

3. Steiner, et al. Endocrinology 154:363, 1997.

4. Wilson, JS and Pirola RC. Gastroenterology 113:355, 1997.

5. Kaplowitz, N. J Hepatol 32 (suppl 1):39, 2000.

6. Bikle DD, et al. Ann Intern Med 103:42-48, 1985.

7. Hoek JB, et al. Semin Liver Disease 8:36, 1988.

8. Diamond I and Gordon AS. Physiol Rev 77:1, 1997.

9. Mochly-Rosen D, et al. Nature 333:848, 1988.

10. Hoek JB, et al. J Biol Chem 262:682, 1988.

11. Slater SJ, et al. Nature 364:82, 1993.

12. Constantinescu AI, et al. J Biol Chem 274:26985, 1999.

13. Resnicoff M, et al. Alcohol Clin Exp Res 20:961, 1996.

14. Miyakawa T, et al. Science 278:698, 1997.

15. Harris RA. Alcohol Clin Exp Res 23:1563, 1999.

16. Wilkemeyer MF, et al. Proc Natl Acad Sci USA 97:3690, 2000.

17. Abou Hashieh I, et al. J Hepatol 24:360, 1996.

18. Turner RT et al. Alcohol Clin Exp Res 22:591, 1998.

19. The animal studies were performed following approval of the Institutional Animal Welfare Committee. Sexually mature Sprague Dawley female rats obtained from Harlan Sprague Dawley, Madison, WI, were administered either ethanol 1 g/kg body weight as a 40% aqueous solution or water only sc. The rats were anesthetized 24 h later with ketamin HCL (120

mg/kg:xylazine (24 mg/kg) prior to decapitation. Total cellular RNA was isolated as described (Cavolina, et al. Endocrinology 138:1567, 1997) using a modified organic solvent method (Chomcynski P and Sacchi M. 162:156, 1987). Gene filter microarrays are performed using rat Gene Filters microarrays release 1 (GF300) and software from Research Genetics (Huntsville, AL). Total RNA (1 μg) isolated from bone was used for cDNA synthesis. The RNA was pooled from 4 animals from each treatment group to reduce differences due to individual animal variation. The synthesis of cDNA, prehybridization, hybridization and washings were performed as described in the manufacturer's protocol (Research Genetics). The radioactive Gene Filters were exposed for 48 h on a phosphor screen to obtain the phosphor image of the gel using the Cyclone Storage Phosphor System (Packard Instrument Company, Meriden, CT). The phosphor image was analyzed using Pathways software (Research Genetics) to determine gene specific changes. A complete listing of the cDNAs contained in the gene microarray is available (http://www.resgen.com).

20. A complete list of the gene changes in the 3 organs can be obtained upon request (turner.russell@mayo.edu).

21. Murdoch RN and Edwards T. Biochemistry Int 28:1029, 1992.

22. Mitchell JA, Van Kainen BR. Alcohol Clin Exp Res 16:308, 1992.

23. Murdoch RN and Sim B. Biochem Med Metab Biol 47:54, 1992.

24. Chaud MA, et al. Prostaglandins Leukot Essent Fatty Acids 42:119, 1991.

25. Murdoch RN. Teratology 35:169, 1987.

26. Lieber, et al. Proc Natl Acad Sci USA 72:437, 1975.

27. Kaplowitz N and Tsukamoto H. Prog Liver Disease XIV:131, 1996.

28. Kaplowitz N. J Hepatol 32 (Suppl 1):39, 2000.

29. Porta, et al. Lab Invest 18:1437, 1965.

30. Tsukamoto H and French SW. Alcohol 10:437, 1993.

31. Thurman RG, Am J Physiol 275:G605, 1998.

32. Tsukamoto H, et al. J Clin Invest 96:620, 1995.

33. Iimuro Y, et al. Am J Physiol 272:G1186, 1997.

34. Enomoto N, et al. Am J Physiol 277:G671, 1999.

35. Spencer H, et al. Am J Med 80:393, 1986.

36. Bikle DD, et al. Alcohol Clin Exp Res 17:690, 1993.

37. Diez A, et al. J Bone Miner Res 9:825, 1994.

38. Gonzalez-Calvin JL, et al. Alcohol 28:571, 1993.

39. Lalor BC et al. Quarterly J Med 59:497, 1986.

40. Pumarino H, et al. Revista Medica de Chile 124:423, 1996.

41. Schnitzler CM and Solomon L. S Afr Med J 66:730, 1984.

42. Labid M, et al. Alcohol 24:141, 1989.

43. Laitinen K, et al. Bone Miner 13:139, 1991.

44. Laitinen K, et al. Bone Miner 24:171, 1994.

45. Nielsen HK, et al. Calcif Tissue Int 46:173, 1990.

46. Rico H, et al. Bone Miner 2:221, 1987.

47. Peng TC, et al. Endocrinology 91:586, 1972.

48. Peng TC, et al. Alcohol Clin Exp Res 12:1655, 1988.

49. Turner RT, et al. Alcohol Clin Exp Res 12:151, 1988.

50. Turner RT, et al. Cell Mater Suppl 1:167, 1991.

51. Wezeman FH, et al. Alcohol Clin Exp Res 23;1534, 1999.

52. Turner RT, et al. J Bone Miner Res 2:61, 1987.

53. Dyer SA, et al. Alcohol 16:337, 1998.

54. Hogan HA, et al. Alcohol Clin Exp Res 21:809, 1997.

55. Sampson HW. Alcohol Clin Exp Res 22:2029, 1998.

56. Sampson HW, et al. Alcohol Clin Exp Res 21:352, 1997.

57. Sampson HW, et al. Alcohol Clin Exp Med 23:324, 1999.

58. Turner RT, et al. Alcohol Clin Exp Res 22:1591, 1998.

59. Nieto N, et al. Hepatology 30:987, 1999.

60. The authors acknowledge Lori M. Rolbiecki for secretarial assistance and Peggy Backup for editorial assistance. These studies were supported by NIH grant AA11140 and Department of Defense grant DAMD17-98-1-8517.

Table 1: Organ-Specific Effects of Alcohol on Gene Expression			
Organ(s)	Named Genes (# changed)	ESTs (# changed)	Total Genes (# changed)
Uterus	28[1]	26	54
Tibia	134	363	497
Liver	1237	1938	3175
Uterus & Tibia	0	2/3[2]	2/3
Uterus & Liver	28/28	14/14	42/42
Tibia & Liver	16/45	50/124	66/169
All organs	0	0/1	0/1

[1]Number of genes which mRNA levels differ from control by $\geq$ 2.5 fold from a total of 5531 genes assayed.

[2]x/y where x = number of genes where mRNA levels change in same direction and y = total number of genes in common regulated by alcohol.

Table 2: Named Genes Regulated by Ethanol in Uterus and Liver		
Gene	Uterus (fold change)	Liver (fold change)
Keratin (K5)	-2.6[1]	-3.3
RGS8	-2.7	-3.8
Calcium-independent alpha-latrotoxin receptor	-2.5	-2.8
Beta-tubulin T beta 15	-2.9	-2.9
Syntaxin binding protein Munc18-2 mRNA	-2.7	-3.1
Pancreatic phospholipase A-2	-2.9	-4.3
Proteasomal ATPase (Tat-binding protein 7)	-2.6	-2.9
Transcription factor USF-1	-2.5	-3.2
cdc25A	-2.6	-2.9
PMF31	-2.7	-3.1
Alternatively spliced aggrecan, large aggregating cartilage proteoglycan core protein	-2.6	-4.2
RB13-6 antigen	-2.5	-3.4
Iron-responsive element-binding protein	-2.5	-4.2
190 kDa ankyrin isoform	-2.8	-2.9
120 Kd lysosomal membrane glycoprotein	-2.5	-4.1
Farnesyltransferase beta subunit	-2.6	-3.8
Cortactin isoform B	-3.0	-4.2
BTG3 mRNA	-2.8	-4.6
Mitochondrial 3-2trans-enoyl-CoA isomerase	-2.7	-3.7
Oxidosqualene cyclase mRNA	-2.7	-3.6
Spermatid protein RSP29	-2.6	-3.5
RNB6	-2.6	-3.0
Zinc finger transcriptional activator (NGFI-C)	-2.8	-3.3
Transition protein 2 (TP2)	-2.9	-3.2
Cytochrome P450 2D18	-2.8	-3.1
P2X5 protein	-2.5	-3.3
Delta-aminolevulinate synthase	-2.6	-4.3
RAB10	-2.5	-3.3
[1]Values are fold change in steady-state mRNA levels compared to rats given water only.		

Table 3: Named Genes Regulated by Ethanol in Liver and Bone		
Gene	Liver (fold change)	Bone (fold change)
Alpha-lactalbumin (alpha-LA)	-5.9[1]	3.2
Brain acyl-CoA synthetase II	-8.6	4.1
Complex polypeptide 1 (Tcp-1)	-5.9	4.7
GTP cyclohydrolase I	-6.6	3.3
Carboxylesterase precursor	-6.8	3.1
Gamma subunit of sodium potassium ATPase	-6.6	3.9
F1-ATPase alpha subunit	2.8	-7.7
Farnesyltransferase alpha subunit peptide	-4.4	3.0
Equilbrative nitrobenzylthioninosine-insensitive nucleoside transporter	-9.6	4.7
CD30	3.6	-9.3
G protein gamma-5 subunit	-7.8	4.3
Bone morphogenetic protein 2 related peptide	-5.5	3.2
Lamina-associated polypeptide 1C (LAPIC)	-8.8	2.9
Cardiac troponin T mRNA	-4.1	-4.1
Microvascular endothelial differentiation gene 1	-9.5	2.5
Rab3B protein	-4.8	2.5
Long-chain acyl-CoA synthetase	-5.5	3.0
Gephyrin	-5.9	2.8
MIFR	-3.7	3.0
Alpha 2,6-sialyltransferase	-9.9	3.3
250 kDa estrous-specific protein	-3.5	2.5
Retrovirus-related gag protein	-9.4	4.1
EGF-like growth factor	-7.5	2.6
Galanin receptor type 2 (GALR2)	-7.4	2.6
RET ligand 1 (RETL1)	-9.5	5.8
Nedd2/Ich-1 mRNA	-2.7	-2.5
Very-long-chain Acyl-CoA dehydrogenase	-7.4	-4.2
mRNA for ST1B1	-3.2	2.5
Vesicular GABA transporter (VGAT)	-3.3	-2.6
Peroxisome assembly factor-2	-3.1	2.6
Retinol binding protein (CRBP)	-3.2	-3.2
Proto-oncogene FYN (p59fyn)	-4.8	-2.8
Clathrin-associated protein 17 (AP17)	-8.0	-3.8
V-1 protein	-3.4	-5.4
Neurabin mRNA	-2.9	-4.4
Collagen alpha 1 type 1	-3.7	2.6
Intercellular calcium-binding protein (MRP8)	-4.4	-4.1
p-450, phenobarbital-inducible	3.2	5.8
AlphaB crystallin-related protein	-2.9	-2.7
Ferritin-H subunit	-3.9	2.5
Acyl-CoA synthetase	2.9	3.0
Alpha-globin mRNA	-6.9	2.6
Peptidylarginine deiminase	-3.4	-2.9
Mannose 6-phosphate/insulin-like growth factor II receptor	-3.0	2.6
Ribosomal protein S10	-3.4	-2.8
[1]Values are fold change in steady-state mRNA levels compared to rats given water only.		

FIGURE LEGEND

Figure 1: cDNA microarrays used to detect genes regulated by alcohol in uterus (top), proximal tibial metaphysis (middle), and liver (bottom). The microarrays were sequentially hybridized to total RNA from control rats and alcohol treated rats. Only genes expressing differences in mRNA levels of $\geq$ 2.5 fold are shown. Red spots indicate genes with increased expression following alcohol whereas blue indicates decreased expression.

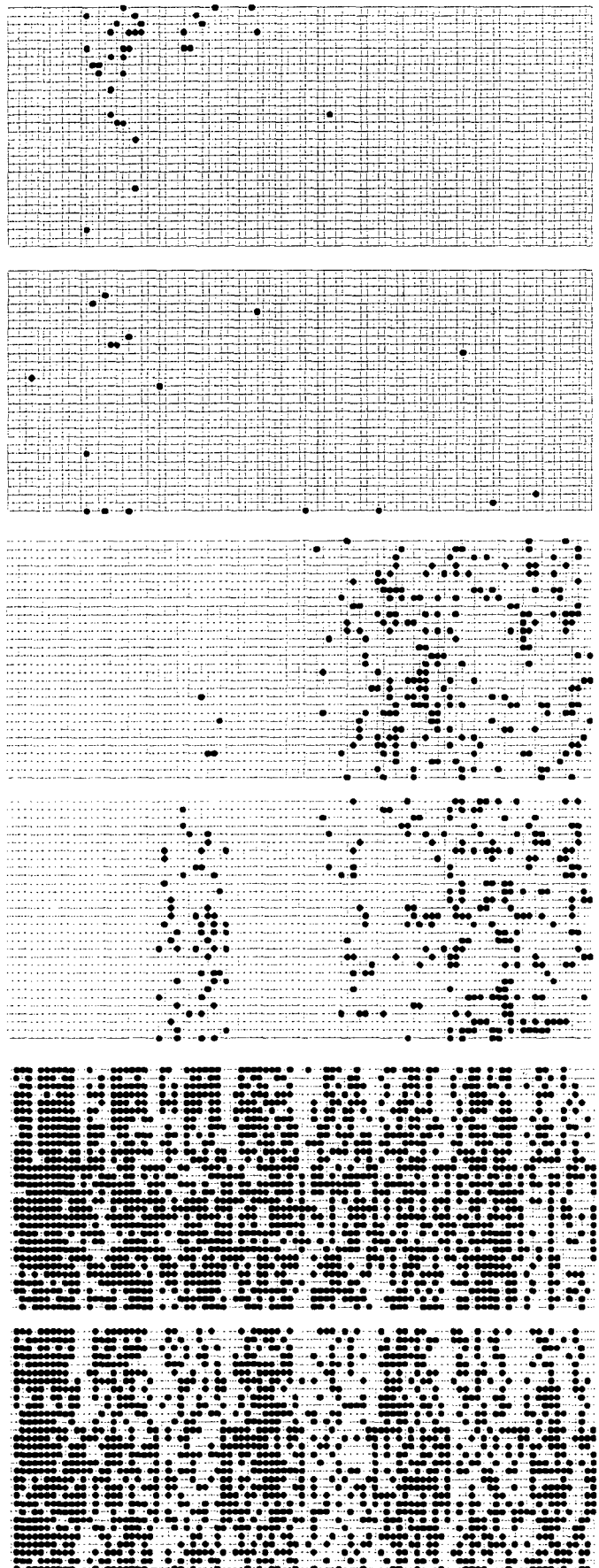

PH946777_1

0145-6008/01/2505-0667$03.00/0
ALCOHOLISM: CLINICAL AND EXPERIMENTAL RESEARCH

Vol. 25, No. 5
May 2001

Effects of Parathyroid Hormone on Bone Formation in a Rat Model for Chronic Alcohol Abuse

Russell T. Turner, Glenda L. Evans, Minzhi Zhang, and Jean D. Sibonga

Background: Alcoholism is a risk factor for osteoporosis and it is not clear whether the detrimental effects of alcohol on bone are reversible. Parathyroid hormone (PTH) is a potent stimulator of bone matrix synthesis and is being investigated as a therapeutic agent to reverse bone loss. The present investigation was designed to determine the effects of PTH on bone formation in a rat model for chronic alcohol abuse.

Methods and Results: Alcohol was administered in the diet of female rats (35% caloric intake) for 2 weeks. Human (1-34) PTH (80 μg/kg/day) was administered subcutaneously during the second week of the study. Alcohol resulted in a transient reduction in steady-state mRNA levels for the bone matrix proteins type 1 collagen, osteocalcin, and osteonectin compared with rats that were fed an alcohol-free (control) diet. As expected, alcohol decreased and PTH increased histologic indices of bone formation. Additionally, two-way ANOVA demonstrated that alcohol antagonized PTH-induced bone formation. Despite antagonism, bone formation and mRNA levels for bone matrix proteins in alcohol-fed rats treated with PTH greatly exceeded the values in rats fed the control diet.

Conclusions: The results of this study contribute to a growing body of evidence that alcohol-induced bone loss is primarily due to reduced bone formation. We conclude that alcohol does not prevent the stimulatory effects of PTH on bone formation. This is evidence that the effects of alcohol on the skeleton are reversible. Additionally, the positive effects on bone formation in rats that consumed high concentrations of alcohol suggested that PTH may be useful as an intervention to treat alcohol-induced osteoporosis.

Key Words: Alcoholism, Osteoblasts, Osteoclasts, Bone Histomorphometry, Bone Resorption.

ALCOHOLICS OFTEN HAVE radiographic evidence of osteopenia, a greatly reduced bone mineral density, and reduced histologic and biochemical indices of bone formation (Bikle et al., 1985, 1993; Crilly et al., 1988; Diez et al., 1994; Gonzalez-Calvin et al., 1993; Harding et al., 1988; Labib et al., 1989; Laitinen et al., 1992, 1993; Lalor et al., 1986; Nielsen et al., 1990; Odvina et al., 1995; Pumarino et al., 1996; Schnitzler and Solomon, 1984; Spencer et al., 1986). There is also evidence that alcoholics are at a greater risk for receiving fractures than healthy individuals (Kanis et al., 1999; Kelepouris et al., 1995). Alcohol-induced osteoporosis differs from postmenopausal bone loss in that the pronounced increase in bone turnover that follows the menopause is not observed in alcoholics (Felson et al., 1993; Heaney et al., 1978). The principal mechanism for alcohol-induced bone loss appears to be reduced bone formation (Bikle et al., 1993; Gonzalez-Calvin et al., 1993; Labib et al., 1989; Laitinen et al., 1992; Nielsen et al., 1990; Schnitzler and Solomon, 1984); indices of bone resorption may be increased, decreased, or unchanged (Bikle et al., 1985, 1993; Crilly et al., 1988; Diez et al., 1994; Laitinen et al., 1991a, 1994; Lalor et al., 1986; Schnitzler and Solomon, 1984). The net reduction in bone formation appears to result in a negative remodeling balance and ultimately to osteopenia (Turner, 2000).

At present, there is no specific intervention to treat alcoholics who have osteoporosis, but a rat model for the skeletal effects of alcohol abuse has been established to investigate possible therapies. Rats fed ethanol at a rate (adjusted for the difference in body mass) comparable to alcoholics develop abnormalities in bone and mineral homeostasis similar to alcoholics (Peng et al., 1972; Peng and Gitelman, 1974; Sampson, 1998; Sampson et al., 1997; Turner et al., 1987, 1988, 1991). These abnormalities include osteopenia and a pronounced inhibition of bone formation (Sampson, 1998; Sampson et al., 1997; Turner et al., 1987, 1988, 1991).

Parathyroid hormone (PTH) is under investigation for treatment of osteoporosis. Pulsatile administration of PTH increases bone formation and bone mass in humans and laboratory animals (Dobnig and Turner, 1995). The principle purpose of the present study was to evaluate the efficacy of PTH as a therapy to reverse the inhibitory effects of alcohol abuse on bone formation in the rat model.

From the Departments of Orthopedics (RTT, GLE, MZ, JDS) and Biochemistry and Molecular Biology, (RTT), Mayo Clinic, Rochester, Minnesota.

Received for Publication June 28, 2000; accepted February 19, 2001.

Supported by NIH grant AA11140, Department of Defense grant DAMD 17–98–1-8517, and the Mayo Foundation.

Reprint requests: Russell T. Turner, Room 3-69 Medical Science Building, Mayo Clinic 200 First Street SW, Rochester, MN 55905; Fax: 507-284-5075; E-mail: turner.russell@mayo.edu

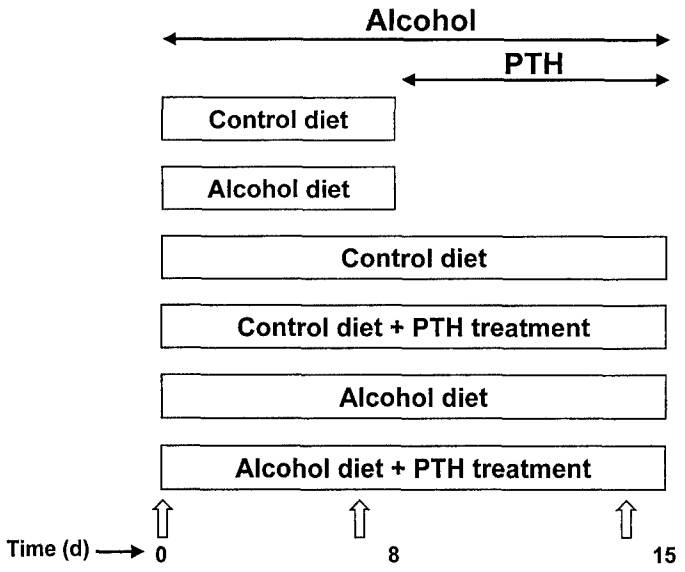

Fig. 1. A schematic showing the experimental design. Alcohol treatment was started on day 0 and PTH treatment was started on day 8. Fluorochrome labels (⇑) were administered on day 0, 7, and 14. The baseline control groups were killed on day 8 and the remaining groups on day 15.

MATERIALS AND METHODS

Animals

Six-month-old female Sprague Dawley® rats (Harlan, Sprague Dawley, Indianapolis, IN) weighing an average of 294 ± 2 g (mean ± SE) were randomly assigned to one of six groups (n = 10 rats/group). All animal procedures were approved by the Institutional Animal Welfare Committee. Rats were individually housed in a temperature- and humidity-controlled animal facility on a 12-hr light/dark cycle. All animals were acclimated to a modified Lieber-DeCarli liquid diet (BioServe, Frenchtown, NJ) for one week. The three alcohol-supplemented groups were subsequently fed, ad libitum, a liquid diet containing increasing concentrations of ethanol (95% v/v) until they received 35% of total caloric intake as alcohol at the end of the first treatment week (Kidder and Turner, 1998). This dose of alcohol results in blood alcohol levels and changes in bone and mineral metabolism similar to alcoholics (Kidder and Turner, 1998; Sampson, 1998; Sampson et al., 1997; Turner et al., 1987, 1988, 1991). Rats were not given water. The three control diet groups did not receive ethanol and were fed the same liquid diet isocalorically supplemented with maltose/dextran, as per the manufacturer's instructions. All animal weights were recorded on the first day of study (day 1), on the first day of treatment with PTH (day 8), and on the day of necropsy (day 15). The 24-hr consumptions were recorded daily and the rats that were fed the control diet were pair-fed to the mean consumption of the alcohol-treated animals.

A schematic of the experimental design is shown in Fig. 1. On the first day of ethanol treatment, all rats were injected with a 20 mg/kg BW dose of a bone fluorochrome, tetracycline-hydrochloride (Sigma, St. Louis, MO), perivascularly at the base of the tail. All rats were injected 7 days later with another bone fluorochrome, calcein (20 mg/kg BW; Sigma). One group of rats that were fed alcohol and one group of rats that were fed the control diet were euthanized on day 8 to provide baseline measurements for the PTH intervention study.

Starting on day 8, two groups of rats (one fed the control diet and one fed the alcohol diet) were administered human PTH (1–34) daily (80 μg/kg) subcutaneously, as described (Dobnig and Turner, 1997). Also, starting on day 8, the remaining two groups of rats (one control diet and one alcohol diet) were given carrier only. All remaining rats were given the fluorochrome demeclocyline (20 mg/kg BW; Sigma) on day 14 and euthanized on day 15.

Rats were anesthetized using ketamine (100 mg/ml) and xylazine (100 mg/ml) and killed by decapitation. Tibiae were defleshed and either frozen in liquid nitrogen and stored at −80°C prior to RNA analysis or fixed by immersion in 70% ethanol for bone histomorphometry. Uteri were harvested and wet weights recorded.

Bone Histomorphometry

Tibiae were dehydrated by immersion in a series of increasing concentrations of ethanol, and embedded without demineralization in a methylmethacrylate mixture (methylmethacrylate:2-hydroxyethyl-methacrylate 12.5:1). Longitudinal sections were taken from the middle of the proximal tibia with a Reichert-Jung microtome (5 μm thick) and permanently mounted on slides for histomorphometric measurements. Cancellous bone measurements were performed in a standard sampling site located on the long axis of the bone, one millimeter from the epiphyseal growth plate at its most distal point. This site is distal to the primary spongiosa, within the secondary spongiosa, and extends bilaterally to exclude the endocortical edges. The sampling site encompassed a tissue area of 2.88 mm^2.

All histomorphometric measurements were carried out with a semiautomatic image-analysis system, which consisted of a Compaq computer interfaced with a microscope and image analysis software (OsteoMetrics, Inc., Atlanta, GA). Skeletal indices were measured by registering the movement of a digitizing mouse across a graphics tablet as a tracing was superimposed on an image of the section displayed on a video screen. The computer software recorded lengths and calculated the enclosed areas. The following histomorphometric indices were determined as described (Kidder and Turner, 1998): cancellous bone volume (BV), trabecular number (Tb.N), trabecular thickness (Tb.Th), trabecular separation (Tb.Sp), mineralizing surface (LS), mineral apposition rate (MAR), and bone formation rate (BFR). Measurements were performed in accordance with standardized nomenclature and methods (Parfitt et al., 1987).

Northern Hybridizations

Total RNA was isolated from tibial metaphyses for Northern analysis of steady-state mRNA levels for selective bone matrix proteins. Metaphyses from frozen tibiae were individually crushed into powder using a Spex freezer mill (Edison, NJ) and total cellular RNA was extracted and isolated with a modified organic solvent method as described (Turner et al., 1998a). Ten μg of total RNA from each sample were denatured in 1 M glyoxal, 50% dimethylsulfoxide 0.01 M NaH_2PO_4 at 52°C, separated by electrophoresis on a 1% agarose gel, transferred by capillary action in 20X SSC to nylon membranes (Amersham Hybond nylon membrane, Arlington Heights, IL) and crosslinked using a UV source (Stratagen, LaJolla, CA) before hybridization procedures. Membranes were prehybridized for 1–2 hrs at 65°C in a Rapid-Hyb Buffer (Amersham). Hybridization was carried out for 80 min in a buffer containing the above ingredients in addition to a minimum of $4x10^6$ cpm/ml ^{32}P-labeled cDNA for the following bone matrix proteins: prepro-α (I) subunit of type I collagen (collagen), osteocalcin, and osteonectin. The amounts of RNA loaded and transferred were assessed by methylene blue staining of the membranes and by hybridization with ^{32}P-labeled cDNA for 18S ribosomal RNA. Representative Northern blots of bone extracts from ethanol and from PTH-treated rats are published (Dobnig and Turner, 1997; Turner et al., 1998a).

cDNA probes were labeled by random sequence hexanucleotide primer extension using the Megaprime DNA labeling kit (Amersham). The membranes were washed for 30 min at RT in 3X SSC and for 15 min in 1X SSC at 43–65°C.

The mRNA bands on the Northern blots were quantitated by densitometric scanning (Molecular Dynamics Phosphor Imager, Sunnyvale, CA) and values normalized to 18S ribosomal RNA. Representative photographs of phosphor images of Northern blots for type 1 collagen, osteocalcin, and osteonectin are published (Turner et al., 1998a).

Statistical Analysis

Values are expressed as mean ± SE. Group comparisons between the alcohol-treated and nonalcohol fed groups after the first week of treat-

Table 1. Effects of Alcohol and PTH on Body Weight and Uterine Weight

Group	Final body weight (g)	Uterine weight (mg)
Baseline		
Control diet	305 ± 5	865 ± 83
Alcohol diet	295 ± 6	657 ± 64
t-test		
Effect of Alcohol	NS	NS
Treatment		
Control Diet		
Vehicle	307 ± 5	558 ± 48
PTH	305 ± 5	637 ± 69
Alcohol Diet		
Vehicle	280 ± 5	509 ± 34
PTH	285 ± 5	496 ± 49
Two-way ANOVA		
Effect of Alcohol	NS (0.09)	NS
Effect of PTH	NS	NS
Interaction	NS	NS

Values are mean ± SE; $n = 10$.
NS, not significant.

Table 2. Effects of Alcohol on Cancellous Bone Histomorphometry After 1 Week Treatment

Measurement	Control diet	Alcohol diet	p Value (t-test)
BV/TV (%)	25.1 ± 2.9	29.2 ± 1.9	NS
Tb.Th (μm)	56.8 ± 3.2	59.7 ± 3.1	NS
Tb.N (mm^{-1})	4.35 ± 0.32	4.88 ± 0.19	NS
Tb.Sp (μm)	180 ± 20	147 ± 9	NS
LS/BS (%)	2.30 ± 1.6	1.40 ± 0.60	NS
BFR/BS ($\mu m^3/\mu m^2$/d)	0.022 ± 0.007	0.011 ± 0.006	NS
BFR/BV (%/d)	0.080 ± 0.025	0.033 ± 0.016	NS
BFR/TV (%/d)	0.018 ± 0.004	0.011 ± 0.006	NS
MAR (μm/d)	0.94 ± 0.05	0.78 ± 0.10	NS

Values are mean ± SE; n = 7–8. NS is $p > 0.05$.
BV, bone volume; TV, tissue volume; LS, labeled surface; BS, bone surface; MAR, mineral apposition rate; BFR, bone formation rate; Tb, trabecular; Th, thickness; N, number; Sp, separation.
NS, not significant.

ment were determined by Student's t test. The respective effects of ethanol and PTH were analyzed by two-way analysis of variance. Significance was established at p values ≤ 0.05.

RESULTS

Body weights and uterine weights are shown in Table 1. Neither alcohol nor PTH had an effect on body weight or uterine weight.

The effects of 1 week of dietary alcohol on bone histomorphometry are shown in Table 2. Alcohol had no significant effects but there was a consistent tendency toward reduced dynamic measurements, especially LS/BS, BFR/TV, BFR/BS, and BFR/BV.

The effects of 1 week of dietary alcohol on steady-state mRNA levels for bone matrix proteins are shown in Fig. 2. Alcohol resulted in significant decreases in mRNA levels for type 1 collagen, osteonectin, and osteocalcin.

Table 3 shows the effects of 2 weeks of dietary alcohol with and without PTH treatment on bone histomorphometry. Alcohol decreased and PTH treatment increased several indices of bone formation, including LS/BS, BFR/BS, BFR/BV,

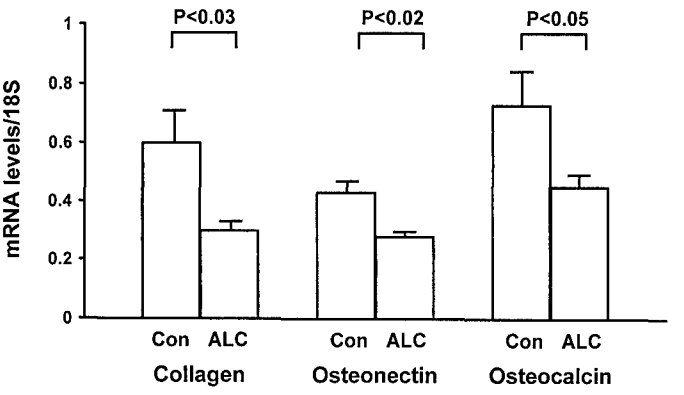

Fig. 2. The effects of a 1-week treatment with alcohol on steady-state mRNA levels for bone matrix proteins. Values are mean ± SE; $n = 4$. Alcohol diet (Alc), control diet (Con).

and BFR/TV. Neither treatment had a significant effect on MAR, although there was a strong tendency for alcohol to reduce this measurement. Alcohol significantly reduced but did not prevent the stimulatory effect of PTH on bone formation.

The effects of PTH treatment with and without alcohol on steady-state mRNA levels for bone matrix proteins are shown in Table 4. PTH increased mRNA levels for type 1 collagen, osteocalcin, and osteonectin. Alcohol had no significant effect on mRNA levels for the three bone matrix proteins after 2 weeks of treatment. However, it tended to decrease the mRNA levels for type 1 collagen and osteocalcin and tended to decrease the stimulatory effects of PTH on mRNA levels for all three bone matrix proteins.

DISCUSSION

Alcohol abuse leads to decreased bone formation in humans (Bikle et al., 1993; Gonzalez-Calvin et al., 1993; Labib et al., 1989; Laitinen et al., 1992; Nielsen et al., 1990; Schnitzler and Solomon, 1984) and experimental animals (Sampson, 1998; Sampson et al., 1997; Turner et al., 1987, 1988, 1991). The present studies demonstrate that the pronounced inhibitory effects of alcohol on bone formation in adult rats can be reversed by PTH, even while rats continue an alcohol intake comparable to alcoholics.

The inhibitory effect of alcohol consumption on bone formation occurred within 2 weeks of initiating treatment. The decreased mRNA levels for bone matrix proteins and strong tendency toward reduced dynamic bone measurements observed in the alcohol-consuming baseline group suggest that the inhibitory effects of alcohol on bone formation were established prior to initiation of PTH treatment. The failure to detect significant changes in dynamic bone histomorphometry in the alcohol-treated rats after 1 week is not unexpected. The fluorochrome based measurements would underestimate an inhibitory response because LS, MAR, and BFR are calculated using two fluorochrome labels, one of which was administered at the time treatment was started, at which time bone formation would not differ

Table 3. Effect of PTH on Bone Histomorphometry in Rats Fed Alcohol for 2 Weeks

Measurement	Group				Two-Way ANOVA		
	Control diet + vehicle	Alcohol diet + vehicle	Control diet + PTH	Alcohol diet + PTH	Alcohol	PTH	Interaction
BV/TV (%)	22.2 ± 1.9	29.4 ± 2.2	27.1 ± 1.9	24.9 ± 1.5	NS	NS	NS
Tb.Th (μm)	55.2 ± 2.2	60.0 ± 2.9	64.7 ± 2.4	59.8 ± 1.8	NS	NS (.06)	NS
Tb.Sp (μm)	204.6 ± 18.7	165.9 ± 12.8	182.4 ± 15.7	186.7 ± 14.8	NS	NS	NS
Tb.N (mm^{-1})	4.0 ± .2	4.7 ± 0.4	4.2 ± .2	4.1 ± .2	NS	NS	NS
LS/BS (%)	4.8 ± 1.3	1.0 ± .4	30.1 ± 3.1	11.7 ± 1.8	.0001	.0001	.0007
MAR (μm/d)	1.09 ± .06	.88 ± .02	1.15 ± .04	.98 ± .03	NS (.06)	NS	NS
BFR/BS ($\mu m^3/\mu m^2$/d)	.05 ± .02	.01 ± .005	.35 ± .04	.12 ± .02	.0001	.0001	.0009
BFR/BV (%/d)	.19 ± .05	.04 ± .01	1.10 ± .12	.40 ± .07	.0001	.0001	.001
BFR/TV (%/d)	.04 ± .01	.01 ± .004	.29 ± .04	.08 ± .009	.0001	.0001	.0005

BV/TV, bone volume/tissue volume; Tb.Th, trabecular thickness; Tb.Sp, trabecular separation; Tb.N, trabecular number; LS/BS, label surface/bone surface; BFR/BS, bone formation rate/bone surface; MAR, mineral apposition rate; BFR/BV, bone formation rate/bone volume; BFR/TV, bone formation rate/tissue volume. NS, not significant.

Table 4. Effect of PTH on Steady-State mRNA Levels for Bone Matrix Proteins in Rats Fed Alcohol for 2 Weeks

Group	Type 1 Collagen/18S	Osteonectin/18S	Osteocalcin/18S
Control diet	10.4 ± 2.9	3.7 ± 0.9	12.0 ± 2.9
Alcohol diet	9.1 ± 1.7	3.9 ± 0.4	11.6 ± 0.7
Control diet + PTH treated	53.8 ± 4.6	16.3 ± 2.1	54.5 ± 3.6
Alcohol diet + PTH treated	35.3 ± 7.1	11.1 ± 1.2	39.1 ± 9.1
Two-way ANOVA			
Effect of Alcohol	NS ($p = 0.05$)	NS ($p = 0.08$)	NS
Effect of PTH	$p < 0.0001$	$p < 0.0001$	$p < 0.0001$
Interaction	NS ($p = 0.09$)	NS ($p = 0.06$)	NS

Values are mean ± SE; $n = 4$.
NS, not significant.

from the controls. Although the present study was only 2 weeks in duration, we have shown that bone formation is also suppressed in adult rats that were continuously fed a diet in which ethanol contributed 35% of the caloric intake after 2 (Turner, unpublished data, 2001) and 4 months (Turner et al., 2001).

The inhibitory effects of alcohol on steady-state mRNA levels for bone matrix proteins were transient; mRNA levels returned toward normal after 2 weeks of alcohol consumption. This finding was, not surprisingly, based on the results of time course studies showing that the effects of alcohol on gene expression can change dramatically over short intervals (Turner et al., 1998a), which suggests that the mRNA levels for bone matrix proteins may depend upon the interval between feeding and sacrifice.

PTH resulted in histomorphometric changes consistent with those reported in published studies, including increases in mineralizing surface and bone formation rate (Dobnig and Turner, 1995; Turner et al., 1998b). The large increases in mRNA levels for bone matrix proteins after PTH-treatment have also been reported (Dobnig and Turner, 1995). The lack of an effect of PTH on bone area and architecture was anticipated because of the short duration of the study (Dobnig and Turner, 1995; Turner et al., 1998b).

In the current study, LS was measured as an index of osteoblast number, and MAR was calculated as an index of osteoblast activity (Turner, 1994). Alcohol consumption inhibited bone formation by decreasing LS and had little effect on MAR. These findings are in agreement with prior rat (Sampson, 1998; Sampson et al., 1997; Turner et al., 1987, 1988, 1991) and human studies (Bikle et al., 1985, 1993; Diez et al., 1994; Gonzalez-Calvin et al., 1993; Lalor et al., 1986; Pumarino et al., 1996; Schnitzler and Solomon, 1984). PTH increases bone formation in rats by increasing osteoblast number and to a lesser extent, activity (Dobnig and Turner, 1995; Turner et al., 1998b).

Prolonged exposure to high concentrations of alcohol inhibits proliferation of cultured osteosarcoma cells (Klein and Carlos, 1995; Klein et al., 1996), immortalized cells derived from the osteoblast lineage (Maran et al., 2001), and primary osteoblastic cell cultures from chick calvaria (Farley et al., 1985). Alcohol, however, had little effect on differentiated osteoblasts which suggests that the reduction in LS in rats that consume alcohol may be due in part to decreased cell proliferation (Klein and Carlos, 1995; Klein et al., 1996; Maran et al., 2001). On the other hand, modulation of osteoblasts to the quiescent bone lining cell phenotype would also result in a reduction in LS. This latter explanation is more likely because the rate of osteoblast turnover in adult rats is very slow (Dobnig and Turner, 1995).

In the present study, chronic alcohol consumption blunted the anabolic effects of PTH on bone. Others have reported that alcohol reduces PTH levels in humans (Laitinen et al., 1991b) and antagonizes the hypercalcemic effects of PTH in rats and dogs (Peng and Gitelman, 1974; Peng et al., 1972). Thus, reduced circulating levels of PTH and/or end organ resistance to the hormone may contribute to alcohol-induced bone loss. Despite the observed antagonism, PTH-treatment increased bone formation in the alcohol-treated rats to values which greatly exceeded those observed in rats fed the control diet. Furthermore, PTH treatment reversed the reduction in LS observed after chronic alcohol consumption. These findings suggest that PTH treatment may be useful as an intervention to reverse alcohol-induced osteopenia. However, additional long-term studies will be necessary to demonstrate that PTH treatment is capable of restoring bone mass in rats with alcohol-induced osteopenia.

ACKNOWLEDGMENT

The authors thank Ms. Lori Rolbiecki for typing this manuscript.

REFERENCES

Bikle DD, Genant HK, Cann C, Recker RR, Halloran BP, Strewler GJ (1985) Bone disease in alcohol abuse. Ann Intern Med 103:42–48.

Bikle DD, Stesin A, Halloran B, Steinbach L, Recker R (1993) Alcohol-induced bone disease: Relationship to age and parathyroid hormone levels. Alcohol Clin Exp Res 17:690–695.

Crilly RG, Anderson C, Hogan D, Delaquerriere-Richardson L (1988) Bone histomorphometry, bone mass, and related parameters in alcoholic males. Calcif Tissue Int 43:269–276.

Diez A, Puig J, Serrano S, Marinoso ML, Bosch J, Marrugat J, Mellibovsky L, Nogues X, Knobel H, Aubia J (1994) Alcohol-induced bone disease in the absence of severe chronic liver damage. J Bone Miner Res 9:825–831.

Dobnig H, Turner RT (1995) Evidence that intermittent treatment with parathyroid hormone increases bone formation in adult rats by activation of bone lining cells. Endocrinology 136:3632–3638.

Dobnig H, Turner RT (1997) The effects of programed administration of human parathyroid hormone fragment (1–34) on bone histomorphometry and serum chemistry in rats. Endocrinology 188:4607–4612.

Farley JR, Fitzsimmons R, Taylor AK, Jorch UM, Lau KH (1985) Direct effects of ethanol on bone resorption and formation in vitro. Arch Biochem Biophys 238:305–314.

Felson DT, Zhang Y, Hannan MT, Kiel DP, Wilson PWF, Anderson JJ (1993) The effect of postmenopausal estrogen therapy on bone density in elderly women. N Engl J Med 329:1141–1146.

Gonzalez-Calvin JL, Garcia-Sanchez A, Bellot V, Munoz-Torres M, Raya-Alvarez E, Salvatierra-Rios D (1993) Mineral metabolism, osteoblastic function and bone mass in chronic alcoholism. Alcohol Alcohol 28:571–579.

Harding A, Dunlap J, Cook S, Mattalino A, Azar F, O'Brien M, Kester M (1988) Osteoporotic correlates of alcoholism in young males. Orthopedics 11:279–282.

Heaney RP, Recker RR, Saville PD (1978) Menopausal changes in bone remodeling. J Lab Clin Med 92:964–970.

Kanis J, Johnell O, Gullberg B, Allander E, Elffors L, Ranstam J, Dequeker J, Dilsen G, Gennari C, Vaz AL, Lyritis G, Mazzuoli G, Miravet L, Passeri M, Perez Cano R, Rapado A, Ribot C (1999) Risk factors for hip fracture in men from southern Europe: The MEDOS study. Mediterranean Osteoporosis Study Osteoporos Int 9:45–54.

Kelepouris N, Harper KD, Gannon F, Kaplan FS, Haddad JG (1995) Severe osteoporosis in men. Ann Intern Med 123:452–460.

Kidder LS, Turner RT (1998) Dietary ethanol does not accelerate bone loss in ovariectomized rats. Alcohol Clin Exp Res 22:2159–2164.

Klein RF, Carlos AS (1995) Inhibition of osteoblastic cell proliferation and ornithine decarboxylase activity by ethanol. Endocrinology 136: 3406–3411.

Klein RF, Fausti KA, Carlos AS (1996) Ethanol inhibits human osteoblastic cell proliferation. Alcohol Clin Exp Res 20:572–578.

Labib M, Abdel-Kader M, Ranganath L, Teale D, Marks V (1989) Bone disease in chronic alcoholism: The value of plasma osteocalcin measurement. Alcohol Alcohol 24:141–144.

Laitinen K, Karkkainen M, Lalla M, Lamberg-Allardt C, Tunninen R, Tahtela R, Valimaki M (1993) Is alcohol an osteoporosis-inducing agent for young and middle-aged women? Metab Clin Exp 42:875–881.

Laitinen K, Lamberg-Allardt C, Tunninen R, Harkonen M, Valimaki M (1992) Bone mineral density and abstention-induced changes in bone and mineral metabolism in noncirrhotic male alcoholics. Am J Med 93:642–650.

Laitinen K, Lamberg-Allardt C, Tunninen R, Karonen SL, Ylikahri R, Valimaki M (1991a) Effects of 3 weeks' moderate alcohol intake on bone and mineral metabolism in normal men. Bone Miner 13:139–151.

Laitinen K, Lamberg-Allardt C, Tunninen R, Karonen SL, Tahtela R, Ylikahri R, Valimaki M (1991b) Transient hypoparathyroidism during acute alcohol intoxication. N Engl J Med 324:721–727.

Laitinen K, Tahtela R, Luomanmaki K, Valimaki MJ (1994) Mechanisms of hypocalcemia and markers of bone turnover in alcohol-intoxicated drinkers. Bone Miner 24:171–179.

Lalor BC, France MW, Powell D, Adams PH, Counihan TB (1986) Bone and mineral metabolism and chronic alcohol abuse. Quarterly J Med 59:497–511.

Maran A, Zhang M, Spelsberg TC, Turner RT (2001) The dose-response effects of ethanol on the human fetal osteoblastic cell line. J Bone Miner Res 16:270–276.

Nielsen HK, Lundby L, Rasmussen K, Charles P, Hansen C (1990) Alcohol decreases serum osteocalcin in a dose-dependent way in normal subjects. Calcif Tissue Int 46:173–178.

Odvina CV, Safi I, Wojtowicz CH, Barengolts EI, Lathon P, Skapars A, Desai PN, Kukreja SC (1995) Effects of heavy alcohol intake in the absence of liver disease on bone mass in black and white men. J Clin Endo Metab 80:2499–2503.

Parfitt AM, Drezner MK, Glorieux FH, Kanis JA, Malluche H, Meunier PJ, Ott SM, Recker RR (1987) Bone histomorphometry: Standardization of nomenclature, symbols and units. J Bone Miner Res 2:595–610.

Peng TC, Cooper CW, Munson PL (1972) The hypocalcemic effect of alcohol in rats and dogs. Endocrinology 91:586–593.

Peng TC, Gitelman HJ (1974) Ethanol-induced hypocalcemia, hypermagnesemia and inhibition of the serum calcium-raising effect of parathyroid hormone in rats. Endocrinology 94:608–611.

Pumarino H, Gonzalez P, Oviedo S, Lillo R, Bustamante E (1996) Assessment of bone status in intermittent and continuous alcoholics, without evidence of liver damage. Revista Medica de Chile 124:423–430.

Sampson HW (1998) Effect of alcohol consumption on adult and aged bone: A histomorphometric study of the rat animal model. Alcohol Clin Exp Res 22:2029–2034.

Sampson HW, Chaffin C, Lange J, DeFee B II (1997) Alcohol consumption by young actively growing rats: A histomorphometric study of cancellous bone. Alcohol Clin Exp Res 21:352–359.

Schnitzler CM, Solomon L (1984) Bone changes after alcohol abuse. S Afr Med J 66:730–734.

Spencer H, Rubio N, Rubio E, Indeika M, Seitam A (1986) Chronic alcoholism: Frequently overlooked cause of osteoporosis in men. Am J Med 80:393–397.

Turner RT (1994) Cancellous bone turnover in growing rats: Time-dependent changes in association between calcein label and osteoblasts. J Bone Miner Res 9:1419–1424.

Turner RT, Aloia RC, Segel LD, Hannon KS, Bell NH (1988) Chronic alcohol treatment results in disturbed vitamin D metabolism and skeletal abnormalities in rats. Alcohol Clin Exp Res 12:151–155.

Turner RT, Evans GL, Cavolina JM, Halloran B, Morey-Holton E (1998b) Programmed administration of parathyroid hormone (PTH) increases bone formation and reduces bone loss in hindlimb unloaded ovariectomized rats. Endocrinology 139:4086–4091.

Turner RT, Greene VS, Bell NH (1987) Demonstration that ethanol inhibits bone matrix synthesis and mineralization in the rat. J Bone Miner Res 2:61–66.

Turner RT, Spector M, Bell NH (1991) Ethanol induced abnormalities in bone formation, turnover, mechanical properties, and mineralization in young adult rats. Cell and Materials (Suppl 1):167–173.

Turner RT, Wronski TJ, Zhang M, Kidder LS, Bloomfield SA, Sibonga JD (1998a) Effects of ethanol on gene expression in rat bone: Transient dose-dependent changes in mRNA levels for bone matrix proteins, skeletal growth factors, and cytokines are followed by reductions in bone formation. Alcohol Clin Exp Res 22:1591–1599.

Turner RT, (2000). Skeletal response to alcohol. Alcohol Clin Exp Res 24:1693–1701.

Turner RT, Kidder LS, Kennedy A, Evans GL, Sibonga JD (2001) Moderate alcohol consumption suppresses bone turnover in adult female rats. J Bone Miner Res 16:589–594.

JOURNAL OF BONE AND MINERAL RESEARCH
Volume 16, Number 3, 2001

Moderate Alcohol Consumption Suppresses Bone Turnover in Adult Female Rats

R.T. TURNER,[1,2] L.S. KIDDER,[1] A. KENNEDY,[1] G.L. EVANS,[1] and J.D. SIBONGA[1]

ABSTRACT

Chronic alcohol abuse is a major risk factor for osteoporosis but the effects of moderate drinking on bone metabolism are largely uninvestigated. Here, we studied the long-term dose-response (0, 3, 6, 13, and 35% caloric intake) effects of alcohol on cancellous bone in the proximal tibia of 8-month-old female rats. After 4 months of treatment, all alcohol-consuming groups of rats had decreased bone turnover. The inhibitory effects of alcohol on bone formation were dose dependent. A reduction in osteoclast number occurred at the lowest level of consumption but there were no further reductions with higher levels of consumption. An imbalance between bone formation and bone resorption at higher levels of consumption of alcohol resulted in trabecular thinning. Our observations in rats raise the concern that moderate consumption of alcoholic beverages in humans may reduce bone turnover and potentially have detrimental effects on the skeleton. (J Bone Miner Res 2001;16:589–594)

Key words: rat bone, alcohol abuse, bone formation, bone resorption

INTRODUCTION

ALCOHOLICS OFTEN have radiographic and histomorphometric evidence of osteopenia and a greatly reduced bone mineral density (BMD).[1–3] Histomorphometric analysis of bone biopsy specimens and measurement of biochemical markers of bone metabolism have revealed consistent evidence that alcohol excess inhibits bone formation.[4–13] The effects of ethanol on bone resorption are less certain; increases, decreases, and no change have been reported.[2,4–7,11,13]

The inability to assign a role for bone resorption in mediating alcohol-induced bone loss highlights the difficulties associated with performing studies in alcoholics. Human studies often are difficult to interpret because of the small number of patients who can be studied and wide variations of the patient population in age, duration, and pattern of alcohol abuse and accompanying risk factors. It is difficult to distinguish the direct effects of ethanol from secondary factors such as magnesium and zinc deficiency, reduced mechanical loading of the skeleton caused by decreased physical activity and weight loss, malabsorption caused by chronic pancreatitis, and skeletal abnormalities associated with increased cigarette smoking and increased use of aluminum-containing antacids. The role of abnormal liver function is especially controversial, with some investigators reporting bone loss in alcoholics free of liver disease and others reporting no bone loss.[4,8,12,14–17] It is especially difficult to control for nutrition, in part because alcoholics have a larger caloric intake than their peers but frequently are underweight.[18,19]

A rat model for alcohol abuse has been developed to circumvent the limitations of human studies. Weight and nutrition can be controlled carefully in this animal model. Growing rats who consume ethanol at a rate (adjusted for the difference in body mass) comparable with alcoholics develop osteopenia and other abnormalities in bone and mineral metabolism.[20,21] All of the changes described in the rat model have been reported in alcoholic patients.[2–4,6,7,11–13,15,17]

[1]Department of Orthopedics, Mayo Foundation, Rochester, Minnesota, USA.
[2]Department of Biochemistry and Molecular Biology, Mayo Foundation, Rochester, Minnesota, USA.

The skeletal response to low and moderate alcohol consumption is relevant to a much larger segment of the adult population than is alcohol abuse but has not been studied extensively in either humans or laboratory animals. The present investigation was designed to investigate the long-term dose-response effects of ethanol on the skeleton of adult female rats. Specifically, the study was designed to determine the minimum consumption of ethanol required to induce bone loss.

MATERIALS AND METHODS

Animal experiment

Female Sprague–Dawley rats (Harlan, Indianapolis, IN, USA) were received at 8 months of age (body weight [BW], 279 ± 3 g; mean ± SE). Subsequent procedures performed on animals were approved by the Mayo Institutional Animal Care and Use Committee in accordance with the National Institutes of Health (NIH) Guide for the Care and Use of Laboratory Animals. Rats were weight-matched into seven study groups (n = 9–12) comprised of four ethanol-treated groups (3, 6, 13, and 35% caloric intake), a control group fed ad libitum, a control group pair fed to the 6% ethanol-treated group, and a control group killed at the start of the experiment (baseline). As described for a previous study,[22] rats were housed individually in a temperature- and humidity-controlled animal facility on a 12-h light/dark cycle. During the first week of the study, all animals were acclimated to a modified Lieber-DeCarli liquid diet (Bio-Serve, Frenchtown, NJ, USA). This diet contains 1.3 g/liter calcium and 1.7 g/liter phosphorous. Protein, fat, and carbohydrates contribute 18, 35, and 47% of caloric intake, respectively. The alcohol-supplemented groups were subsequently fed, ad libitum, a liquid diet containing increasing concentrations of ethanol (95% vol/vol) until receiving the appropriate percent of total caloric intake at the end of the first treatment week. Treatment continued for 4 months. Rats were not given water. Control rats did not receive ethanol and were fed a liquid diet isocalorically supplemented with maltose/dextran, as per the manufacturer's instructions. All animal weights were recorded weekly for the last 12 weeks of the study. On the first day of ethanol treatment, all rats were injected with a 20 mg/kg BW dose of a bone fluorochrome (tetracycline-hydrochloride; Sigma, St. Louis, MO, USA) perivascularly at the base of the tail. The baseline control rats were killed 24 h later. The remaining rats were injected (20 mg/kg BW) with the fluorochromes calcein (Sigma) and demeclocycline (Sigma) 9 days and 2 days before death, respectively. Rats were anesthetized using ketamine and xylazine, weighed, and killed by decapitation. Tibiae were harvested, defleshed, and fixed by immersion in 70% ethanol for bone histomorphometry. Wet weights of uteri were recorded.

Cancellous bone histomorphometry

Tibiae were processed for plastic embedding without demineralization and sectioned as described.[22] Histomorphometry of cancellous bone was performed on unstained longitudinal sections (5 μm thick) in a standard sampling site in the proximal tibial metaphysis.[22] Terminology and abbreviations are consistent with the standardized histomorphometric nomenclature.[23]

All measurements were conducted on an image-analysis system employing OsteoMeasure software (OsteoMetrics, Atlanta, GA, USA) as described.[22]

The following measured and derived histomorphometric values were obtained: total cancellous bone area (BA) measured at a magnification of ×10 in a metaphyseal sampling site divided by the total area of the tissue sampling site (2.88 mm^2) and expressed as a percentage; cancellous BA was compared between the ad libitum and the pair-fed control groups to determine if there was a significant effect of diet on BA; and trabecular thickness (Tb.Th), trabecular number (Tb.N), and trabecular separation (Tb.S) were estimated using the method of Parfitt et al.[24]

Fluorochrome-based measurements and derived values consisting of double-labeled perimeter, mineral apposition rate (MAR), and bone formation rate (BFR) were determined as described.[22] The measurements were performed at a magnification of ×10.

The length of cancellous bone perimeter covered by osteoclasts was measured in toluidine blue–stained sections at ×20, divided by total bone perimeter, and expressed as a percentage. Osteoclasts were morphologically distinguished as large, multinucleated cells with a foamy cytoplasm juxtaposed to bone surface.

Statistics

All values are expressed as means ± SE. Significant differences between alcohol-treated groups and controls were determined by Fisher's protected least significant difference post hoc test for multiple group comparisons after detection of significance by one-way analysis of variance (ANOVA). Significance was considered at values of $p < 0.05$. Dose-response effects were evaluated by linear regression analysis.

RESULTS

Pair feeding had no effect on any measured value. For this reason, the pair-fed and ad libitum control groups were combined.

The effects of ethanol on BW; change in BW, food, and ethanol consumption; and uterine weight are shown in Table 1. The initial BWs did not differ between the treatment groups. Ethanol had minor effects on final BW and food consumption. The lowest concentration of ethanol (3% caloric intake) increased final BW and rate of change in BW as well as consumption of the diet, whereas the highest concentration (35% of caloric intake) significantly decreased food consumption and rate of change in BW. There was a nearly linear increase in total ethanol consumed per day as the concentration of ethanol was increased in the diet. Ethanol treatment tended to decrease uterine weight; the reductions were significant for the groups with 6% and 35% caloric intakes.

TABLE 1. BODY AND UTERINE WEIGHTS

Group	Initial BW (g)	Necropsy BW (g)	Change in BW (g/day)	Diet consumed (ml/day)	Ethanol consumed (ml/day)	Uterine weight (g)
Control	277 ± 5	321 ± 9	0.40 ± 0.06	67.8 ± 2.3	0	0.931 ± 0.047
3% Ethanol	279 ± 6	358 ± 15*	0.75 ± 0.10*	76.6 ± 1.5*	0.44 ± 0.01*	0.946 ± 0.069
6% Ethanol	281 ± 5	339 ± 12	0.54 ± 0.12	69.3 ± 1.4	0.80 ± 0.02*	0.778 ± 0.063*
13% Ethanol	272 ± 9	323 ± 15	0.47 ± 0.08	64.1 ± 1.3	1.60 ± 0.03*	0.835 ± 0.078
35% Ethanol	285 ± 6	291 ± 7	0.06 ± 0.03*	61.5 ± 2.4*	4.12 ± 0.16*	0.722 ± 0.045*

Values are mean ± SEM.
* $p < 0.05$ treatment (n = 9–12) versus control (n = 20–22).

TABLE 2. CANCELLOUS BONE ARCHITECTURE

Group	BA/TA (%)	Tb.Th (μm)	Tb.N (mm^{-1})	Tb.S (μm)
Baseline	25.6 ± 1.3	70.1 ± 1.9	3.7 ± 0.2	208 ± 13
Control	20.6 ± 1.2	64.9 ± 2.6	3.2 ± 0.1	260 ± 15
3% Ethanol	19.5 ± 1.4	62.5 ± 3.0	3.1 ± 0.1	267 ± 16
6% Ethanol	18.3 ± 1.7	57.6 ± 2.3*	3.2 ± 0.2	274 ± 26
13% Ethanol	15.7 ± 2.3*	52.5 ± 2.4*	2.9 ± 0.4	359 ± 73
35% Ethanol	15.8 ± 1.0*	50.9 ± 1.7*	3.1 ± 0.1	281 ± 20

Values are mean ± SEM.
* $p < 0.05$ treatment (n = 8–11) versus control (n = 19).

The effects of ethanol on static bone histomorphometry are summarized in Table 2. BA/tissue area (TA) was significantly decreased in the 13% and 35% caloric intake groups and Tb.Th was decreased for intake levels at and above 6%. Tb.N and Tb.S were not significantly influenced by ethanol.

The effects of ethanol on cancellous bone dynamic and cellular histomorphometry are summarized in Table 3. Ethanol treatment decreased mineralizing perimeter (M.Pm) and BFR (perimeter referent). Ethanol had no effect on MAR. All concentrations of ethanol treatment reduced osteoclast perimeter (Oc.Pm) to a similar magnitude.

We were unable to measure longitudinal bone growth because of inadequate separation between the tetracycline label given at the start of the experiment and the mineralized hypertrophic cartilage.

The dose-response effects of alcohol are summarized in Table 4. Linear regression revealed significant dose-dependent decreases in BA/TA, Tb.Th, M.Pm, and BFR. There was no dose-dependent effect of alcohol on BW, uterine wet weight, Tb.N, Tb.S, MAR, or Oc.Pm.

DISCUSSION

The observed results are disturbing because we did not observe a no-effect dose for alcohol consumption. Pronounced changes in bone metabolism were observed at the lowest consumption level of alcohol. Dietary intake of alcohol comprising as little as 3% of total calories dramatically reduced histological indices of bone turnover. Higher consumption levels of alcohol resulted in alterations in trabecular architecture and even net cancellous bone loss.

Analysis of the cancellous bone architecture revealed that alcohol-induced bone loss was caused by a reduction in Tb.Th; Tb.N was not altered. Oc.Pm was not increased, indicating that cancellous bone loss was caused by a disturbance in the bone remodeling balance rather than increased bone remodeling. Indeed, the present results indicate that alcohol consumption results in reduced bone remodeling as evidenced by the decreases in histomorphometric indices of bone resorption (Oc.N) and bone formation (M.Pm).

Cancellous bone remodeling occurs when focal resorption (remodeling unit) is initiated on a previously quiescent trabecular surface.[25] A small amount of bone is resorbed and the resulting resorption lacuna is filled shortly thereafter as a result of new bone formation. There are two cellular mechanisms that could lead to trabecular thinning: (1) excessive erosion during the resorption phase and (2) incomplete refilling of the erosion cavity during the formation phase. The maximum inhibition of osteoclast number was achieved at the lowest level of alcohol consumption, whereas M.Pm showed a striking dose-dependent decrease. These findings suggest that incomplete filling of the erosion cavity during the formation phase of the remodeling cycle is the more likely cellular mechanism for trabecular thinning. The MAR was not altered, suggesting that alcohol inhibits onset of the bone formation phase of the remodeling cycle but not its continuation once initiated. These results are consistent with Dyer et al.[26] who concluded that alcohol

TABLE 3. FLUOROCHROME AND OSTEOCLAST MEASUREMENTS

Group	*M.Pm/B.Pm (%)*	*MAR (μm/d)*	*BFR/BV (%/d)*	*Oc.Pm (%)*
Control	11.05 ± 0.75	0.94 ± 0.04	0.325 ± 0.019	15.77 ± 1.15
3% Ethanol	5.79 ± 1.07*	0.92 ± 0.02	0.169 ± 0.032*	10.78 ± 1.85*
6% Ethanol	5.14 ± 0.78*	0.91 ± 0.03	0.171 ± 0.031*	10.62 ± 1.18*
13% Ethanol	3.71 ± 0.77*	1.01 ± 0.04	0.150 ± 0.035*	10.66 ± 0.99*
35% Ethanol	2.37 ± 0.56*	0.86 ± 0.04	0.077 ± 0.019*	10.09 ± 1.52*

Values are mean ± SEM.
* $p < 0.05$ treatment ($n = 11$) versus control ($n = 18$–20).
B.Pm, bone perimeter.

TABLE 4. DOSE-RESPONSE EFFECTS OF ETHANOL ANALYZED BY LINEAR REGRESSION

Measurement	r Value	p Value
Necropsy BW (g)	—	NS
Uterine wet weight (g)	—	NS
BA/TA (%)	0.31	0.0001
Tb.Th (μm)	0.43	0.0012
Tb.N (mm^{-1})	—	NS
Tb.S (μm)	—	NS
M.Pm/B.Pm	0.77	0.0001
MAR (μm/d)	—	NS
BFR (%/d)	0.79	0.0001
Oc.Pm	—	NS

B.Pm, bone perimeter.

inhibits osteoblast proliferation and activity in the rat. This observation also is consistent with in vitro studies showing that ethanol delays recruitment of osteoblasts but has little effect on bone matrix protein gene expression and peptide secretion by mature osteoblasts.[27,28] Similarly, ethanol did not increase apoptosis in vitro,[25] suggesting that osteoblast lifespan is unaffected.

At first glance, the observed nondose-dependent reduction in uterine weight in rats fed some doses of ethanol suggests that gonadal insufficiency contributes to the bone changes. However, the histological changes are not consistent with this possibility. Ovariectomy results in greatly elevated bone turnover[29,30] whereas alcohol reduced bone turnover. In addition, the pattern of bone loss differs from ovariectomy. Gonadal insufficiency decreases Tb.N, whereas ethanol resulted in a decrease in Tb.Th.[22] The mechanism for the uterine atrophy is not clear but alcohol has been reported to induce a variety of pathophysiological changes in the uterus, including uterine atrophy.[31] Furthermore, we have identified numerous genes in which expression is altered dramatically after acute administration of 1 mg/kg of ethanol, suggesting that alcohol has direct effects on the uterus (Turner et al., unpublished results, 2000).

Studies performed in growing male[21,32–35] and female[36,37] rats indicated that chronic consumption of large doses of alcohol in the diet suppresses bone growth. The resulting relative osteopenia is caused by the failure to acquire a normal bone mass and is relevant to juvenile alcohol abusers. The present study in older rats is more relevant to adult humans and shows alcohol-induced bone loss in rats. Our failure to detect measurable longitudinal bone growth at the proximal tibial growth plate provides definitive evidence that the observed changes were not influenced by growth. The present study also differs from previous work in that it attempts to model moderate as well as abusive alcohol consumption.

There is no universal agreement as to what constitutes moderate drinking. Additionally, the level of ethanol consumption in rats in this study cannot be related directly to humans because the rates of metabolism differ between the two species. The variables that must be considered and evaluated in these studies include: total ethanol consumed, the percent caloric intake contributed by ethanol, and peak blood levels of ethanol.

The low-dose group (3% caloric intake) consumed approximately 0.4 ml ethanol/day. On a body mass basis, this would be equivalent to approximately three standard drinks by a 50-kg woman, which is on the high end of moderate alcohol consumption. However, relative to caloric intake, this level of consumption would be the equivalent of <0.5 daily drinks, which is on the low end. Blood ethanol levels may be more important than the absolute amount of alcohol consumed. Ethanol administered at 35% of caloric intake resulted in measured blood ethanol levels of 0.09–0.15%.[21,32,33,36] The measured levels are likely to underestimate peak blood alcohol levels because sequential measurements have not been performed throughout the rat feeding cycle. Nevertheless, these levels are near to or exceed the impairment level, which generally is considered to be between 0.08 and 0.10%. This high blood alcohol level contrasts with the 3% caloric intake dose rate, which results in blood alcohol levels below the assay detection limit. Taken as a whole, the data suggest that our dose range in the rat extends from the human equivalent of low-moderate to alcohol abuse.

Bone formation generally is reduced in alcoholics.[3,4,7,17] Additionally, administration of ethanol to healthy volunteers results in an acute decrease in serum osteocalcin levels.[8–10] The similarity between our results and those seen in humans indicates that in addition to being a good model for alcohol abuse in adults, the mature rat also may be predictive for the skeletal effects of moderate drinking.

The implications of a reduction in bone turnover in moderate drinkers may depend on age and other factors. On one

hand, ethanol consumption by adolescents might reduce peak bone mass, which would predispose the individual to osteoporosis. On the other hand, a reduction in bone turnover is likely to reduce the risk of osteoporosis in postmenopausal women because these individuals are losing bone at a rapid rate because of, in part, elevated bone turnover. This speculation is supported by epidemiological data indicating that postmenopausal moderate drinkers have a higher bone mass than abstainers.[38–41] It also is supported by studies in ovariectomized rats, which show that ethanol does not accelerate the bone loss associated with gonadal insufficiency and may reduce osteoclast number.[22,42,43]

Neither moderate nor high doses of alcohol prevented bone loss in ovariectomized rats.[22,42,43] Ovariectomy is likely to result in a more extreme depletion of gonadal hormones than menopause. Epidemiological studies suggest that estrogen replacement accentuates the putative beneficial skeletal response to alcohol in postmenopausal women.[41] Thus, it is possible that the combined antiremodeling actions of estrogen replacement and alcohol have additive effects in women and rats.

In summary, these studies in rats show that alcohol consumption results in dose-dependent bone loss and decreased bone turnover. A no-effect dose for alcohol was not observed. The findings in rats suggest that even moderate levels of alcoholic beverage consumption in humans may reduce bone turnover and potentially have detrimental effects on the skeleton.

ACKNOWLEDGMENTS

The authors thank Ms. Lori Rolbiecki for typing this manuscript and Ms. Peggy Backup for editorial assistance. The authors also thank Mr. Charles Rowland for his biostatistical analysis. These studies were supported by the National Institutes of Health grant AA11140 and the Department of Defense grant DAMD17–98-1–8517 as well as the Mayo Foundation.

REFERENCES

1. Spencer H, Rubio N, Rubio E, Indeika M, Seitam A 1986 Chronic alcoholism: Frequently overlooked cause of osteoporosis in men. Am J Med **80:**393–397.
2. Bikle DD, Genant HK, Cann C, Recker RR, Halloran BP, Strewler GJ 1985 Bone disease in alcohol abuse. Ann Intern Med **103:**42–48.
3. Gonzalez-Calvin JL, Garcia-Sanchez A, Bellot V, Munoz-Torres M, Raya-Alvarez E, Salvatierra-Rios D 1993 Mineral metabolism, osteoblastic function and bone mass in chronic alcoholism. Alcohol Alcohol **28:**571–579.
4. Lalor BC, France MW, Powell D, Adams PH, Counihan TB 1986 Bone and mineral metabolism and chronic alcohol abuse. QJM **59:**497–511.
5. Schnitzler CM, Solomon L 1984 Bone changes after alcohol abuse. S Afr Med J **66:**730–734.
6. Diez A, Puig J, Serrano S, Marinoso ML, Bosch J, Marrugat J, Mellibovsky L, Nogues X, Knobel H, Aubia J 1994 Alcohol-induced bone disease in the absence of severe chronic liver damage. J Bone Miner Res **9:**825–831.
7. Bikle DD, Stesin A, Halloran B, Steinbach L, Recker R 1993 Alcohol-induced bone disease: Relationship to age and parathyroid hormone levels. Alcohol Clin Exp Res **17:**690–695.
8. Nielsen HK, Lundby L, Rasmussen K, Charles P, Hansen C 1990 Alcohol decreases serum osteocalcin in a dose-dependent way in normal subjects. Calcif Tissue Int **46:**173–178.
9. Labib M, Abdel-Kader M, Ranganath L, Tealem D, Marks V 1989 Bone disease in chronic alcoholism: The value of plasma osteocalcin measurement. Alcohol Alcohol **24:**141–144.
10. Rico H, Cabranes JA, Cabello J, Gomez-Castresana F, Hernandez ER 1987 Low serum osteocalcin in acute alcohol intoxication. A direct toxic effect of alcohol on osteoblasts. Bone Miner **2:**221–225.
11. Laitinen K, Tahtela R, Luomanmaki K, Valimaki MJ 1994 Mechanisms of hypocalcemia and markers of bone turnover in alcohol-intoxicated drinkers. Bone Miner **24:**171–179.
12. Laitinen K, Lamberg-Allardt C, Tunninen R, Harkonen M, Valimaki M 1992 Bone mineral density and abstention-induced changes in bone and mineral metabolism in noncirrhotic male alcoholics. Am J Med **93:**642–650.
13. Laitinen K, Lamberg-Allardt C, Tunninen R, Karonen SL, Ylikahri R, Valimaki M 1991 Effects of 3 weeks' moderate alcohol intake on bone and mineral metabolism in normal men. Bone Miner **13:**139–151.
14. Pumarino H, Gonzalez P, Oviedo S, Lillo R, Bustamante E 1996 Assessment of bone status in intermittent and continuous alcoholics, without evidence of liver damage. Rev Med Chil **124:**423–430.
15. Crilly RG, Anderson C, Hogan D, Delaquerriere-Richardson L 1988 Bone histomorphometry, bone mass, and related parameters in alcoholic males. Calcif Tissue Int **43:**269–276.
16. Harding A, Dunlap J, Cook S, Mattalino A, Azar F, O'Brien M, Kester M 1988 Osteoporotic correlates of alcoholism in young males. Orthopedics **11:**279–282.
17. Diamond T, Stiel D, Lunzer M, Wilkinson M, Posen S 1989 Ethanol reduces bone formation and may cause osteoporosis. Am J Med **86:**282–288.
18. Preedy VR, Reilly ME, Patel VB, Richardson PJ, Peters TJ 1999 Protein metabolism in alcoholism: Effects on specific tissues and the whole body. Nutrition **15:**604–608.
19. Preedy VR, Peters TJ, Why H 1997 Metabolic consequences of alcohol dependency. Adverse Drug React Toxicol Rev **16:**235–256.
20. Peng TC, Gitelman HJ 1974 Ethanol-induced hypocalcemia, hypermagnesemia and inhibition of the serum calcium-raising effect of parathyroid hormone in rats. Endocrinology **94:**608–611.
21. Turner RT, Aloia RC, Segel LD, Hannon KS, Bell NH 1988 Chronic alcohol treatment results in disturbed vitamin D metabolism and skeletal abnormalities in rats. Alcohol Clin Exp Res **12:**151–155.
22. Kidder LS, Turner RT 1998 Dietary ethanol does not accelerate bone loss in ovariectomized rats. Alcohol Clin Exp Res **22:**2159–2164.
23. Parfitt AM, Drezner MK, Glorieux FH, Kanis JA, Malluche H, Meunier PJ, Ott SM, Recker RR 1987 Bone histomorphometry: Standardization of nomenclature, symbols, and units. Report of the ASBMR Histomorphometry Nomenclature Committee. J Bone Miner Res **2:**595–610.
24. Parfitt AM, Mathews CH, Villanueva AR, Kleerekoper M, Frame B, Rao DS 1983 Relationships between surface, volume, and thickness of iliac trabecular bone in aging and in osteoporosis. Implications for the microanatomic and cellular mechanisms of bone loss. J Clin Invest **72:**1396–1409.
25. Frost HM 1969 Tetracycline-based histological analysis of bone remodeling. Calcif Tissue Res **3:**211–237.
26. Dyer SA, Buckendahl P, Sampson HW 1998 Alcohol consumption inhibits osteoblastic cell proliferation and activity in vivo. Alcohol **16:**337–341.

27. Klein RF 1997 Alcohol-induced bone disease: Impact of ethanol on osteoblast proliferation. Alcohol Clin Exp Res **21:** 392–399.
28. Maran A, Zhang M, Spelsberg TC, Turner RT 2001 Evidence that ethanol-mediated changes in bone metabolism are due to indirect effects on osteoblast bone matrix gene expression. J Bone Miner Res (in press).
29. Wronski TJ, Walsh CC, Ignaszewski LA 1986 Histological evidence for osteopenia and increased bone turnover in ovariectomized rats. Bone **7:**119–123.
30. Cavolina JM, Evans GL, Harris SA, Zhang M, Westerlind KC, Turner RT 1997 The effects of orbital spaceflight on bone histomorphometry and mRNA levels for bone matrix proteins and skeletal signaling peptides in ovariectomized growing rats. Endocrinology **138:**1567–1576.
31. Mello NK, Bree MP, Mendelson JH, Ellingboe J, King MW, Sehgal P 1983 Alcohol self-administration disrupts reproductive function in female macaque monkeys. Science **221:**677–679.
32. Turner RT, Greene VS, Bell NH 1987 Demonstration that ethanol inhibits bone matrix synthesis and mineralization in the rat. J Bone Miner Res **2:**61–66.
33. Turner RT, Wronski TJ, Zhang M, Kidder LS, Bloomfield SA, Sibonga JD 1998 Effects of ethanol on gene expression in rat bone: Transient dose-dependent changes in mRNA levels for matrix proteins, skeletal growth factors, and cytokines are followed by reductions in bone formation. Alcohol Clin Exp Res **22:**1591–1599.
34. Turner RT, Spector M, Bell NH 1991 Ethanol induced abnormalities in bone formation, turnover, mechanical properties, and mineralization in young adult rats. Cell Mater **1:**167–173.
35. Peng TC, Kusy RP, Hirsch PF, Hagman JR 1988 Ethanol-induced changes in morphology and strength of femurs of rats. Alcohol Clin Exp Res **12:**1655–1659.
36. Sampson HW, Perks N, Champney TH, DeFee B II 1996 Alcohol consumption inhibits bone growth and development in young actively growing rats. Alcohol Clin Exp Res **20:** 1375–1384.
37. Hogan HA, Sampson HW, Cashier E, Ledoux N 1992 Alcohol consumption by young actively growing rats: A study of cortical bone histomorphometry and mechanical properties. Alcohol Clin Exp Res **21:**809–816.
38. Laitinen K, Karkkainen M, Lalla M, Lamberg-Allardt C, Tunninen R, Tahtela R, Valimaki M 1993 Is alcohol an osteoporosis-inducing agent for young and middle-aged women? Metab Clin Exp **42:**875–881.
39. Laitinen K, Valimaki M, Keto P 1991 Bone mineral density measured by dual-energy X-ray absorptiometry in healthy Finnish women. Calcif Tissue Int **48:**224–231.
40. Feskanich D, Korrick SA, Greenspan SL, Rosen HN, Colditz GA 1999 Moderate alcohol consumption and bone density among postmenopausal women. J Womens Health **8:**65–73.
41. Felson DT, Zhang Y, Hannon MT, Kiel DP, Wilson PWF, Anderson JJ 1993 The effect of postmenopausal estrogen therapy on bone density in elderly women. N Engl J Med **329:**1141–1146.
42. Sampson HW, Shipley D 1997 Moderate alcohol consumption does not augment bone density in ovariectomized rats. Alcohol Clin Exp Res **21:**1165–1168.
43. Fanti P, Monier-Faugere MC, Geng Z, Cohen D, Malluche HH 1997 Moderately high consumption of ethanol suppresses bone resorption in ovariectomized but not in sexually intact adult female rats. Alcohol Clin Exp Res **21:**1150–1154.

Address reprint requests to:
Russell T. Turner
Orthopedic Research
Room 3–69 Medical Science Building
Mayo Clinic
200 First Street Southwest
Rochester, MN 55905, USA

Received in original form May 9, 2000; in revised form August 18, 2000; accepted October 12, 2000.

DISUSE EXAGGERATES THE DETRIMENTAL EFFECTS OF ALCOHOL ON CORTICAL BONE

RUNNING TITLE: Alcohol, Disuse and Bone

Theresa Hefferan, Angela M. Kennedy, Glenda L. Evans, Russell T. Turner

Department of Orthopedics, Mayo Clinic, Rochester, MN

Address correspondence to: Russell T. Turner, Ph.D.
Orthopedic Research
Room 3-69 Medical Science Bldg.
Mayo Clinic
200 First Street SW
Rochester, MN 55905
Phone: (507) 284-4062/Fax: (507) 284-5075
E-mail: turner.russell@mayo.edu

ABSTRACT

Background: Alcohol abuse is associated with an increased risk for osteoporosis. However, co-morbidity factors may play an important role in the pathogenesis of alcohol-related bone fractures. Sub-optimal mechanical loading of the skeleton, an established risk factor for bone loss, may occur in some alcohol abusers due to reduced physical activity, muscle atrophy or both. The purpose of the present study was to determine if mechanical disuse alters bone metabolism in a rat model for chronic alcohol abuse.

Methods: Alcohol was administered in the diet (35% caloric intake) of 6-month-old male rats for 4 weeks. Rats were hindlimb unloaded the final 2 weeks of the experiment in order to prevent dynamic weight bearing. Afterwards, cortical bone histomorphometry was evaluated at the tibia-fibula synostosis.

Results: At the periosteal surface of the tibial diaphysis, alcohol and hindlimb unloading independently decreased mineralizing perimeter, mineral apposition rate and bone formation rate. In addition, alcohol, but not hindlimb unloading, increased endocortical bone resorption. The respective detrimental effects of alcohol and hindlimb unloading to inhibit bone formation were additive; there was no interaction between the two variables.

Conclusion: Reduced weight bearing accentuates the detrimental effects of alcohol on cortical bone in adult male rats by further inhibiting bone formation. This finding suggests that reduced physical activity may be a co-morbidity factor for osteoporosis in alcohol abusers.

Key Words: Osteoblasts, osteoclasts, osteoporosis, bone remodeling, rat bone

INTRODUCTION

Over 6 million fractures occur in the United States per year of which roughly 5% do not heal properly and require additional and often costly interventions. The consequences of fractures (including ones that heal normally) are especially severe in the elderly. Hip fractures, because of the prolonged recovery interval and loss of mobility, are devastating with more than 275,000 occurring annually in women and an additional 100,000 in men (Cooper and Melton, 1992). Approximately 70% of the hip fractures are attributable to osteoporosis (Cumming et al., 1985). Patients with hip fractures have increased mortality (up to 20% die within 6 months) and those who survive generally have a poor prognosis for complete recovery; 20% will require long term institutionalization (>1 year) and a similar percentage will face a permanent decrease in quality of life (e.g., mobility limited to a walker or wheelchair) (Cooper and Melton, 1992). The number of hip fractures is increasing at an alarming rate. Compared to 1990, the number of annual hip fractures is projected to increase worldwide during the next 50 years from 1.2 to 4.5 million in women and 0.5 to 1.8 million in men (Cooper et al., 1992).

Vertebral fractures represent the other common severe fracture that is specifically associated with osteoporosis. The estimated lifetime risk in 50-year-old Americans of European descent for a clinically diagnosed vertebral fracture is 15.6% for women and 5.0% for men (Cooper and Melton, 1992). Until recently, it was believed that osteoporotic vertebral fractures were not accompanied by significant mortality. However, population based studies show that the overall survival among patients with a vertebral fracture is substantially reduced (Cooper and Melton, 1992). In contrast to mortality associated with hip fractures, which typically occurs within 6 months, there is a sustained reduction in survival in patients with vertebral fractures

such that the excess mortality reaches nearly 20% by 5 years following the fracture (Poor et al., 1995).

Insidious bone loss combined with the great difficulty of restoring bone to an osteopenic skeleton makes it imperative to identify risk factors for bone loss and to effectively intervene prior to fracture. European heritage and menopause are inherent risk factors for osteoporosis. However, avoidable lifestyle risk factors are responsible for the majority of osteoporotic fractures (Cooper and Melton, 1992). Alcohol abuse is one such risk factor (Bikle et al 1985, 1993; Diez et al, 1994; Gonzalex-Calvin et al., 1993; Lalor et al., 1986; Pumarino et al., 1996; Schnitzler and Solomon, 1984); reduced bone mass in alcoholics has been detected by histomorphometry of iliac crest bone biopsies (Bikle et al., 1985, 1993; Schnitzler and Solomon, 1984), as well as by densitometry (Diez et al., 1994; Gonzalez-Calvin et al., 1993; Lalor et al., 1986; Pumarino et al., 1996).

The cellular mechanisms leading to bone loss in alcoholics have been investigated. Histological indices of bone formation and serum osteocalcin, a biochemical marker of bone matrix synthesis, are consistently reduced in alcoholics clearly implicating reduced bone formation as a contributing factor to bone loss (Gonzalez-Calvin et al., 1993; Labib et al., 1989; Laitinen et al., 1991a, 1992, 1994; Nielson et al., 1990; Rico et al., 1987). The effects of alcohol on bone resorption are more variable, with increases, decreases and no change having been reported (Bikle et al., 1993, 1985; Crilley et al., 1988; Diez et al., 1994; Laitinen et al., 1991a, 1994; Lalor et al., 1986; Schnitzler and Solomon, 1984).

Prospective and retrospective studies have been performed in an attempt to establish an association between alcohol and bone mass in the general population. In contrast to studies in alcoholics, these population-based studies have not consistently detected either a decrease in

bone mineral density or increase in fracture incidence associated with alcohol consumption (Felson et al., 1995; Feskanisch et al., 1999; Grainge et al., 1998; Hoidrup et al., 1999a, 1999b; Holbrook and Barrett-Connor, 1993; Jouanny et al., 1995; Krogsgaard et al., 1994; Laitinen et al., 1992; May et al., 1995; Orwoll et al., 1996; Perry et al., 1999). It is well established that the presence of multiple risk factors can greatly enhance the likelihood of a woman developing a postmenopausal fracture (Cummings et al., 1995). By analogy, alcohol abuse in concert with additional risk factors may be more likely to lead to osteoporosis than alcohol abuse alone.

Abnormal liver function, poor nutritional status and cigarette smoking are common in alcohol abusers. Limited investigation suggests that these independent risk factors for osteoporosis may contribute to bone loss in alcoholics (Bikle et al., 1985; Laitinen et al., 1992; Crilly and Delaquerriere-Richardson, 1990). Physical activity, another well-recognized determinant of bone mass (Kanis et al., 1999), has not been extensively investigated in relationship to alcohol abuse. The purpose of the present study in sexually mature male rats was to determine whether reduced mechanical loading of the skeleton induced by unloading the hindlimbs exaggerates the detrimental effects of alcohol on cortical bone histomorphometry.

METHODS

Six-month old, intact, male Fisher 344 rats were obtained from Harlan Laboratory (Indianapolis, IN) and maintained in accordance with the procedures approved by the Mayo Institutional Animal Care and Use Committee as outlined by the NIH Guide for the Care and Use of Laboratory Animals. The animals were weight-matched (330 ± 3 g, mean $\pm$ SE) and assigned to treatment groups. The treatment groups consisted of: baseline loaded (normal weight bearing) control (n=9), baseline loaded alcohol (N=10), loaded control (N=11), loaded alcohol (N=11), hindlimb unloaded control (N=11), and hindlimb unloaded alcohol (N=11). The

experimental design is outlined in Figure 1. The animals were individually housed in either standard cages for the loaded treatment groups or specially equipped cages (Harper et al., 1994; Turner et al., 1998) for the hindlimb unloaded group. Hindlimb unloading is a well established method to reduce weight bearing that was originally developed as a ground-based model for spaceflight (Globus, et al. 1996). The room temperature was maintained at 22°C with a 12-hour light/dark cycle.

The alcohol-fed groups were acclimated during the first week to a modified Lieber-DeCarli liquid diet (BioServe, Frenchtown, NJ, USA). To maintain normal food consumption, the amount of alcohol for the alcohol-treated groups was gradually increased from 11.5% of caloric intake to 23% to 35% on day 1, day 4, and day 7, respectively. The control groups received liquid diet containing isocaloric substitution of maltose/dextran for alcohol. All other groups were pair-fed to the hindlimb unloaded alcohol group to control for weight loss associated with reduced caloric intake.

On day 8, when the caloric contribution of alcohol was increased to 35%, the baseline animals were given calcein (Sigma, St Louis, MO) 20 mg/kg body weight by perivascular injection at the base of the tail. The second fluorochrome, tetracycline hydrochloride, (Sigma), 20 mg/kg body weight, was given by tail injection on day 15. The baseline control and baseline alcohol control groups were sacrificed two days later. The four remaining experimental groups were given fluorochrome labels (20 mg/kg body weight) by tail injection on day 15 (calcein), day 19 (tetracycline hydrochloride), and day 28 (calcein). The animals were anesthetized with ketamine (100 mg/ml) and xylazine (100mg/ml), bled by cardiac puncture, and killed by decapitation; baseline animals on day 17, and the experimental groups on day 31.

Bone Histomorphometry

The tibiae were isolated and adherent muscle tissue was removed prior to fixation in 70% ethanol for bone histomorphometric analysis. A precision caliper (Buehler, Lake Bluff, IL) was used to measure the length of the tibiae. Ground sections were cut proximal to the tibia-fibula synostosis and prepared as described previously (Cavolina et al., 1997). Histomorphometric analysis was conducted using an image-analysis system coupled with OsteoMeasure software (OsteoMetrics, Atlanta, GA). Cross-sectional area, cortical area, medullary area, double label surface, mineral apposition rate, and bone formation rate were determined (Turner et al., 1998). The endocortical resorption rate was calculated by subtracting the mean baseline medullary area from the final medullary area and dividing the differences by the 14 d experimental interval. This method underestimates bone resorption if there is concurrent endocortical bone formation. However, in the present study endocortical bone formation was too low to measure.

Statistical Analysis

All values are expressed as means $\pm$ SE. Comparisons among treatment groups were made by analysis of variance (ANOVA) using StatView (Abacus Concepts, Berkeley, CA) software. Post hoc comparisons were made using Fisher's protected least significant difference test. SuperANOVA software (Abacus Concepts, Berkeley, CA) was used for the two-way ANOVA.

RESULTS

The data was analyzed by two-way ANOVA; hindlimb unloading and alcohol were the two interacting variables. No significant interaction term was detected fro any measurement indicating that the two variables had independent additive effects.

The animals weighed ~335 g at the start of the experiment; at that time there were no differences between groups in body weight. There was no change in body weight during the 4 w experiment in the weight bearing groups. Alcohol had no effect on body weight but, despite pair-feeding, hindlimb unloading resulted in a significant (10-14%) decrease in body weight.

The static bone measurements are tabulated in Table 1. There were no differences between groups in tibia length, cross-sectional area and cortical bone area. The medullary area was increased in rats fed alcohol compared with the alcohol baseline group. Two-way ANOVA confirmed that alcohol but not hindlimb unloading increased medullary area.

The effects of alcohol and unloading on the calculated endocortical bone resorption rate are shown in Figure 2. Alcohol but not unloading increased bone resorption.

Alcohol had no effect on dynamic bone histomorphometry (dl.Pm, MAR and BFR) during the two week baseline interval (data not shown). Also, there was no difference in dynamic measurements between the baseline control and post-treatment weight bearing control groups (data not shown).

The effects of alcohol and hindlimb unloading on dynamic bone measurements performed at the periosteum are shown in Figure 3. Alcohol and hindlimb unloading decreased fluorochrome double label surface (3a), mineral apposition rate (3b), and bone formation rate (3c) compared to their respective baseline value. Two-way ANOVA confirmed that alcohol and hindlimb unloading have independent additive inhibitory effects on double label surface, mineral apposition rate, and bone formation rate.

DISCUSSION

The detrimental changes in cortical bone histomorphometry observed in rats fed alcohol were anticipated because of the well documented inhibition of periosteal and endocortical bone formation by ethanol in rapidly growing male and female rats (Turner et al., 1987; Turner et al., 1991; Hogan et al., 1997; Turner et al., 1988; Sampson et al., 1997; Sampson et al., 1999; Sampson et al., 1996; Sampson et al., 1997b; Peng et al., 1988). The present study extends earlier work by showing that alcohol inhibits cortical bone formation in rats approaching skeletal maturity and by investigating the combined effects of alcohol and reduced weight bearing on cortical bone.

Insignificant changes in most static bone measurements were noted in the present study, the exception being a significant increase in medullary area. The failure to detect changes in cross-sectional area and cortical bone area was not unexpected because of the relatively short duration of the experiment. Additionally, in contrast to growing rats in whom bone formation was suppressed during the first week of alcohol feeding (Turner, et al., 2001a), no change occurred in adults during the first two weeks. However, the reduction in bone formation in alcohol-fed rats during the final two weeks of the present study is consistent with the detrimental effects of alcohol on bone mass observed in longer duration experiments (Sampson et al., 1999b; Turner et al., 1988; Turner et al., 2001). An alcohol-induced increase in marrow area has been previously reported (Turner et al., 1988; Turner et al., 1987) but the cellular mechanism for the change could not be determined with certainty because the rats were growing and pre-treatment baseline values were not measured. In growing animals, it is generally not possible to distinguish between bone loss (osteoclast-mediated) and failure to gain normal amounts of bone (osteoblast-mediated). The present study in adults showed that alcohol resulted in an increase in medullary area compared to baseline control values as well as age-matched controls. This

finding demonstrates that alcohol resulted in a net increase in endocortical bone resorption. Furthermore, these results show that the net change was primarily due to an increase in bone resorption; the prevailing rate of bone formation was too small for a change in that parameter to contribute much to the increase in size of the bone marrow cavity.

Reduced dynamic weight bearing, whether due to spaceflight (Morey and Baylink, 1978; Wronski and Morey, 1983), sciatic neurotomy (Turner and Bell, 1986), limb casting (Li et al., 1990), tendonotomy (Thompson and Rodan, 1988), or hindlimb unloading (Globus et al., 1986), results in osteopenia in rats. The bone formation rate is decreased in the unweighted skeleton but bone resorption is either unchanged or transiently increased (Marino et al., 1979; Turner and Bell, 1986; Thompson and Rodan, 1988; Mack et al., 1967). We have detected increased bone resorption in the proximal tibial metaphysis following spaceflight and hindlimb unloading but have not observed a change in the bone resorption in the diaphysis (Cavolina et al., 1997; Turner et al., 1998).

There is no compelling evidence that disuse osteopenia in humans or laboratory animals is dependent upon abnormal levels of systemic factors such as calcium regulating hormones (e.g., parathyroid hormone or 1,25-dyhydroxyvitamin D_3) or gonadal hormones, although changes in the circulating levels of these hormones might accompany and influence the magnitude of bone loss as well as the cellular and molecular mechanisms mediating it (Turner and Bell, 1986; Backup et al., 1994; Wergedal et al., 1986; Linkhart et al., 1986; Pfeilschifter et al., 1988; Turner 2000; Turner et al., 1988). Studies in which different methods were used to modify skeletal loading, including unilateral sciatic neurotomy, limb casting, tendonotomy, hindlimb unloading, spaceflight and local loading, strongly suggest that the beneficial skeletal effects of weight bearing are due to the direct local actions of repetitive mechanical loading on

bone (Turner and Bell, 1986; Li et al., 1990; Thompson and Rodan, 1988). It is less clear whether the detrimental effects of alcohol on bone metabolism are similarly direct. Cultured osteoblasts are relatively insensitive to alcohol (Klein et al., 1996; Maran et al., 2001). In addition, there is evidence that deletion of the gene for interleukin-6 renders mice resistant to alcohol-induced bone loss (Dai et al., 2000). These findings suggest, but do not prove, that changes in systemic factors may be important in mediating the skeletal response to alcohol.

We did not include an *ad lib* fed control group of rats in the present study because we were interested in the specific effects of alcohol on bone metabolism. We and others have shown that caloric intake is reduced in alcohol-fed growing rats. Reduced caloric intake results in decreased bone growth which in turn results in a decrease in peak bone mass (Hogan et al., 1997; Turner et al., 1988; Sampson et al., 1996). Altered caloric intake was controlled for by pair-feeding the controls to alcohol-fed rats. Consistently, (Hogan et al., 1997; Turner et al., 1988; Sampson et al., 1996) alcohol leads to a further reduction in bone growth over and above that caused by caloric restriction. In contrast to growing rats, with proper acclimation, alcohol has minimal effects on food consumption and body weight in adults. On the other hand, hindlimb unloading results in reductions in body weight and caloric intake. The effects of alcohol but not skeletal unloading on body weight was successfully controlled for by pair-feeding the weight bearing rats to the hindlimb unloaded animals.

The association between alcohol consumption and physical activity has not been well studied. There are, however, suggestions of an inverse relationship (Fihter and Elton, 1993; Korelitz et al., 1993). Our findings showing that the hindlimb unloading exaggerates the inhibitory effects of alcohol on bone formation suggest that physical activity might be a co-morbidity factor in the pathogenesis of alcohol-induced osteoporosis. Additionally, muscle

atrophy commonly associated with alcohol abuse (Pendergast et al., 1990; Preedy et al., 2001) could potentiate bone loss by reducing the peak loads applied to the skeleton by muscle contraction during activity. Acute illness and injury in an alcohol abuser may result in episodes of greatly reduced physical activity which could, in turn, lead to accelerated bone loss that is not fully reversed following restoration of normal physical activity. This speculation is supported by recent studies demonstrating that treadmill exercise does not counteract the inhibitory effects of alcohol consumption on bone formation (Reed et al., 2001).

Although performed in rats, our results are likely to be relevant to humans. The rat model for chronic alcohol abuse appears to replicate changes in bone metabolism in human alcohol abusers with a high degree of fidelity (Turner, 2000). Similarly, hindlimb unloading is a well-established model which recapitulates the bone changes in humans associated with physical inactivity (Turner, 2000a).

In summary, disuse and alcohol consumption had additive inhibitory effects on bone formation in adult male rats. Our findings support the concept that co-morbidity factors may contribute to the high incidence of osteoporosis in alcoholics. Recognition and treatment of these additional risk factors may be important in successful prevention and treatment of alcohol-induced bone loss.

ACKNOWLEDGMENTS

The authors thank Ms. Lori M. Rolbiecki for typing this manuscript. These studies were supported by grants from the Department of Defense (DAMD17-98-1-8517), National Institutes of Health (AA11140), and NASA (NAG9-1150) and the Mayo Foundation.

REFERENCES

Backup P, Westerlind KC, Harris S, Spelsberg T, Kline B, Turner R (1994) Spaceflight results in reduced mRNA levels for tissue-specific proteins in the musculoskeletal system. Am J Physiol 266:E567-E573.

Bikle DD, Genant HK, Cann C, Recker RR, Halloran BP, Strewler GJ (1985) Bone disease in alcohol abuse. Ann Intern Med 103:42-48.

Bikle DD, Stesin A, Halloran B, Steinbach L, Recker R (1993) Alcohol-induced bone disease: Relationship to age and parathyroid hormone levels. Alcohol Clin Exp Res 17:690-695.

Cavolina JM, Evans GL, Harris SA, Zhang M, Westerlind KC, Turner RT (1997) The effects of orbital spaceflight on bone histomorphometry and mRNA levels for bone matrix proteins and skeletal signaling peptides in ovariectomized growing rats. Endocrinology 138:1567-1576.

Cooper C, Campion G, Melton LJ III (1992) Hip fractures in the elderly: A worldwide projection. Osteoporosis Int 2;285-289.

Cooper C, Melton LJ III (1996) Magnitude and impact of osteoporosis and fractures, in Osteoporosis (Marcus R, Feldman D, Kelsey J eds), pp 419-434. Academic Press, San Diego.

Crilly RG, Anderson C, Hogan D, Delaquerriere-Richardson L (1988) Bone histomorphometry, bone mass, and related parameters in alcoholic males. Calcif Tissue Int 43;269-276.

Cummings SR, Kelsey JL, Nevitt MC, O'Dowd KJ (1985) Epidemiology of osteoporosis and osteoporotic fractures. Epidemiologic Rev 7:178, 1985.

Cummings SR, Nevitt MC, Browner WS, Stone K, Fox KM, Ensrud KE, Cauley J, Black D, Vogt TM (1995) Risk factors for hip fracture in white women. Study of Osteoporotic Fractures Research Group. N Engl J Med 332:814-815.

Dai J, Lin D, Zhang J, Habib P, Smith P, Murtha J, Fu Z, Yao Z, Qi Y, Keller ET (2000) Chronic alcohol ingestion induces osteoclastogenesis and bone loss through IL-6 in mice. J Clin Invest 106:887-895.

Diez A, Puig J, Serrano S, Marinoso ML, Bosch J, Marrugat J, Mellibovsky L, nogues X, Knobel H, Aubia J (1994) Alcohol-induced bone disease in the absence of severe chronic liver damage. J Bone Miner Res 9:825-831.

Felson DT, Zhang Y, Hannan MT, Kannel WB, Kiel DP (1995) Alcohol intake and bone mineral density in elderly men and women. The Framingham Study. Am J Epidemiol 142:485-492.

Feskanch D, Korrick SA, Greenspan SL, Rosen HN, Colditz GA (1999) Moderate alcohol consumption and bone density among postmenopausal women. J Womens Health 8:65-73.

Globus RK, Bikle DD, Morey-Holton E (1986) The temporal response of bone to unloading. Endocrinology 118:733-742.

Gonzalez-Calvin JL, Garcia-Sanchez A, Bellot V, Munoz-Torres M, Raya-Alvarez E, Salvatierra-Rios D (1993) Mineral metabolism, osteoblastic function and bone mass in chronic alcoholism. Alcohol Alcohol 28:571-579.

Grainge MJ, Coupland CA, Cliffe SJ, Chilvers CE, Hosking DJ (1998) Cigarette smoking, alcohol and caffeine consumption, and bone mineral density in postmenopausal women. The Nottingham EPIC Study Group. Osteoporos Int 8:355-363.

Harper JS, Mulenburg GM, Evans J, Navidi M, Wolinsky I, Arnaud SB (1994) Metabolic cages for a space flight model in the rat. Lab Animal Sci 44:645-647.

Hogan HA, Sampson HW, Cashier E, Ledoux N (1997) Alcohol consumption by young actively growing rats: A study of cortical bone histomorphometry and mechanical properties. Alcohol Clin Exp Res 21;809-816.

Hoidrup S, Gronbaek M, Gottschau A, Lauritzen JB, Schroll M (1999a) Alcohol intake, beverage preference, and risk of hip fracture in men and women. Copenhagen Centre for Prospective Population Studies. Am J Epidemiol 149:993-1001.

Hoidrup S, Gronbaek M, Pedersen AT, Lauritzen JB, Gottschau A, Schroll M (1999b) Hormone replacement therapy and hip fracture risk: Effect of modification by tobacco smoking, alcohol intake, physical activity, and body mass index. Am J Epidemiol 150:1085-1093.

Holbrook TL, Barrett-Connor E (1993) A prospective study of alcohol consumption and bone mineral density. BMJ 306:1506-1509.

Jouanny P, Guillemin F, Kuntz C, Jeandel C, Pourel J (1995) Environmental and genetic factors affecting bone mass: Similarity of bone density among members of healthy families. Arthritis Rheum 38:61-67.

Kanis J, johnell O, Gullberg B, Allander E, Elffors L, Ranstam J, Dequeker J, Dilsen G, Gennari C, Vaz AL, Lyritis G, Mazzuoli G, Miravet L, Passeri M, Perez Cano r, Rapado A, Ribot C (1999) Risk factors for hip fracture in men from southern Europe: The MEDOS study. Osteoporos In 9:45-54.

Klein RF, Fausti KA, Carlos AS (1996) Ethanol inhibits human osteoblastic cell proliferation. Alcohol Clin Exp Res 20:572-578.

Korelitz JJ, Fernandez AA, Uyeda VJ, Spivey GH, Browdy BL, Schmidt RT (1993) Health habits and risk factors among truck drivers visiting a health booth during a trucker trade show. Am J Health Promot 8:117-123.

Krogsgaard MR, Frolich A, Lund B, Lund B (1995) Long-term changes in bone mass after partial gastrectomy in a well-defined population and its relation to tobacco and alcohol consumption. World J Surg 19:867-871.

Labib M, Abdel-Kader M, Ranganath L, Teale D, Marks V (1989) Bone disease in chronic alcoholism: The value of plasma osteocalcin measurement. Alcohol Alcohol 24:141-144.

Laitinen K, Lamberg-Allardt C, Tunninen R, Karkonen M, Valimaki M (1992) Bone mineral density and abstention-induced changes in bone and mineral metabolism in noncirrhotic male alcoholics. Am J Med 93:642-650.

Laitinen K, Lamberg-Allardt C, Tunninen R, Karonen SL, Ylikahri R, Valimaki M (1991a) Effects of 3 weeks moderate alcohol intake on bone and mineral metabolism in normal men. Bone Miner 13:139-151.

Laitinen K, Tahtela R, Luomanmaki K, Valimaki MJ (1994) Mechanisms of hypocalcemia and markers of bone turnover in alcohol-intoxicated drinkers. Bone Miner 24;171-179.

Lalor BC, France MW, Powell D, Adams PH, Counihan TB (1986) Bone and mineral metabolism and chronic alcohol abuse. Quarterly J Med 59:497-511.

Li XJ, Jee WSS, Chow S-Y, Woodbury DM (1990) Adaptation of cancellous bone to aging and immobilization in the rat: A single photon absorptiometry and histomorphometry study. Anat Rec 2271:12-24.

Linkhart TA, Jennings JC, Mohan S, Wakley GK, Baylink DJ (1986) Characterization of mitogenic activities extracted from bovine bone matrix. Bone 7:479-487.

Mack PD, LaChance PA, Vose GP, Vogt FB (1967) Bone demineralization of foot and hand of Gemini-Titan IV, V and VII astronauts during orbital spaceflight. Am J Roentgenol 100:503-511.

Maran A, Zhang M, Spelsberg TC, Turner RT (2001) The dose response effects of ethanol on the human fetal osteoblastic cell lines. J Bone Miner Res 16:270-276.

Marino AA, Becker RO, Hart FX, Anders F (1979) Space osteoporosis: An electromagnetic hypothesis. Aviation Space Environ Med 50:409-410.

May H, Murphy S, Khaw KT (1995) Alcohol consumption and bone mineral density in older men. Gerontology 41:152-158.

Morey ER, Baylink DJ (1978) Inhibition of bone formation during spaceflight. Science 201:1138-1141,

Nielsen HK, Lundby L, Rasmussen K, Charles P, Hansen C (1990) Alcohol decreases serum osteocalcin in a dose-dependent way in normal subjects. Calcif Tissue Int 46:173-178.

Orwoll ES, Bauer DC, Vogt TM, Fox KM (1996) Axial bone mass in older women. Study of Osteoporotic Fractures Research Group. Ann Intern Med 124:187-196.

Pendergast DR, York JL, Fisher NM (1990) A survey of muscle function in detoxified alcoholics. Alcohol 7:361-366.

Peng TC, Kusy RP, Hirsch PF, Hagman JR (1988) Ethanol-induced changes in morphology and strength of femurs of rats. Alcohol Clin Exp Res 12:1655-1659.

Perry HM III, Horowitz m, Fleming S, Kaiser Fe, Patrick P, Morley JE, Cushman W, Bingham S, Perry HM Jr (1999) The effects of season and alcohol intake on mineral metabolism in men. Alcohol Clin Exp Res 23:214-219.

Pfeilschifter J, Seyedin SM, Mundy GR (1988) Transforming growth factor-beta inhibits bone resorption in fetal rat long bone cultures. J Clin Invest 82:680-685.

Poor G, Atkinson EJ, O'Fallon WM, Melton LJ III (1995) Determinants of reduced survival following fractures in men. Clin Orthop 319:260-265.

Preedy VR, Adachi J, Ueno Y, Ahmed S, Mantle D, Mullatti N, Rajendram R, Peters TJ (2001) Alcoholic skeletal muscle myopathy: definitions, features, contribution of neuropathy, impact and diagnosis. Eur J Neurol 8:677-687.

Pumarino H, Gonzalez P, Oviedo S, Lillo R, Bustamante E (1996) Assessment of bone status in intermittent and continuous alcoholics, without evidence of liver damage. Revista Medica de Chile 124;423-430.

Reed AH, McCarty JL, Evans GL, Turner RT, Westerlind KC (2001) Effects of endurance exercise and chronic alcohol consumption on musculoskeletal components in skeletally mature male rats. Alcohol Clin Exp Res, In press.

Rehm J, Fichter MM, Elton M (1993) Effects on mortality of alcohol consumption, smoking, physical activity, and close personal relationships. Addiction 88:101-112.

Rico H, Cabranes JA, Cabello J, Gomez-Castresana F, Hernandez ER (1987) Low serum osteocalcin in acute alcohol intoxication: A direct toxic effect of alcohol on osteoblasts. Bone Miner 2;221-225.

Sampson HW, Chaffin C, Lange J, DeFee B 2nd (1997) Alcohol consumption by young actively growing rats: A histomorphometric study of cancellous bone. Alcohol Clin Exp Res 21:352-359.

Sampson HW, Gallager S, Lange J, Chondra W, Hogan JA (1999) Binge drinking and bone metabolism in a young actively growing rat model. Alcohol Clin Exp Res 23:1228-1231.

Sampson HW, Perks N, Champney TH, DeFee B 2nd (1996) Alcohol consumption inhibits bone growth and development in young actively growing rats. Alcohol Clin Exp Res 20:1375-1384.

Sampson HW, Shipley D (1997a) Moderate alcohol consumption does not augment bone density in ovariectomized rats. Alcohol Clin Exp Res 21:1165-1168.

Sampson HW, Spears H (1999a) Osteopenia due to chronic alcohol consumption by young actively growing rats is not completely reversible. Alcohol Clin Exp Res 23:324-327.

Schnitzler CM, Solomon L (1984) Bone changes after alcohol abuse. S Afr Med J 66:730-734.

Thompson DD, Rodan GA (1988) Indomethacin inhibition of tenotomy-induced bone resorption in rats. J Bone Miner Res 3:409-414.

Turner RT (2000) Skeletal response to alcohol. Alcohol Clin Exp Res 24:1693-1701.

Turner RT (2000a) Physiology of a microgravity environment. Invited Review: What do we know about the effects of spaceflight on bone? J Appl Physiol 89:840-847.

Turner RT, Aloia RC, Segel LD, Hannon KS, Bell NH (1988) Chronic alcohol treatment results in disturbed vitamin D metabolism and skeletal abnormalities in rats. Alcohol Clin Exp Res 12:151-155.

Turner RT, Bell NH (1986) The effects of immobilization on bone histomorphometry in rats. J Bone Miner Res 1:399-407.

Turner RT, Evans GL, Cavolina JM, Halloran B, Morey-Holton E (1998) Programmed administration of parathyroid hormone (PTH) increases bone formation and reduces bone loss in hindlimb unloaded ovariectomized rats. Endocrinology 139:4086-4091.

Turner RT, Evans GL, Zhang M, Sibonga JD (2001a) Effects of parathyroid hormone on bone formation in a rat model for chronic alcohol abuse. Alcohol Clin Exp Res 25:667-671.

Turner RT, Greene VS, Bell NH (1987) Demonstration that ethanol inhibits bone matrix synthesis and mineralization in the rat. J Bone Miner Res 2:61-66.

Turner RT, Kidder LS, Kennedy A, Evans GL, Sibonga JD (2001) Moderate alcohol consumption suppresses bone turnover in adult female rats. J Bone Miner Res 16;589-594.

Turner RT, Spector M, Bell NH (1991) Ethanol induced abnormalities in bone formation, turnover, mechanical properties, and mineralization in young adult rats. Cell and Materials (Suppl 1):167-173, 1991.

Wergedal JE, Mohan S, Taylor A, Baylink DJ (1986) Skeletal growth factor is produced by human osteoblast-like cells in culture. Biochem Biophys Acta 889:163-170.

Wronski TJ, Morey ER (1983) Effect of spaceflight on periosteal bone formation in rats. Am J Physiol 244:R305-R309,

FIGURE LEGENDS

Figure 1: Experimental design. The experiment consisted of two intervals: 1) alcohol pretreatment and 2) hindlimb unloading. The alcohol-fed groups were acclimated to the alcohol containing diet during the alcohol pretreatment interval. An alcohol fed group and control group was sacrificed following the pretreatment interval in order to obtain baseline measurements. The effects of hindlimb unloading on control and alcohol-fed rats was determined following the hindlimb unloading interval. Fluorochrome labels were administered during the alcohol pretreatment interval (baseline groups only) and hindlimb unloading interval to evaluate bone formation (⇑, calcein; ↑, tetracycline).

Figure 2: Effects of alcohol and hindlimb unloading on endocortical bone resorption rate. Values are mean ± SE; n=11. The experimental groups are: normal weight bearing (loaded control), alcohol-fed weight bearing (loaded alcohol), hindlimb unloaded (unloaded control) and alcohol-fed hindlimb unloaded (unloaded alcohol). Two-way ANOVA detected a significant increase in endocortical bone resorption in alcohol-fed ($p=0.0015$) rats, no effect of weight bearing, and no interaction between the two variables.

Figure 3: Effects of alcohol and hindlimb unloading on periosteal bone formation. Double labeled perimeter (dL.Pm) (a), mineral apposition rate (MAR) (b), and bone formation rate (BFR) (c) are shown. The values are mean ± SE; n=11. The experimental groups are normal weight bearing controls (loaded control), alcohol-fed weight bearing (loaded alcohol), hindlimb unloaded controls (unloaded control), and alcohol-fed hindlimb unloaded (unloaded alcohol). dL.Pm was decreased ($^{a}p<0.05$) compared to baseline control and ($^{b}p<0.05$) compared to baseline alcohol. MAR was decreased ($^{a}p<0.001$) compared to baseline control and ($^{b}p<0.001$) compared to baseline alcohol. BFR was decreased ($^{a}p<0.05$) compared to baseline control and ($^{b}p<0.05$)

compared to baseline alcohol. Two-way ANOVA detected significant decreases in dL.Pm (NS, alcohol-fed; $p<0.0001$, hindlimb unloaded), MAR ($p=0.0003$ alcohol-fed, $p=0.0001$ hindlimb unloaded, and BFR ($p=0.019$ alcohol-fed, $p=0.0001$ hindlimb unloaded). There was no interaction between the two variables for any index of bone formation.

Table 1: The Effect of Hindlimb Unloading and Ethanol on Static Bone Measurements

	Baseline		Loaded		Unloaded		Two-way ANOVA		
	Control (n=9)	Ethanol (n=10)	Control (n=11)	Ethanol (n=11)	Control (n=11)	Ethanol (n=11)	Effect of weight bearing	Effect of ethanol	Interaction
Length (cm)	4.20±0.02	4.16±0.04	4.19±0.03	4.21±0.03	4.22±0.02	4.21±0.03	NS	NS	NS
CA (mm^2)	4.10±0.15	4.15±0.15	3.87±0.10	3.98±0.06	3.99±0.08	4.01±0.14	NS	NS	NS
CSA (mm^2)	5. 10±0.15	5.01±0.18	4.82±0.11	5.06±0.08	4.96±0.10	5.03±0.17	NS	NS	NS
MA	0.91±0.05	0.87±0.09	0.95±0.03	1.08±0.04[a,b]	0.97±0.04	1.03±0.04[b]	NS	P<0.05	NS

Mean ± SE; n=9-11; [a]$p<0.05$ compared to baseline control; [b]$p<0.05$ compared to baseline alcohol. Cortical area (CA), cross-sectional area (CSA), medullary area (MA).

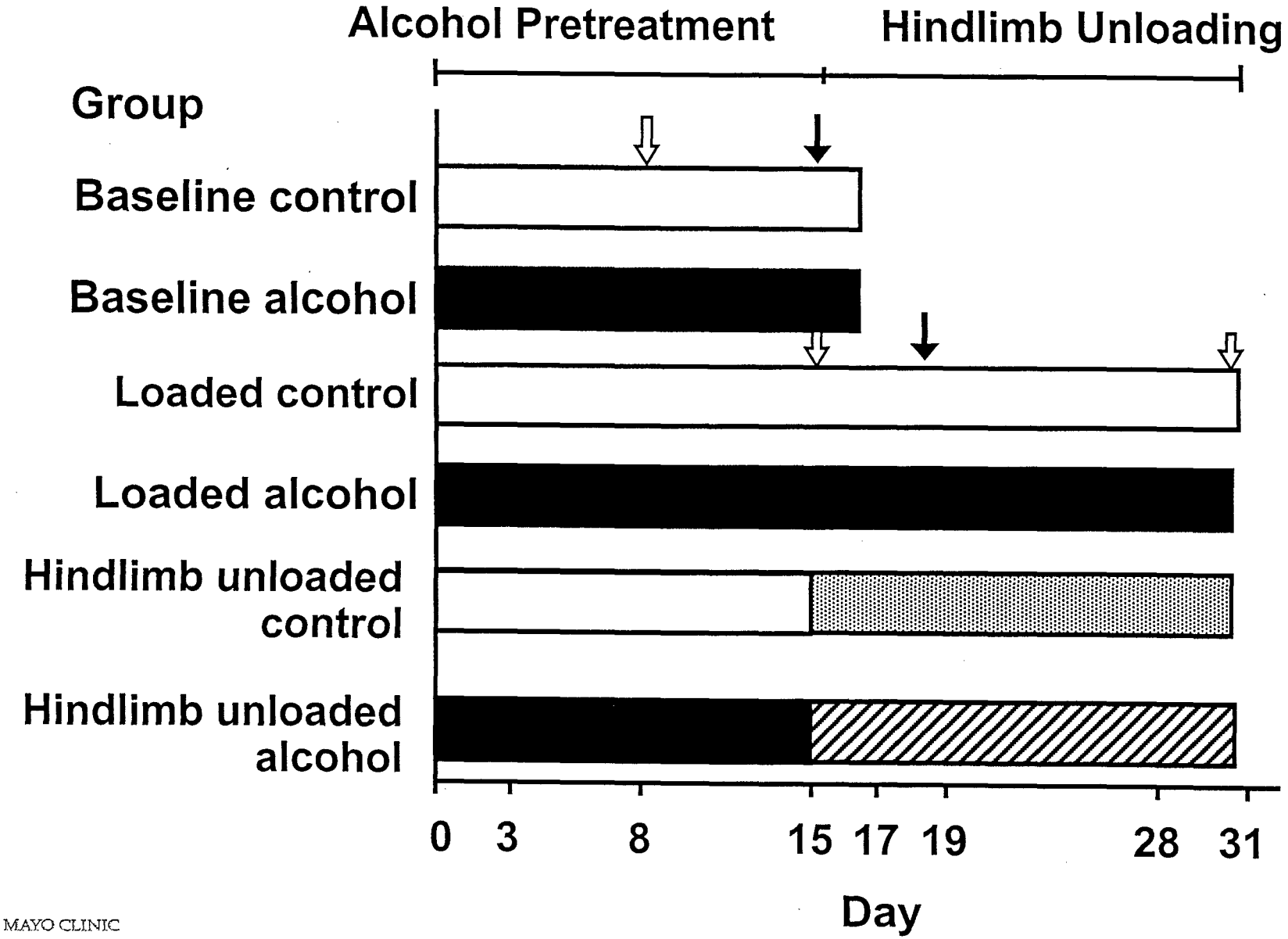

MAYO CLINIC

CP1062621B-1

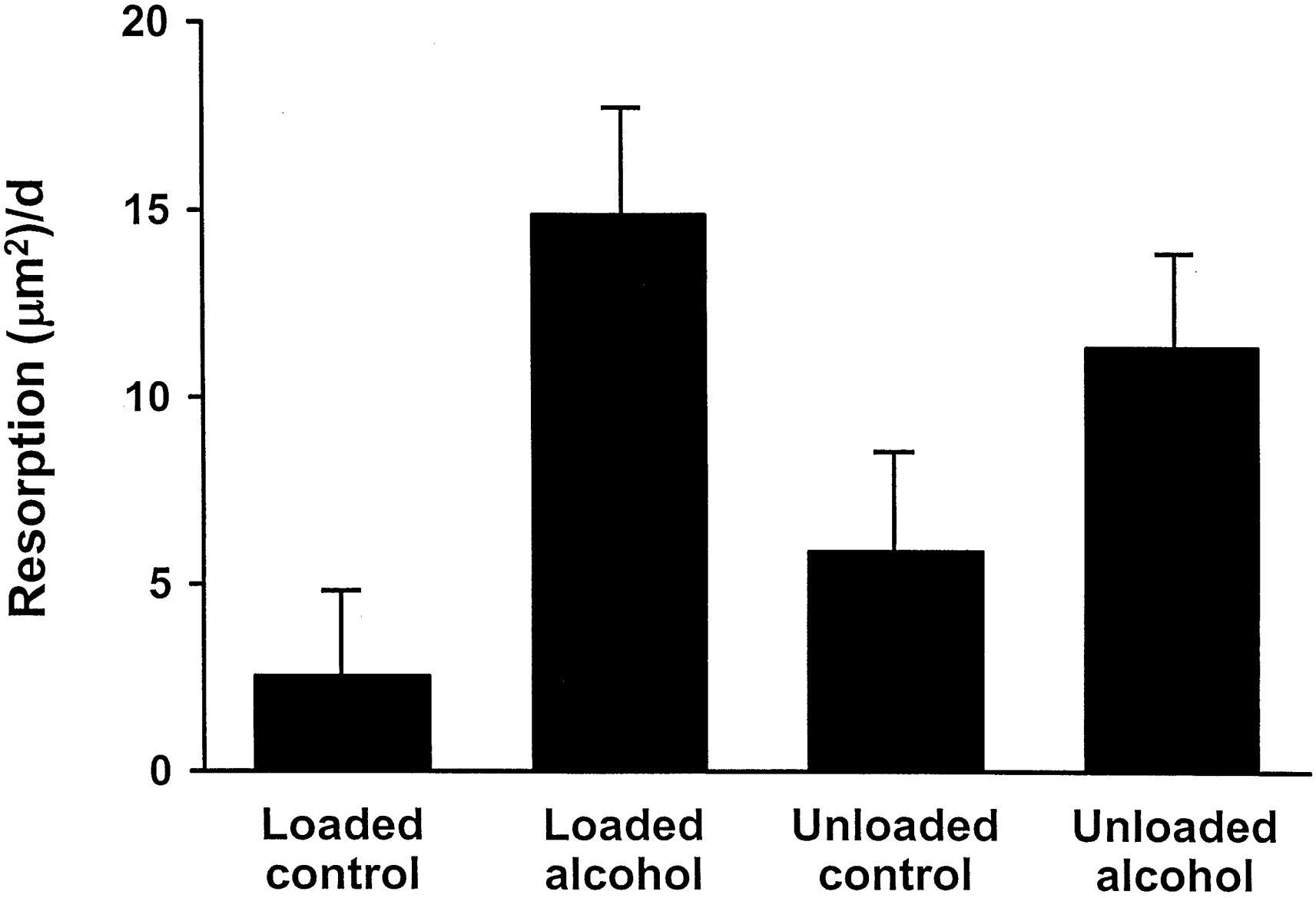

MAYO CLINIC

CP1062621B-5

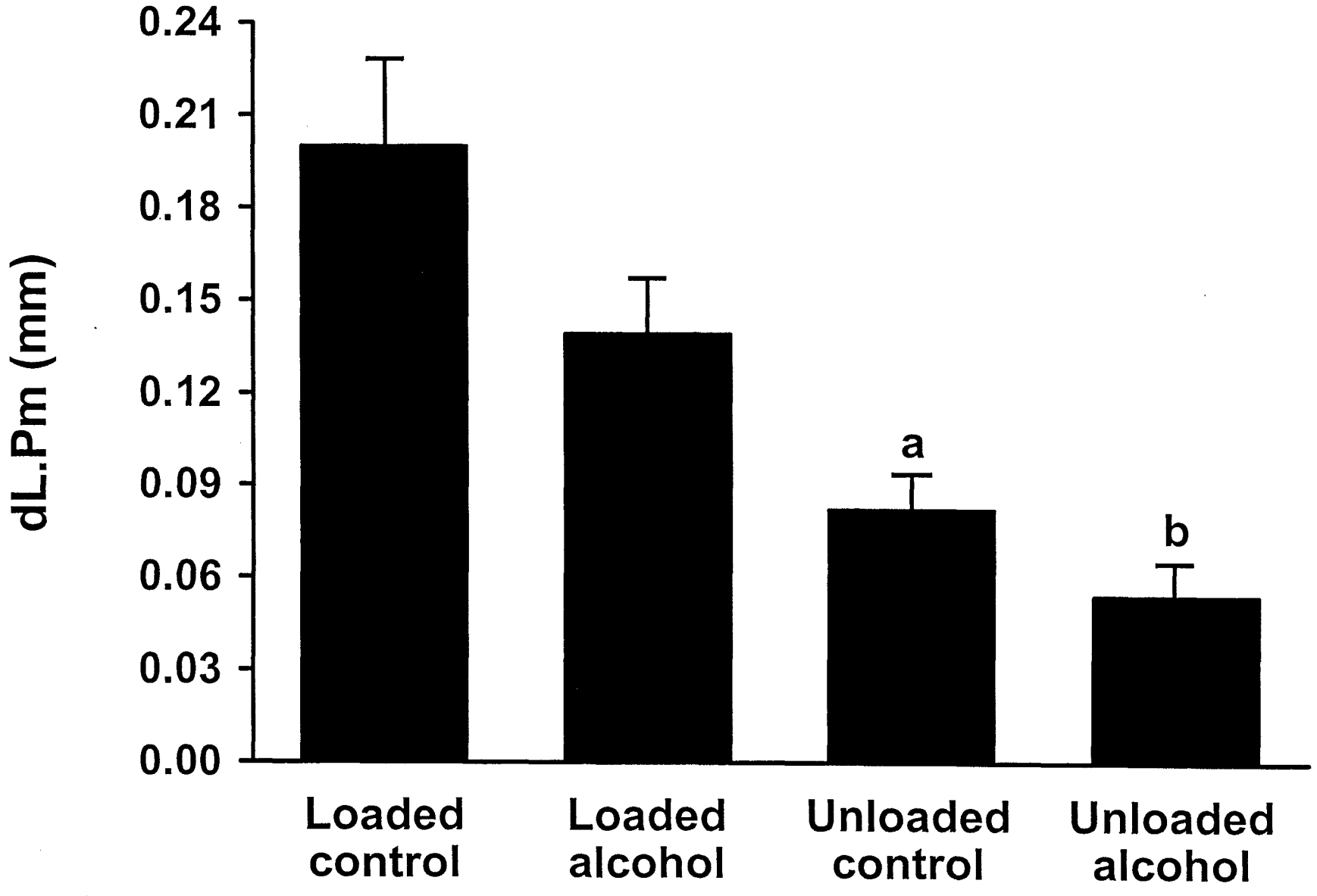

MAYO CLINIC

CP1062621B-2

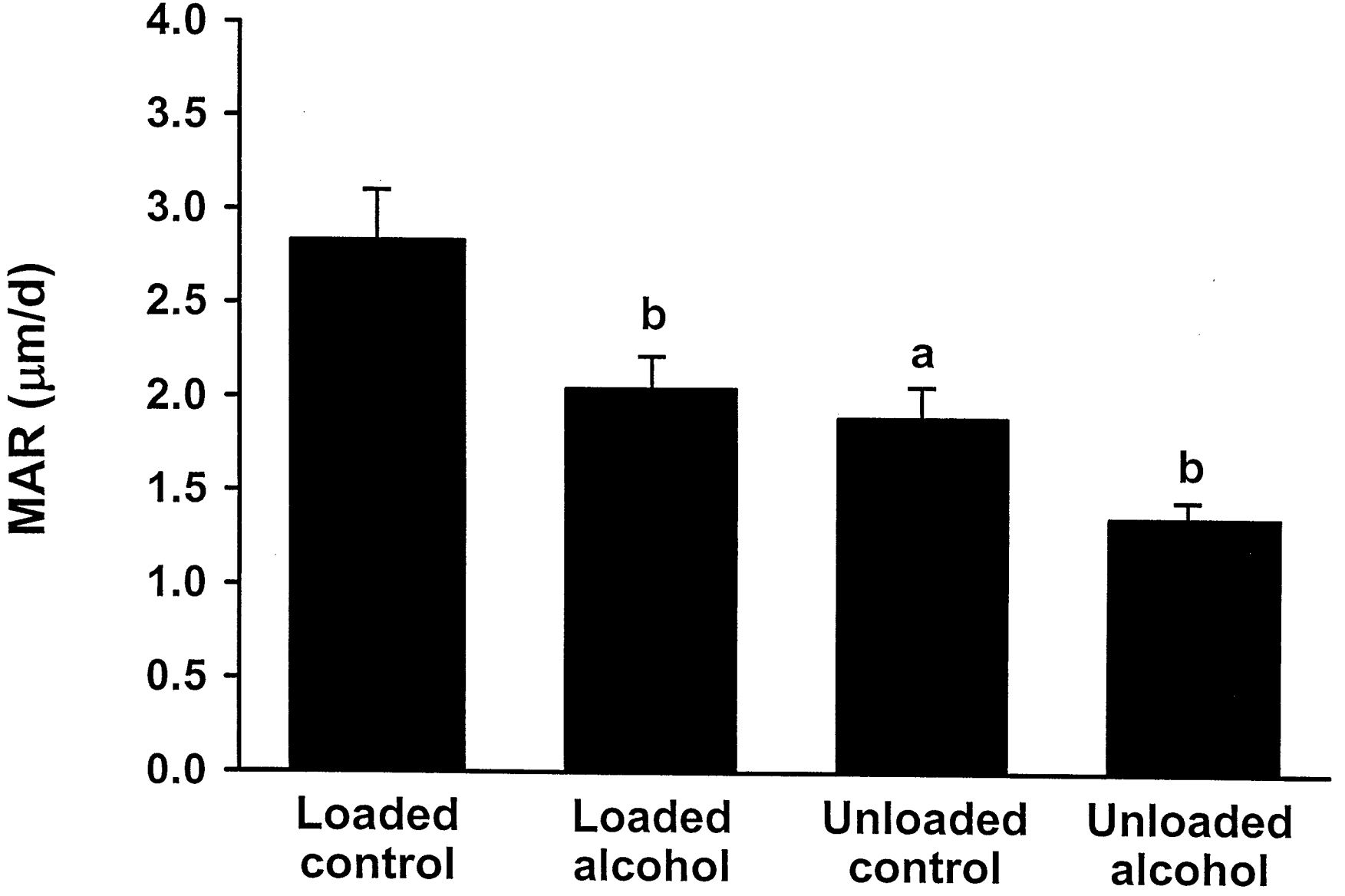

MAYO CLINIC

CP1062621B-4

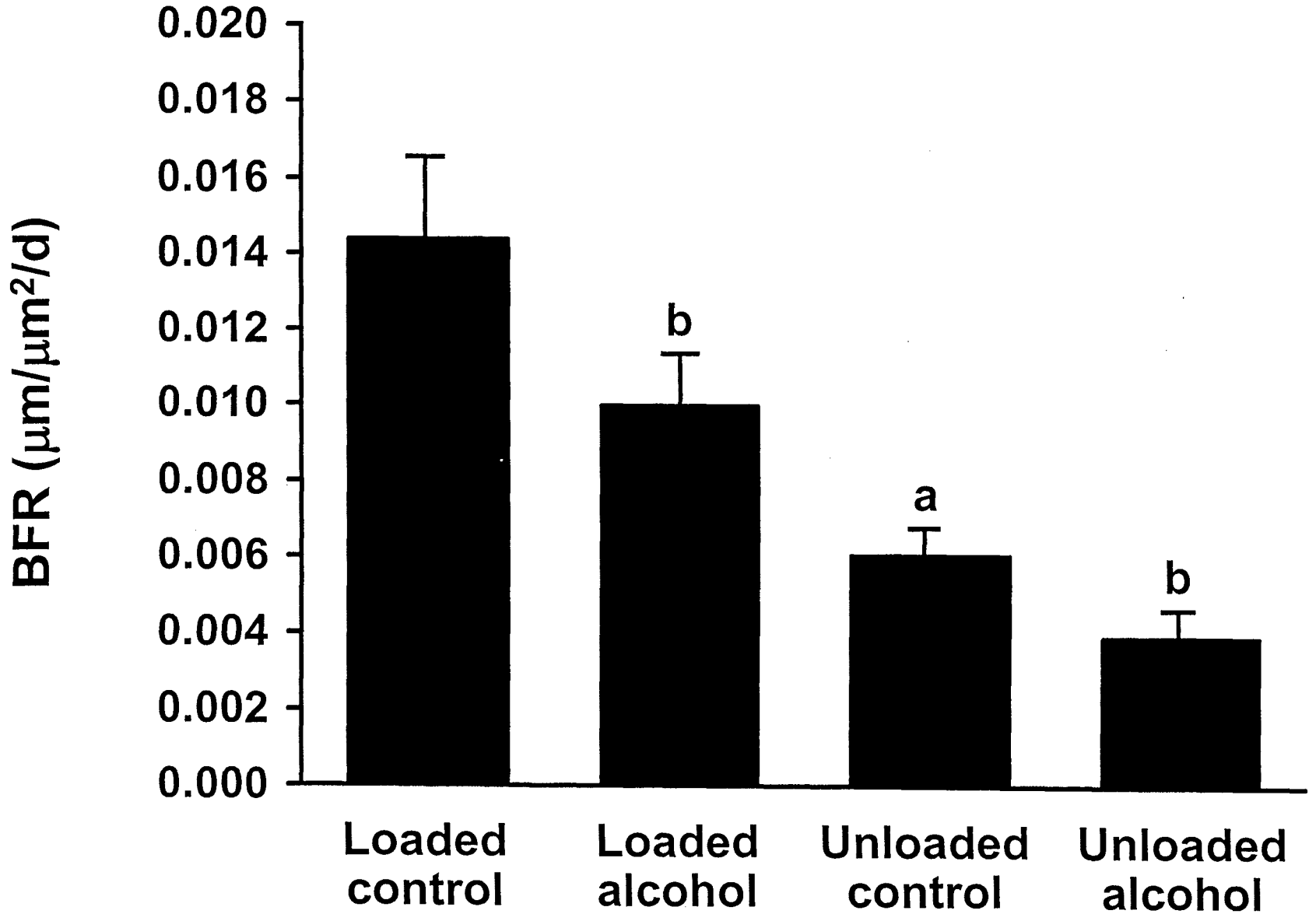

MAYO CLINIC

CP1062621B-3

0145-6008/02/2608-1269$03.00/0
ALCOHOLISM: CLINICAL AND EXPERIMENTAL RESEARCH

Turner, Russell T.
Appendix 8

Vol. 26, No. 8
August 2002

The effects of chronic alcohol consumption and exercise on the skeleton of adult male rats

Adam H. Reed, Heidi L. McCarty, Glenda L. Evans, Russell T. Turner, and Kim C. Westerlind

Background: Lifestyle factors are known to affect skeletal development and integrity. Specifically, running has been reported to increase risk of fatigue fractures, whereas chronic alcohol consumption has been shown to reduce bone formation and bone mass. The combined effect of exercise and alcohol on the skeleton has yet to be explored, although alcohol consumption is common among certain physically active populations (e.g., military recruits, college athletes). It was hypothesized that chronic alcohol consumption would accentuate the inherent risk associated with endurance running exercise.

Methods: Six-month-old male Sprague Dawley® rats were assigned to one of five groups: baseline, exercise-alcohol diet, exercise-normal diet, sham-alcohol diet, and sham-normal diet. Alcohol-fed rats (35% caloric intake) received a liquid diet ad libitum. Normal animals were pair-fed the identical diet with a maltose dextrin caloric substitute. Exercise was conducted on a motorized treadmill 5 days/wk for 16 weeks. Sham rats were placed on a stationary treadmill for matching time periods. Fluorochrome labels were administered 3 days before baseline and at 10 and 2 days before animals were killed. Heart, soleus, and rectus femoris muscles were wet weighed to assess the effects of training. Tibiae were collected for static and dynamic histomorphometric measurements on cancellous and cortical bone.

Results: Muscle weights were larger in the exercised rats versus the sham rats. Alcohol had no significant effect on skeletal muscle weight but did result in larger heart weights in both alcohol-treated groups. Cancellous and periosteal bone formation rates were significantly decreased in the alcohol-fed rats versus rats on the normal diet and were associated with a significant reduction in trabecular thickness in the tibial metaphysis. Cortical and cross-sectional areas were also significantly lower in the alcohol-fed groups compared with the non-alcohol-fed groups. Exercise had no significant effect on cancellous or cortical bone measurements.

Conclusions: Chronic alcohol consumption significantly reduced bone formation. Exercise had no effect on the bone and did not attenuate any of the negative effects of alcohol. The results suggest that alcohol consumption weakens the skeleton and increases the incidence of endurance-exercise-related bone injuries. Thus, individuals who are participating in endurance exercise and consuming alcohol may be at greater risk for exercise-related skeletal injuries. Further investigation of the potential for alcohol to induce detrimental effects on the hearts of individuals participating in endurance exercise is indicated.

Key Words: Endurance Exercise, Rat Model, Histomorphometry, Bone Formation.

LIFESTYLE FACTORS, SUCH as chronic alcohol consumption, are known to have detrimental effects on skeletal development and integrity and can decrease peak bone mass and increase the incidence of osteoporosis (Turner et al., 2001). Furthermore, the effects of alcohol consumption may not be reversible with cessation of alcohol intake (Sampson and Spears, 1999). Alcohol may reduce the activity and/or number of osteoblasts, promote the uncoupling of bone formation and resorption, and/or decrease the expression of genes for bone matrix proteins and skeletal growth factors (Dyer et al., 1998; Sampson et al., 1997; Turner et al., 1998; Wezeman et al., 2000). Alcohol also has been reported to disrupt the availability or efficacy of various anabolic hormones, thereby decreasing the rate of protein synthesis and skeletal muscle mass, which may directly affect bone strength (Lang et al., 2001).

In contrast, exercise generally is perceived to be beneficial for the musculoskeletal system. However, the evidence for specific bone modeling or remodeling changes that result from exercise differs, depending on the type of exercise as well as its intensity, load, and frequency. Endurance exercise may stimulate calcium deposition in the bones and increase formation of the connective tissue matrix essential for mineral deposition. In addition, endurance exercise may depress remodeling to maintain bone mass (Beyer et al., 1985; Frost, 1988; Wheeler et al., 1995).

Alcohol consumption and weight-bearing exercise have

From the AMC Cancer Research Center (AHR, HLM, KCW), Denver, Colorado; and the Department of Orthopedics (GLE, RTT), Mayo Clinic, Rochester, Minnesota.

Received for publication February 13, 2002; accepted May 7, 2002.

Supported by Grant DOD-DAMD 17-98-1-8517, NASA and by the Mayo Foundation.

Reprint requests: Kim C. Westerlind, PhD, AMC Cancer Research Center, 1600 Pierce Street, Denver, CO 80214; Fax: 303-239-3560; E-mail: westerlind@amc.org.

DOI: 10.1097/01.ALC.0000023984.47311.6E

potentially opposite effects on bone, but their interactions are unknown. In certain physically active populations where there is a high prevalence of alcohol consumption (e.g., military recruits, college athletes), stress fractures occur with suspicious regularity, yet the combined effect of exercise and alcohol consumption on the skeleton has not been evaluated (Lappe et al., 2001; Nelson and Wechsler, 2001). Shin splints and stress fractures are common among military recruits and college athletes. Stress fractures are small cracks in bones that typically develop from chronic or excessive impact. They can be difficult to diagnose, even with the assistance of magnetic resonance imaging. If the diagnosis is missed or delayed and fracture displacement results, serious complications such as avascular necrosis may occur, which require prompt surgical intervention. Even without displacement, stress fracture can be painfully debilitating, especially to individuals who are required to be physically active. Duration and intensity of training may be compromised by recurring injury in an individual whose bones are made more susceptible to stress fracture/injury because of alcohol consumption. Moreover, stress fractures of the cancellous bone may be a warning sign of early onset of osteopenia (Marx et al., 2001).

Nearly one in five individuals in the military reports having engaged in heavy drinking, and college athletes, despite repetitive athlete-targeted anti-alcohol education campaigns, are more likely to drink than their nonathlete counterparts (Hunter et al., 2000; Nelson and Wechsler, 2001). These populations are regularly involved in endurance exercise, and their propensity for alcohol consumption presents a bone environment that has yet to be explored. The purpose of this study was to investigate the independent and interactive effects of exercise and alcohol on the skeleton in skeletally mature rats. Six-month-old male rats were used to model the late adolescent/early adult skeleton. It was hypothesized that chronic alcohol consumption would exacerbate the skeletal risks of running exercise

METHODS

Fifty-six male Sprague Dawley® rats (Harlan, Indianapolis, IN) were received at 6 months of age (body weight, 444.5 ± 4.8 g; mean ± SE). All procedures were approved by the AMC Institutional Animal Care and Use Committee. Before the start of the study, rats were acclimatized to handling and the treadmill. Animals were housed individually for daily monitoring of diet intake in a temperature- and humidity-controlled animal facility on a 12-hr light/dark cycle. Rats were stratified by body weight and randomized to one of five groups (n = 10/group); baseline, exercise + alcohol diet (Ex-EtOH), exercise + normal diet (Ex), sham exercise + alcohol diet (sham-EtOH), and sham exercise + normal diet (sham). Initially, Ex-EtOH and Ex group sizes were larger (n = 13), to accommodate potential noncompliance with the exercise protocols. In our experience, approximately 10% of the animals will refuse to run regardless of stimuli or motivation.

During the first week, all animals were acclimated to Bio-Serv Liquid Rat Diet LD'82 (Bio-Serv, Frenchtown, NJ). All diets contained 1.3 g/liter calcium, 0.95 g/L potassium, 0.13 g/L magnesium, and 1.75 g/L phosphorus. Protein, fat, and carbohydrate constituted 28%, 30%, and 21% of the caloric value of the diet, respectively. Alcohol (ethyl alcohol, AAPER Alcohol and Chemical Co., Shelbyville, KY) concentration in the diet was increased from ~12% to a final 35% of kcal intake over a 1 week period. Non-alcohol-fed rats received Bio-Serv Liquid Rat Diet LD'82 as well, with a maltose dextrin caloric substitute in place of alcohol, according to the manufacturer's instructions. The alcohol diet was administered ad libitum throughout the 4 month study to the Ex-EtOH and Sham-EtOH groups. Non-alcohol-fed animals were pair-fed to their respective counterparts (exercise or sham-exercised). Animals were weighed twice per week throughout the experiment.

Exercise was conducted on a motorized 20-lane treadmill (Stanhope Instruments, Davis, CA) 5 days/wk for 16 weeks. All training was conducted in the dark under red light, was started at 0% grade, and was performed 10 to 15 m/min for 15 to 25 min. Intensity and duration were increased gradually and were adjusted to reach a final level of 25 m/min at 15% grade for 30 min. This protocol was used to minimize the "stress" associated with treadmill running. 92% of the animals were compliant with the exercise protocol; when necessary, manual prodding was used for motivation. No electrical stimulation was required. Sham-exercise rats were placed on a stationary treadmill for matching time periods.

Blood was drawn at 4 week intervals and at the time animals were killed to assess blood alcohol content (BAC). BAC was measured by using an alcohol kit (333-UV; Sigma Chemical, St. Louis, MO), and concentration of alcohol was determined spectrophotometrically at 340 nm in a Shimadzu (Kyoto, Japan) UV-VIS Recording Spectrophotometer (UV2100U). All samples were analyzed in duplicate. Any duplicates differing by more than 10% were reassayed. Intra-assay coefficient of variation was 8.6%.

Three days before commencement of training, all animals received a fluorochrome label (oxytetracycline, Sigma Chemical; 20 mg/kg body weight) via perivascular injection at the base of the tail. Baseline rats were killed 3 days later. The remaining rats were injected with calcein (Sigma Chemical; 20 mg/kg body weight) at 10 and 2 days before they were killed. Rats were killed 24 hr after the final exercise session by CO_2 inhalation and cervical dislocation. Tibiae were removed, defleshed, and fixed by immersion in 70% EtOH for bone histomorphometry. Tibia lengths were measured with a Mitutoyo vernier caliper (Mitutoyo American Corporation, Aurora, IL) and recorded. Rectus femoris, heart, and soleus muscle wet weights were recorded.

Bone histomorphometric parameters were measured by using the Osteomeasure semiautomatic image analysis system (OsteoMetrics, Atlanta, GA) as described by Cavolina et al. (1997) and Kidder and Turner (1998). To measure cortical bone, cross sections of tibial diaphyses, approximately 150 μm thick, were cut at a site just proximal to the tibiofibular synostosis with a low-speed Isomet saw equipped with a diamond wafer blade (Buehler, Lake Bluff, IL). They were ground on a roughened glass plate to a thickness of 20 μm and mounted on a glass slide with Eukitt mounting reagent (O Kindler, Frieborg, Germany). Two sections from each animal were examined at ×18.75 magnification. The zone of measurement was 1 mm below the growth plate on the tibial metaphysis, and total area measured was 2.94 mm. Cortical bone area (mm^2) was calculated by subtracting medullary area from cross-sectional area. Periosteal bone formation rate ($mm^2 \times 10^{-3}$/day) was calculated as the area of the bone between the first and last labels divided by the labeling period in days. Periosteal mineral apposition rate (μm/day) was calculated as the periosteal bone formation rate divided by the double-labeled perimeter.

For cancellous bone measurements, the proximal metaphyses were dehydrated through an ascending series of ethanol, infiltrated, embedded in methylmethacrylate, and sectioned at a thickness of 5 μm (Reichert-Jung Supercut microtome, Heidelberg, Germany). Sections were mounted for unstained static and dynamic determination of cancellous bone. Bone volume was defined as the percentage of tissue volume consisting of cancellous bone. Double labeled surface, expressed as a percentage of bone surface, was the trabecular surface covered with both calcein labels. Mineral apposition rate was the mean distance between the two calcein labels divided by the interval of 8 days. Bone formation rate was the product of the labeled surface and mineral apposition rate and was presented relative to bone surface, bone volume, and total bone tissue.

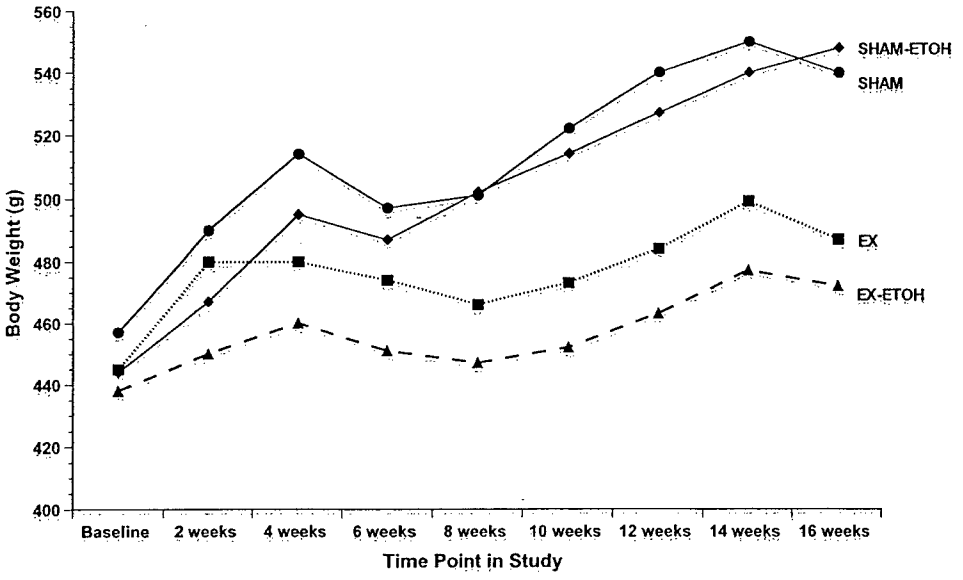

Fig. 1. The effect of exercise and alcohol consumption on body weight.

Table 1. The Effects of Exercise and Alcohol Consumption on Muscle Weights

					Two-way ANOVA		
Variable	Ex	Ex-EtOH	Sham	Sham-EtOH	Effect of exercise	Effect of EtOH	Interaction
Heart (g/100 g BW)	0.310 ± 0.007	0.328 ± 0.005	0.279 ± 0.008	0.295 ± 0.005	$p < 0.001$	$p = 0.02$	NS
Rectus (g/100 g BW)	0.297 ± 0.004	0.285 ± 0.004	0.255 ± 0.004	0.257 ± 0.005	$p < 0.001$	NS	NS
Soleus (g/100 g BW)	0.041 ± 0.001	0.040 ± 0.001	0.034 ± 0.002	0.034 ± 0.001	$p < 0.001$	NS	NS

All data are expressed as mean ± SE (n = 9–13/group). Muscle weights are presented per 100 g of body weight (BW) to adjust for differences in body weight at death between exercised and sham-exercised animals. NS, nonsignificant.

Trabecular thickness, trabecular number, and trabecular separation were determined by using the method of Parfitt et al. (1983).

All data are presented as mean ± SE. Two way ANOVAs were used to detect overall significant differences for the main effects (exercise and alcohol consumption) and the interaction of these two factors. Statistical significance was set at $p \leq 0.05$.

RESULTS

Final group sizes were Ex-EtOH (n = 10), Sham-EtOH (n = 10), Ex (n = 13), and Sham (n = 9). Two animals in the Ex-EtOH group were noncompliant, and one spontaneously developed a tumor that prohibited running. One rat in the Sham group was lost due to technical reasons.

The average BAC (mean ± SD) over the 16-week study for the alcohol-fed animals was 91.0 ± 18.9 mg/dl (Ex-EtOH) and 90.4 ± 15.1 mg/dl (Sham-EtOH), whereas the Ex and Sham animals had mean BACs of 3.7 ± 0.4 mg/dl and 3.2 ± 0.6 mg/dl, respectively. Blood alcohol levels were not affected by exercise.

No significant difference was observed in mean body weight between the baseline (448.6 ± 10.5 g) and other four groups (452.9 ± 10.4 g) at the beginning of the study. There was no significant difference in body weight change over the course of the study with alcohol treatment. Exercising animals gained, on average, 51 g less than their sedentary counterparts ($p < 0.001$; Fig. 1).

No differences in absolute muscle weights were observed among the four groups, but when normalized to body weight, heart and skeletal muscle weights were significantly greater in the exercised animals (Table 1). Heart, rectus, and soleus muscles weights were adjusted per 100 g/body weight, because of the differences in body weight gained over time. Skeletal muscle weights were not affected by alcohol, but the heart weights from the alcohol-fed animals were greater than those from the non-alcohol-fed animals ($p = 0.02$).

Periosteal bone formation and mineral apposition rates were significantly reduced (~40%) with alcohol consumption (Table 2). Cortical and cross-sectional areas were decreased by 6% ($p = 0.02$) and 5% ($p = 0.02$), respectively, when averaged for the two alcohol-fed groups compared with the two normal diet groups. Exercise, in contrast, had no significant effect on static or dynamic measurements in the cortical bone. There was no significant difference in medullary area across groups. There was no significant difference in tibia length among the four groups or when compared with the baseline animals.

Static and dynamic bone histomorphometry data from the tibial metaphysis are presented in Table 3. Cancellous bone volume was 19.5% lower in the animals fed alcohol, but this difference failed to reach statistical significance ($p = 0.15$). Cancellous bone formation rates were significantly reduced (38%; $p = 0.01$) in the animals fed the alcohol diet, regardless of exercise status. The reduction in

Table 2. The Effects of Exercise and Alcohol Consumption on Cortical Bone and Tibia Length

Variable	Baseline	Ex	Ex-EtOH	Sham	Sham-EtOH	Two-way ANOVA		
						Effect of Exercise	Effect of EtOH	Interaction
Cortical area (mm^2)	5.06 ± 0.09	5.33 ± 0.10	5.01 ± 0.14	5.16 ± 0.07	4.79 ± 0.09	NS	$p = 0.01$	NS
Cross-sectional area (mm^2)	6.18 ± 0.12	6.86 ± 0.13	6.59 ± 0.17	6.68 ± 0.07	6.29 ± 0.12	NS	$p = 0.02$	NS
Medullary area (mm^2)	1.12 ± 0.06	1.53 ± 0.06	1.58 ± 0.07	1.52 ± 0.05	1.49 ± 0.08	NS	NS	NS
Periosteal BFR ($mm^2 \times 10^{-3}$/day)		2.44 ± 0.36	1.01 ± 0.41	2.12 ± 0.41	0.85 ± 0.39	NS	$p = 0.001$	NS
Periosteal MAR (μm/day)		0.40 ± 0.03	0.24 ± 0.04	0.29 ± 0.04	0.22 ± 0.04	NS	$p = 0.003$	NS
Tibia length (mm)	41.0 ± 0.8	42.6 ± 0.6	42.4 ± 0.6	42.8 ± 0.6	42.1 ± 0.6	NS	NS	NS

All data are expressed as mean ± SE (n = 9–13/group). NS, non significant; BFR, bone formation rate; MAR, mineral apposition rate.

Table 3. The Effects of Exercise and Alcohol Consumption on Cancellous Bone Histomorphometry

Variable	Ex	Ex-EtOH	Sham	Sham-EtOH	Two-way ANOVA		
					Effect of exercise	Effect of EtOH	Interaction
BV/TV (%)	16.62 ± 2.12	12.69 ± 2.25	14.71 ± 2.63	12.48 ± 1.80	NS	NS	NS
BFR/BS ($\mu m^3/\mu m^2$/day)	0.132 ± 0.016	0.069 ± 0.012	0.136 ± 0.020	0.088 ± 0.022	NS	$p = 0.01$	NS
BFR/BV (%/day)	0.325 ± 0.033	0.211 ± 0.031	0.383 ± 0.067	0.272 ± 0.056	NS	$p = 0.02$	NS
BFR/TV (%/day)	0.052 ± 0.007	0.027 ± 0.006	0.056 ± 0.013	0.034 ± 0.011	NS	$p = 0.02$	NS
LS/BS (%)	20.66 ± 4.61	9.31 ± 1.36	15.64 ± 1.78	9.80 ± 1.73	NS	$p = 0.01$	NS
MAR (μm/day)	0.797 ± 0.025	0.727 ± 0.054	0.850 ± 0.040	0.829 ± 0.056	NS	NS	NS
Tb.Th (μm)	81.90 ± 5.48	64.24 ± 5.61	74.59 ± 8.22	63.57 ± 4.82	NS	$p = 0.02$	NS
Tb.N (No./μm)	1.95 ± 0.15	1.83 ± 0.23	1.89 ± 0.21	1.87 ± 0.17	NS	NS	NS
Tb.Sp (μm)	472.08 ± 49.97	587.31 ± 103.05	523.64 ± 87.80	521.28 ± 68.82	NS	NS	NS

All data are expressed as mean ± SE (n = 9–13/group). NS, nonsignificant; BV, bone volume; TV, tissue volume; BFR, bone formation rate; LS, labeled surface; BS, bone surface; MAR, mineral apposition rate; Tb.Th, trabecular thickness; Tb.N, trabecular number; Tb.sp, trabecular separation.

bone formation was associated with a 47% decrease in calcein-labeled surface. Bone surface/bone volume was increased with alcohol intake ($p = 0.02$) and is indicative of the reduction in trabecular thickness that was observed in the alcohol-fed animals ($p = 0.02$). Alcohol treatment had no effect on mineral apposition rate, trabecular number, or trabecular separation. Treadmill exercise had no effect on any of the cancellous measurements in either the alcohol-fed or non-alcohol-fed rats.

DISCUSSION

The majority of the exercising animals, regardless of alcohol intake, successfully completed the exercise program. The body weights increased in all animals, although the exercising groups gained less weight over the 16 week period. This is consistent with data from Bourrin et al. (1995), who reported that male rats do not compensate for increased physical activity by increasing their food intake.

Although absolute muscle weights did not differ among groups, when expressed relative to body weight at the time animals were killed, exercise-trained animals had significantly larger muscles, which suggested an effect of the treadmill-training protocol. This exercise-training effect was observed in both alcohol- and non-alcohol-fed rats. Interestingly, the heart is the only muscle that displayed a significant independent and interactive effect of exercise and alcohol. In the United States, long-term, excessive alcohol consumption is the leading cause of nonischemic, dilated cardiomyopathy, otherwise known as alcoholic heart muscle disease (Fauchier et al., 2000). In the human heart, alcoholic heart muscle disease is associated with dilation of the left ventricle and mild hypertrophy. In animal models, similar hypertrophy has been observed when heart weight is adjusted for body weight (Kim et al., 2001). Consistent with these data, in the present study heart weights were greater in the Ex-EtOH and Sham-EtOH than in the Ex and Sham groups, respectively.

Consistent with the majority of human studies, we found that endurance-exercise training (running and brisk walking) resulted in no significant positive effect on skeletal mass or bone formation in skeletally mature male rats (Forwood and Burr, 1993). Other animal studies have presented comparable results (Barengolts et al., 1993), and findings to the contrary generally have involved longer duration (>1 hr) training protocols (Bourrin et al., 1995; Chen et al., 1994) or exercise protocols that were varied to create novel stimuli (Bourrin et al., 1995). In contrast, animal studies that have involved resistance exercise have reported significant increases in bone formation as a result of the physical activity. For example, 6-month-old male rats trained to perform a "squat" exercise with weights applied to a Velcro backpack had significantly greater cancellous bone volume than sedentary controls in less than 2 months of training when both the number of repetitions and amount of weight lifted per repetition were continually increased (Westerlind et al., 1998).

The fundamental differences between resistance and

running/walking exercise training may be responsible for the differences in outcome. During a session of running/walking, each successive heel strike subjects the skeleton to a specific amount of strain; each repetition provides no greater strain than the one preceding. This strain may not be significantly greater than that created by normal daily activity. Endurance exercise may, therefore, not provide a "peak strain" that is great enough to stimulate bone formation. Peak strain is comparable to the minimum effective strain, a threshold that must be attained or exceeded in an exercise regimen to increase bone formation (Frost, 1988). Like the minimum effective strain, an exercise protocol must attain or surpass the level of the peak strain to "turn on" the metabolic processes of bone formation. Once the peak strain is attained, additional strain will dictate the strength, function, and shape of the skeleton. Higher strains produce greater osteogenesis than lower strains (Lanyon, 1996).

Regardless of the magnitude of strain, the accumulation of skeletal fatigue as a result of repeated cycles of loading, like that incurred during running, can create microcracks in cancellous and cortical bone. The presence of such cracks may catalyze new bone formation (Zioupos et al., 1996), but as the number of loading cycles is increased, the risk for fatigue-type injuries, such as shin splints or stress fractures, also is increased (Frost, 1988).

The mechanism of action for alcohol on the osteoblast has yet to be fully understood, although Maran et al. (2001) showed that direct cell toxicity is not the cause. Despite questions on how alcohol affects bone formation, there is little controversy that alcohol abuse negatively affects the bone. In the present study, alcohol consumption significantly reduced periosteal bone formation and mineral apposition rates and resulted in smaller cortical and cross-sectional areas. These data are consistent with those of Wezeman et al. (2000), who reported a reduction of cortical bone width after a chronic alcohol consumption study in 35-day-old male rats. Likewise, Dyer et al. (1998) reported a 52% reduction in osteoblast activity (expressed as wall thickness). They observed trabecular thinning in alcohol-treated animals (35% daily caloric intake) similar to that observed in this study. Turner et al. (2001) also observed trabecular thinning that was attributed to a net reduction in bone formation as a result of alcohol consumption. In these dose-response studies, a small intake of alcohol led to parallel reductions in bone formation and bone resorption, whereas higher consumption levels led to further reductions in bone formation with no additional change in bone resorption. The histomorphometric changes in the present study provide additional evidence for a reduction in bone formation in adult alcohol-treated animals.

Data from the present study demonstrate that the detrimental effects of alcohol are not prevented or attenuated by running endurance exercise. Shin splints and stress fractures are common risks associated with running exercise, and the present data suggest that alcohol consumption may increase such risks because of its deleterious effects on bone mass and architecture. All tissues develop microscopic mechanical fatigue damage as a result of repeated strain. Under normal conditions, bone remodeling would repair the fatigue damage. To accelerate bone healing, Lanyon (1996) asserted that exercise should include many cycles of increased strain. Even under ideal circumstances, the rate of bone remodeling is controlled and relatively slow. Therefore, if the structure of bone was challenged and damaged at a rate greater than the rate of repair, the incidence of stress fracture and shin splints could be expected to increase (Frost, 1988). With the added insult of alcohol consumption and its reduction of bone remodeling, the repair of microcracks may become inadequate, thereby increasing the risk of running-related injuries.

CONCLUSION

This study examined the independent and interactive effects of running exercise and alcohol consumption in skeletally mature male rats. Long-distance running increases the risk for bone fractures, in part because the peak mechanical strain is insufficient to induce a net increase in bone formation and because the bone remodeling rate is insufficient to fully repair fatigue damage. Our results suggest that alcohol abuse potentiates the inherent risks of running by decreasing bone remodeling and reducing bone mass.

REFERENCES

Barengolts EI, Curry DJ, Bapna MS, Kukreja SC (1993) Effects of endurance exercise on bone mass and mechanical properties in intact and ovariectomized rats. J Bone Miner Res 8:937–942.

Beyer RE, Huang JC, Wilshire GB (1985) The effect of endurance exercise on bone dimensions, collagen, and calcium in the aged male rat. Exp Gerontol 20:315–323.

Bourrin S, Palle S, Pupier R, Vico L, Alexandre C (1995) Effects of physical training on bone adaptation in three zones of the rat tibia. J Bone Miner Res 10:1745–1752.

Cavolina JM, Evans GL, Harris SA, Zhang M, Westerlind KC, Turner RT (1997) The effects of orbital spaceflight on bone histomorphometry and messenger ribonucleic acid levels for bone matrix proteins and skeletal signaling peptides in ovariectomized growing rats. Endocrinology 138: 1567–1576.

Chen MM, Yeh JK, Aloia JF, Tierney JM, Sprintz S (1994) Effect of treadmill exercise on tibial cortical bone in aged female rats: a histomorphometry and dual energy X-ray absorptiometry study. Bone 15: 313–319.

Dyer SA, Buckendahl P, Sampson HW (1998) Alcohol consumption inhibits osteoblastic cell proliferation and activity in vivo. Alcohol 16: 337–341.

Fauchier L, Babuty D, Poret P, Casset-Senon D, Autret ML, Cosnay P, Fauchier JP (2000) Comparison of long-term outcome of alcoholic and idiopathic dilated cardiomyopathy. Eur Heart J 21:306–314.

Forwood MR, Burr DB (1993) Physical activity and bone mass: exercises in futility. Bone Miner 21:89–112.

Frost HM (1988) Vital biomechanics: proposed general concepts for skeletal adaptations to mechanical usage. Calcif Tissue Int 42:145–156.

Hunter CL, Talcott GW, Klesges RC, Lando H, Haddock K (2000) Demographic, lifestyle, and psychosocial predictors of frequency of

intoxication and other indicators as estimates of alcohol-related problems in air force basic military recruits. Mil Med 165:539–545.

Kidder LS, Turner RT (1998) Dietary ethanol does not accelerate bone loss in ovariectomized rats. Alcohol Clin Exp Res 22:2159–2164.

Kim SD, Beck J, Bieniarz T, Schumacher A, Piano MR (2001) A rodent model of alcoholic heart muscle disease and its evaluation by echocardiography. Alcohol Clin Exp Res 25:457–463.

Lang CH, Kimball SR, Frost RA, Vary TC (2001) Alcohol myopathy: impairment of protein synthesis and translation initiation. Int J Biochem Cell Biol 33:457–473.

Lanyon LE (1996) Using functional loading to influence bone mass and architecture: objectives, mechanisms, and relationship with estrogen of the mechanically adaptive process in bone. Bone (Suppl 1) 18:37S–43S.

Lappe JM, Stegman MR, Recker RR (2001) The impact of lifestyle factors on stress fractures in female army recruits. Osteoporos Int 12:35–42.

Maran A, Zhang M, Spelsberg TC, Turner RT (2001) The dose-response effects of ethanol on the human fetal osteoblastic cell line. J Bone Miner Res 16:270–276.

Marx RG, Saint-Phard D, Callahan LR, Chu J, Hannafin JA (2001) Stress fracture sites related to underlying bone health in athletic females. Clin J Sports Med 11:73–76.

Nelson TF, Wechsler H (2001) Alcohol and college athletes. Med Sci Sports Exerc 33:43–47.

Parfitt AM, Mathews CH, Villanueva AR, Kleerekoper M, Frame B, Rao DS (1983) Relationships between surface, volume, and thickness of iliac trabecular bone in aging and in osteoporosis. Implications for the microanatomic and cellular mechanisms of bone loss. J Clin Invest 72:1396–1409.

Sampson HW, Chaffin C, Lange J, DeFee B II (1997) Alcohol consumption by young actively growing rats: a histomorphometric study of cancellous bone. Alcohol Clin Exp Res 21:352–359.

Sampson HW, Spears H (1999) Osteopenia due to chronic alcohol consumption by young actively growing rats is not completely reversible. Alcohol Clin Exp Res 23:324–327.

Turner RT, Kidder LS, Kennedy A, Evans GL, Sibonga JD (2001) Moderate alcohol consumption suppresses bone turnover in adult female rats. J Bone Miner Res 16:589–594.

Turner RT, Wronski TJ, Zhang M, Kidder LS, Bloomfield SA, Sibonga JD (1998) Effects of ethanol on gene expression in rat bone: transient dose-dependent changes in mRNA levels for matrix proteins, skeletal growth factors, and cytokines are followed by reductions in bone formation. Alcohol Clin Exp Res 22:1591–1599.

Westerlind KC, Fluckey JD, Gordon SE, Kraemer WJ, Farrell PA, Turner RT (1998) Effect of resistance exercise training on cortical and cancellous bone in mature male rats. J Appl Physiol 84:459–464.

Wezeman FH, Emanuele MA, Moskal SF, Steiner J, Lapaglia N (2000) Alendronate administration and skeletal response during chronic alcohol intake in the adolescent male rat. J Bone Miner Res 15:2033–2041.

Wheeler DL, Graves JE, Miller GJ, Vander Griend RE, Wronski TJ, Powers SK, Park HM (1995) Effects of running on the torsional strength, morphometry, and bone mass of the rat skeleton. Med Sci Sports Exerc 27:520–529.

Zioupos P, Wang XT, Currey JD (1996) The accumulation of fatigue microdamage in human cortical bone of two different ages in vitro. Clin Biomech 11:365–375.

Triazolopyrimidine (Trapidil) Inhibits Parathyroid Bone Disease in an Animal Model for Chronic Hyperparathyroidism

Sutada Lotinun[1], Jean D. Sibonga[1], and Russell T. Turner[1,2]

Department of Orthopedics[1] and Biochemistry and Molecular Biology[2]

Running Title: Parathyroid Bone Disease

Key Words: PDGF-A, osteitis fibrosa, bone histomorphometry, bone resorption, rat bone

Correspondence should be addressed to:
Russell T. Turner, Ph.D.
Department of Orthopedics
Mayo Clinic
200 First Street SW
Rochester, MN 55905
Phone: (507) 284-4062
Fax: (507) 284-5075
Email: turner.russell@mayo.edu

Abstract

Parathyroid bone disease in humans is caused by chronic hyperparathyroidism (HPT). Continuous infusion of parathyroid hormone (PTH) into rats results in histological changes similar to parathyroid bone disease, including increased bone formation, focal bone resorption and severe peritrabecular fibrosis whereas pulsatile PTH increases bone formation without skeletal abnormalities. Using a cDNA microarray having over 5000 genes, we identified an association between increased platelet-derived growth factor-A (PDGF-A) signaling and PTH-induced bone disease in rats. Verification of PDGF-A over-expression was accomplished with an RNase Protection Assay. Using immunohistochemistry, PDGF-A peptide was localized to mast cells in PTH-treated rats. We also report a novel strategy for prevention of parathyroid bone disease using triazolopyrimidine (trapidil). Trapidil, an inhibitor of PDGF signaling, did not have any effect on indices of bone turnover in normal rats. However, dramatic reductions in marrow fibrosis and bone resorption, but not bone formation, were observed in PTH-treated rats given trapidil. Also, trapidil antagonized the PTH-induced increases in mRNA levels for PDGF-A. These results suggest that PDGF signaling is important for the detrimental skeletal effects of HPT, and drugs which target the cytokine or its receptor might be useful in reducing or preventing parathyroid bone disease.

Introduction

Parathyroid hormone (PTH) is an important physiological regulator of bone metabolism. Chronic elevation of PTH level leads to parathyroid bone disease (1, 2). Primary hyperparathyroidism (HPT) is a common disorder with an incidence rate of ~ 28 per 100,000 person years (3). Because of early medical intervention, severe forms of parathyroid bone disease are now rarely encountered (prevalence < 2%) in developed countries in patients with primary HPT (4). Severe disease occurs frequently (prevalence ~50%), however, in primary HPT patients in less developed countries (5). Also, parathyroid bone disease due to secondary HPT is common in renal dialysis patients (6). A renal impairment in the conversion of 25-hydroxyvitamin D_3 to 1α, 25-dihydroxyvitamin D_3 and the excretion of phosphate results in hypocalcemia and phosphate retention, leading to a chronic increase in PTH secretion (7, 8).

The precise skeletal changes associated with chronic HPT are diagnostic of the severity and duration of the parathyroid bone disease: the hierarchy of disease severity is 1) increased bone turnover; 2) dissecting osteitis, tunneling of trabeculae by osteoclasts and an excess of osteoid formation by osteoblasts; 3) osteitis fibrosa, bone resorption accompanied by fibrosis around the weakened trabeculae; and 4) osteitis fibrosa cystica, replacement of marrow by fibrous tissue, hemorrhage from microfractures and hemosiderin-laden macrophages that often display multinucleated osteoclast-like giant cells resulting in a cystic brown tumor (5, 9). The etiology of these histological changes is incompletely understood, but uncontrolled chronic HPT results in bone pain, bone deformities and pathological fractures. Treatments currently used to control parathyroid bone disease are vitamin D supplementation and partial parathyroidectomy; the latter can reduce symptoms but can lead to undesirable side effects, including adynamic bone disease (10).

To find a therapeutic alternative, an animal model for parathyroid bone disease was developed. Continuous infusion of PTH into rats via a subcutaneous implanted osmotic pump for 6 days results in skeletal changes that are strikingly similar to severe parathyroid bone disease observed in patients with chronic HPT. In contrast, daily s.c. injection of PTH increases bone formation without detrimental skeletal effects (11). This observation indicates that the anabolic and pathological skeletal effects of PTH can be disassociated, implying different signaling pathways. The histological presentation of the skeletal abnormalities, specifically the well-defined peritrabecular fibrosis and focal bone resorption, suggest that HPT results in excessive local levels of growth factors in the vicinity of bone surfaces which in turn mediate the abnormal accumulation of fibroblasts and osteoclasts to bone surfaces. To evaluate this hypothesis in rats, we used a cDNA microarray to identify candidate PTH-regulated growth factor genes. Using this approach, we identified platelet-derived growth factor-A (PDGF-A) as a potential causative factor for parathyroid bone disease. We then investigated antagonism of PDGF-A signaling as a novel therapeutic strategy for the disease.

Materials and Methods

Animals

Three-month-old female Sprague Dawley rats (Harlan Sprague Dawley, Inc., Indianapolis, IN) were housed on a 12-h light, 12-h dark cycle with standard laboratory chow and water ad libitum. All procedures were approved by the Mayo Foundation institutional animal care and use committee.

Study 1: Induction of parathyroid bone disease

This experiment was performed to identify candidate genes and localize target cells which play a role in the detrimental effects of continuous PTH on bone. Animals were randomly divided into 3 groups with 5 animals per group. One group was given daily s.c. injection with 80 μg/kg BW/day human PTH (1-34) (hPTH) for 7 days. The two other groups received s.c. implanted osmotic pumps (Alza Corp., Mountainview, CA) which delivered vehicle or 40 μg/kg BW/day hPTH at the rate of 1 μl/hr for 7 days. On day 8, animals were anesthetized with ketamine (50 mg/kg BW) : xylazine HCl (5 mg/kg BW) and sacrificed by decapitation, and both tibiae and femora were removed. Right tibiae were fixed by immersion in 70% ethanol and processed for bone histology in order to verify an appearance of peritrabecular fibrosis. Left tibiae were frozen in liquid N_2, stored frozen at –80 °C until processed for RNA isolation, cDNA microarray and RNase Protection Assay. Femora were fixed in 10% neutral buffered formalin for immunohistochemistry.

Study 2: Effect of trapidil on parathyroid bone disease

This experiment was performed to evaluate the effect of trapidil, PDGF-A antagonist, on bone in rat-treated with continuous PTH. Rats were divided into 4 groups [Vehicle (n = 9), trapidil (n = 10), PTH (n = 8) and PTH+trapidil (n = 10)]. The animals were implanted s.c with 1

wk osmotic pumps containing either vehicle or 40 μg/kg BW/day hPTH. They also received daily s.c. injections of vehicle or 40 mg/kg BW/day trapidil (Rodleben Pharma GmbH, Rodleben, Germany) for 8 days. This dosage was estimated on the basis of an effective inhibitory effect of trapidil on several types of cells in the rat (12, 13, 14). Fluorochrome labels (20 mg/kg BW, Sigma Chemical Co., St. Louis, MO) were injected at the base of the tail on day 0 (tetracycline) and day 6 (calcein). At the end of experiment (day 8), the rats were anesthetized and blood was collected by cardiac puncture for determination of serum chemistry and PTH levels before sacrifice. Tibiae were removed and fixed in 70% ethanol for bone histomorphometry. Femora were stored frozen at –80 °C for RNA isolation and RNase Protection Assay.

Isolation of RNA

The frozen proximal tibial metaphyses and distal femoral metaphyses were individually homogenized in guanidine isothiocyanate using a Spex freezer mill (Spex Industries, Inc., Edison, NJ). Total RNA was extracted and isolated using a modified organic solvent method and the RNA yields were determined spectrophotometrically at 260 nm (15).

cDNA microarray analysis

Rat genefilter microarrays (GF 300), consisting of 5531 genes were purchased from Research Genetics (Huntsville, AL). cDNA probes were generated from 1 μg total RNA isolated from tibial metaphyses from each group of animals by reverse transcription (Superscript II, Life Technologies, Rockville, MD). First-strand cDNA probes were primed by addition of Oligo dT and labeled with [α-^{33}P]dCTP (ICN Radiochemicals, Costa Mesa, CA). The probes were subsequently purified by passage through Sephadex G-50 DNA Grade Column (Amersham Pharmacia Biotech AB, Uppsala, Sweden). Hybridization was carried out as recommended by

manufacturer's protocol. After the hybridization, the array was washed and wrapped with plastic wrap before placing it in a phosphor imaging cassette containing Cyclone Storage Phosphor Screen (Packard, Downers Groves, IL) for 24 hours. The array was scanned and the image was analyzed using Pathways 2.01 software to compare the signal intensities of spots.

RNase Protection Assay

Steady-state mRNA levels for PDGF-A were determined using an RNase Protection Assay according to the manufacturer's protocol (Pharmingen, San Diego, CA). Quantitation of protected RNA fragments was performed by PhosphoImager analysis and normalized to glyceraldehyde-3-phosphate dehydrogenase (GAPDH) and ribosomal structural protein L32.

Immunohistochemistry of PDGF-A

Immunohistochemical staining for PDGF-A in paraffin-sections (5 μm) of demineralized rat femora was achieved with a perioxidase ABC rabbit kit (VectorElite, Vector Laboratories, Burlingame, CA) and a polyclonal antibody specific for PDGF-A (Santa Cruz Biotechnology, Santa Cruz, CA). Sections were pretreated by incubation in hydrogen peroxide (0.6% in methanol at RT) and digestion in hyaluronidase (250 U/ml in Na acetate/NaCl buffer at 37 °C). Incubation with primary antibody (1/33 dilution in Tris HCl buffer) was performed at either 37 °C (1 hr), followed by incubation at room temperature in goat anti-rabbit antibody (1 hr) and peroxidase labeled avidin-biotin complex (30 min., VectorElite ABC). Positive PDGF-A staining was localized with the chromagen diaminobenzidine upon incubation with hydrogen peroxide substrate. Specificity of antibody was confirmed with the omission and increasing dilutions of primary antibody, with staining in tissue from vehicle-treated rats and with staining performed with a non-PDGF-A rabbit antisera.

Serum chemistry and PTH

Total serum calcium, phosphate, and magnesium were measured by Central Clinical Laboratory Research at the Mayo Clinic using an automated procedure. Serum PTH was measured using an immunoradiometric assay for rat PTH (Immunotopics International, LLC, San Clementa, CA) which has approximately 100% cross-reactivity to human PTH.

Bone histomorphometry

The proximal metaphyses were dehydrated in a graded series of ethanol, infiltrated and embedded in methylmethacrylate (Fisher Scientific, Fair Lawn, NJ). Tissue sections were cut at 5 μm thickness (Reichert-Jung Model 2065 Microtome, Heidelberg, Germany) and mounted unstained for dynamic cancellous bone measurements. Consecutive sections were stained with toluidine blue for bone cell and peritrabecular fibrosis measurements and Goldner's method for photomicrographs. A standard sampling site of 2.8 mm^2 was established in the secondary spongiosa of the metaphysis 1.5 mm distal to the growth plate. All histomorphometric measurements were carried out with an Osteomeasure image analysis system (OsteoMetrics, Atlanta, GA) and parameters were calculated according to the standardized nomenclature (16). The following measurements were obtained as described (11): bone volume per tissue volume, tetracycline and calcein labels, mineral apposition rate, osteoblast surface, osteoclast surface and fibrotic perimeter. Bone formation rate was calculated as the product of mineral apposition rate and the calcein labeled perimeter, expressed per bone surface, bone volume or tissue volume.

Statistical analysis

Multiple group comparisons were determined using one-way analysis of variance (one-way ANOVA) with statistical significance at $P < 0.05$. Differences between pairs of groups were compared by the Fisher's protected least significant difference post-hoc test. Two-way analysis

of variance (two-way ANOVA) was performed to determine significant effects of PTH and trapidil or interaction between PTH and trapidil.

Results

Continuous PTH Induces Parathyroid Bone Disease in Rats.

We confirmed the differential effect of two types of PTH administration on bone histology (11). As expected, continuous PTH for 7 days induced tibial metaphysis histopathology resembling high turnover parathyroid bone disease. The PTH-treated rats had increased bone formation and resorption and extensive peritrabecular bone marrow fibrosis. The histological changes contrast with pulsatile administration of PTH which dramatically increased bone formation without inducing development of peritrabecular fibrosis or abnormal bone resorption.

Increased PDGF-A Signaling is Associated with Parathyroid Bone Disease.

To understand the etiopathogenesis of parathyroid bone disease, we identified differentially expressed genes using cDNA microarrays. Total cellular RNA was isolated from the same region of contralateral tibiae of rats on which histological measurements were performed. The RNA was hybridized with rat genefilter microarrays containing 5531 genes, and data from rats treated with continuous PTH were compared to pulsatile PTH. Approximately 14 % of total genes measured were differentially expressed. We detected increased expression of several growth factors. We focused our attention on one of these, PDGF-A, a known mitogenic and chemotactic factor for fibroblasts. We next verified the differential regulation of PDGF-A expression using an RNase Protection Assay (Fig. 1a). Pulsatile PTH had no effect on steady-state mRNA levels for PDGF-A, whereas continuous PTH resulted in a statistically significant 3.3-fold increase in expression of PDGF-A mRNA (Fig. 1b). Additionally, we localized PDGF-A protein in bone by immunohistochemistry. Mast cells in PTH-treated rats stained intensely

positive for PDGF-A (Fig. 2). Much weaker staining was observed in growth plate hypertrophic chondrocytes. PDGF staining was weaker yet in osteoblasts, osteoclasts and fibroblasts.

Trapidil Antagonizes PDGF-signaling and Decreases Parathyroid Bone Disease in Rats.

Triazolopyrimidine (trapidil) is a competitive inhibitor of PDGF receptor (17) and decreases mRNA levels for PDGF-receptor and peptide (18). We examined the effects of PTH and trapidil on serum chemistry (Table 1). Continuous PTH had no effect on serum concentrations of phosphorous and magnesium, and increased serum PTH and calcium. Trapidil alone had no effect on serum chemistry but in combination with PTH it reduced serum calcium.

Trapidil had no effect on mRNA levels for PDGF-A but prevented the PTH-induced increase in mRNA levels (Fig. 3). Similarly, trapidil alone had no effect but when combined with PTH antagonized the PTH-induced increase in mRNA levels for PDGF-α receptor (data not shown), the principal receptor for the PDGF-A homodimer.

We further investigated the effects of trapidil on parathyroid bone disease using bone histomorphometry. Continuous PTH stimulated cancellous bone formation, whether the rate was expressed per bone surface, bone volume or tissue volume, due largely to an increase in osteoblast number as deduced by increased calcein labeled surface (Table 1). The fluorochrome-based analyses were confirmed by measurements showing that PTH increased osteoblast surface (Fig. 4*a*). Continuous PTH slightly increased mineral apposition rate, an index of osteoblast activity. Trapidil, when given alone or in combination with PTH, had no significant effect on indices related to bone formation. As expected, continuous PTH increased osteoclast surface, an index of bone resorption (Fig. 4*b*, 5*c*), and induced extensive peritrabecular fibrosis (Fig. 4*c*, 5*c*). Trapidil decreased osteoclast perimeter and peritrabecular fibrosis induced by PTH by 73 and 63 %, respectively. Two-way ANOVA revealed an interaction between PTH and trapidil on

osteoclast and peritrabecular fibrotic perimeter, confirming that trapidil antagonized the detrimental skeletal effects of continuous PTH but had no effect on normal rats. Combination treatment with PTH and trapidil resulted in histological changes (Table 1 and Fig. 5*d*) similar to those observed following pulsatile PTH treatment, as shown by an increase in bone formation and osteoblast surface. These data suggest that trapidil, by antagonizing PDGF-A, selectively reduces skeletal pathology induced by continuous infusion of PTH.

Discussion

In this study, we identify PDGF-A as a potential causative factor for parathyroid bone disease in an animal model for HPT. PDGF-A expression increases in skeletal tissue in this model. Treating PTH-infused animals with trapidil, an inhibitor of PDGF signaling, provides a highly effective intervention for preventing the skeletal disorders, leading to a striking reduction of peritrabecular fibrosis and osteoclastic bone resorption.

PTH has incongruous effects on bone metabolism depending on the pattern of exposure to the hormone (19-21). Pulsatile PTH increases bone formation, whereas continuous PTH stimulates bone resorption as well as bone formation, and induces marrow fibrosis. The signal transduction pathways of PTH begin with the hormone binding to the highly conserved PTH/PTH-related peptide receptor at the osteoblast surface. Upon binding to its receptor, early signaling events are sufficient to induce the anabolic response. However, late events, associated with continuously elevated PTH, lead to parathyroid bone disease. Therefore, understanding the differential gene expression of these two regimens is essential for determining what signals mediate PTH-induced parathyroid bone disease. Identification of genes induced by continuous versus pulsatile PTH was performed using cDNA microarray, a powerful tool for profiling gene expression. Using this approach, we obtained preliminary evidence that PDGF-A mRNA becomes elevated by continuous but not pulsatile PTH. These gene array data was confirmed using an RNase Protection Assay.

PDGF is a homo- or heterodimer polypeptide encoded by two distinct genes, PDGF-A and PDGF-B (22). The PDGF-A and PDGF-B chains share 56% homology and join by disulfide bond to form three different dimers, AA, AB or BB (23, 24). Cellular responses are mediated via two high-affinity receptor subunits, α and β. PDGF-A binds primarily to the α-receptor, whereas

PDGF-B binds to the α- or β-receptors (25). PDGF has potent mitogenic and chemotactic actions on mesenchymal cells. PDGF plays a role in physiological repair mechanisms and pathogenesis of proliferative diseases, including tumorigenesis, atherosclerosis, inflammatory disorders and most relevant to the present investigation, fibrosis (26, 27).

^{3}H-Thymidine radioautography was used to determine the origin of the peritrabecular fibroblasts induced by continuous infusion of PTH and indicated extensive proliferation of the fibroblasts lining bone surfaces (28). This finding suggests a role for a PTH-induced growth factor, possibly PDGF-A, in the recruitment to bone surfaces and expansion of fibroblast populations by PTH.

PDGF-A peptide was localized to mast cells by immunohistochemistry. This intriguing result suggests that cytokines that are released by mast cells, including PDGF, mediate parathyroid bone disease. This mechanism of action is supported by evidence implicating mast cells in pathological fibrosis as well as pathological bone resorption (29-31). Additionally, HPT patients have increased numbers of mast cells in the vicinity of trabecular surfaces of cancellous bone (32) and PTH is reported to induce mast cell degranulation (33).

Trapidil, originally developed as a vasodilator and anti-platelet agent, has proven to be clinically effective in the treatment of coronary heart disease (34). Trapidil has been reported to antagonize PDGF signaling by acting as a PDGF receptor antagonist, and by reducing PDGF and PDGF receptor gene expression (17, 18). Trapidil has been reported to have additional actions *in vitro*; including inhibition of phosphodiesterase (35), thromboxane A_2 (36), and CD40 signaling (37), and direct activation of protein kinase A signaling (38).

The observed decreases in mRNA levels for PDGF-A and PDGF receptor α demonstrate that trapidil antagonizes PDGF-A signaling in PTH-treated rats. The lack of an effect of trapidil

on normal rats indicates that the drug is unlikely to have inhibited phosphodiesterase or have activated protein kinase A signaling, since these actions would have been expected to have dramatic effects on bone turnover (39, 40).

PTH treatment decreased mRNA levels for thromboxane A_2 (data not shown) so it is unlikely that a further decrease by trapidil could be responsible for the actions of the drug on bone. Finally, we did not detect an effect of trapidil on mRNA levels for TNF-α, IL-6 and IL-12 (data not shown), genes reported to be down-regulated in response to blockade of the CD40 pathway. Although we cannot rule out the possibility of multiple pathways of action, we have established that trapidil antagonizes PDGF signaling and have uncovered no evidence to implicate alternative pathways.

Treatment of animals with trapidil did not alter serum PTH levels, demonstrating that the drug did not act by accelerating the metabolism of the hormone. Trapidil, however, did decrease serum calcium in PTH-treated rats. This reduction of serum calcium was likely due to an inhibitory effect of trapidil on bone resorption, as shown by a decrease in osteoclast surface. There are a variety of mechanisms by which PDGF-A signaling could act as an indirect factor in PTH-induced bone resorption. For example, fibroblasts have been reported to express RANKL, a critical factor in the differentiation of osteoclasts. The combination of marrow fibrosis induced by PDGF-A and additional factors that induce RANKL expression could be responsible for the focal bone resorption associated with hyperparathyroidism. This possibility is consistent with clinical observations; peritrabecular fibrosis and increased bone resorption generally occur in combination in patients with renal osteodystrophy (10). Alternatively, PDGF-A signaling could play a role in the release from mast cells of one or more cytokines that stimulate osteoclast function (41). Further research will be necessary to test these and other possibilities.

All three isoforms of PDGF were shown to induce proliferation of osteoblastic cells in culture (PDGF-BB > -AB > -AA)(42, 43). In cultured calvariae, PDGF increases the number of cells capable of synthesizing collagen, and inhibits matrix synthesis in intact calvariae (44). Other studies have reported that the effects of PDGF on in vitro mineralization depend upon the duration of exposure to the cytokine; pulsed exposure increases mineralization whereas, continuous exposure antagonizes mineralization (31).

Continuous infusion of PTH resulted in tibial metaphysis histological changes similar to a previous report, including multilayers of fibroblasts lining trabeculae (11). Trapidil was found to inhibit Balb/c 3T3 fibroblast proliferation induced by PDGF (45) and we demonstrated that trapidil markedly reduced peritrabecular fibrosis. Trapidil was also reported to strongly decrease gene expression of PDGF-α and -β receptors and to moderately suppress mRNA levels of PDGF-A and –B in injured rat arteries (18). We have found that trapidil similarly decreases mRNA levels for PDGF-A and PDGF-α receptor in bone.

In conclusion, PDGF-A signaling appears to be critical to the pathogenesis of parathyroid bone disease. Trapidil, an antagonist of PDGF signaling, suppressed the development of peritrabecular fibrosis and osteoclastic bone resorption while allowing the elevated bone formation to continue. The latter finding suggests that increased PDGF-A signaling is unnecessary for the initial stimulation of bone formation by PTH. The beneficial effects of trapidil on bone with no adverse effects at the dosage tested in this study suggest a use of PDGF antagonists in parathyroid bone disease. Whether or not trapidil can reduce established marrow fibrosis requires further investigation.

Acknowledgements

The authors acknowledge Dr. Reiner Ludwig (Rodleben Pharma GmbH, Germany) for a gift of trapidil, Ms. Glenda Evans and Minzhi Zhang for technical assistance, and Ms. Peggy Backup and Lori Rolbiecki for editorial assistance. This work was supported by grants from the National Institutes of Health (NIH AR 45233), the National Aeronautics and Space Administration through the NASA Cooperative Agreement NCC 9-58 with the National Space Biomedical Research Institute (NASA NAG 9-1150) and the Mayo Foundation.

References

1. Bereket A, Casur Y, Firat P, Yordam N. 2000 Brown tumour as a complication of secondary hyperparathyroidism in severe long-lasting vitamin D deficiency rickets. Eur J Pediatr 159:70-73
2. Kulak CA, Bandeira C, Voss D, Sobieszczyk SM, Silverberg SJ, Bandeira F, Bilezikian JP 1998 Marked improvement in bone mass after parathyroidectomy in osteitis fibrosa cystica. J Clin Endocrinol Metab 83:732-735
3. Khosla S, Melton LJ 3rd, Wermers RA, Crowson CS, O'Fallon W, Riggs B 1999 Primary hyperparathyroidism and the risk of fracture: a population-based study. J. Bone Miner Res 14:1700-1707
4. Silverberg SJ, Bilezikian JP 2001 Clinical presentation of primary hyperparathyroidism in the United States. In: Bilezikian JP, Marcus R, Levine MA, eds. The Parathyroids: Basic and Clinical Concepts. 2nd ed. San Diego: Academic Press; 349-360
5. Mithal A, Bandeira F, Meng X, Silverberg SJ, Shi Y, Mishra SK, Griz L, Macedo G, Celdas G, Bandeira C, Bilezikian JP, Rao SD 2001 Clinical presentation of primary hyperparathyroidism: India, Brazil, and China. In: Bilezikian JP, Marcus R, Levine MA, eds. The Parathyroids: Basic and Clinical Concepts. 2nd ed. San Diego: Academic Press; 375-386
6. Rosenberg AE 1994 Skeletal system and soft tissue tumors. In: Cotran RS, Kumar V, Robbins SL, eds. Pathologic Basis of Disease Philadelphia: W.B. Saunders Company; 1213-1272
7. Rubin E, Farber JL 1994 The endocrine system. In: Rubin E, Farber JL, eds. Pathology. 2nd ed. Philadelphia: J.B. Lippincott Company; 1098-1147
8. Coburn JW, Henry DA 1984 Renal osteodystrophy. Adv Intern Med 30: 387-424

9. Schiller AL, Teitelbaum SL 1990 Bones and joints. In: Rubin E, Farber JL, eds. Pathology. 3rd ed. Philadelphia: Lippincott-Raven; 1336-1413

10. Coburn JW, Salusky IB 2001 Renal bone diseases: clinical features, diagnosis and management. In: Bilezikian JP, Marcus R, Levine MA, eds. The Parathyroids: Basic and Clinical Concepts. 2nd ed. San Diego: Academic Press; 635-661

11. Dobnig H, Turner RT 1997 The effects of programmed administration of human parathyroid hormone fragment (1-34) on bone histomorphometry and serum chemistry in rats. Endocrinology 138:4607-4612

12. Tiell ML, Sussman II, Gordon PB, Saunders RN 1983 Suppression of fibroblast proliferation in vitro and of myointimal hyperplasia in vivo by the triazolopyrimidine, trapidil. Artery 12:33-50

13. Gocer AI, Polat S, Ozel S, Tuna M, Kaya M, Cetinalp E, Haciyakupoglu S 1998 The effect of trapidil on the reactive astrocytic proliferation following spinal cord trauma in rats: light and electron microscopic findings. Neurol Res 20:365-373

14. Futamura A, Izumino K, Nakagawa Y, Takata M, Inoue H, Iida H. 1999 Effect of the platelet-derived growth factor antagonist trapidil on mesangial cell proliferation in rats. Nephron 81:428-433

15. Chomczynski P, Sacchi N 1987 Single-step method of RNA isolation by acid guanidinium thiocyanate-phenol-chloroform extraction. Anal. Biochem 162:156-159

16. Parfitt AM, Drezner MK, Glorieux FH, Kanis JA, Malluche H, Meunier PJ, Ott SM Recker RR 1987 Bone histomorphometry: standardization of nomenclature, symbols, and units. Report of the ASBMR Histomorphometry Nomenclature Committee. J Bone Miner Res 2:595-610

17. Poon M, Cohen J, Siddiqui Z, Fallon JT, Taubman MB 1999 Trapidil inhibits monocyte chemoattractant protein-1 and macrophage accumulation after balloon arterial injury in rabbits. Lab. Invest 79:1369-1375

18. Deguchi J, Abe J, Makuuchi M, Takuwa Y 1999 Inhibitory effects of trapidil on PDGF signaling in balloon-injured rat carotid artery. Life Sci 65:2791-2799

19. Jerome CP, Gubler HP 1991 Experimental determination of the "the law of bone remodeling" and effect of rat parathyroid hormone (1-34) infusion on derived parameters Calcif. Tissue Int. 49:398-402

20. Podbesek R, Edouard C, Meunier PJ, Parsons JA, Reeve J, Stevenson RW, Zanelli JM 1983 Effects of two treatment regimens with synthetic human parathyroid hormone fragment on bone formation and the tissue balance of trabecular bone in greyhounds. Endocrinology 112:1000-1006

21. Nishida S, Yamaguchi A, Tanizawa T, Endo N, Mashiba T, Uchiyama Y, Suda T, Yoshiki S, Takahashi HE 1994 Increased bone formation by intermittent parathyroid hormone administration is due to the stimulation of proliferation and differentiation of osteoprogenitor cells in bone marrow Bone 15:717-723

22. Betsholtz C, Johnsson A, Heldin C-H., Westermark B, Lind P, Urdea MS, Eddy R, Shows TB, Philpott K, Mellor AL., Knott TJ, Scott J 1986 cDNA sequence and chromosomal localization of human platelet-derived growth factor A-chain and its expression in tumor cell lines. Nature 320:695-699

23. Heldin C-H, Westermark B 1987 PDGF-like growth factors in autocrine stimulation of growth. J Cell Physiol 5 (Suppl):S31-S34.

24. Waterfield MD, Scrace GT, Whittle N, Stroobant P, Johnsson A, Wasteson A, Westermark B, Heldin C-H, Huang JS, Deuel TF 1983 Platelet-derived growth factor is structurally related to the putative transforming protein $p28^{sis}$ of simian sarcoma virus. Nature 304:35-39

25. Seifert RA, Hart CE, Phillips PE, Forstrom JW, Ross R, Murray MJ, Bowen-Pope D F 1989 Two different subunits associate to create isoform-specific platelet-derived growth factor receptors. J Biol Chem 264:8771-8778

26. Heldin C–H, Westermark B 1996 Role of platelet-derived growth factor in vivo. In: Clark RAF, eds The Molecular and Cellular Biology of Wound Repair. 2nd ed. New York: Plenum Press; 249-273

27. Raines EW, Bowen-Pope DF, Ross R 1990 Platelet-derived growth factor. In: Sporn, MB, Robert AB, eds. Handbook of Experimental Pharmacology. Peptide Growth Factors and Their Receptors. Heidelberg: Springer-Verlag; 173-262

28. Lotinun S, Sibonga JD, Turner RT 2002 Differential effects of intermittent and continuous administration of parathyroid hormone on bone histomorphometry and gene expression. Endocrine 17:29-36

29. Hiragun T, Morita E, Tanaka T, Kameyoshi Y, Yamamoto S 1998 A fibrogenic cytokine, platelet-derived growth factor (PDGF), enhances mast cell growth indirectly via a SCF- and fibroblast-dependent pathway. J Invest Dermatol 111:213-217

30. Johansson C, Roupe G, Lindstedt G, Mellstrom D 1996 Bone density, bone markers and bone radiological features in mastocytosis. Age Ageing 25:1-7

31. Hsieh SC, Graves DT 1998 Pulse application of platelet-derived growth factor enhances formation of a mineralizing matrix while continuous application is inhibitory. J Cell Biochem 69:169-180

32. Peart KM, Ellis HA 1975 Quantitative observations on iliac bone marrow mast cells in chronic renal failure. J Clin Pathol 28:947-955

33. Nakamura M, Kuroda H, Narita K, Endo Y 1996 Parathyroid hormone induces a rapid increase in the number of active osteoclasts by releasing histamine from mast cells. Life Sci 58:1861-1868

34. Okamoto S, Inden M, Setsuda M, Konishi T, Nakano T 1992 Effects of trapidil (triazolopyrimidine), a platelet-derived growth factor antagonist, in preventing restenosis after percutaneous transluminal coronary angioplasty. Am Heart J 123:1439-1444

35. Mazurov AV, Menshikov M, Yu Leytin VL, Tkachuk VA, Repin VS 1984 Decrease of platelet aggregation and spreading via inhibition of cAMP phosphodiesterase by trapidil. FEBS Lett 172:167-171

36. Ohnishi H, Kosuzume H, Hayashi Y, Yamaguchi K, Suzuki Y, Itoh R 1981 Effects of trapidil on thromboxane A2-induced aggregation of platelets, ischemic changes in heart and biosynthesis of thromboxane A2. Prostaglandins Med 6:269-281

37. Zhou L, Ismaili J, Stordeur P, Thielemans K, Goldman M, Pradier O 1999 Inhibition of CD40 pathway of monocyte activation by triazolopyrimidine. Clin Immunol 93:232-238

38. Bonisch D, Weber AA, Wittpoth M, Osinski M, Schror K 1998 Antimitogenic effects of trapidil in coronary artery smooth muscle cells by direct activation of protein kinase A. Mol Pharmacol 54:241-248

39. Kinoshita T, Kobayashi S, Ebara S, Yoshimara Y, Horiuchi H, Tsutsumimoto T, Wakabayashi S, Takaoka K 2000 Phosphodiesterase inhibitors, pentoxifylline and rolipram, increase bone mass mainly by promoting bone formation in normal mice. Bone 27:811-817

40. Swarthout JT, D'Alonzo RC, Selvamurugan N, Partridge NC 2002 Parathyroid hormone-dependent signaling pathways regulating genes in bone cells. Gene 282:1-17

41. Nilsson G, Svensson V, Nilsson K 1995 Constitutive and inducible cytokine mRNA expression in the human mast cell line HMC-1. Scand J Immunol 42:76-81

42. Centrella M, McCarthy TL, Kusmik WF, Canalis E 1991 Relative binding and biochemical effects of heterodimeric and homodimeric isoforms of platelet-derived growth factor in osteoblast-enriched cultures from fetal rat bone. J Cell Physiol 147:420-426

43. Pfeilschifter J, Krempien R, Naumann A, Gronwald RG, Hoppe J, Ziegler R 1992 Differential effects of platelet-derived growth factor isoforms on plasminogen activator activity in fetal rat osteoblasts due to isoform-specific receptor functions. Endocrinology 130:2059-2066

44. Hock JM, Canalis E 1994 Platelet-derived growth factor enhances bone cell replication, but not differentiated function of osteoblasts. Endocrinology 134:1423-1428

45. Ohnishi H, Yamaguchi K, Shimada S, Suzuki Y, Kumagai A 1981 A new approach to the treatment of atherosclerosis and trapidil as an antagonist to platelet-derived growth factor. Life Sci 28:1641-1646

Figure Legends

Fig. 1 Continuous but not pulsatile PTH increases mRNA levels for PDGF-A. Rats were treated with vehicle, daily s.c. injection of hPTH (1-34) (pulsatile PTH) or s.c. implanted hPTH (1-34) osmotic pump (continuous PTH) for 7 days. Tibial metaphyses were removed for total RNA extraction. A, Representative RNase Protection Assay for PDGF-A and housekeeping genes, L32 and GAPDH. B, Results are expressed in arbitrary densitometric units normalized for the expression of L32 in each group. Continuous PTH significantly increased PDGF-A either expressed per L32 or GAPDH (data not shown). Each bar represents mean ± SEM. (n = 5). [a], $P <$ 0.001 compared with vehicle, [b], $P < 0.01$ compared with pulsatile PTH.

Fig. 2 PDGF-A immunohistochemistry. Specific staining for PDGF-A was localized to mast cells (arrows) in the femoral metaphysis of rats treated with vehicle (A), and PTH (B). Immunohistochemistrically stained cells were identified as mast cells by metachromatic staining of granules by 0.1% toluidine blue in serial paraffin sections. Staining was completely eliminated in sections incubated in the absence of primary antibody or with a non PDGF-A rabbit antiserum. B indicates cancellous bone.

Fig. 3 Trapidil prevented the PTH-induced increase in PDGF-A mRNA levels. Total RNA from femoral metaphyses was isolated for RNase Protection Assay for PDGF-A. PTH increased PDGF-A/L32 mRNA levels. Trapidil alone had no effect but when combined with PTH prevented the PTH-induced increase in PDGF-A mRNA levels. Each bar represents mean ± s.e.m. (n = 5). [a], $P < 0.01$ compared with vehicle, [b], $P < 0.001$ compared with trapidil, [c], $P <$ 0.001 compared with PTH.

Fig. 4 Effects of trapidil, PTH and combination of PTH and trapidil on bone cells and fibroblasts. Five-micron-thick tibial longitudinal sections were stained with toluidine blue for

measuring: A, Osteoblast surface per bone surface (Ob.S/BS). B, Osteoclast surface per bone surface (Oc.S/BS). C, Fibroblasts surrounding trabecular surface (fibrotic perimeter). Two-way ANOVA indicated significant effects of PTH on Ob.S/BS whereas there were significant effects of PTH, trapidil or interaction between PTH and trapidil on Oc.S/BS and fibrotic perimeter. Each bar represents mean ± SEM. (n = 8-10). [a], $P < 0.05$ compared with vehicle, [b], $P < 0.05$ compared with trapidil, [c], $P < 0.05$ compared with PTH.

Fig. 5 Inhibitory effects of trapidil on peritrabecular fibrosis induced by continuous PTH. Photomicrograph of Goldner's stain from tibial metaphyses in rats treated with vehicle (A), trapidil (B), PTH (C), PTH and trapidil (D). Note numerous fibroblasts (black arrows) and osteoclasts (white arrows) in C and osteoblasts (black arrows) in D.

A.

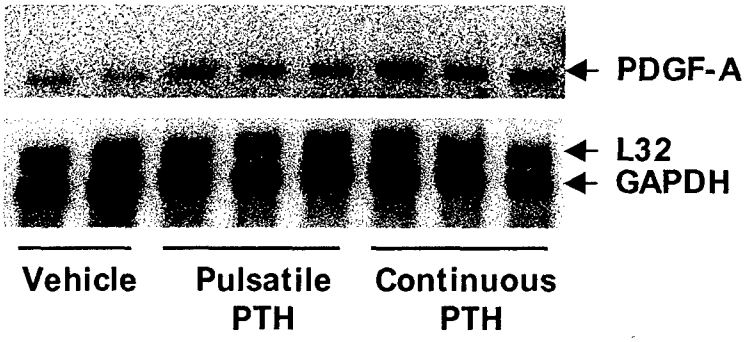
PDGF-A
L32
GAPDH
Vehicle
Pulsatile PTH
Continuous PTH

B.

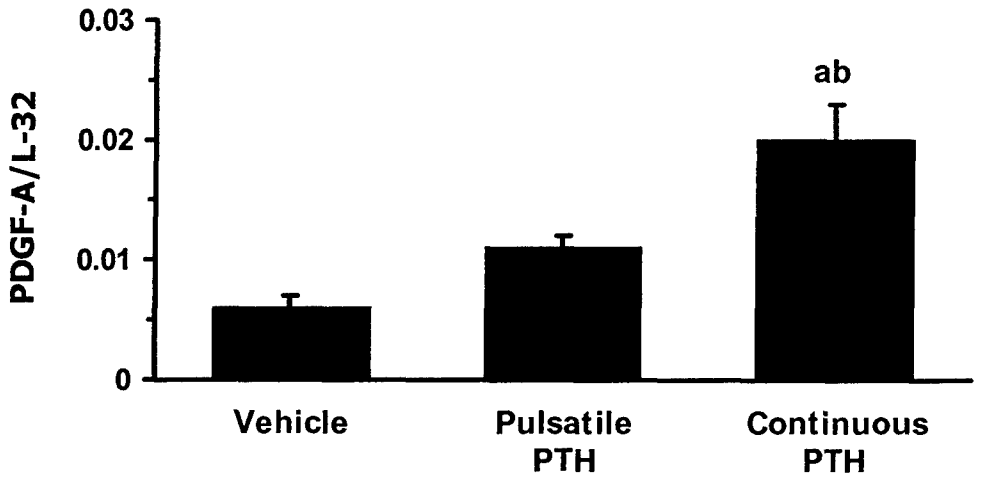
0.03
0.02
0.01
0
PDGF-A/L-32
ab
Vehicle
Pulsatile PTH
Continuous PTH

Fig. 1

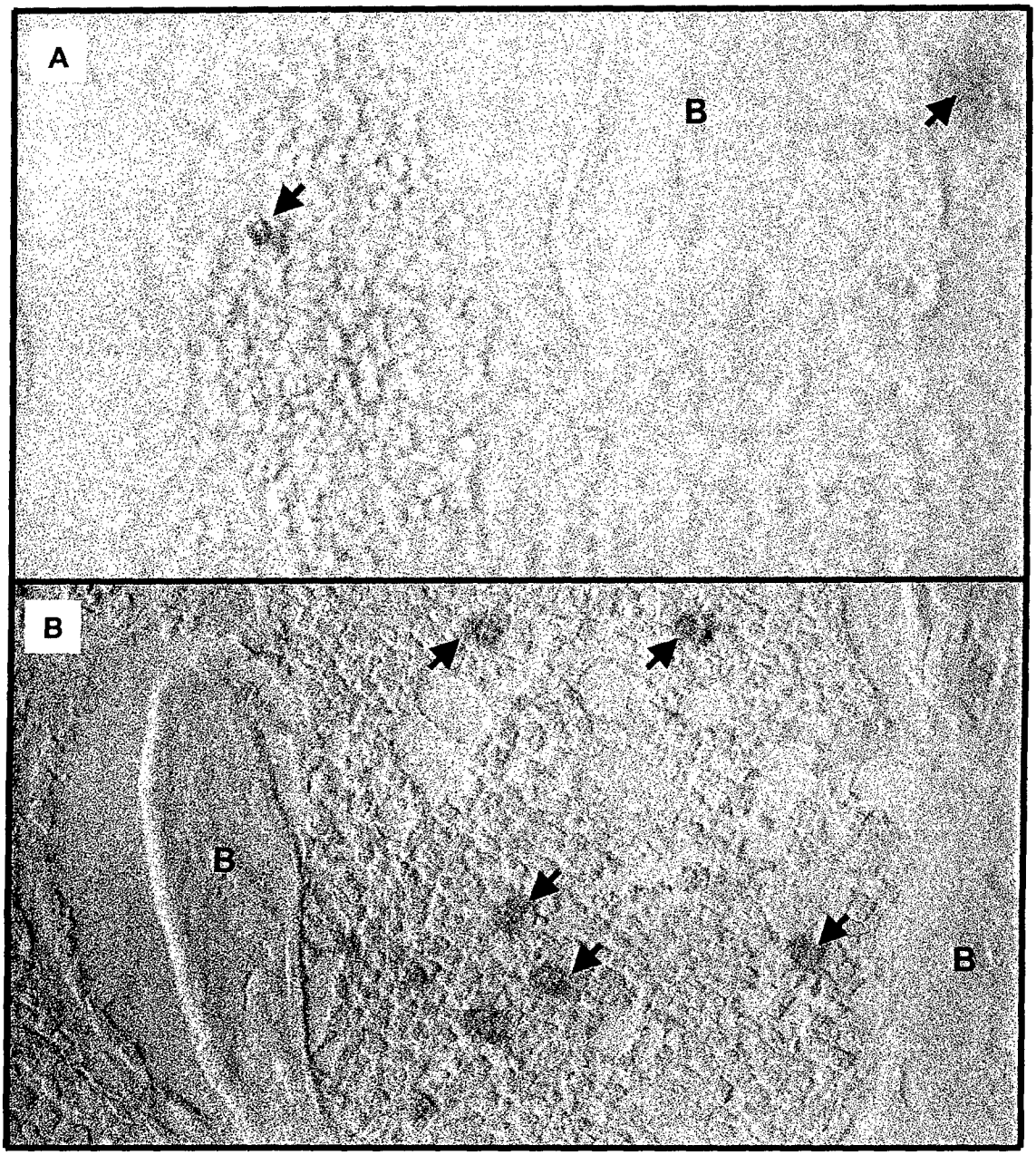

Fig 2

Table 1 Serum chemistry and bone histomorphometric measurements.

Parameters	Vehicle ($n = 9$)	Trapidil ($n = 10$)	PTH ($n = 8$)	PTH+Trapidil ($n = 10$)	Two-way ANOVA		
					PTH	Trapidil	Interaction
Serum							
Calcium (mg/dl)	10.26 ± 0.07	10.10 ± 0.05	11.65 ± 0.28[ab]	10.94 ± 0.32[abc]	$P < 0.001$	$P < 0.05$	NS
Phosphorus (mg/dl)	7.89 ± 0.27	7.33 ± 0.29	7.95 ± 0.48	7.46 ± 0.29	NS	NS	NS
Magnesium (mg/dl)	2.34 ± 0.05	2.40 ± 0.05	2.49 ± 0.04	2.46 ± 0.07	NS	NS	NS
PTH (pg/ml)	19.45 ± 8.37	28.80 ± 9.62	85.29 ± 13.82[ab]	108.23 ± 41.06[ab]	$P < 0.001$	NS	NS
Bone							
BV/TV (%)	24.89 ± 0.94	24.83 ± 0.87	27.25 ± 1.14	23.79 ± 0.86	NS	NS	NS
Tetracycline label (%)	7.86 ± 0.94	9.65 ± 1.76	5.65 ± 2.48	6.91 ± 1.71	NS	NS	NS
Calcine label (%)	18.63 ± 2.22	18.32 ± 1.39	48.08 ± 5.35[ab]	43.24 ± 4.42[ab]	$P < 0.001$	NS	NS
MAR (μm/day)	1.09 ± 0.05	1.06 ± 0.04	1.29 ± 0.08	1.18 ± 0.07	$P < 0.05$	NS	NS
BFR/BS ($\mu m^3/\mu m^2$/day)	0.29 ± 0.03	0.30 ± 0.03	0.71 ± 0.10[ab]	0.59 ± 0.06[ab]	$P < 0.001$	NS	NS
BFR/BV (%)	1.04 ± 0.11	0.99 ± 0.08	2.30 ± 0.31[ab]	2.06 ± 0.18[ab]	$P < 0.001$	NS	NS
BFR/TV (%)	0.26 ± 0.03	0.25 ± 0.02	0.63 ± 0.09[ab]	0.49 ± 0.05[ab]	$P < 0.001$	NS	NS

Data represent mean ± SEM. [a], $P < 0.05$ compared with vehicle, [b], $P < 0.05$ compared with trapidil, [c], $P < 0.05$ compared with PTH. Abbreviation: bone volume per tissue volume (BV/TV), mineral apposition rate (MAR), bone formation rate (BFR) expressed per bone surface (BS), bone volume (BV) or tissue volume (TV).

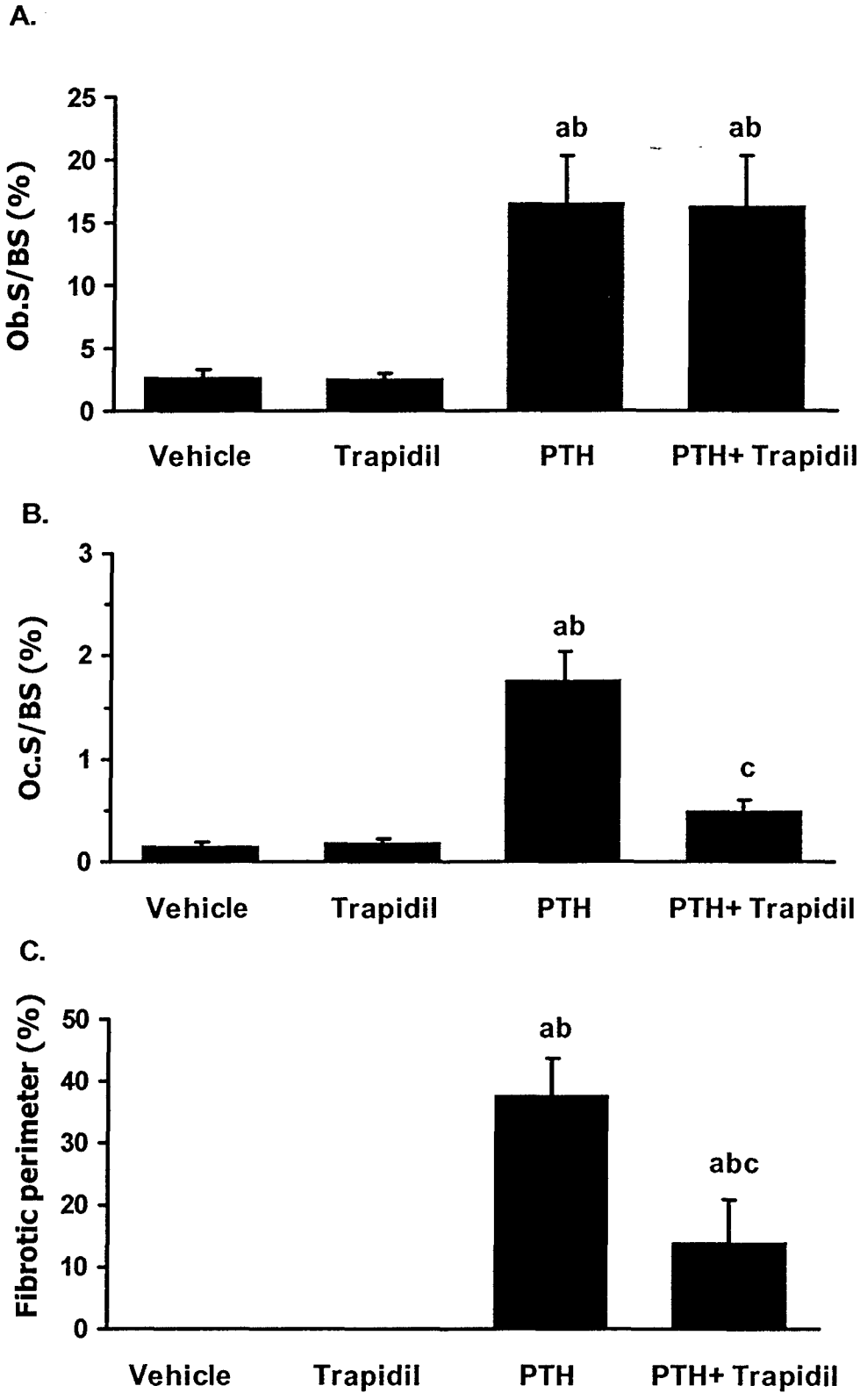
A.
Ob.S/BS (%)
25
20
15
10
5
0
ab
ab
Vehicle
Trapidil
PTH
PTH+ Trapidil
B.
Oc.S/BS (%)
3
2
1
0
ab
c
Vehicle
Trapidil
PTH
PTH+ Trapidil
C.
Fibrotic perimeter (%)
50
40
30
20
10
0
ab
abc
Vehicle
Trapidil
PTH
PTH+ Trapidil

Fig. 4

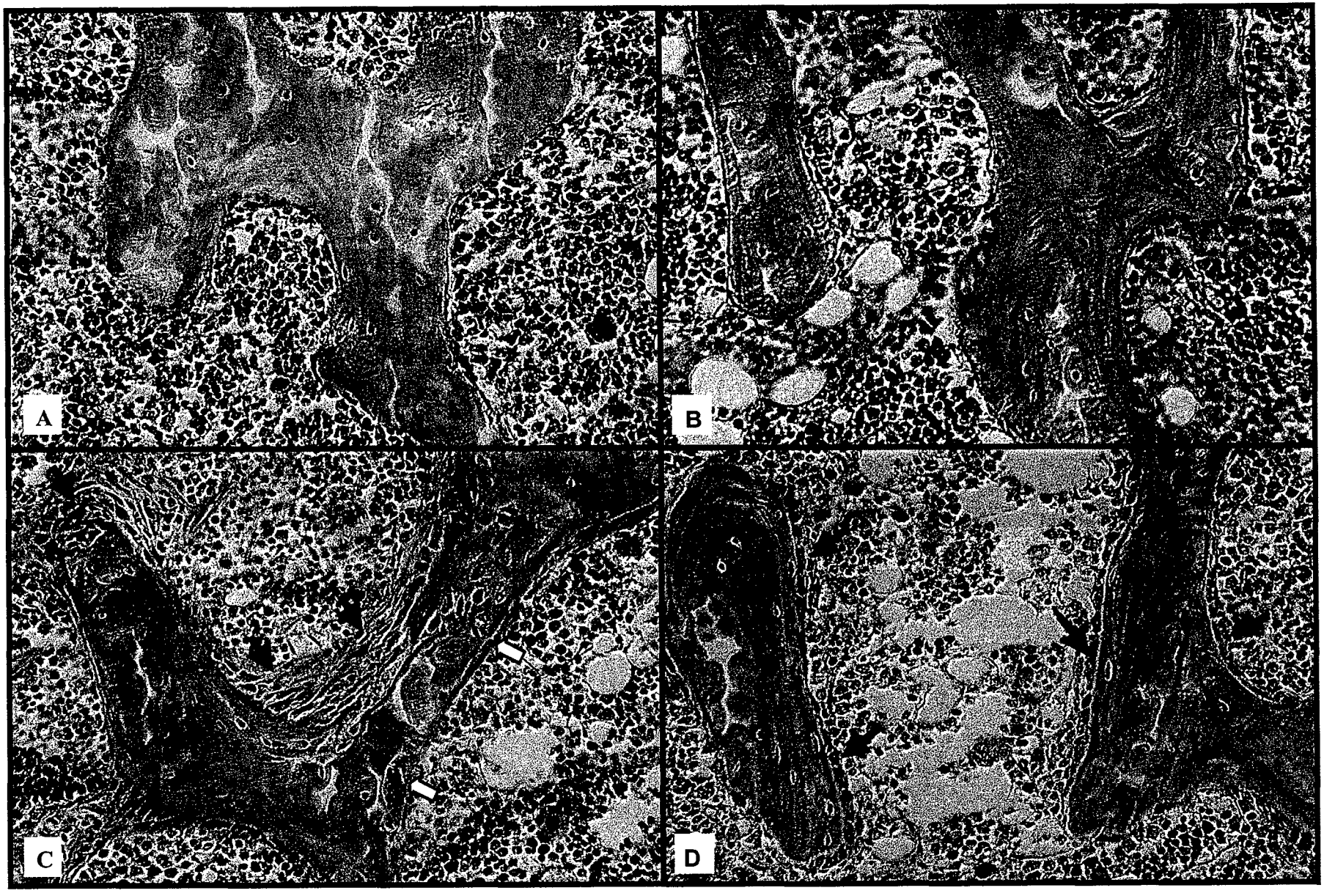

Fig. 5